EXPLORING THE CLINICAL UTILITY OF OPTICAL QUALITY AND FUNDUS AUTOFLUORESCENCE METRICS FOR MONITORING AND SCREENING FOR DIABETES MELLITUS

PROGRAMA DE DOCTORADO EN OPTOMETRÍA Y CIENCIAS DE LA VISIÓN

DOCTORANDO:

Ana María Calvo Maroto

DIRECTORES DE TESIS

Alejandro Cerviño Expósito

Rafael J. Pérez Cambrodí

José Juan Esteve Taboada

Burjasot, Febrero 2017

EXPLORING THE CLINICAL UTILITY OF OPTICAL QUALITY AND FUNDUS AUTOFLUORESCENCE METRICS FOR MONITORING AND SCREENING FOR DIABETES MELLITUS

PROGRAMA DE DOCTORADO EN OPTOMETRÍA Y CIENCIAS DE LA VISIÓN

DOCTORANDO:

Ana María Calvo Maroto

DIRECTORES DE TESIS

Alejandro Cerviño Expósito

Rafael J. Pérez Cambrodí

José Juan Esteve Taboada

Burjasot, Febrero 2017

EXPLORING THE CLINICAL UTILITY OF OPTICAL QUALITY AND FUNDUS AUTOFLUORESCENCE METRICS FOR MONITORING AND SCREENING FOR DIABETES MELLITUS

Memoria presentada por

Ana María Calvo Maroto

Para optar al grado de

DOCTOR en OPTOMETRÍA Y CIENCIAS DE LA VISIÓN

2017

DECLARATION

No portion of the work referred to in the thesis has been submitted in support of an application for another degree or qualification of this or any other university or other institution of learning.

El Dr. Alejandro Cerviño Expósito, Profesor Titular de Óptica de la Universidad de Valencia, el Dr. Rafael José Pérez Cambrodí, Responsable de la unidad de Optometría de Oftalmar (Departamento de Oftalmología) en el Hospital Internacional Vithas Medimar de Alicante, y el Dr. Juan José Esteve Taboada, Investigador Doctor Senior de la Universidad de Valencia.

CERTIFICAN que la presente memoria "EXPLORING THE CLINICAL UTILITY OF OPTICAL QUALITY AND FUNDUS AUTOFLUORESCENCE METRICS FOR MONITORING AND SCREENING FOR DIABETES MELLITUS", resume el trabajo de investigación realizado, bajo su dirección, por Dª. Ana María Calvo Maroto y constituye su Tesis para optar al Grado de Doctor en Optometría y Ciencias de la Visión.

Y para que así conste, y en cumplimiento de la legislación vigente, firma el presente certificado en Valencia, a Febrero de dos mil diecisiete.

Fdo. Dr. Alejandro Cerviño Expósito. Fdo. Dr. Rafael José Pérez Cambrodí

Fdo. Dr. José Juan Esteve Taboada

A mis padres,

Ángel y Ana

AGRADECIMIENTOS

Esta Tesis Doctoral es el resultado de varios años de estudio y cuesta creer que ha llegado a su fin. A lo largo de estos años, muchas han sido las personas que me han acompañado en esta etapa y a las que tengo que agradecer que ahora me encuentre escribiendo estas palabras de mi Tesis Doctoral.

En primer lugar, quiero dar las gracias a mis tutores de Tesis, Alejandro Cerviño Expósito, Rafael J. Pérez Cambrodí y José J. Esteve Taboada grandes profesionales y, si cabe, mejores personas. Aunque en tan pocas palabras no puedo agradeceros todo lo que me habéis ayudado, en especial, os agradezco vuestra confianza, apoyo, paciencia e implicación en este trabajo. Ha sido un auténtico lujo trabajar y aprender de vosotros.

A cada una de las personas que componen el Grupo de Investigación en Optometría (GIO), por vuestra acogida, ayuda y colaboración.

También me gustaría agradecer al Dr. Antonio Hernández Mijares y a Leo por abrirme las puertas del hospital Doctor Peset y por hacerme sentir como una más durante los días que ha durado el proyecto.

Evidentemente no pueden faltar mis amigas, que aunque no nos veamos todo lo que quisiéramos, siempre están ahí cuando las necesitas. Gracias por preocuparos por mí, por vuestros ánimos, y por los momentos tan buenos que pasamos cuando estamos juntas.

A Carlos, gracias por tu apoyo, cariño, y comprensión; gracias por haber creído y confiado en mí, por aguantarme en mis malos momentos, por tu optimismo en la vida, y por sacarme siempre una sonrisa.

Y para finalizar, y para mí lo más importante en mi vida, me gustaría dar las gracias con mayúsculas a mi familia, especialmente a mis padres, por vuestro apoyo y ayuda incondicional, no sólo a lo largo de esta etapa sino durante toda mi vida. Gracias por respetar mis decisiones, por vuestra comprensión en los momentos difíciles, y por compartir mi alegría en los éxitos. Gracias a vosotros he conseguido ser quien soy. Y a mi hermano, por cuidarme y protegerme, y por ser un ejemplo de constancia y perseverancia en la vida.

A pesar de que hace algunos años que nos dejó, no puedo olvidarme de mi abuelo Julio (q.e.p.d.), a quién recuerdo siempre con un libro entre las manos, y de quién aprendí muchas cosas, entre ellas la pasión por aprender y el valor del conocimiento.

GRACIAS A TODOS

RESUMEN

La Diabetes Mellitus (DM) es una enfermedad sistémica que se caracteriza por una hiperglucemia crónica asociada a daños a largo plazo de diferentes órganos, como son los ojos, riñones, corazón y vasos sanguíneos, entre otros. Normalmente, la DM se clasifica en DM tipo 1 y DM tipo 2, a los que también hay que añadir la diabetes gestacional y otros tipos de diabetes causados por factores genéticos y otras enfermedades o infecciones.

La DM es una enfermedad que constituye un gran impacto socio-sanitario debido al incremento que ha experimentado su prevalencia y a su alta tasa de mortalidad asociada. Según la Organización Mundial de la Salud (en inglés, World Health Organization (WHO)), para el año 2030 habrá 366 millones de personas con diabetes a nivel mundial, y según la Federación Internacional de Diabetes (en inglés, International Diabetes Federation (IDF)), esta cifra es aún mayor, alcanzando los 552 millones de diabéticos.

Sin embargo, es una enfermedad que no puede evitarse en el caso de la DM tipo 1, y aunque la DM tipo 2 presenta un perfil hereditario, es cierto que existen ciertos factores que contribuyen a tener un mayor riesgo a desarrollarla, como son la edad, la obesidad y la falta de actividad física. Aunque un buen control de glucemia, de los

niveles de colesterol y de la tensión arterial pueden prevenir ciertas complicaciones, aquellas más importantes no pueden ser evitadas, pero sí se puede retrasar su aparición y su progreso.

A nivel ocular, la DM causa una serie de complicaciones, como son la catarata, glaucoma, queratopatía, cambios refractivos, parálisis de nervio oculomotor, inflamación crónica de los párpados, retinopatía diabética (RD) y edema macular diabético (EMD). Desde un punto de vista óptico, las estructuras involucradas en la potencia refractiva ocular y que pueden sufrir un deterioro en su calidad óptica son la película lagrimal, la córnea, el cristalino y el vítreo. Cada una de estas estructuras es vulnerable a cambios estructurales, morfológicos y fisiológicos causados por la DM.

En la práctica clínica, la valoración de la calidad óptica de los dioptrios oculares y de la imagen retiniana puede realizarse mediante las medidas de aberraciones y dispersión ocular. El ojo humano es un sistema óptica imperfecto, siendo la córnea y el cristalino las principales fuentes de aberraciones, cuyas imperfecciones causan una desviación de los rayos respecto a la trayectoria deseada, causando una degradación en la calidad de la imagen retiniana. Las aberraciones pueden clasificarse en aquellas de bajo y de alto orden, siendo éstas últimas las analizadas en esta Tesis Doctoral.

La dispersión intraocular es otro fenómeno que afecta a la imagen retiniana, y que se produce cuando la luz es reflejada, refractada, difractada o una combinación de las tres debido a variaciones del índice de refracción o a partículas presentes a lo largo de su trayectoria ocular. Cabe destacar que la dispersión intraocular puede dividirse en dispersión hacia adelante (en inglés, forward scattering) y hacia atrás (en inglés, backward scattering). En esta tesis la dispersión hacia atrás o retrodispersión ha sido utilizada para valorar la calidad óptica de la córnea. Cabe destacar que esta luz no llega a la retina, y por lo tanto no afecta a la calidad de la imagen retiniana, pero disminuye la cantidad de luz que llega a ésta.

Dado la alta prevalencia de esta enfermedad, que continúa en aumento a causa del envejecimiento de la población y de los hábitos de vida no saludables, y a su impacto en la sanidad debido a sus complicaciones y a su alta tasa de mortalidad, es de gran interés determinar una serie de métricas que nos permitan valorar la progresión de la enfermedad, además de llegar a ser útiles en métodos de screening mediante la detección precoz de signos oculares relacionados con la DM. Por lo tanto, sabiendo

todos los cambios que sufren las estructuras oculares debido a la DM, cómo pueden afectar tanto a la calidad óptica de sus estructuras como a la de la imagen retiniana y al desarrollo de instrumentos para valorar de una forma objetiva la calidad óptica del ojo, esta tesis está centrada en las complicaciones oculares producidas por la DM, además de cómo afectan a la calidad óptica tanto de los componentes oculares, como al resultado global que causan en la calidad de la imagen retiniana. Además, las complicaciones retinianas, como RD y el EMD, también han sido valoradas mediante la técnica de autofluorescencia de fondo de ojo, método que en el capítulo 5 se explica con detalle. Esta tesis tiene como objetivo principal explorar la utilidad de medidas no invasivas, tanto de calidad óptica como de autofluorescencia, que permitan el manejo y la detección temprana de complicaciones.

En el capítulo 2, se muestra el objetivo principal de esta Tesis, así como los objetivos de cada uno de los estudios llevados a cabo para confirmar dicha hipótesis.

El capítulo 3 se divide en dos medidas realizadas sobre córneas de pacientes diabéticos, en primer lugar, se evalúa el efecto que tiene la duración de la DM sobre dos parámetros estructurales corneales, como son la densidad endotelial y el espesor central en DM tipo 2, y en segundo lugar se valora la retrodispersión corneal en imágenes Scheimpflug mediante el desarrollo de una métrica con ayuda de un software médico llamado NIH ImageJ, tanto en pacientes diabéticos tipo 1 como tipo 2, y comparados con sujetos sanos.

Así, en la primera parte de este capítulo, se valoran las diferencias de densidad endotelial y espesor central corneal (ECC) entre pacientes diabéticos tipo 2 y sujetos control sanos emparejados por edad, y las posibles consecuencias que tiene la duración de la enfermedad sobre ambos parámetros.

Los resultados mostraron que el ECC era significativamente mayor y la densidad celular endotelial significativamente menor en pacientes diabéticos de larga duración (mínimo 10 años desde el diagnóstico) comparados con pacientes diabéticos recién diagnosticados (menos de un año desde el diagnóstico) y con los sujetos control. Ya que ambos grupos de pacientes diabéticos presentan un grupo control emparejado por edad, ambos parámetros corneales fueron comparados entre los dos grupos control y no hubo diferencias significativas para ningún parámetro. Además, mediante un análisis multivariado de varianza, se demostró que la duración de la diabetes tiene un efecto

significativo sobre el ECC y la densidad celular endotelial. Además, en pacientes diabéticos, se observó que el ECC era significativamente diferente para un valor de hemoglobina glucosilada (HbA1c) de 7.5%, y la densidad celular endotelial para los valores de 7.0% y 7.5% de HbA1c.

Por lo tanto, la diabetes tipo 2 altera de manera significativa la estructura y función corneal a largo plazo. Así, este estudio confirma el efecto que tiene la duración de la diabetes y el bajo control glicémico en los cambios de CCT y densidad endotelial.

En la segunda parte se determinó la calidad óptica de la córnea mediante retrodispersión corneal central con imágenes de Scheimpflug en pacientes diabéticos tipo 1 y tipo 2, y los resultados fueron comparados con sujetos sanos. Para ello, se realizó un análisis de imagen con NIH ImageJ de los sietes meridianos centrales y se determinaron dos regiones de estudio, los 3 mm y 5 mm centrales. Las medidas de retrodispersión corneal se realizaron en unidades de densidad óptica tras la correspondiente calibración de las imágenes en escala de grises a densidad óptica.

Los resultados de este estudio piloto mostraron que la retrodispersión corneal fue significativamente mayor en pacientes diabéticos para ambas zonas de estudio. Sin embargo, cuando estos valores fueron comparados entre diabéticos tipo 1 y tipo 2 no se encontraron diferencias significativas. En pacientes diabéticos tipo 2 ambas zonas de estudio, 3 mm y 5mm, estaban relacionadas con la edad y el ECC, mientras que estas correlaciones no fueron significativas para los diabéticos tipo 1. Además, mediante el test Krukall-Wallis se determinó que la presencia de DM tenía un efecto significativo sobre la retrodispersión corneal central.

Por lo tanto, según los resultados expuestos anteriormente, el análisis de densidad óptica corneal mediante las medidas de retrodispersión corneal podría ser una herramienta muy útil para el seguimiento y valoración de los cambios corneales causados por la DM.

En el capítulo 4 se examinó la calidad óptica del ojo completo mediante el análisis de la distribución de aberraciones de alto orden totales, corneales e internas, en pacientes diabéticos tipo 1 y tipo 2. En este estudio piloto, los pacientes diabéticos tipo 1 presentaban unos valores de aberraciones totales que fueron ligeramente mayores que los que mostraban los diabéticos tipo 2. Se observó que el coeficiente de Zernike más

predominante, y por lo tanto, que más contribuía al aumento de las aberraciones oculares totales, era el coma vertical interno para ambos grupos de diabéticos. En pacientes diabéticos tipo 1 las aberraciones totales estaban correlacionadas con la asfericidad posterior e inversamente correlacionadas con la edad. En diabéticos tipo 2, las aberraciones totales estaban correlacionadas con la edad y el ECC, e inversamente correlacionado con el volumen de cámara anterior.

Por lo tanto existen cambios en la cara posterior de la córnea y el cristalino que causan un aumento de las aberraciones totales, creando así una degradación de la imagen retiniana. De este modo, la medida de calidad óptica ocular podría ayudar al seguimiento de los cambios oculares causados por la DM.

En el capítulo 5 se muestra una revisión bibliográfica sobre el proceso de autofluorescencia, los fluoróforos endógenos oculares presentes en córnea, cristalino y epitelio pigmentario de la retina y la autofluorescencia ocular en DM. Centrándonos en la autofluorescencia de fondo de ojo, causada por los fluoróforos del epitelio pigmentario de la retina y que es la que atañe a esta Tesis, este capítulo además proporciona una revisión sobre los instrumentos disponibles en el mercado para la obtención de imágenes de fondo de ojo, sus diferencias en los principios básicos de cada uno de ellos, y también en la diferencias técnicas, como las longitudes de onda utilizadas para la excitación y detección, el proceso de adquisición de la imagen y los algoritmos usados en el procesado posterior de la imagen.

En el capítulo 6 se estudia la utilidad de las imágenes de autofluorescencia obtenidas con una cámara retiniana no midriática en la detección de la RD y el EMD. En primer lugar, se valoró la autofluorescencia de fondo y la función visual en pacientes diabéticos. Las imágenes de autofluorescencia fueron obtenidas con la cámara digital CR 2-Plus, y la función visual fue valorada con la medida de la función de sensibilidad al contraste. Cuestionarios como “Visual-Functionning Questionnaire-25” y “Diabetes Self-Management Questionnaire (DSMQ) fueron utilizados para valorar la calidad de vida y el autocontrol de la diabetes que presentaban los pacientes, además de un nuevo cuestionario que valora el riesgo de padecer diabetes basado en preguntas sobre el estilo de vida y antecedentes familiares.

Las imágenes fueron normalizadas y homogeneizadas utilizando MATLAB 2013b para mejorar la posible detección de alteraciones retinianas, y que fueron

denominadas como imágenes de autofluorescencia optimizadas. Se obtuvieron por lo tanto tres tipos de imagen del fondo de ojo por paciente, imagen en color, de autofluorescencia y de autofluorescencia optimizada.

En los resultados de este estudio piloto se observó que tanto las imágenes de autofluorescencia como las optimizadas mostraban un mayor número de alteraciones retinianas relacionadas con la RD cuando fueron comparadas con las imágenes en color. En los pacientes diabéticos se observaron signos compatibles con microaneurismas, dilataciones capilares y hemorragias, que fueron más numerosos en las imágenes de autofluorescencia, tanto en la no optimizada como en la optimizada, que en la imagen de color. En sujetos controles con riesgo a desarrollar DM se observó un mayor número de defectos del epitelio pigmentario de la retina que en sujetos sin riesgo de padecer dicha enfermedad, observados en menor cantidad en las imágenes en color. En relación a la función visual y a la calidad de vida no hubo diferencias entre pacientes diabéticos y sujetos control.

Por lo tanto, las imágenes de autofluorescencia y las de autofluorescencia optimizada muestran alteraciones relacionadas con la RD que no son observadas en las imágenes de fondo de ojo en color. Ambos tipos de imágenes de autofluorescencia podrían utilizarse como prueba complementaria para la detección precoz de alteraciones asociadas al desarrollo y progresión de la RD.

En segundo lugar, se valoró la capacidad de las imágenes de autofluorescencia en la detección del EMD. Para ello, se utilizó la misma cámara retiniana no midriática y se llevó a cabo el mismo procesamiento de imágenes con MATLAB 2013b. En una valoración cualitativa de las imágenes se observó que aquellos pacientes con EMD presentaban unas alteraciones hiperautofluorescentes en la zona macular compatibles con EMD.

Además, se realizó un análisis cuantitativo de la señal de autofluorescencia. Para ello, la zona macular fue dividida en tres zonas: fóvea, parafovea y perifovea. La señal de autofluorescencia fue medida en escala de grises. Los resultados del análisis cuantitativo mostraron que los pacientes diabéticos con EMD tenían mayores valores de autofluorescencia en todas las zonas estudiadas. La señal de autofluorescencia en la zona de la fóvea fue estadísticamente menor que las correspondientes a las zonas parafoveal y perifoveal. Además, los valores de autofluorescencia estaban

correlacionados con los niveles de HbA1c en pacientes diabéticos con EMD. Aunque se trata de un estudio piloto con una muestra reducida, los resultados muestran que las imágenes de autofluorescencia obtenidas con una cámara retiniana no midriática podrían llegar a ser una prueba complementaria para la valoración y seguimiento del EMD en pacientes diabéticos con RD.

En el capítulo 7 se muestra la discusión de la hipótesis inicial y de los objetivos establecidos en esta Tesis, en función de los resultados obtenidos en cada uno de los estudios realizados.

Finalmente en el capítulo 8 se reúnen las conclusiones generales, en función de lo expuesto en cada capítulo, así como las sugerencias para posibles estudios futuros.

CONTENTS

CHAPTER 1. INTRODUCTION 1

1.1 Definition and classification of Diabetes Mellitus 3

1.2 Epidemiology and Risk factors 6

1.3 Diagnosis and Glycaemic control 7

1.4 Ocular complications of Diabetes Mellitus 10

1.5 Refractive power of the eye and Diabetes Mellitus 13

1.5.1 Tear film 13

1.5.2 Cornea 15

1.5.3 Crystalline lens 18

1.5.4 Vitreous 20

1.6 Ocular optical quality in Diabetes Mellitus 22

1.6.1 Wavefront aberrations 22

1.6.2 Ocular scattering 27

CHAPTER 2. HYPOTHESIS AND OBJECTIVES 33

CHAPTER 3. CORNEA AND DIABETES MELLITUS 37

3.1 Quantitative corneal anatomy: evaluation of the effect of diabetes duration on the endothelial cell density and corneal thickness 39

3.2 Corneal backscatter in type 1 and type 2 diabetes mellitus patients 49

CHAPTER 4. OCULAR OPTICAL QUALITY AND DIABETES MELLITUS ..65

4.1 Total, corneal, and internal aberrations in type 1 and type 2 diabetes mellitus patients 67

CHAPTER 5. STATE-OF-THE-ART IN FUNDUS AUTOFLUORESCENCE IMAGING METHODS 81

5.1 Basic mechanism of autofluorescence 83

5.2 Ocular endogenous fluorophores 85

5.3 Corneal autoflurorescence in Diabetes Mellitus 91

5.4 Crystalline lens autofluorescence in Diabetes Mellitus 93

5.5 Fundus autofluorescence 95

5.5.1 Fundus autofluorescence imaging acquisition 95

5.5.2 Normal Fundus autofluorescence imaging 109

5.5.3 Fundus autofluorescence imaging in Diabetes Mellitus 110

CHAPTER 6. FUNDUS AUTOFLUORESCENCE IN DIABETES MELLITUS 115

6.1. Visual function and fundus autofluorescence assessment in diabetic patients 117

6.2. Diabetic macular oedema assessment by fundus autofluorescence analysis using a non-mydriatic retinal camera 134

CHAPTER 7. DISCUSSION 153

CHAPTER 8. CONCLUSIONS AND FUTURE WORK 163

REFERENCES 167

APPENDIX 1. PUBLICATIONS RESULTING FROM THE THESIS 205

APPENDIX 2. TABLE 6.1.3, TABLE 6.1.4 209

ACRONYMS

AAO: American Academy of Ophthalmology

ACD: Anterior Chamber Depth

ACV: Anterior Chamber Volume

ADA: American Diabetes Association

AGEs: Advanced Glycation End products

AF: Autofluorescence

AH: Asteroid Hyalosis

ANOVA: Analysis of Variance

AMD: Age-related Macular Degeneration

A2E: N-retinylidine-N-retininylethalonamin

A2PE: N-retinylidine N-retinyl Phospatidylethanolamine

B: overall blurring strength of spherocylindrical refraction error

BCVA: Best Corrected Visual Acuity

BMI: Body Mass Index

CCD: Charged Couple Device

CCT: Central Corneal Thickness

CH: Corneal Hysteresis

CI: Confidence Interval

CME: Cystoid Macular Oedema

CSF: Contrast Sensitivity Function

cpd: cycles per degree

cSLO: confocal Scanning Laser Ophthalmoscopy

CSME: Clinically Significant Macular Oedema

CV: Coefficient of Variation

DCCT: Diabetes Control and Complications Trials

DLS: Dynamic Light Scattering

DM: Diabetes Mellitus

DME: Diabetes Mellitus Oedema

DSMQ: Diabetes Self-Management Questionnaire

DOPA: Dihydroxyphenylalanine

DR: Diabetes Retinopathy

ECD: Endothelial Cell Density

ETDRS: Early Treatment Diabetic Retinopathy Study

FAD: Flavin Adenine Dinucleotide

FAF: Fundus Autofluorescence

FAM: Fundus Autofluorescence in age-related Macular degeneration

FMN: Flavin Mononucleotide

GA: Geographic Atrophy

GP: General Practitioner

GU: Grey level Units

HbA1c: Glycated Haemoglobin A1c

HDL: High-Density Lipoprotein

HNE: 4-Hydroxynoneual

HOAs: Higher-Order Aberrations

HRA: Heidelberg Retinal Angiography

IDDM: Insulin-Dependent Diabetes Mellitus

IDF: International Diabetes Federation

IFG: Impaired Fasting Glucose

IGT: Intolerance Glucose Tolerance

IRB: Institutional Review Board

IRMA: Intraretinal Microvascular Abnormalities

IVB: Intravitreal Injection of Bevacizumab

LADA: Latent Autoimmune Diabetes Mellitus

LASIK: Laser-Assisted In Situ Keratomileusis

LDL: Low-Density Lipoprotein

LOAs: Low-Order Aberrations

logMAR: logarithm of the minimum of angle resolution

LSDS: Light Scattering Detection System

LSI: Light Scattering Index

M: Mean spherical equivalent

MANOVA: Multivariate Analysis of Variance

MDA: Malondialdehyde

MODY: Maturity-Onset Diabetes Mellitus of the young

MPOD: Macular Pigment Optical Density

NAD: Nicotinamide Dinucleotide

NADP: Nicotinamide Dinucleotide Phosphate

NIDDM: Non-Insulin-Dependent Diabetes Mellitus

NPDR: Non-Proliferative Diabetic Retinopathy

NPDRS: Non-Proliferative Diabetic Retinopathy Severe

NVD: New Vessels near the optic Disc

NVE: New Vessels Elsewhere in the retina

NVI: New Vessels at level of Iris

OCT: Optical Coherence Tomography

o.d.u.: optical density units

OGTT: Oral Glucose Test Tolerance

OMCIAS: Oxford Modular Cataract Image Analysis System

PDR: Proliferative Diabetic Retinopathy

PE: Phospatidylethanolamine

PKC: Protein Kinasa C

Q: Asphericity

RcSLO: Rodenstock confocal Scanning Laser Ophthalmoscopy

RMS: Root Mean Square

RNFL: Retinal Nerve Fibre Layer

RPE: Retinal Pigment Epithelium

SD-OCT: Spectral-Domain Optical Coherence Tomography

TBUT: Tear Film Break-Up Time

TCSPC: Time-Correlated Single Photon Counting

T1DM: Type 1 Diabetes Mellitus

T2DM: Type 2 Diabetes Mellitus

UKPDS: United Kingdom Prospective Diabetes Study

UV: Ultraviolet

VA: Visual Acuity

VFQ-25: Visual-Functioning Questionnaire-25

VLDL: Very Low-Density Lipoprotein

WHO: World Health Organization

ZcSLO: Zeiss prototype SM confocal Scanning Laser Ophthalmoscopy

3-HGK: 3-Hydroxy-Kynurenine Glycoside

LIST OF TABLES

Table 1.1: Diagnosis of hyperglycaemia states according to WHO criteria (World Health Organization, 1999).

Table 1.2: International clinical diabetic retinopathy disease severity scale (American Academy of Ophthalmology Retina/Vitreous, 2016).

Table 1.3: International clinical diabetic macular oedema disease severity scale (American Academy of Ophthalmology Retina/Vitreous, 2016).

Table 3.1.1: Diabetic patients with age-matched healthy subjects. Mean (SD) values.

Table 3.2.1: Diabetic patients with age-matched normal subjects. Mean (SD) values.

Table 4.1.1: Demographic data of the diabetic groups.

Table 4.1.2: Total aberrations in T1DM and T2DM patients. Mean (SD) values.

Table 4.1.3: Internal aberrations in T1DM and T2DM patients. Mean (SD) values.

Table 4.1.4: Corneal aberrations in T1DM and T2DM patients. Mean (SD) values.

Table 5.1: Characteristics of ocular endogenous fluorophores.

Table 5.2: Technical characteristics of the commercially available cSLO devices.

Table 5.3: Technical characteristics of the commercially available conventional fundus cameras.

Table 6.1.1: Descriptive statistics and scoring of Visual Functioning Questionnaire-25 (VFQ-25) of the diabetic patients and control subjects. Mean (SD) values.

Table 6.1.2: Scoring of Diabetes Self-Management Questionnaire (DSMQ) in diabetic patients.

Table 6.2.1: Demographic data of diabetic patients with and without DR. Mean (SD) values.

Table 6.2.2: Demographic data of diabetic patients with and without DME. Mean (SD) values.

LIST OF FIGURES

Figure 1.1: Representation of first 28 Zernike polynomials ordered vertically by radial degree and horizontally by azimuthal degree (Pérez-Vives et al., 2010).

Figure 1.2: Schematic representation of the combination of ocular and corneal wavefront aberrations to estimate wavefront aberrations of internal optics (Pérez-Vives et al., 2010).

Figure 1.3: Wavefront aberration for 5 mm pupil diameter for the cornea, internal surfaces, and the whole eye. The internal surfaces aberrations compensate partially those present in the cornea (Artal, 2014).

Figure 1.4: Simulation of night vision in a patient with glare complaints due to a significant amount of ocular scattering (Pinero et al., 2010).

Figure 1.5: Schematic diagram showing sources of scattering in the human eye (Pinero et al., 2010).

Figure 3.1.1: Estimated marginal means of CCT at different cut-off values of HbA1c between short-term (circles) and long-term (squares) diabetic subjects. Error bars represent 95% CI.

Figure 3.1.2: Estimated marginal means of ECD at different cut-off values of HbA1c between short-term (circles) and long-term (squares) diabetic subjects. Error bars represent 95% CI.

Figure 3.2.1: Image processing using ImageJ (a. 8-bit image, pixels with value of zero are black and pixels with value 255 are white; b. 8-bit image with contrast-reverted; c. 8-bit image with contrast and pixel values reverted, pixels with value of zero are white and pixels with value 255 are black; d. Determination of central region of 3 mm; e. Determination of central region width; f. Outline of central region of 3 mm).

Figure 3.2.2: Mean of central corneal backscatter in both types of DM and control subjects for central 3 mm. Error bars represent 95% Confidence Interval (CI).

Figure 3.2.3: Mean of central corneal backscatter in both types of DM and control subjects for central 5 mm. Error bars represent 95% CI.

Figure 3.2.4: Correlation between corneal backscatter for central 3 mm and age in control subjects (squares and solid line; r = 0.062; p>0.05), T1DM (circles and dotted line; r = 0.523; p>0.05) and T2DM (crosses and dotted/dashed line; r = 0.604; p<0.05) patients.

Figure 3.2.5: Correlation between corneal backscatter for central 3 mm and CCT in control subjects (squares and solid line; r = 0.400; p>0.05), T1DM (circles and dotted line; r = -0.071; p>0.05) and T2DM (blades and dotted/dashed line; r = 0.641; p<0.05) patients.

Figure 3.2.6: Corneal images from Scheimpflug photography and corneal densitometry profile in diabetic patients and control age-matched. (a. T1DM patient; b. Control age-matched T1DM patient; c. T2DM patient; d. Control age-matched T2DM patient).

Figure 4.1.1: Correlations between total HOAs and age in T1DM patients (circles and solid line, r = -0.644; p=0.013) and T2DM patients (squares and dashed/dotted line, r = 0.821, p<0.001).

Figure 4.1.2: Correlation between total HOAs and posterior Q in T1DM patients (r = 0.754; p=0.002).

Figure 4.1.3: Correlation between age and total vertical coma (Z_3^{-1}) in T2DM patients (r = -0.782; p<0.001).

Figure 4.1.4: Correlations between age and internal vertical coma (Z_3^{-1}) in T2DM patients (r = -0.732; p<0.001).

Figure 4.1.5: Correlation between total vertical coma (Z_3^{-1}) and CCT in T2DM patients (r = -0.524; p=0.012).

Figure 5.1: Jablonski diagram illustrating the basic mechanism of fluorescence. Bold lines represent the limits of electronic energy states. Within each electronic energy states are represented several vibrational energy states (Calvo-Maroto et al., 2016a).

Figure 5.2: The visual cycle that represents several steps of lipofuscin metabolism and N-retinylidine-N-retinylethanolamin (A2E) formation (Calvo-Maroto et al., 2016b).

Figure 5.3: Schematic diagram of cSLO showing illumination and imaging paths (Calvo-Maroto et al., 2016a).

Figure 5.4: Central macular area in a healthy subject acquired with SPECTRALIS®. (Available at www.heidelbergengineering.com; Last accessed July 2016).

Figure 5.5: Schematic diagram of conventional fundus camera showing illumination and imaging paths (Calvo-Maroto et al., 2016a).

Figure 5.6: Central macular area in a healthy subject acquired with CR 2-Plus retinal camera. (Available at www.canon-europe.com; Last accessed July 2016).

Figure 5.7: FAF image in a healthy subject. Note the hypofluorescence in the macular area and the increased signal in parafoveal zone (Calvo-Maroto et al., 2016b).

Figure 6.1.1: Division of fundus images into four quadrants centred at the optic nerve.

Figure 6.1.2: CSF between diabetic patients (solid line) and control subjects (dashed/dotted line) ($p>0.05$).

Figure 6.1.3: CSF between control subject with (dashed/dotted line) and without (solid line) risk of undergo DM.

Figure 6.1.4: Colour fundus imaging (a), FAF imaging (b) and optimized-FAF (c) of 1: T1DM patient, diabetes duration 18 years; 2: T2DM patient, diabetes duration 30 years; 3: Control subject with risk of developing DM; 4: Control subject without risk of developing DM. Signs compatible with microaneurysms were represented by circles, capillary dilation by squares, haemorrhages by triangles, and hard exudates by rhombus.

Figure 6.2.1: Division of FAF images intro three concentric rings centred at the fovea. A: Foveal Zone; B: Parafoveal Zone; C: Perifoveal Zone.

Figure 6.2.2: Colour fundus imaging (a), FAF imaging (b), and homogenized and normalized FAF imaging (c) of (1) control subject; (2) diabetic patient without diabetic retinopathy; (3) diabetic patient with diabetic retinopathy but not diabetic macular oedema; (4) diabetic patient with diabetic macular oedema. Signs compatible with cystoid alteration were represented by circle form.

Figure 6.2.3: FAF signal measurements (GU) of macular zones (foveal, parafoveal, and perifoveal) in different groups of diabetic patients.

Figure 6.2.4: Correlations between FAF signal measurements in three macular zones and fasting glucose levels, in diabetic patients without DR. (Foveal: circles and solid line r = -0.685, p=0.014; Parafoveal: squares and dotted line r = -0.674, p=0.016; Perifoveal: crosses and dash-dot line r = -0.676, p=0.016).

Figure 6.2.5: Scatter diagram between FAF signal measurements in three macular zones and HbA1c levels, in diabetic patients with DME. (Foveal: circles; Parafoveal: squares; Perifoveal: crosses).

CHAPTER 1

Introduction

1.1 DEFINITION AND CLASSIFICATION OF DIABETES MELLITUS

Diabetes Mellitus (DM) is a clinical syndrome characterized by a disorder in the metabolism of carbohydrates, caused by a defect in insulin secretion, insulin action, or both. This disease is determined by a chronic hyperglycaemia associated with long-term damage of different organs, particularly eyes, kidneys, nerves, heart and blood vessels (American Diabetes Association, 2005; American Diabetes Association, 2010). In all cases, the development of the disease is attributed to a combination of predisposing genetic factors and a number of environmental factors that may act as triggers.

The most widely accepted classification divides DM in type 1, type 2, and gestational.

Type 1 DM (T1DM), is also known as insulin-dependent or juvenile-onset DM (IDDM). This form of the disease includes only 5-10% of those patients with DM (American Diabetes Association, 2010) and can be divided further into type 1A DM and type 1B DM (American Diabetes Association, 2005; American Diabetes Association, 2010; Conget, 2002).

Type 1A DM is due to a cellular-mediated autoimmune selective destruction of pancreatic β-cells mediated by activated T lymphocytes (known as latent autoimmune

DM of adult (LADA) or type 1.5). The rate of β-cells destruction is variable, being rapid in some individuals, mainly infants and children, and slow in others, mainly adults. Some patients, particularly children and adolescents, may present with ketoacidosis as the first manifestation of the disease; this condition is caused when body cannot produce enough insulin and start to break down fat as source of energy leading to a production of high levels of blood acids, called ketones, through the bloodstream. However, others patients show modest fasting hyperglycaemia that can rapidly change to severe hyperglycaemia and/or ketoacidosis in the presence of infection or other stress situations. This kind of diabetes commonly occurs in childhood and adolescence, but it can occur at any age, even in the 8^{th} and 9^{th} decades of life (American Diabetes Association, 2005; American Diabetes Association, 2010; Conget, 2002).

Autoimmune destruction of β-cells presents multiple genetic predispositions and is also related to environmental factors that are still poorly defined. Although patients are rarely obese when they present this type of diabetes, the presence of obesity is not incompatible with the diagnosis. These patients are also prone to other autoimmune disorder such as Grave's disease, Hashimoto's thyroiditis, Addison's disease, vitiligo, celiac sprue, autoimmune hepatitis, myasthenia gravis, and pernicious anaemia (American Diabetes Association, 2005; American Diabetes Association, 2010; Conget, 2002).

Type 1B or idiopathic DM are some forms of type 1 diabetes with aetiologies unknown, however, these patients have permanent insulinopenia and are prone to ketoacidosis with no evidence of autoimmunity. Patients with this form of diabetes undergo episodic ketoacidosis and exhibit varying degrees of insulin deficiency between episodes. This form of diabetes is strongly inherited, lacks immunological evidence for β-cell autoimmunity (American Diabetes Association, 2005; American Diabetes Association, 2010; Conget, 2002).

Both subtypes are treated with insulin (American Diabetes Association, 2005; American Diabetes Association, 2010; Conget, 2002).

The type 2 DM (T2DM) or noninsulin-dependent DM (NIDDM) affects about 90-95% of people with DM (American Diabetes Association, 2010). This type of DM may occur in genetically susceptible individuals with impaired insulin secretion, or with

insulin resistance and bad regulation of glucose production at the liver. Although the specific aetiologies are not known, autoimmune destruction of β-cells does not occur. Most patients with this form of diabetes are obese, and obesity itself causes some degree of insulin resistance. Patients who are not obese according to traditional weight criteria, they may have an increase percentage of body fat in the abdominal region. Ketoacidosis seldom occurs spontaneously in this type of diabetes. This form of diabetes frequently goes undiagnosed for many years due to the fact that hyperglycaemia develops gradually, and at earlier stages is often not severe enough for the patient to notice any of the classic symptoms of diabetes. These patients may have insulin levels that appear normal o elevated, but the higher blood glucose levels in these diabetic patients would result in higher insulin values, despite their β-cell function had been normal. Thus, insulin secretion is defective in these patients and insufficient to compensate for insulin resistance. Insulin resistance can be improved by weight loss and/or pharmacological treatment; although these patients do not develop ketoacidosis, they may suffer hyperglycaemic comma (American Diabetes Association, 2005; American Diabetes Association, 2010; Conget, 2002).

Gestational DM is characterized by a certain degree of insulin resistance that could be due to a combination of maternal adiposity and desensitizing effects of several substances produced by the placenta. Most of the cases usually resolve with childbirth (Vambergue and Fajardy, 2011).

There are other causes that can lead to the development of DM, such as genetic β-cell function defects. several forms of this type of DM are also known as maturity-onset DM of the young (MODY), characterized by the onset of hyperglycaemia before the age of 25 and autosomal-dominant inheritance, genetic defects in insulin action, diseases of the exocrine pancreas, endocrinopathies, drug-induced DM, infections, antibodies against insulin receptors, and specific diseases such as Down syndrome, Turner syndrome, Klinefelter syndrome, Wolfram syndrome, among others (American Diabetes Association, 2005; American Diabetes Association, 2010; Conget, 2002).

People with raised blood glucose levels that are not high enough for a diagnosis of diabetes are said to have impaired glucose tolerance (IGT) and impaired fasting glucose (IFG) (American Diabetes Association 2005; American Diabetes Association 2010; International Diabetes Federation, 2015). These conditions are sometime called

"pre-diabetes". The term IFG defines those individuals with fasting plasma glucose (FPG) between the upper limit of normal and the lower limit of diabetic FPG. And IGT refers to those individuals with a 2-hour post-load plasma glucose between the upper limit of normal and the lower limit of diabetic (Genuth et al., 2003). People with IGT are at increased risk of developing T2DM. IGT shares many characteristics with T2DM and is associated with advancing age and the inability of the body to use the insulin it produces (International Diabetes Federation, 2015). The International Diabetes Federation IFG/IGT Consensus Workshop concluded that IGT and IFG differ in their prevalence, population distribution, phenotype, sex distribution, and risk for total mortality and cardiovascular disease (Unwin et al., 2002).

Both pre-diabetic states are associated with glycaemic disturbances showing different metabolic processes with different prognostic consequences. Some evidences suggest that IGT is primarily associated with insulin resistance and IFG is associated with impaired insulin secretion and suppression of hepatic glucose output (Hassan et al., 2003). The magnitude of the risk for developing DM differs for these two metabolic states.

1.2 EPIDEMIOLOGY AND RISK FACTORS

Worldwide, DM is a disease with a great healthcare impact due to its increased prevalence and high mortality rate. A prospective study shows that, in developed countries there will be an 11% increase in the adult population, a 27% increase in the prevalence of adult DM and 42% increase in the number of people with DM between the years 1995 and 2015; while for developing countries there will be an 82% increase in the adult population, a 48% increase in the prevalence of adult DM and a 170% increase in the number of people with DM, between the years 1995 and 2025 (King et al., 1998).

According to the World Health Organization (WHO), by 2030 it may reach 366 million of people with DM in the world (Wild et al., 2004); however the International Diabetes Federation (IDF) states that the prevalence of DM will be 9.9% and the

number of people with DM will rise to 552 million people by 2030 (Whiting et al., 2011).

Currently, the number of people with diabetes worldwide is estimated in 415 million (6% of the worldwide population) according to IDF, due to population growth, aging, obesity increase and lack of physical activity. Approximately, there are 94.2 million people aged > 65 years with DM; however, there are 320.5 million working-age people with DM, aged 20 to 64 years, and therefore will have more years to develop chronic complications due to DM (International Diabetes Federation, 2015). The prevalence of DM is similar in men and women, but is slightly higher in men under 60 years of age and women over 60 years of age (Wild et al., 2004).

At present, T1DM cannot be prevented; although having a family member with T1DM, pancreas disease, exposure to some viral infections and increased mother´s age during pregnancy could contribute to its development (American Diabetes Association 2005; American Diabetes Association 2010; International Diabetes Federation, 2015).

Type 2 DM presents a pattern of family heritage but the risk of developing this form of DM increases with older age, ethnicity, obesity, lack of physical activity, genetics, poor nutrition, and past history of gestational diabetes (American Diabetes Association 2005; American Diabetes Association 2010; International Diabetes Federation, 2015) and polycystic ovary syndrome (Legro et al., 1999).

1.3 DIAGNOSIS AND GLYCAEMIC CONTROL

The criteria for the diagnosis of DM are shown in Table 1.1. Three ways to diagnose DM are possible, and each, in the absence of unequivocal hyperglycaemia, must be confirmed, on a subsequent day, by any one of the three methods given in Table 1.1.

- **Diabetes Mellitus**
1. **Fasting plasma glucose (FPG) ≥ 126mg/dl (7.0 mmol/l).** Fasting is defined as no caloric intake for at least 8h.
2. **Plasma glucose level ≥ 200mg/dl (11.1 mmol/l) after 2 hours of oral glucose test tolerance (OGTT).** The test should be performed with glucose load containing the equivalent of 75 g anhydrous glucose dissolved in water.
3. **Symptoms of hyperglycaemia and casual glucose levels ≥200mg/dl (11.1 mmol/l)*.** Casual is defined as any time of day without regard to time since last meal. The classic symptoms of diabetes include polyuria, polydipsia, and an unexplained weight loss.
- **Impaired glucose tolerance (IGT)**
OGTT values after 2h ≥ 140 mg/dl (7.8 mmol/l) and < 200 mg/dl (11.1 mmol/l)
- **Impaired fasting glucose (IFG)**
FPG ≥ 110 mg/dl (6.1 mmol/l) and < 126 mg/dl (7.0 mmol/l)

*In the absence of unequivocal hyperglycaemia, these criteria should be confirmed by repeat testing on a different day.

Table 1.1: Diagnosis of hyperglycaemia states according to WHO criteria (World Health Organization, 1999).

The diagnosis of DM can be established with situations similar at IDF and WHO institutions, although the use of glycated haemoglobin A1c (HbA1c) is the main difference between both diagnostic criteria, (because of it is not approved by WHO). HbA1c is a marker of chronic glycaemia, reflecting average blood glucose levels over a 2 to 3 months period of time. This test plays a critical role in the management of the patient with diabetes, since it correlates well with both microvascular and macrovascular complications, and is widely used as the standard biomarker for the adequacy of glycaemic management (American Diabetes Association, 2010). An International Expert Committee (2009) recommended the use of the HbA1c test to diagnose diabetes, with a threshold of $\geq 6.5\%$. The diagnostic HbA1c cut point of 6.5% is associated with an inflection point for retinopathy prevalence, as are the diagnostic thresholds for FPG and 2-h plasma glucose (International Expert Committee, 2009). The diagnostic test should be performed using a method that is certified by the National

Glycohaemoglobin Standardization Program and standardized to the Diabetes Control and Complications Trial reference assay.

In cases of gestational DM the criteria is FPG ≥ 95mg/dl (5.3 mmol/l), and when levels of glucose are ≥ 180mg/dl (10.0 mmol/l) or ≥ 155mg/dl (8.6 mmol/l) after 1 hour or 2 hours respectively, after an oral glucose load of 75 grams. When glucose load concentration used is 100 grams, the criteria for the diagnosis of gestational DM is established when glucose levels are ≥ 180mg/dl (10.0 mmol/l) after 1 hour, ≥ 155mg/dl (8.6 mmol/l) after 2 hours and ≥ 140mg/dl (7.8 mmol/l) after 3 hours (American Diabetes Association, 2010).

All major complications of diabetes are not inevitable, and they can be prevented by good glycaemic control, as well as good control of blood pressure and cholesterol levels. This requires a high educational level of people with diabetes in managing their condition, as well as access to insulin, oral medications and monitoring equipment. People with diabetes should be supported by a well-educated health work force as well as health systems that provide regular blood tests and eye and foot examinations (International Diabetes Federation, 2015).

A good glycaemic control can reduce morbidity and mortality from chronic complications derivated from diabetes and improve the quality of life of diabetic patients. Multicentre clinical trials, such as the Diabetes Control and Complications Trial (DCCT) and the United Kingdom Prospective Diabetes Study (UKPDS) have shown an association between the degree of hyperglycaemia and the increased risk of developing macrovascular and microvascular complications.

The DCCT was a multicentre, randomized clinical trial performed in T1DM patients. They examined whether intensive treatment, maintaining blood glucose concentrations close to the normal range, could decrease the frequency and severity of complications. After an average follow-up of 6.5 years, they concluded that intensive therapy reduced by 76% the development of diabetic retinopathy, by 54% that of nephropathy and by 60 % that of neuropathy compared with conventional therapy (The Diabetes Control and Complications Trial Research Group, 1993).

For the UKPDS study, T2DM patients from 23 centres across the UK were monitored for 10 years (UK Prospective Diabetes Study Group, 1998a). As well as the

DCCT study, they compared risk of developing complications between diabetic groups treated with conventional therapy, and with intensive therapy. The findings were similar to those the DCCT study. They confirmed that the predominant effect of intensive glucose control was a reduction of microvascular complications. They also observed a trend towards a reduction in macrovascular disease.

Further epidemiological analysis showed relation between glycaemic control and the risk of developing microvascular complications (UK Prospective Diabetes Study Group, 1998b; Stratton et al., 2000), so that each 1% reduction in HbA1c values was associated with a 37% decrease in risk for microvascular complications (Stratton et al., 2000). Thus, any reduction in HbA1c values is likely to reduce the risk of complications, with the lowest risk being in those with HbA1c values in the normal range (<6.0%).

1.4 OCULAR COMPLICATIONS OF DIABETES MELLITUS

DM is associated to the development of several complications within the eye, such as cataract (Ederer et al., 1981; Klein et al., 1985; Nielsen and Vinding, 1984) (2 to 4 times more than healthy people), glaucoma (Şahin et al., 2009), keratopathy (Inoue et al., 2001), refractive changes, oculomotor nerve paralysis, chronic inflammation of the eyelids, or diabetic retinopathy (DR) and diabetic macular oedema (DME) (American Academy of Ophthalmology, 2016; Williams et al., 2004).

DR is a leading cause of visual impairment in working-age adults. In patients with DM, some defects in neurosensory function have been demonstrated prior to the onset of vascular lesions. The most common early clinically visible manifestations of DR include microaneurysms formation and intraretinal haemorrhages. DR is characterized by microvascular damage leading to retinal capillary nonperfusion, cotton wool spots, increased numbers of haemorrhages, venous abnormalities and intraretinal microvascular abnormalities (IRMA) (American Academy of Ophthalmology Retina/Vitreous Panel, 2016).

According to the American Association of Ophthalmology (AAO) (American Academy of Ophthalmology Retina/Vitreous Panel, 2016), DR can be divided into two main stages: non-proliferative (NPDR) and proliferative (PDR) (Table 1.2).

NPDR is considered as the initial stage of the ocular disease and usually visual acuity (VA) is not seriously damaged. This stage can be subdivided in different stages according to disease severity (Table 1.2). The earliest ophthalmoscopic findings of DR usually are microaneurysms, although these stages are characterized by presence of intraretinal haemorrhages, venous dilation, and cotton-wool spots. At these or later stages, an increased retinal vascular permeability occurs and it may result in retinal thickening (oedema) and lipid deposits (hard exudates). Clinically significant macular oedema (CSME) is used to describe retinal thickening and/or adjacent hard exudates that either located on the centre of the macular or threaten to involve it. CSME can be divided into centre-involving macular and non-centre-involving macular oedema (American Academy of Ophthalmology Retina/Vitreous Panel, 2016).

As DR progresses, there is a gradual closure of retinal vessels resulting in an impaired perfusion and retinal ischemia. Some signs of this increasing ischemia include venous abnormalities, IRMA, and more severe and extensive vascular leakage characterized by increasing retinal haemorrhages and exudation (American Academy of Ophthalmology Retina/Vitreous Panel, 2016).

PDR is characterized by the onset of neovascularization at the inner surface of the retina induced by retinal ischemia. These new vessels can be originated on, or near the optic disc (NVD), or elsewhere in the retina (NVE), which may bleed into the vitreous, resulting in vitreous haemorrhage. These new vessels may undergo fibrosis and contraction; this and other fibrous proliferation may result in epiretinal membrane formation, vitreoretinal traction bands, retinal tears, and traction or rhegmatogenous retinal detachments (Table 1.2). The presence of severe ischemia produces the proliferation of new vessels at the level of anterior chamber structures such the iris (NVI) and trabeculum. Main consequence of this proliferation is neovascular glaucoma (American Academy of Ophthalmology Retina/Vitreous Panel, 2016).

Disease Severity Level	Findings observable upon dilated
No apparent retinopathy	No abnormalities
Mild NPDR	Microaneurysms only
Moderate NPDR	More than just microaneurysms but less than severe NPDR
Severe NPDR	Any of the following and no signs of proliferative retinopathy: - More than 20 intraretinal haemorrhages in each of four quadrants - Definite venous beading in two or more quadrants - Prominent IRMA in one or more quadrants
PDR	One of the following: - Neovascularization - Vitreous/preretinal haemorrhages

IRMA: intraretinal microvascular abnormalities; NPDR: nonproliferative diabetic retinopathy; PDR: proliferative diabetic retinopathy.

Table 1.2: International clinical diabetic retinopathy disease severity scale (American Academy of Ophthalmology Retina/Vitreous, 2016).

DME is one of the major complications of DR and also one of the leading causes of severe visual loss in working-age population (Klein et al., 1998; Klein et al., 2008; World Health Organization, 2005). Although DME may appear at any stage of DR (Lopes de Faria et al., 1999), around 12% of patients with DR develop DME (Paulus and Gariano, 2009). T1DM patients can develop DME within the first five years following diagnosis (White et al., 2010), however around 5% of T2DM patients already have DME at time of diagnosis (Gundogan et al., 2016). The prevalence rate of DME is associated with duration, type of diabetes, proteinuria, gender, cardiovascular disease, high levels of HbA1c and the use of diuretics (White et al., 2010). In addition to glycaemic control and regulation of hypertension and hyperlipidaemia, there are several ophthalmic treatments intended to resolve DME, such as focal/grid laser photocoagulation (ETDRS Research Group, 1987; Olk, 1986;), intravitreal injection of bevacizumab (IVB) (Haritoglou et al., 2006) or triamcinolone acetonide (Avitabile et al., 2005), and pars plana vitrectomy (Harbour and Smiddy, 1996).

According to the AAO (American Academy of Ophthalmology Retina/Vitreous Panel, 2016), Table 1.3 shows the international classification of DME.

Disease Severity Level	Findings observable upon dilated
DME apparently absent	No apparent retinal thickening or hard exudates in posterior pole
DME apparently present	Some apparent retinal thickening or hard exudates in posterior pole
If DME is present, it can be classified as follows:	
Disease Severity Level	**Findings observable upon dilated**
DME present	Mild DME: some retinal thickening or hard exudates in posterior pole but distant from the centre of the macula

DME: Diabetic macular oedema

Table 1.3: International clinical diabetic macular oedema disease severity scale (American Academy of Ophthalmology Retina/Vitreous, 2016).

1.5 REFRACTIVE POWER OF THE EYE AND DIABETES MELLITUS

From an optical perspective, the structures directly involved in the overall refractive power of the eye that might deteriorate its optical quality are the tear film, the cornea, the crystalline lens and the vitreous. All of them are susceptible of changing as a consequence of DM.

1.5.1 TEAR FILM

Due to the great impact of DM in the ocular surface and the fact that maintaining a normal ocular surface is essential for retinal image quality, changes in tear film with DM have been studied in detail over the recent decades (Cousen et al., 2001; Dogru et al., 2001; Figueroa-Ortiz et al., 2011; Goebbels, 2000; Grus et al., 2002; Herber et al., 2001; Ozdemir et al., 2003; Peponis et al., 2002; Peponis et al., 2004; Saito et al., 2003; Yoon et al., 2004).

Some ocular manifestations of DM are associated with lachrymal gland dysfunction and have been related to dry eye. Several clinical studies have demonstrated

that people with DM are more vulnerable to dry eye than healthy subjects (Cousen et al., 2001; Dogru et al., 2001; Figueroa-Ortiz et al., 2011; Goebbels, 2000).

In people with DM, the most frequent and measurable alterations of the tear film function are reduced tear secretion (Cousen et al., 2001; Dogru et al., 2001; Figueroa-Ortiz et al., 2011; Goebbels, 2000; Ozdemir et al., 2003; Saito et al., 2003; Yoon, et al., 2004), tear film instability (tear film break-up time (TBUT)) (Dogru et al., 2001; Figueroa-Ortiz et al., 2011; Ozdemir et al., 2003; Yoon et al., 2004), higher degree of conjunctival squamous metaplasia (Dogru et al., 2001; Figueroa-Ortiz et al., 2011; Goebbels, 2000; Yoon et al., 2004), lower globet cell density (Dogru et al., 2001; Yoon et al., 2004) and reduced corneal sensitivity (Cousen et al., 2001; Dogru et al., 2001; Saito et al., 2003; Yoon et al., 2004).

Although the exact mechanisms of these changes in the ocular surface with DM are still unclear, some studies suggest that diabetic neuropathy affects the innervation of the lachrymal gland and that the fluctuation in the glycaemic control could affect the ocular surface and lachrymal gland secretory function, causing a decrease in basal tear secretion and TBUT (Dogru et al., 2001; Ozdemir et al., 2003; Yoon et al., 2004). However, other studies showed that basal tear secretion and TBUT values do not change but total and reflex tear secretions are significantly reduced in subjects with DM, suggesting that the decreased reflex tearing is due to a diminished sensitivity in cornea and conjunctiva (Goebbels, 2000; Saito et al., 2003).

Usually the aforementioned findings are accompanied by globet cell loss and conjunctival squamous metaplasia. Goebbels (2000) suggested that a decrease in tear secretion together with a disturbed trophic function of the tear film, such as vitamin A and epithelial growth factors, might cause chronic conjunctival damage leading to conjunctival metaplasia. Dogru et al. (2001), showed however that the conjunctival metaplasia was due to a loss of neurotrophic effects as a result of corneal hypoesthesia, glucose level fluctuation and metabolic control insufficiency.

DM is often associated with increased oxidative stress and free radical production (Peponis et al., 2002; Peponis et al., 2004), which may damage epithelial tissues such as the conjunctiva and the lachrymal glands. As the tear film is rich in several antioxidants such as ascorbic acid (vitamin C), found in high concentrations in the eye, Peponis et al. (2002) demonstrated that orally administered antioxidant

supplements for a period of 10 days improved the tear film stability and secretion, and the antioxidant properties of vitamins C and E could protect the ocular surface from the attack of free radicals and preserve the integrity of the epithelium.

According to the tear composition in subjects with DM, some studies have shown significant differences compared to healthy subjects, as the number of peaks in diabetic tear protein is significantly higher compared to tear protein patterns of nondiabetic subjects (Grus et al., 2002; Herber et al., 2001). This could be the result of glycosylation of tear proteins that often leads to changes in the protein structure that may influence protein function (Herber et al., 2001). Moreover, Grus et al. (2002) observed differences in protein patterns in the molecular weight range of 30-50 kDa, although they could not identify one single peak that was present in all diabetic patients. These proteins were not observed in healthy subjects and could be decisive therefore in the pathogenesis of DM and/or the development of eye-related complications of diabetic disease.

1.5.2 CORNEA

DM has important effects on every corneal structure and shows significant and characteristic signs, such as epithelial defects, recurrent epithelial erosions, delayed reepithelization, slower wound repair, increased epithelial fragility, reduced sensitivity, increased autofluorescence (AF), altered epithelial and endothelial barrier functions, ulcers, oedema and increased susceptibility to injury (Herse, 1988; Sánchez-Thorin, 1998), all of these affecting morphological, metabolic, physiological, and clinical aspects of the cornea. All these signs are included within the term “diabetic keratopathy” and are present in more than 70% of the people with DM (Quadrado et al., 2006).

The corneal epithelium acts as a diffusion barrier that avoids the penetration of polarized substances such as water or ions and participates in maintaining the dehydrated state of the corneal stroma (Göbbels et al., 1989). Some studies with fluorophotometry show this barrier function is weakened in DM leading to an increase in permeability to fluorescein (Göbbels et al., 1989; Ljubimov et al., 1998).

The corneal epithelium in patients with DM exhibits alterations in both cellular components and basal membrane, which could impair the physiology of the corneal epithelial barrier function (Rehany et al., 2000) and cause the cornea to be more vulnerable to foreign pathogens such as bacteria and fungi.

The abnormalities observed in corneal epithelial cells include a decrease in the number of cells, bullae, polymorphism, polymegathism, changes in the cellular coefficient of variation (Sánchez-Thorin, 1998), an accumulation of glycogen granules and areas of epithelial cell degeneration (Rehany et al., 2000). Although the cause of theses abnormalities is not clear, some studies suggested that these disorders may be due to altered basal membrane structure and/or epithelial integrin expression (Herse, 1988; Ljubimov et al., 1998), increased glycosylation of type IV collagen (Rehany et al., 2000) and fibronectin, abnormal regulation of the synthesis of extracellular matrix, increased in type IV collagen and decreased laminin (Ljubimov et al., 1998) and heparin sulphate (Sánchez-Thorin, 1998).

As far as epithelial basal membrane alteration is concerned, people with DM show an accumulation of fibrillar and granular material between the epithelial cells and Bowman´s membrane, thickening and multilayering of the basal membrane (Friend and Thoft, 1984; Rehany et al., 2000) and accumulation of advanced glycation end products (AGEs) (Gekka et al., 2004). Despite this, Quadrado et al. (2006) found that basal membrane in DM was lower in density compared to healthy subjects, and they suggested that this could be a result of the combination of different mechanisms, such as decreased innervation at the subbasal nerve plexus, basal membrane alterations, and higher turnover rate in basal epithelial cells.

These disorders are associated with alterations in the basal membrane anchoring complex (anchoring fibrils, anchoring plaques, basal lamina and hemidesmosomes) (Friend and Thoft, 1984; Herse, 1988; Sánchez-Thorin, 1998) resulting in a critical adherence of the basal membrane to the corneal stroma, causing delayed epithelial healing rates and epithelial instability (Herse, 1988; Ljubimov et al., 1998; Sánchez-Thorin, 1998).

With regards to corneal stroma, Rehany et al. (2000) observed that stromal keratocytes contain vacuoles of lipids and prominent endoplasmic reticulum, and in DM both stroma and Descemet´s membrane are loaded with randomly distributed aggregates

of normally spaced collagen fibrils. Also, wrinkles in Descemet`s membrane may occur, and may be considered as a sign of increased corneal hydration (Busted et al., 1981).

The maintenance of a relative degree of dehydration of the strongly hydrophilic stroma is mainly due to the action of fluid barrier and pumping mechanisms in the corneal epithelium and endothelium (Sánchez-Thorin, 1998). Although this dehydration state is essential for corneal transparency and thickness, in the corneal endothelium of subjects with DM, hyperglycaemia can inhibit Na^+/K^+-ATPase activity, and therefore corneal hydration (McNamara et al., 1998) and corneal thickness will increase affecting corneal transparency.

Some researchers indicate that corneas of patients with DM have a tendency to present greater central corneal thickness (CCT). Roszkowska et al. (1999) reported significantly increased CCT values in people with T2DM compared to non-diabetic subjects. Inoue et al. (2002), however, reported that people with T2DM have damaged corneal endothelial structure but found similar CCT values compared to non-diabetic subjects (Choo et al., 2010; Schultz et al., 1984). In people with T1DM, Schultz et al. (1984) observed similar CCT values to those of healthy subjects, while Roszkowska et al. (1999) found a significant increase in T1DM patients.

Aldose reductase in the corneal endothelium and the osmotic stress that occurs secondary to sorbitol accumulation could recur periodically over the life of people with DM and lead to altered endothelial morphology and cell loss. In diabetic corneas, endothelial cells show morphological abnormalities such as a high coefficient of variation of cell area and a decrease in the percentage of hexagonal cells (Choo et al., 2010; Herse, 1988; Inoue et al., 2002; Roszkowska et al., 1999; Sánchez-Thorin, 1998; Schultz et al., 1984). Although there are many reports about corneal endothelium in people with DM, the results remain controversial. Inoue et al. (2002) found a decrease of 4.1% in endothelial cell density (ECD) in patients with T2DM and a higher coefficient of variation of cell area but did not observe a decrease in percentage of hexagonal cells. Despite these results, there are also some studies reporting that the ECD in patients with T2DM is similar to that found in healthy subjects (Quadrado et al., 2006; Schultz et al., 1984).

Regarding endothelial cell hexagonality loss (pleomorphism), some authors reported a decrease in percentage of hexagonal cells (Roszkowska et al., 1999; Schultz et al., 1984).

A number of studies have shown that people with DM have decreased corneal sensitivity (Cousen et al., 2007; Dogru et al., 2001; Friend and Thoft, 1984; Herse, 1988; Saito et al., 2003; Sánchez-Thorin, 1998; Yoon et al., 2004), making them more vulnerable to corneal trauma. Thickening and thinning of Schwann cell basal lamina, irregular distribution in the nerve beading pattern, and occasional axonal degeneration of the nonmyelinated corneal nerves have been found in people with DM (Sánchez-Thorin, 1998). Dogru et al. (2001) suggested that keratopathy and corneal neuropathy might be manifestations of distal peripheral neuropathy of DM and proposed that changes of intraneural concentration of myoinositols and increased sorbitol levels within the Schwann cell basal lamina could be responsible for either mechanical compression or toxic axonal damage. McNamara et al. (1998) showed reduced corneal sensitivity during episodes of hyperglycaemia as a consequence of changes in corneal hydration control.

1.5.3 CRYSTALLINE LENS

People with DM often complain of discomfort in certain activities, such as reading or driving, and blurred vision with their own glasses. In patients with DM, a rapid reduction in blood glucose could cause an aggravation of both retinopathy status and refractive changes and so that, VA often decreases. Refractive changes occur frequently in people with DM and can be either acute or long-term.

Regarding long-term changes, Duke-Elder in 1925 described that hyperglycaemia led to the development of myopia, while relative hypoglycaemia respect to initial hyperglycaemia state, led to hyperopic changes. Qwinup and Villareal (1976) supported his theory 50 years later, both in acute and chronic changes; and demonstrated that the hyperopic changes are mainly due to the lens.

As for the acute changes, a reduction of plasma glucose levels leads to hyperopic refractive changes, and hyperglycaemia causes variations in the refractive index of the lens in people with DM (Okamoto et al., 2000; Saito et al., 1993) that may lead to

transient cataract development. However, it has been also reported that hyperopic changes occur with plasma glucose level, regardless of whether it was increased or decreased (Eva et al., 1982). The underlying mechanism of the relation between plasma glucose concentration and refractive changes in subjects with DM remains therefore to be established.

A possible hypothesis to explain what happens in the crystalline lens during transient hyperopic changes in people with DM could be that when the body rapidly changes from a hyperglycaemic to a hypoglycaemic state, an excess of glucose accumulated in the lens flows out into the aqueous humour and freely enters the intracellular space, but sorbitol (less permeable) remains in the lens for a longer time (Gabbay, 1973). This process causes a difference in osmotic pressure leading to an influx of water from the aqueous humour into the crystalline lens, and therefore the lens becomes thicker with hyperopic refractive changes (Okamoto et al., 2000).

Some researchers support this hypothesis, like Saito et al. (1993), who found that the lens thickness increased and the anterior chamber depth decreased significantly during transient hyperopia in ten eyes of five patients with DM. Other researchers, however, observed that the lens thickness did not increase significantly and the anterior chamber depth did not decrease significantly during hyperopic changes, explaining why this hypothesis cannot be confirmed without knowing the effects of each of these contributing factors in the power of the lens (thickness, curvature of anterior and posterior surfaces, refractive index of the aqueous humour lens and vitreous body), as an increase in lens thickness resulted in myopic changes by reducing the radius of curvature (Okamoto et al., 2000).

The human lens continues to grow throughout life due to the addition of new fibres, becoming thicker and more convex; in addition, the refractive index of crystalline lens undergoes changes due to ageing and cataract development. In patients with DM the lens has been found thicker and more convex compared to healthy subjects (Bron et al., 1993; Løgstrup et al., 1996; Sparrow et al., 1992a). Wiemer et al. (2008a) observed an increase in the average lens thickness of 0.2 mm and a significant decrease in equivalent refractive index with age in both diabetic patients and control subjects, the greater decrease corresponding however, to patients with T1DM. The fact that crystalline lens is thicker in people with DM might be due not only to an abnormality in

the growth of the lens, greater cortical thickness, or osmotic swelling, but also as a result of an increase in cell membrane permeability or deficiency in the ions pump (Wiemer et al., 2008b).

Sparrow et al. (1990) found that in people with T1DM the duration of the condition had a determining power on the biometry of the lens, a finding corroborated by Wiemer et al. (2008a), who also found that T2DM had no effect on the lens thickness, shape or equivalent refractive index.

1.5.4 VITREOUS

The vitreous is a hydrated gel matrix composed of a complex network of cross-linked collagen (types II, V, IX and XI), fibrils and the hydrophilic glycosaminoglycan, hyaluran. With aging or disease development, vitreous gel may undergo liquefaction due to biochemical and physiological changes that cause dissociation of collagen and hyaluran. Many of these disorders manifest as opacities in an optical structure that is normally transparent.

Patients with DM experience vitreous degeneration earlier than those without DM (Stitt et al., 1998), such as asteroid hyalosis (AH), a degenerative process resulting in small, white vitreous opacities consisting of calcium phosphate and complex layered lipid deposits. The prevalence of this condition in the general population is 1.2% (Moss et al., 2001), affecting all races with a male to female ratio of 2:1 (Akram et al., 2003) and associated with age. AH is unilateral in the 75% cases (Akram et al., 2003). Although its aetiology is still not clear, a significant association between AH and DM has been reported (Akram et al., 2003), although Moss et al. (2001) found no evidence to suggest a relationship between HA and DM, remaining therefore controversial.

Hyperglycaemia may play a direct role in vitreous pathology by altering the structure and function of the collagen network through increased glycation (non-enzymatic glycosylation) and abnormal cross-linking of the collagen fibrils, resulting in vitreous destabilization (Lundquist and Österlin, 1994; Stitt et al., 1998). Lundquist and Österlin (1994) showed that whereas the glucose level in the vitreous is generally lower than in the blood, in people with DM it will reach levels that might increase the

glycation rate, which might in turn lead to the formation of cross-links in the vitreous collagen.

Increased AGEs in serum and tissues is a characteristic of DM and may have an important role in the destabilization, premature liquefaction, and complicated posterior vitreous detachment (Stitt et al., 1998). The vitreous in people with DM manifests changes in angiogenic and metabolic factors concordant with abnormalities in the retinal microvasculature occurring in the pathogenesis of DR. Retinal neovascularization occurs toward the vitreous cavity, with microproliferation and migration of cells onto the posterior vitreous cortex (Cohen et al., 2008). As disease progresses, angiogenic factors that induce the growth of new retinal blood vessels (neovascularization) are secreted (Schwartzman et al., 2010). Yokoi et al. (2007) found that the vitreous levels of AGEs and vascular endothelial growth factor (VEGF) correlate with each other, both of which are inversely associated with vitreous total antioxidant capacity in patients with DR. Kinnunen et al. (2009) showed differences in growth factor expression between people with T1DM and T2DM with retinopathy, while VEGF-A was most abundantly present in T1DM patients, and VEGF-D was more copious in the neovascular tissues of patients with T2DM. They suggested the possibility that an inflammatory mechanism accelerates proliferative retinopathy in T2DM, by VEGF-D-dependent pathways, and T1DM hypoxia is more important in the development of proliferative retinopathy than inflammation. This difference in growth factor expression might contribute to the pathogenesis of both forms of the disease.

These abnormalities of diabetic vitreous would produce traction upon the structures attached to the vitreous cortex, such as the new vessels present in PDR, and contribute to the progression of retinopathy by either traction on the new vessels or induction of new vessels rupture, thus causing a vitreous haemorrhage (Sebag, 1993).

1.6 OCULAR OPTICAL QUALITY IN DIABETES MELLITUS

Nowadays, the objective assessment of the optical quality of the eye is of great interest in clinical practice. The optical system of the eye has some limitations due to its shape and the composition of its media. Ocular diffraction, aberrations and scattering influence intraocular retinal image quality, therefore affecting the visual performance of the subject. In human eyes, it is possible to improve image quality by minimizing aberrations and ocular scattering; but it is impossible to exceed the limits of image quality due to diffraction. Both aberrations and ocular scattering, and therefore optical quality of the retinal image, are affected by DM.

1.6.1 WAVEFRONT ABERRATIONS

The human eye is an optical system that has several optical elements whose aim is to focus light rays for representing images onto the retina. However, these components and materials present imperfections that may cause light rays to deviate from the desired path. These deviations result in blurred images and degradation of retinal image quality (Schwiegerling, 2000).

The imperfections of ocular components are measured and represented as wavefront aberrations. The deviation of a wavefront in an optical system from a desired perfect planar wavefront is called the wavefront aberration and is commonly represented by Zernike polynomials (International Organization for Standardization, 2008) (Figure 1.1). Zernike polynomials are a sets of functions that are orthogonal in a continuous mode over the interior of a unit circle (Lombardo et al., 2010). Several different normalization and numbering schemes for these polynomials are in common use (Thibos et al., 2000).

Wavefront aberrations can be further classified based on their order as lower or higher order aberrations. Low-order aberrations (LOAs) extend from the zero to second order, while higher-order aberrations (HOAs) are all those above the second order. LOAs are the predominant optical aberration in optics components of the human eye,

accounting for approximately 90% of the total ocular aberrations. Their correction with spectacles, contact lenses or corneal laser surgery significantly improves vision in most cases. Although HOAs make a small contribution (≤10%) to the overall wavefront aberrations of the eye (Lombardo et al., 2010), some authors have shown a large effect of degradation in the quality of the retinal image and able to affect VA (Applegate et al., 2003).

However, not all Zernike polynomials induce equivalent losses in high and low contrast VA. Zernike polynomials located near the centre of the pyramid adversely affects VA more than those located near the edge of the pyramid (Figure 1.1). Thus, large changes in chart appearance are not reflected in equally large decreases in visual performance (Applegate et al., 2002).

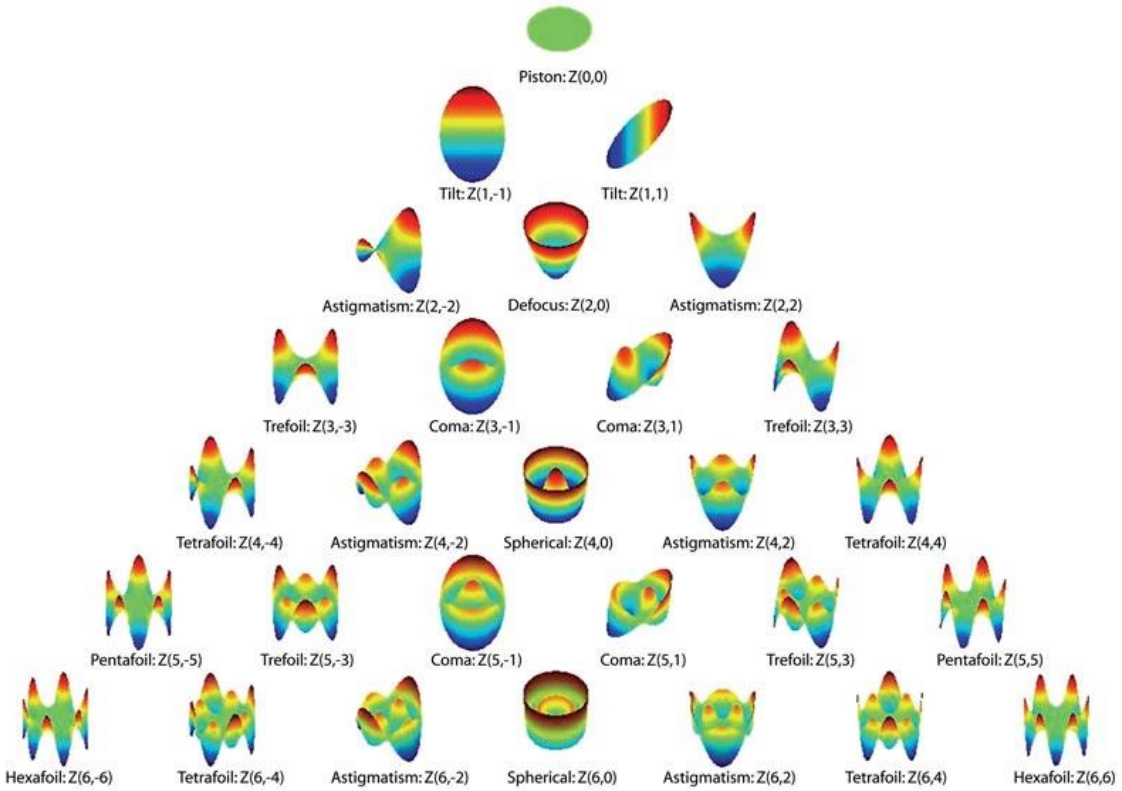

Figure 1.1: Representation of first 28 Zernike polynomials ordered vertically by radial degree and horizontally by azimuthal degree (Pérez-Vives et al., 2010).

Aberrations vary greatly from one individual to another, and these variations have been studied by several authors in large populations of normal subjects (Castejón-Mochón et al., 2002; Howland and Howland, 1977; Liang and Williams, 1997; Porter et al., 2001; Thibos et al., 2002). All authors concluded that there is a high inter-subject variability, although many aberrations showed a good correlation from right and left eye. Beyond defocus and astigmatism, spherical aberration, coma and trefoil are the most significant aberrations in normal eyes.

As previously mentioned, the human eye is constituted by different structures that contribute to overall ocular wavefront aberrations. Mainly, the sources of these aberrations are those induced by the anterior surface of the cornea and by the internal optics of the eye (Figure 1.2). The aberrations associated with the anterior surface of the cornea can be measured by corneal topographers, and the aberrations of the complete eye by several subjective and objective techniques, such as the Hartmann-Shack wavefront sensor. As wavefront aberrations of the whole eye and of the cornea can be easily measured, the relative contributions of the different ocular surfaces to retinal image quality can be evaluated. In particular, the wavefront aberrations of the internal ocular optics are estimated simply by directly subtracting the corneal from the ocular aberrations (Figure 1.2).

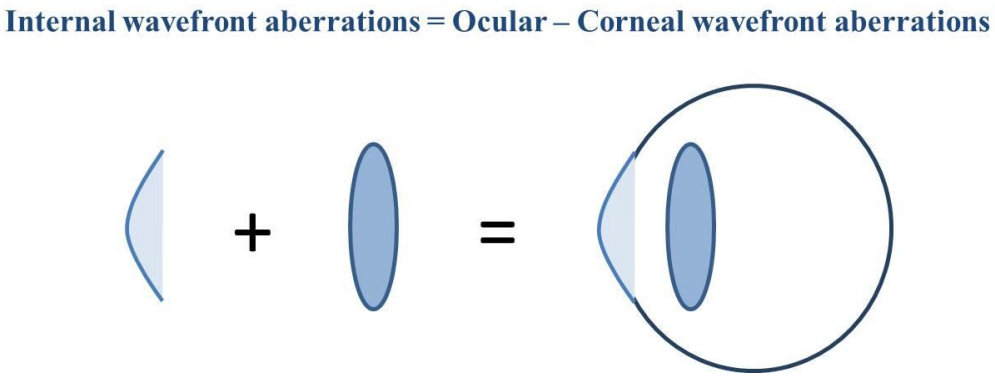

Figure 1.2: Schematic representation of the combination of ocular and corneal wavefront aberrations to estimate wavefront aberrations of internal optics (Pérez-Vives et al., 2010).

The relative contribution of corneal and internal optics wavefront has been evaluated in several studies (Artal and Guirao 1998; Artal et al., 2001; Artal et al., 2002; He et al., 2003). In these studies, the authors observed that the amount of wavefront aberrations of cornea and internal optics taken separately were larger than for the complete eye. Smith et al. (2001) observed that relaxed crystalline lens has negative spherical aberration, approximately the same level as the positive values of the anterior corneal surface. Therefore, these findings show that the internal optics may play a significant role in compensating for the corneal aberrations in normal young eyes (Figure 1.3). However, this compensation was not present for older subjects, due to optics degradation with ageing.

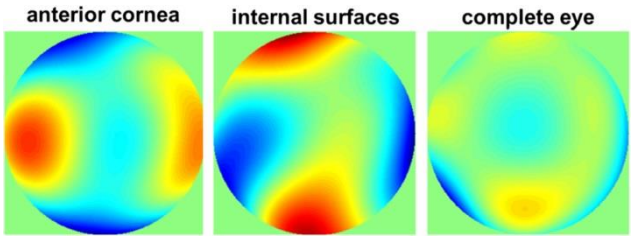

Figure 1.3: Wavefront aberration for 5 mm pupil diameter for the cornea, internal surfaces, and the whole eye. The internal surfaces aberrations compensate partially those present in the cornea (Artal, 2014).

However, there are several factors such as ageing (Artal et al., 1993; Artal et al., 2003; Glasser and Campbell, 1999; Guirao et al., 1999; Shahidi and Yang, 2004), accommodation (Cheng et al., 2004), photoreceptors (Shahidi and Yang, 2004), pupil size (Castejón-Mochón et al., 2002; Guirao and Artal, 2000; Liang and Williams, 1997; Liang et al., 1997; Lombardo and Lombardo, 2010), refractive surgery (Artal et al., 2003; Marcos et al., 2001; Moreno-Barriuso et al., 2001; Oshika et al., 1999), and tear film (Montés-Micó et al., 2004a; Montés-Micó et al., 2004b), that may contribute to the change in aberrations and therefore influence into the compensation process.

Ocular wavefront aberrations in DM

As previously mentioned, people with DM have a series of morphological, structural, metabolic and physiological changes in different ocular structures. Although there are a few studies that related these changes with the impact on visual quality (Shahidi et al., 2004; Wiemer et al., 2009), people with DM undergo variations in blood glucose levels causing changes in spherical and cylindrical components of refraction (LOAs), both acute and long-term. With reference to HOAs, it is well known that they have an important negative effect over the retinal image, although there are not studies evaluating the impact that these factors could have on HOAs in people with DM. People with DM have a thicker and more convex crystalline lens (Bron et al., 1993; Løgstrup et al., 1996; Sparrow et al., 1992a), can develop premature cataracts (Ederer et al., 1981; Klein et al., 1985; Nielsen and Vinding, 1984), undergo a series of changes associated with lachrymal gland dysfunction and dry eye (Cousen et al., 2007; Dogru et al., 2001; Figueroa-Ortiz et al., 2011; Goebbels, 2000; Grus et al., 2002; Herber et al., 2001; Ozdemir et al., 2003; Peponis et al., 2002; Peponis et al., 2004; Saito et al., 2003; Yoon et al., 2004). Furthermore, patients with DM who undergo laser-assisted in situ keratomileusis (LASIK) are also at a significantly higher risk of developing postoperative epithelial complications and refractive results tend to be worse compared with healthy people (Fraunfelder and Rich, 2002).

Few authors have investigated HOAs in people with DM. Shahidi et al. (2004) found that HOAs were increased in their 22 chronic patients with DM and suggested that the presence of increased ocular aberrations were caused by disease-related changes in the optics (cornea and crystalline lens), although they did not provide information about the relative contribution of these optical components to the total amount of aberrations measured.

Wiemer et al. (2009) measured HOAs, as well as the shape of the cornea and the lens in 25 patients with DM (15 patients with T1DM, 10 patients with T2DM) during the presence and absence of hyperglycaemia and blurred vision. They observed that only 4 patients presented a significant increase in HOAs (mean increase in root mean square (RMS) error: 0.07μm for a 5mm pupil diameter). Although this increase in HOAs might reduce VA (Applegate et al., 2003), they did not detect changes in visual performance. They suggested that symptoms of blurred vision due to hyperglycaemia

should be attributed to other factors such as the cerebral cortex or the retina, which might cause subjective symptoms of blurred vision, or that more serious and long-lasting hyperglycaemia would be needed to induce changes in ocular structures large enough to increase aberrations to a level that produces blurred vision (Shahidi et al., 2004).

1.6.2 OCULAR SCATTERING

Scattering is defined as the physical phenomenon inherent to light propagation through different ocular structures that is characterized by refractive index variations or inhomogeneities on a microscopic scale, specifically on the scale of the order of the wavelength of light (Van de Hulst, 1981). Scattering causes the light rays to spread over much larger angles compared to wavefront aberrations, leading to blur and defocus, and as a consequence, a degradation of retinal quality imaging (Figure 1.4) (van den Berg, 1995; van den Berg et al., 2009).

Ocular scattering can be divided in forward and backward scattering. The first one represents the scattered light that reaches the retina with the potential of inducing veiling illuminance superimposed on the retinal image reducing retinal contrast (de Waard et al., 1992). The second one defines the light that does not reach the retina, decreasing the amount of light on the retina. Due to backscattered light from the transparent ocular structures, these can be observed by several devices, such as slit-lamp or Scheimpflug imaging. Thus, ocular backscattering is typically used to assess the quality of tissues (McCally et al., 2007; Patel et al., 2007).

Figure 1.4: Simulation of night vision in a patient with glare complaints due to a significant amount of ocular scattering (Pinero et al., 2010).

In a normal healthy eye, each optical component may cause light deviations from the ideal trajectories as a consequence of inhomogeneities or non-uniformities in the propagation media. These optical components include both refractive elements of the eye (cornea and crystalline lens), the media in which they are immersed (vitreous and aqueous humour) and the supporting structures (sclera and iris) (Figure 1.5).

The cornea (Olsen, 1982; Patel et al., 2007; Smith et al., 1990) and crystalline lens (van den Berg and Spekreijse, 1999) are sources of back and forward scattering, especially when their transparency has been significantly affected, such as in patients with cataract (de Waard et al., 1992) and corneal haze (Braunstein et al., 1996).

Vitreous and aqueous humours are also sources of scatter light when their transparency may be severely affected, such as posterior uveitis or retinal haemorrhages (Pinero et al., 2010).

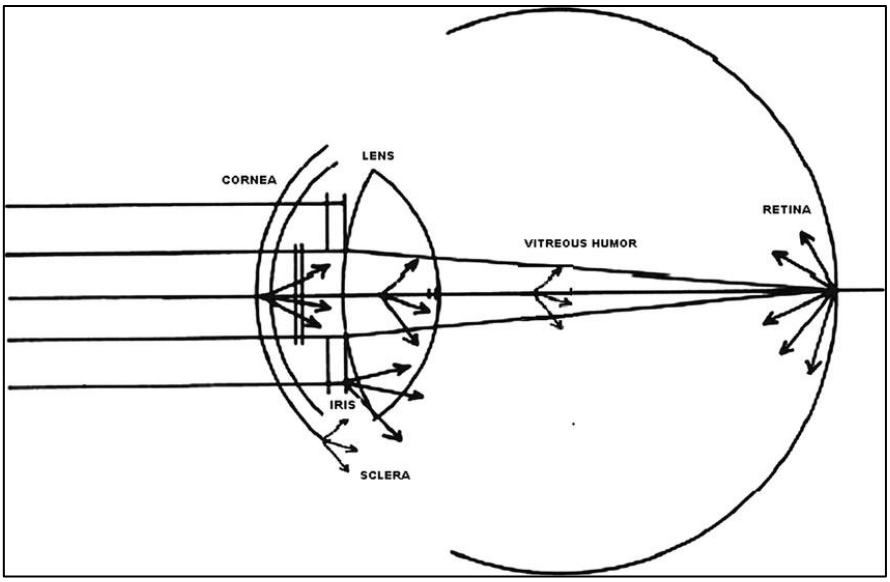

Figure 1.5: Schematic diagram showing sources of scattering in the human eye (Pinero et al., 2010).

Sclera and iris are two important sources of forward scattering, thus light can partly pass through these components depending on the level of pigmentation and density of these structures (van den Berg, 1995). Eyes with high pigmentation (brown eyes) contribute less to global level of ocular scattering than those with less pigmentation (Pinero et al., 2010).

The retina is also a source of scattering. Light is not only absorbed when reaches this structure but also part of this light is reflected to different retinal areas that contributes to intraocular scattering (van den Berg, 1995). This kind of scattering is very dependent on the level of pigmentation of the subject (Pinero et al., 2010).

There are several factors that increases intraocular scattering levels, such as aging (Artal et al., 1993; Shahidi and Yang, 2004), pigmentation (Pinero et al., 2010), associated diseases or ocular surgery (van den Berg et al., 2010).

Ocular scattering in DM

As previously discussed, the cornea undergoes changes associated to DM, such as corneal oedema (McNamara et al., 1998), increased corneal thickness (Inoue et al., 2002; Roszkowska et al., 1999), and abnormalities of basement membrane (Ljubimov et al., 1998; Rehany et al., 2000). These changes could lead to an increase of light scattering as it passes through these media, due to local fluctuations in refractive indices of the oedematous cornea, increased hydration or disruption of the orientation of the collagen fibres. Morishige et al. (2001) measured the scattering of the corneal epithelial basement membrane in 65 patients with T2DM with DR and 18 healthy subjects, and found that the light scattering index (LSI) was significantly higher in people with DM with PDR compared to healthy subjects. They also observed that the LSI correlated with the severity of DR but not with the duration of DM, blood glucose levels in a fasting state or with HbA1c levels, and they suggested that the LSI increases with the stage of DR. Takahashi et al. (2007) described the development of a light scattering detection system (LSDS) for measuring light scattering of corneal epithelial basement membrane, and measured 20 diabetic patients with vascular hyperpermeability, 20 patients with diabetic vascular occlusion and 30 healthy subjects. They observed that LSDS index was significantly higher in people with DM, although they could not specify if this light scattering was generated by the basement membrane or Bowman's layer..

In contrast, Holden et al. (1994) did not detect any difference in central corneal light scattered in a group of patients with T1DM compared with a normal control group.

Another cause of light scattering in a normal eye is that produced by the lens (van den Berg, 1997; van den Berg and Spekreijse, 1999). With aging, the lens loses its transparency due to nuclear sclerosis, becomes yellowish and ends with possible development of premature cataracts in people with DM (Klein et al., 1985; Nielsen and Vinding, 1984). Weiss et al. (1984), in their study with 38 patients with DM and 19 control subjects, observed higher light scattered in people with DM patients and demonstrated that young people with DM seem to have scatter values similar to those older subjects without DM.

Normally, the vitreous does not contribute to the total light scattering, but certain abnormalities such as AH that have been reported in people with DM might increase total light scattering values (Feist et al., 1990). During the course of DM, a partial breakdown of the blood-retinal barrier occurs, causing abnormalities in the tertiary and quaternary structures of the vitreous molecules as well as their diffusivity. Such changes can be detected by dynamic light scattering (DLS) when there are no visible corneal alterations and no onset of DR. Therefore, some authors suggested that DLS in the vitreous should be more effective for an early detection of DR (Rovati et al., 1998).

CHAPTER 2

Hypothesis and Objectives

2.1 HYPOTHESIS

Non-invasive optical methods and fundus AF (FAF) imaging analysis can become useful tools with the potential for early detection and management of the ocular changes caused by DM.

2.2 OBJECTIVES

Several studies have been carried out to prove the hypothesis of this thesis, and the objectives of these studies were as follows:

1. Evaluate the differences in ECD and CCT between T2DM patients and age-matched healthy controls, and determine the impact of time from diagnosis.
2. Determine central corneal backscatter values in both T1DM and T2DM patients from Scheimpflug images and compare results against healthy controls.
3. Explore the distribution of total, corneal, and internal HOAs in both T1DM and T2DM patients.
4. Develop a state-of-the-art review about AF in DM and the differences on FAF imaging acquisition using commercially available devices.
5. Evaluate FAF imaging at early stages of DR and relate findings with conventional colour fundus imaging and visual function in diabetic patients and control subjects.
6. Determine the usefulness of FAF imaging on DME assessment using a non-mydriatic retinal camera.

CHAPTER 3

Cornea and Diabetes Mellitus

3.1 QUANTITATIVE CORNEAL ANATOMY: EVALUATION OF THE EFFECT OF DIABETES DURATION ON THE ENDOTHELIAL CELL DENSITY AND CORNEAL THICKNESS

3.1.1 INTRODUCTION

As previously mentioned, DM is a metabolic disorder which may develop ocular complications, such as dysfunctional lacrimal gland, keratopathy, cataracts, glaucoma, refractive changes and DR. DM brings about a great impact on health, not only because of its increasing prevalence but also because of its high mortality rate. The prevalence of diabetes is estimated to be about 6% worldwide, and in the past two decades alone there has been a dramatic increase in the diagnosis of T2DM (Shaw et al., 2010)

Clinical evidence shows that patients with T2DM present alterations, such as increased epithelial fragility and recurrent erosions, reduced sensitivity, impaired wound healing, altered epithelial barrier function, and persistent stromal oedema after intraocular surgical procedures (Morikubo et al., 2004; Hugod et al., 2011). These changes suggest that diabetic endothelial cells show functional and morphological abnormalities. Studies have demonstrated that diabetic patients present an altered endothelial barrier function, higher polymegathism and pleomorphism of endothelial

cells (Choo et al., 2010), lower ECD (Choo et al., 2010; Inoue et al., 2002; Roszkowska et al., 1999), and increased AF (Weston et al., 1995).

When corneal endothelial function decreases, corneal hydration, and consequently the CCT, increase (Roszkowska et al., 1999). Some studies show a significant increase in CCT in T2DM patients (Roszkowska et al., 1999; Storr-Paulsen et al., 2014), but others do not (Choo et al., 2010; Inoue et al., 2002; Schultz et al., 1984), while the mechanism responsible for these changes in corneal structure and function remains to be fully understood.

In spite of the clinical importance of CCT assessment for diagnosing intraocular pressure pathologies (Lleó et al., 2003), and ECD evaluation to determine the compromise of the endothelial barrier function (Weston et al., 1995), few studies have reported the structural changes with the diabetic duration (Lee et al., 2006) in T2DM. The present study aims to determine if the duration of diabetes and high levels of HbA1c levels (indicating poor glycaemic control) affect CCT and ECD values.

3.1.2 PATIENTS AND METHODS

Subjects

We studied retrospectively 77 eyes from 77 T2DM patients (33 males and 44 females) and 80 healthy control subjects (42 males and 38 females) at the University of Valencia. Institutional review board (IRB) approval was obtained.

The inclusion criterion for diabetic and normal subjects was age between 30 and 60 years. Exclusion criteria for diabetic and normal subjects included prior corneal and/or ocular surgery, corneal and/or ocular disease (i.e. cataract, keratectasia, etc.), clinical corneal changes, contact lens wear, and Goldmann applanation tonometry > 21 mm Hg. The diabetic group and normal subjects had no other ocular or systemic complications.

All diabetic patients had a diagnosis of diabetes in accordance with the guidelines of the American Diabetes Association (ADA) (American Diabetes Association, 2010). Fourteen diabetic patients (18%) were well-controlled. Diabetic

subjects were classified into short-term diabetic subjects, those recently diagnosed (<1 year since diagnosis) and long-term diabetic subjects, those diagnosed and treated for 10 years or more. Two age-matched control groups were used for comparison with the short-term and long-term diabetic groups.

Methods

Diabetic patients and normal subjects underwent an ophthalmic examination that included slit-lamp examination, applanation tonometry, and dilated fundus examination. All patients showed blood glucose levels under 200 mg/dl (11.1 mmol/l) in the ophthalmic examination. HbA1c levels were measured from 8.00 a.m. to 9.00 a.m. one week before CCT and ECD measurements were carried out.

ECD measurements

The ECD was recorded using the Topcon SP-3000P non-contact specular microscope. Photographs of the central cornea were taken using the automatic-mode low flash intensity. Each picture was taken after proper positioning of the alignment dot, circle, and bar references on the screen. The endothelial cell count was performed using built-in image analysis software. Twenty-five cells were counted manually in each image. The estimated ECD was the mean of the three consecutive measurements (Sanchis-Gimeno et al., 2005) and it was expressed as the number of cells/mm^2.

CCT measurements

The CCT measurements were carried out with the DGH 5100E ultrasonic pachymeter. Each patient was asked to blink before CCT measurement to avoid any bias due to corneal drying (Lleó et al., 2003). Ten measurements were made at the centre of the cornea of each eye. The lowest CCT reading was used for analysis as it was thought the most likely to reflect a perpendicular placement of the pachymeter probe and, therefore, to be the most accurate measurement (Copt et al., 1999). All ECD and CCT measurements were performed between 11 and 12 a.m., at least three hours after the patients had woken up (Suzuki et al., 2003) to avoid overnight corneal swelling in CCT measurements (Efron et al., 2002).

Statistical analysis

Only the right eye was contemplated for statistical analysis. The choice of limiting the study to the right eye instead of the left was random. Normality of data distribution for the different groups was determined using the Kolmogorov-Smirnov test. Group differences in corneal parameters were assessed by means of an independent *t* test and two-way analysis of variance (ANOVA). Multivariate analysis of variance (MANOVA) was performed to determine whether corneal changes could be explained by any of the factors measured, for analysis of each individual dependent variable was used a Bonferroni test adjusted alpha level of 0.025. We considered values of $p<0.05$ to be statistically significant. All statistical analysis was performed using SPSS software (version 19, IBM Corp., Armonk, NY-USA).

3.1.3 RESULTS

Characteristics of both groups of T2DM patients compared with their respective age-matched control groups are summarized in Table 3.1.1.

No significant differences in CCT ($t(73) = -0.554$, $p=0.581$) and ECD ($t(73) = 0.559$, $p=0.578$) were found between short-term diabetic subjects and their age-matched controls. However, CCT and ECD were both significantly different in long-term diabetic subjects when compared with their age-matched controls ($t(81) = -8.610$, $p<0.001$; $t(81) = 6.977$, $p<0.001$, respectively). The duration of T2DM was defined as time from diagnosis. The diagnosis of diabetes depends on aspects like access to the health system and knowledge of risk factors, so the time of diagnosis might be considerably different from the time of onset depending on the study population. All our diabetic patients had free access to the health system and were diagnosed at a routine check by their general practitioner. However, time from onset to diagnosis of T2DM was unknown.

Mean CCT was significantly larger for long-term diabetic subjects than for short-term diabetic subjects ($t(75) = -7.826$, $p<0.001$; unpaired t-test) while mean ECD was significantly higher for short-term diabetic subjects than for long-term diabetic subjects ($t(75) = 8.890$, $p<0.001$; unpaired t-test). No significant differences in CCT (t

(79) = -1.039, p=0.302; unpaired t-test) and ECD (t (79) = 1.014, p=0.314; unpaired t-test) were found between control groups.

	Short-term diabetes	Controls	*p*-value	Long-term diabetes	Controls	*p*-value
Number	37	38		40	43	
Gender	16M, 21F	20M,18F		17M,23F	22M,21F	
Age (yr)	45.5 (2.5)	45.3 (2.1)	0.678	52.2 (1.8)	52.3 (2.6)	0.916
CCT (µm)	546 (13)	545 (11)	0.581	569 (11)	547 (11)	<0.001
ECD (cells/mm^2)	2581 (175)	2603 (155)	0.578	2205 (194)	2554 (254)	<0.001
Tonometry (mmHg)	16.4 (1.5)	16.1 (1.8)	0.523	16.6 (1.8)	16.3 (1.9)	0.436
Diabetes duration	4.6 (1.4) (months)	-	-	10.2 (0.8) (years)	-	-
HbA1c levels (%)	7.66 (0.78)	-	-	7.78 (0.66)	-	-

Unpaired t-test; CCT: central corneal thickness; ECD: endothelial cell density

Table 3.1.1: Diabetic with age-matched healthy subjects. Mean (SD) values.

Multivariate analysis of variance indicated that there was a significant effect of the diabetes duration on the combined dependent variable measured (F (4,186) =13.162, p<0.001, Wilks´Lambda= 0.6, partial eta squared = 0.221). Using a Bonferroni adjusted alpha level of 0.025, showed that CCT (F (2,94) = 21.294, p<0.001; R2 = 0.660) and ECD (F (2,94) = 18.221, p<0.001, R2 = 0.632) were statistically different in terms of diabetes duration.

A two-way ANOVA indicated that the estimated marginal means of CCT between short-term and long-term diabetic groups were not significantly different for 6.5% (U (13) = 13.000, p=0.165) and 7.0% (U (14) = 11.000, p=0.177) HbA1c levels (Mann-Whitney U test). Considering a 7.5 % HbA1c cut-off value, there was a significant difference between the diabetic groups (U (47) = 39.500, p<0.001; Mann-Whitney U test) (Figure 3.1.1).

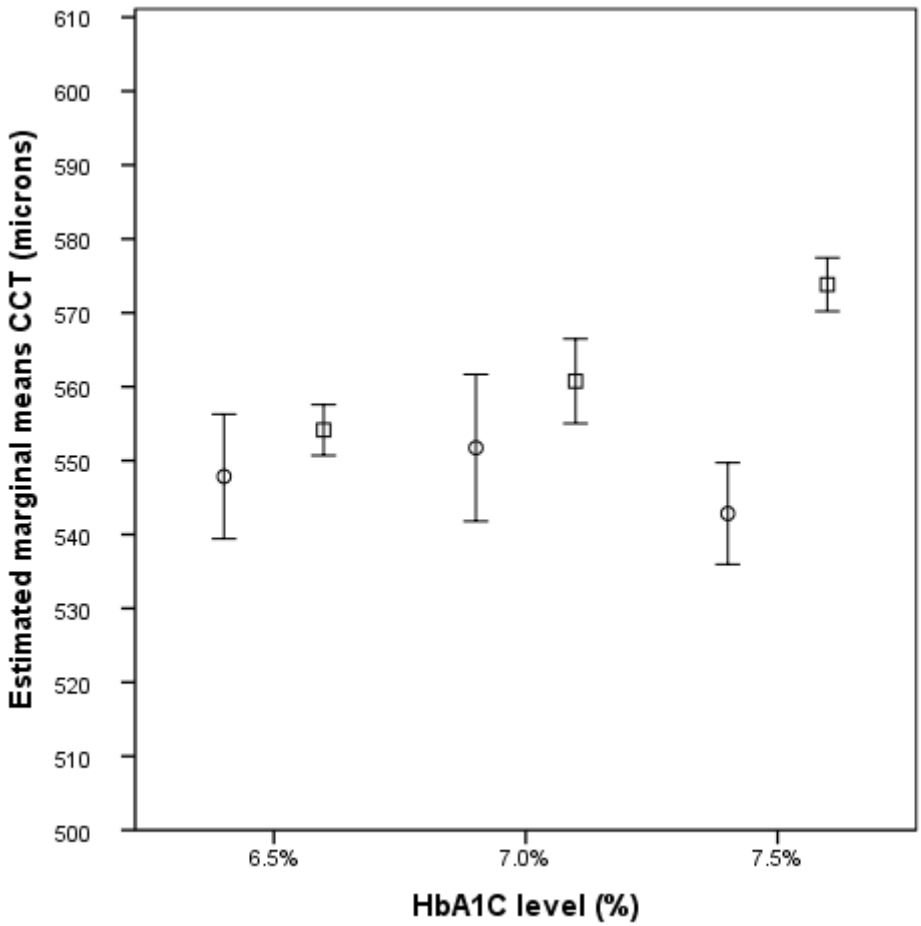

Figure 3.1.1: Estimated marginal means of CCT at different cut-off values of HbA1c between short-term (circles) and long-term (squares) diabetic subjects. Error bars represent 95% CI.

The estimated marginal means of ECD between diabetic groups were significantly different for 7.0% (U (14) = 2.000, p=0.004) and 7.5% (U (47) = 16.000, p<0.001) cut-off values of HbA1c (Mann-Whitney U test), but not for 6.5% HbA1c level (U (13) = 23.000, p=0.902; Mann-Whitney U test) (Figure 3.1.2).

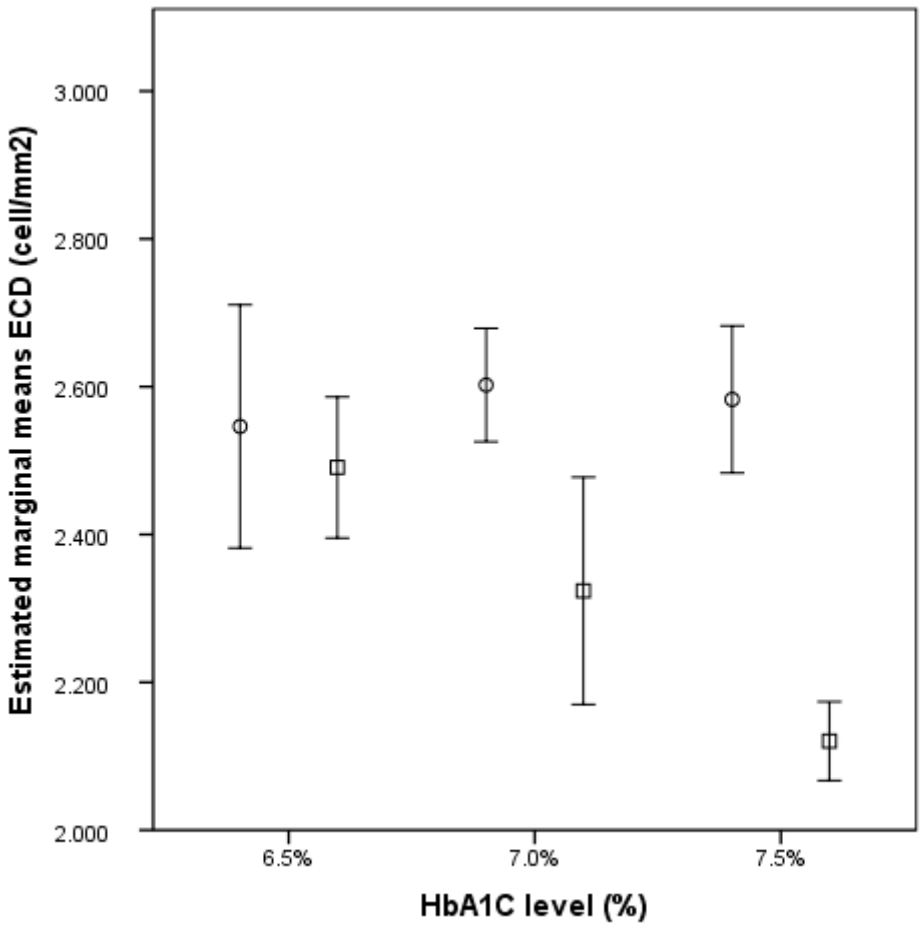

Figure 3.1.2: Estimated marginal means of ECD at different cut-off values of HbA1c between short-term (circles) and long-term (squares) diabetic subjects. Error bars represent 95% CI.

3.1.4 DISCUSSION

The corneal endothelium is responsible for regulating the water and solute transport of aqueous humor to the stroma across the posterior surface of the cornea (endothelial barrier function) and for moving excessive fluid away from the stroma, thus actively maintaining the cornea in the slightly dehydrated state that is required for optical transparency (endothelial pump function). The endothelium is responsible for maintaining the hydration of the cornea (Weston et al., 1995), whose most important enzyme is Na^+/K^+-ATPase which is localized in cellular membranes. This function is essential for good vision since a defective endothelium will lead to corneal oedema and a reduction in corneal transparency (Weston et al., 1995). Endothelial cell analysis provides important clinical information on corneal function and viability. The corneal

endothelium is subjected to cell loss by a number of factors, such as age, contact lens wear, diabetes, intraocular surgery, and penetrating keratoplasty (Storr-Paulsen et al., 2008). DM has serious effects on every structure of the cornea. It is thought to reduce the activity of endothelial Na^+/K^+-ATPase and, since this enzyme is a major component of endothelial cells, it may cause morphological and permeability changes in diabetic corneas (Weston et al., 1995). McNamara et al. (1998) suggested that hyperglycaemia might affect certain aspects of corneal hydration and modify CCT in diabetic patients.

Some investigators have reported that corneas in diabetic patients have a tendency to show higher CCT values (Lee et al., 2006; Roszkowska et al., 1999; Storr-Paulsen et al., 2014). Morphological and functional anomalies have been observed in the corneal endothelium of diabetic patients when compared with corneas of healthy subjects (Choo et al., 2010; Inoue et al., 2002; Lee et al., 2006; Roszkowska et al., 1999; Schultz et al., 1984). These anomalies include changes in cell density, percentage of cells, hexagonality, and variation coefficient. Despite this, some studies showing such morphological changes in corneal endothelium did not find variations in CCT in T2DM patients compared with healthy controls (Choo et al., 2010; Inoue et al., 2002).

In the present study, CCT and ECD values were compared between diabetic patients and age-matched healthy control subjects, and the impact of time from diagnosis was also explored. For this purpose, diabetic subjects were subdivided into two groups: short-term and long-term diabetic subjects.

Although both diabetic and control groups presented the same age difference, our results showed significant CCT and ECD differences between short-term and long-term diabetic subjects. Nevertheless, no significant CCT and ECD differences were found between the control groups. Therefore, these results suggest that the differences observed in both diabetic groups were not due to age.

Choo et al. (2010) found that the corneal endothelial structure was affected by T2DM and that there was a decrease in ECD, but that the CCT was unaffected. These authors also reported that the duration of diabetes and HbA1c levels had no effect on the endothelial structure. Schultz et al. (1984) reported that in T2DM patients, ECD was similar compared with non-diabetic patients. Similarly, Módis et al. (2010) observed that the ECD was normal in T2DM patients compared with healthy age-matched subjects. However, Roszchowska et al. (1999) observed decreased ECD values in

T2DM patients and reported that CCT in these patients was significantly increased when compared with non-diabetic subjects. Inoue et al. (2002) also reported a decrease in ECD compared with controls, but the CCT in T2DM patients was the same as in non-diabetics. Sudhir et al. (2012) in a multivariate regression study carried out on T2DM patients, found that ECD was lower among diabetic patients when compared with normal subjects. Our multivariate analysis of variance indicated that the duration of diabetes had an important effect in CCT and ECD, the latter values being lower and CCT values being higher in long-term than in short-term diabetic subjects and controls.

In the present study, the estimated marginal means of the CCT and ECD were significantly different between short-term and long-term diabetic subjects for a 7.5% HbA1c level. Storr-Paulsen et al. (2014) found that higher HbA1c levels were also associated with lower ECD in T2DM. Since previous reports found a correlation between HbA1c levels and permeability to fluorescein, it may be that hyperglycaemia affects corneal hydration levels (Gekka et al., 2004; McNamara et al., 1998; Weston et al., 1995) This therefore suggests that CCT and ECD values could reflect endothelial anomalies caused by prolonged hyperglycaemia (at 7.5%) due to poor glucose control which may cause corneal endothelial dysfunction, leading to stromal hydration and corneal swelling. Moreover, the results found in the present study seem to support that differences in the ECD and CCT values between the two diabetic groups are caused by the duration of diabetes and poor glycemic control in long-term diabetic patients. The results observed in the present study are of particular importance since it is known that corneal endothelial cells have a limited repair capacity (Joyce, 2003). When endothelial cell loss occurs, the endothelial response is enlargement and migration of the existing cells rather than division, to cover the area previously occupied by the lost cells (Joyce, 2003). Moreover, the endothelial cell population decreases following stressful situations, such as trauma, previous corneal transplant, stress caused by certain systemic diseases like treatment for glaucoma, cataract surgery, intraocular pressure pathologies, and the implantation of intra-ocular lenses (Joyce, 2003; Sihota et al., 2003).

Therefore, assessment of ECD is very important since a decrease in such values seems to be the main indicator of a morphologic alteration (Lee et al., 2001). Excessive reduction in endothelial cell numbers may compromise the endothelial barrier function, leading to VA loss (McNamara et al., 1998; Weston et al., 1995). This could occur, for

instance, in a diabetic patients with reduced ECD undergoing cataract surgery, since cataract surgery itself may also induce a reduction in ECD (Mahdy et al., 2012).

In summary, a significant increase in CCT and decrease in ECD values in T2DM patients, compared with healthy control subjects, were found, as well as a significant impact of the time from diagnosis of the condition. Further studies are required to establish the effect of long-term diabetes and poor glucose control on corneal endothelium, as well as the impact on visual performance and prognosis.

3.2 CORNEAL BACKSCATTER IN TYPE 1 AND TYPE 2 DIABETES MELLITUS PATIENTS

3.2.1 INTRODUCTION

Corneas of diabetic patients undergo several structural, morphological, and physiological changes, such as altered epithelial (Göbbels et al., 1989) and endothelial barrier function (Rehany et al., 2000), corneal oedema (McNamara et al., 1998), abnormalities of basement membrane (Rehany et al., 2000), higher polymegathism and pleomorphism of endothelial cells (Inoue et al., 2002; Roszkowska et al., 1999). And as we have previously observed in section 3.1, diabetic patients also show an increased CCT (Roszkowska et al., 1999) and lower ECD (Inoue et al., 2002). These corneal changes, along with tear film (Grus et al., 2002), crystalline lens (Bron et al., 1993) and vitreous body (Calvo-Maroto et al., 2014) disturbances observed in diabetic patients, imply changes in the optical performance of the eye causing a decrease in the quality of the retinal image (Calvo-Maroto et al., 2014).

The cornea (Olsen, 1982) and crystalline lens (Van Den Berg and Ijspeert, 1995) scatter light, particularly so when their transparency have been significantly affected (Wang et al., 2004). Corneal transparency is determined by the corneal structure and normal metabolism (Olsen, 1982; Van Den Berg and Ijspeert, 1995). In diabetic patients, hyperglycaemia can inhibit Na^+/K^+-ATPase activity causing corneal thickness and hydration to increase, and affecting corneal transparency (McNamara et al., 1998). Its loss implies therefore an increase in the light backscattered by the cornea (Olsen, 1982; Van Den Berg and Ijspeert, 1995).

In clinical practice, several devices have been used to measure light backscatter by means of a digital analysis of the images obtained with slit-lamp (Olsen, 1982), optical tomography (Wang et al., 2004) or Scheimpflug camera (Smith and et al., 1990), and to assess the quality of ocular tissues, mainly crystalline lens (opacities, cataract classification) (Ullrich and Pesudovs, 2012). Previous studies with diabetic patients have shown an increase in corneal epithelial basement membrane light backscatter compared to control subjects (Morishige et al., 2001; Takahashi et al., 2007) and related with the severity of DR (Morishige et al., 2001).

Scheimpflug imaging uses light backscattered from ocular tissues to image the anterior segment noninvasively, allowing the acquisition of multiple photographs of the anterior segment of the eye. Holden et al. (1994) used the Case 2000 CCD (charged couple device) Scheimpflug slit image camera (part of the Oxford Modular Cataract Image Analysis System [OMCIAS]) to measure central corneal backscatter in diabetic patients.

The present pilot study aims to determine the usefulness of Scheimpflug image analysis to detect corneal backscatter changes due to DM and assess the potential of the proposed image analysis for the detection and monitorization of corneal changes related to DM.

3.2.2 PATIENTS AND METHODS

Subjects

18 right eyes from 18 subjects with DM (15 men and 3 women) and 16 eyes from 16 control subjects (4 men and 12 women) were enrolled in the study. Patients and control subjects were recruited from Department of Ophthalmology of the Vithas Medimar International Hospital, in Alicante. All patients provided informed written consent in accordance with the World Medical Association´s Declaration of Helsinki before the procedures took place. IRB approval was obtained prior to the study.

Inclusion criterion was age between 30 and 70 years. Exclusion criteria for both diabetic patients and normal subjects were previous corneal and/or ocular surgery, corneal or ocular disease, retinal photocoagulation, clinical corneal changes and contact lens wear. Both diabetic patients and normal subjects had no other ocular or systemic complications.

All diabetic patients were diagnosed according to the guidelines of ADA (American Diabetes Association, 2010). Diabetic patients had stable and well-controlled blood glucose levels and were classified into T1DM and T2DM groups. A total of 7 patients with T1DM and 11 patients with T2DM were included in the present pilot study. DR was assessed by an ophthalmologist and graded according to the Early Treatment Diabetic Retinopathy Study (ETDRS) classification (Klein et al., 1989).

Methods

Both diabetic patients and control subjects underwent a thorough ophthalmic examination that also included the measurement of best-corrected VA (BCVA) by Snellen chart, slit-lamp examination and Pentacam imaging. VA was recorded in the logarithm of the minimum angle of resolution (logMAR) scale.

Pentacam

Scheimpflug imaging was carried out using the Pentacam rotation Scheimpflug camera (Oculus Inc., Germany). This instrument uses the Scheimpflug principle to acquire cross-sectional images of the anterior segment of the eye.

All measurements were carried out following a standardized procedure to minimize as much as possible external sources of variability. The head of patient was well positioned on the chin and forehead rests, and the patient was asked to fixate to an internal target. A real-time image of the eye appeared on the computer screen, allowing the examiner to change and optimize focus and centration.

All measurements were performed in the morning, and the mean of seven measurements in seven different meridians was taken for each subject. Images of the anterior segment of the eye were obtained using the 25 scans setting. All cross-sectional images were saved in jpeg format.

CCT and anterior chamber depth (ACD) values were also obtained.

Scheimpflug imaging analysis

Imaging analysis was carried out using the NIH ImageJ medical imaging software (NIH ImageJ 1.47v, National Institutes of Health, Bethesda, MD-USA), developed by the National Institutes of Health and available as a free download.

Scheimpflug images provide structure-related data on backscattered light from the eye and allow the assessment of information regarding the transparency of ocular tissues. Cornea is a source of light backscatter when its transparency has been significantly affected (McCally et al., 2007). Therefore, corneal haze with decreased of corneal transparency is associated with increased ocular scattering. Clinically, corneal

haze is assessed as corneal backscatter observed by slit lamp examination or use of Scheimpflug camera (De Brouwere et al., 2008; Wegener and Laser-Junga, 2009). In the imaging analysis, the software of Pentacam Scheimpflug device analyzes the corneal area of interest and the output image is expressed in grayscale units. For the purpose of this study, seven meridians for each eye with orientations ranging from 70º to 110° were analyzed. Imaging analysis is represented in Figure 3.2.1. Firstly, these images of each meridian were first converted to 8-bit images (Figure 3.2.1a), the images were then contrast-reversed from 8-bit images (Figure 3.2.1b). Finally, the "Invert LUT" was applied. This tool reversed the image contrast and pixel values of 8-bit images (Figure 3.2.1c). As a result, pixels with a value of 0 are white and pixels with values of 255 are black. The grayscale image was calibrated on optical density units (o.d.u.) according to Optical Density Calibration tool on the ImageJ software. This tool provides a calibrated optical density step table (density range 0.05 to 3.05 o.d.u.) to calibrate grayscale images. We measured the mean grey value to the white background at the left end image with the same rectangular selection. We obtained 19 measurements listed, and after the "calibrate dialog box" was opened and these measurements were automatically entered into, ImageJ software generated and displayed the calibration curve. As a result of this process, the image is now calibrated to optical density, white pixels representing the highest value of optical density (3.05 o.d.u.) and black pixels the lowest one (0.05 o.d.u.).

The scale was defined by determining the size in pixels of a parameter of known size. A measure of ACD in the center of the image was carried out with the assistance of the "find edges" tool. As a result, 1mm corresponded to 36,36 pixels.

For determining central regions, a central line of 3 mm was drawn and delimited with two vertical lines (Figure 3.2.1d). This region of interest was replicated in each eye. To select the width of the area to be analyzed, and to avoid as much as possible the tear film inclusion into corneal backscatter measurements, we established as a reference point the limit line between corneal endothelium-aqueous humor. Thus, we did match this reference line with an ellipse that was drawn to delimit the second surface of the cornea, and a band with CCT value to delimit the first surface of the cornea (Figure 3.2.1e). Finally, the outline of the 3 mm central region was made (Figure 3.2.1f). The same procedure was carried out for the central 5 mm region.

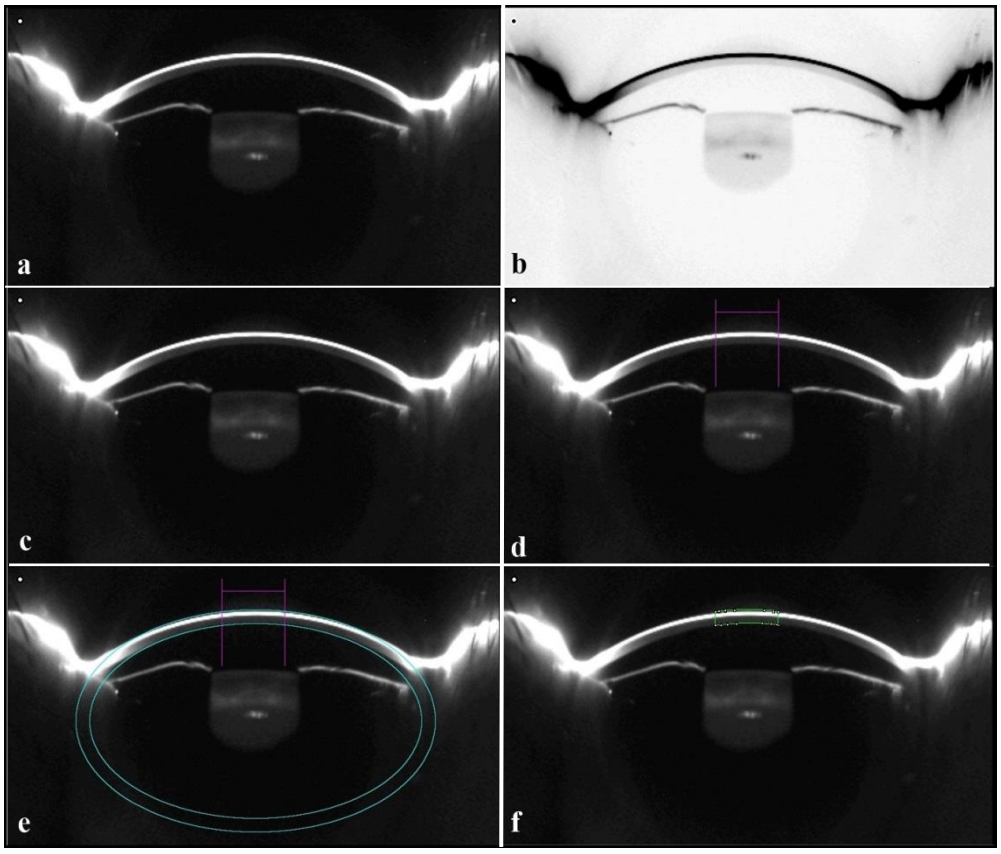

Figure 3.2.1: Image processing using ImageJ (a. 8-bit image, pixels with value of zero are black and pixels with value 255 are white; b. 8-bit image with contrast-reverted; c. 8-bit image with contrast and pixel values reverted, pixels with value of zero are white and pixels with value 255 are black; d. Determination of central region of 3 mm; e. Determination of central region width; f. Outline of central region of 3 mm).

When the image was not properly centered, or any external artifact (shadows) could be affecting the measurements, the image was excluded.

Statistical analysis

In the present study, only the right eye was considered for analysis. The average of central backscatter was calculated for each eye from the seven meridians measured. Normality of data distribution for the different groups was determined using the Kolmogorov-Smirnov test. When parametric analysis was possible, the independent samples Student *t* test was used for comparisons between diabetic patients and control subjects. When parametric analysis was not possible, the U Mann Whitney test was used to assess the significance of such difference.

The homogeneity of these measures was defined by the coefficient of variation (CV). Differences between both central zones (3 mm and 5 mm) were determined using paired *t*-test.

T1DM and T2DM patients and healthy controls differences in central corneal backscatter, and central corneal backscatter differences between stages of DR were assessed by Kruskall-Wallis test. To determine which of pairwise comparisons were responsible for the overall difference between groups, separate Mann-Whitney U tests was performed on each pairwise (3 tests), alpha used 0.05/3 = 0.0167.

Correlation coefficients (Pearson or Spearman) were used to assess the correlation between variables. We considered values of $p<0.05$ to be statistically significant in all statistical tests used. All statistical analysis was performed using SPSS software (version 19, IBM Corp., Armonk, NY-USA).

3.2.3 RESULTS

The mean age of diabetic patients was 51.33 ± 10.63 years (range 33–68 years) and that of healthy subjects was 49.44 ± 9.34 years (range 38–64 years) ($p>0.05$). Both diabetic groups were then compared with age-matched healthy subjects (Table 3.2.1). Diabetes duration difference between T1DM (210.86 ± 150.97 months, range 24–244 months) and T2DM patients (128.82 ± 136.74 months, range 1–480 months) was not found statistically significant ($p=0.246$), although the statistical power in this pilot study is not high enough to determine significance of differences in this parameter.

	T1DM	Controls	*p*-value[§]	T2DM	Controls	*p*-value*
Number	7	6		11	10	
Sex	6M, 1F	3M, 3F		9M, 2F	1M, 9F	
Age (yr)	42.29 (9.57)	40.00 (1.26)	0.94	57.09 (6.59)	55.10 (7.03)	0.56
BCVA (logMAR)	0.06 (0.11)	0	0.23	0	0	-
CCT (µm)	594.70 (19.58)	577. 83 (32.54)	0.37	588.18 (47.03)	555.30 (52.24)	0.28
ACD (mm)	2.68 (0.41)	2.75 (0.27)	90.94	2.60 (0.29)	2.71 (0.34)	0.43
Diabetes Duration (months)	210.86 (150.97)	-		128.82 (136.74)	-	
Central backscatter 3 mm (o.d.u.)	0.266 (0.097)	0.197 (0.021)	<0.05	0.327 (0.167)	0.218 (0.040)	<0.05
Central backscatter 5 mm (o.d.u.)	0.259 (0.090)	0.194 (0.022)	<0.05	0.325 (0.165)	0.214 (0.039)	<0.05

[§]Mann-Whitney U test; * Unpaired *t* test
T1DM: Type 1 diabetes mellitus; T2DM: Type 2 diabetes mellitus
BCVA: Best corrected visual acuity; LogMAR: logarithm of minimum angle of resolution; CCT: Central corneal thickness; ACD: Anterior chamber depth; o.d.u.: optical density units.

Table 3.2.1: Diabetic patients with age-matched normal subjects. Mean (SD) values.

In T1DM group, three patients had moderate NPDR (NPDR II) and a patient showed severe NPDR (NPDRS). In T2DM group, only a patient showed mild NPDR (NPDR I). Diabetic patients did not show any complication caused by DM besides DR.

The mean of central corneal backscatter was calculated for each eye from the seven different meridians analyzed (range 70^{o} to 110^{o}). Differences between diabetic and control groups were statistically significant for central corneal backscatter of 3 mm (0.303 ± 0.144 o.d.u. in diabetic patients and 0.210 ± 0.034 o.d.u. in control subjects, p=0.016), and for central 5 mm (0.299 ± 0.142 o.d.u. in diabetic patients and 0.207 ± 0.034 o.d.u. in control subjects, p=0.014). However, the difference in CCT values between diabetic patients (590.72 ± 38.04 µm) and control subjects (563.75 ± 46.02 µm) was not statistically significant (p=0.071), neither BCVA values were statistically difference between diabetic patients (0.022 ± 0.071) and control subjects (0.00 ± 0.00) (p=0.422).

For corneal backscatter of the central 3 mm, the average CV for the diabetic patients was 2.1% (range 1.0–5.0%) and 2.3% for control subjects (range 0.8–6.6%).

Table 3.2.1 shows the mean values of central corneal backscatter obtained for the central 3 and 5 mm in T1DM patients, T2DM patients, and aged-matched control subjects. Values were significantly higher for T1DM patients than for age-matched control subjects and for T2DM patients compared to age-matched control subjects, for both central zone diameters analyzed.

Corneal backscatter for the 3 mm central zone was significantly higher than for the central 5 mm in control subjects ($p<0.001$) but not so in diabetic patients ($p>0.05$) (paired t-test). Significant differences of corneal backscatter were not found between T1DM and T2DM patients for either zone analyzed ($p>0.05$ in both cases).

Kruskall-Wallis test indicated that for the central backscatter there was a significant effect of presence of DM in both 3 mm and 5 mm central zones ($\chi^2 = 13.546$, $df = 2$, $p=0.001$; $\chi^2 = 13.626$, $df = 2$, $p=0.001$, respectively) (Figures 3.2.2 and 3.2.3).

However, there were not statistically differences for central backscatter between different stages of DR in both 3 mm and 5 mm central zones ($\chi^2 = 2.547$, $df = 3$, $p=0.467$; $\chi^2 = 2.547$, $df = 3$, $p=0.467$, respectively).

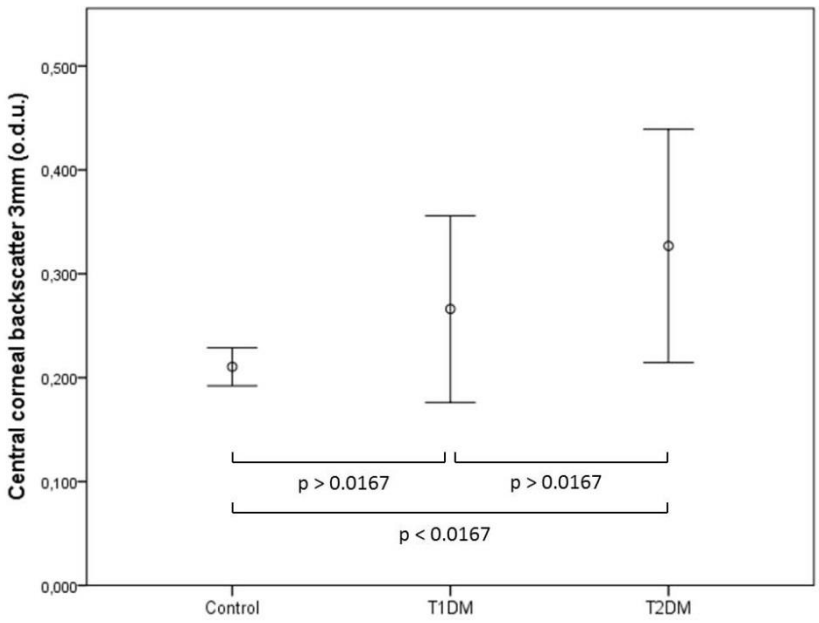

Figure 3.2.2: Mean of central corneal backscatter in both types of DM and control subjects for central 3 mm. Error bars represent 95% Confidence Interval (CI).

Spearman correlation analysis showed that in T1DM patients, central backscatter were not correlated with age for either central zone diameter analyzed (3 and 5 mm) (r = 0.523, p=0.114; r = 0.523, p=0.114 respectively) nor for CCT (r = -0.071, p=0.440; r = -0.071, p=0.440, respectively) (Figures 3.2.4 and 3.2.5). No significant correlations were found between both central backscatter zones, 3 mm and 5 mm, with diabetes duration (r = 0.288, p=0.265; r = 0.288 p=0.265, respectively), or DR stages either (r = -0.077, p=-0.173; r = -0.077, p=-0.173, respectively).

In T2DM, Pearson´s correlation analysis revealed that backscatter for the central 3 mm was significantly correlated with CCT (r = 0.641, p=0.017), and age (r = 0.604, p=0.025), backscatter for the central 5 mm was also significantly correlated with age (r = 0.614, p=0.022) and CCT (r = 0.671, p=0.012) (Figures 3.2.4 and 3.2.5).

Figure 3.2.6 shows optical density profiles of T1DM and T2DM patients with age-matched controls. All participants had a higher peak of optical density that decreased axially across the corneal thickness. This peak was particularly high for T2DM and T1DM patients.

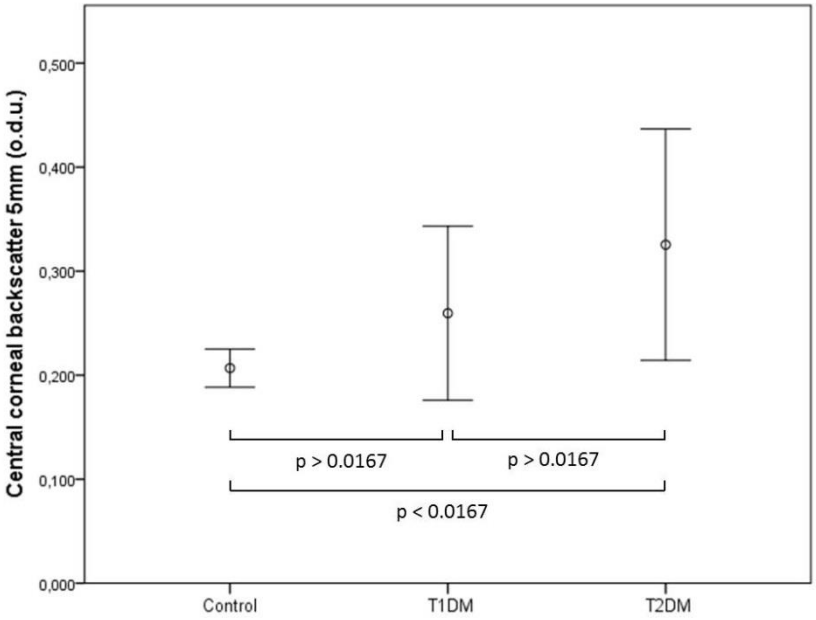

Figure 3.2.3: Mean of central corneal backscatter in both types of DM and control subjects for central 5 mm. Error bars represent 95% CI.

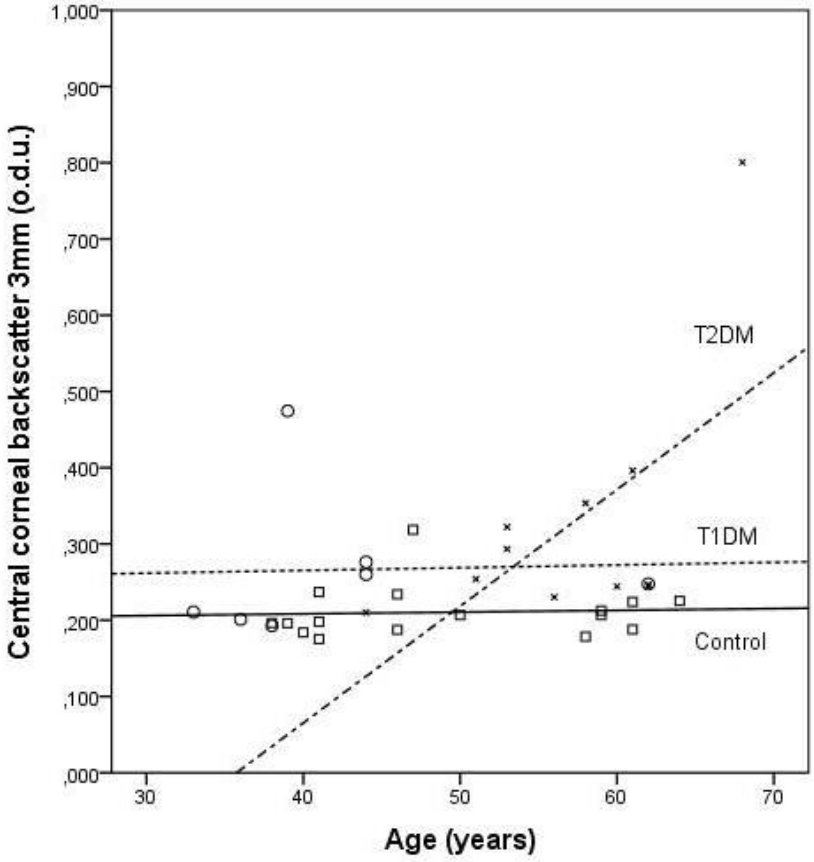

Figure 3.2.4: Correlation between corneal backscatter for central 3 mm and age in control subjects (squares and solid line; r = 0.062; p>0.05), T1DM (circles and dotted line; r = 0.523; p>0.05) and T2DM (crosses and dotted/dashed line; r = 0.604; p<0.05) patients.

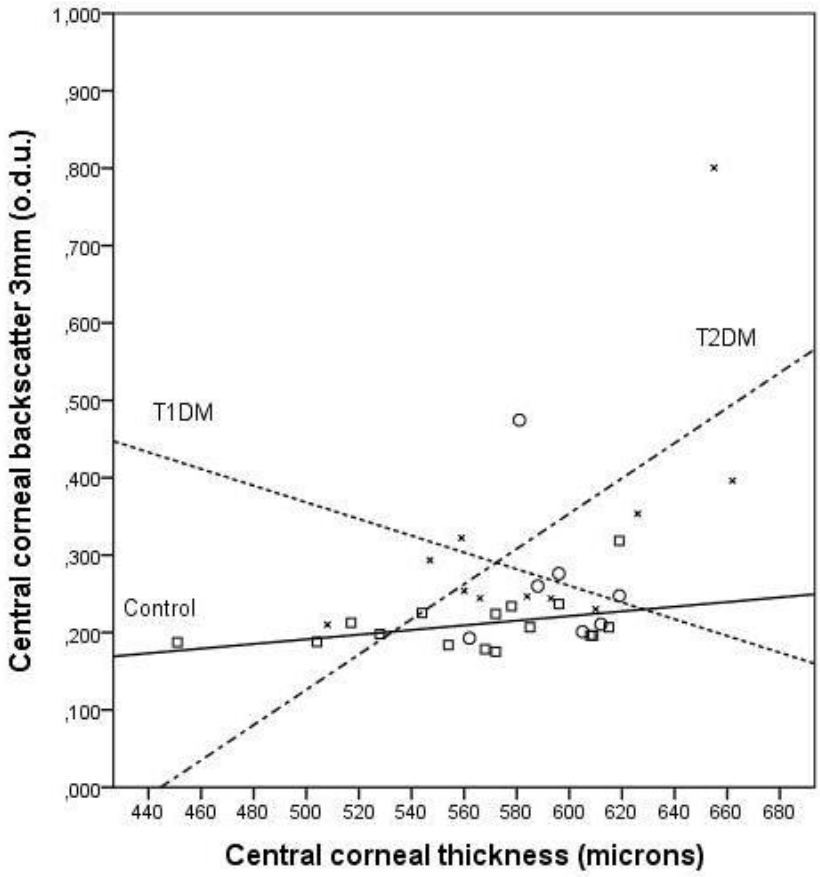

Figure 3.2.5: Correlation between corneal backscatter for central 3 mm and CCT in control subjects (squares and solid line; r = 0.400; p>0.05), T1DM (circles and dotted line; r = -0.071; p>0.05) and T2DM (blades and dotted/dashed line; r = 0.641; p<0.05) patients.

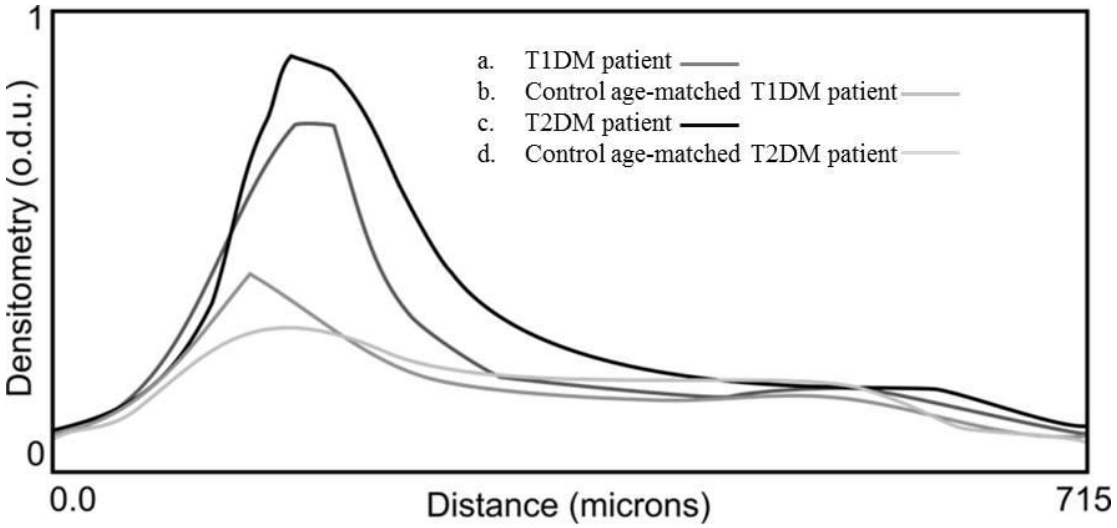

Figure 3.2.6: Corneal images from Scheimpflug photography and corneal densitometry profile in diabetic patients and control age-matched. (a. T1DM patient; b. Control age-matched T1DM patient; c. T2DM patient; d. Control age-matched T2DM patient).

3.2.4 DISCUSSION

Scheimpflug imaging has been widely used to assess the quality of transparent tissues of the anterior segment of eye by measuring of light backscatter. The optical quality of these ocular diopters can be affected by ageing (Artal et al., 1993), ocular/refractive surgery (Moreno-Barriuso et al., 2001; Oshika et al., 1999) or diseases such as DM (Morishige et al., 2001; Shahidi et al., 2004; Takahashi et al., 2007; Wiemer et al., 2009).

In healthy subjects, an increase of corneal light scattering has been related with the disruption of the orientation of collagen fibers with age (Olsen, 1982) or due to fluctuations in refractive indices in oedematous corneas (Goldman et al., 1968). Despite the age-related changes, corneal changes due to DM have been studied in detail in the past. Corneal changes such as abnormalities of the basement membrane (Rehany et al., 2000; Roszkowska et al., 1999), alterations of epithelial (Göbbels et al., 1989) and endothelial barriers function (Rehany et al. 2000), corneal oedema (McNamara et al., 1998), increased corneal thickness (Roszkowska et al., 1999), polymegathism or pleomorphism have been observed in diabetic patients (Roszkowska et al., 1999; Inoue et al., 2002). These structural, physiological and morphological changes could cause an increase in the light backscattered by the cornea.

To determine if these diabetes-related abnormalities cause changes in optical quality of cornea, the present pilot study determined central corneal backscatter by image analysis of Scheimpflug images using external software. Diabetic patients showed higher values of optical density than age-matched control subjects for both 3 mm and 5 mm central zones (Table 3.2.1).

The presence of DM implied a significant effect over corneal backscatter (Figures 3.2.2 and 3.2.3). CCT values were not significantly different between diabetic and control groups (Table 3.2.1), nor were statistically different BCVA values found in diabetic patients compared to control subjects (Table 3.2.1). Although the statistical power in this study is not high enough to determine significance of differences in CCT values, in previous study by authors, the effect of diabetes duration and glycemic control over ECD and CCT was assessed with a larger sample size and found that diabetic patients with more than 10 years of diabetic duration and poor glycemic control (7.5% cut-off values of HbA1c) showed significantly increased in CCT (Calvo-Maroto et al., 2015).

Previously, Holden et al. (1994) using Ocular Modular Cataract Image Analysis System (OMCIAS) did not observe differences in central corneal backscatter between diabetic patients and control subjects (22 patients with T1DM at least 10 years' duration and 29 control subjects). The lack of agreement with the results reported here could be partly due to their control subjects being statistically older than the diabetic patient sample (did not use age-matched controls).

An increase in light scattering in corneal epithelial basement membrane has been observed in diabetic patients (Morishige et al., 2001; Takahashi et al., 2007). Smith et al. (1990) suggested that the most scatter observed occurred in areas where there was a large change in refractive index, such as epithelial and endothelial surfaces. Morishige et al. (2001) identified three peaks in the tissue reflectivity diagram. These peaks corresponded to the interface between the tear film and the corneal epithelium, between epithelial basal cell layer and the anterior stroma, and between posterior stroma, Descemet´s membrane, and endothelium with aqueous humor. Stroma was located between the second and third interfaces. Given the limited resolution of the Scheimpflug imaging system used in this study, the tear film and the different corneal layers could not be differentiated. Corneal backscatter was not evenly distributed along

the corneal axis. A peak of light backscatter in the anterior corneal layers that might correspond to interface between tear film and epithelium-Bowman´s membrane was observed. This peak was higher in most of diabetic patients compared to control subjects (Figure 3.2.6). Therefore not only corneal changes related with DM may cause an increase of backscatter, but also changes in tear film composition (Grus et al., 2002), and dry eye as consequence of diabetes could contribute to this increase. The optical quality and thickness of tear film were not considered in Scheimpflug imaging analysis in the present study, nor dry eye analysis. Our diabetic patients did not report dry eye symptoms, however this condition is strongly linked to diabetes (Dogru et al., 2001; Goebbels, 2000).

The peaks of optical density corresponding to the anterior cornea were similar to those observed by Takahashi (2007) and Morishige (2001). In their studies, all patients presented different stages of DR, and they also showed high peaks of light backscattering corresponding to the interface of Descemet´s membrane and endothelium with aqueous humor.

This increase of backscatter in posterior cornea has not been reported in healthy subjects (Dhubhghaill et al. 2013; Rozema et al. 2011). We have observed that none of the participants enrolled of this study showed high peak values at the level of posterior surface interface.

Even though we did not have ECD values in this study, in a previous study diabetes duration and poor glycemic control (7% and 7.5% cut-off values of HbA1c) caused significantly decreased in ECD in patients with diabetes duration more than 10 years (Calvo-Maroto et al., 2015). It could be possible that ECD values were decreased in this study owing to our diabetic patients showed diabetes duration more than 10 years. Age-related corneal changes are more evident in corneal periphery than in central zone (Smith et al., 1990). Although in this study diabetic patients did not show significantly differences between both zones, in T2DM only patients' age was correlated with the central 5 mm corneal backscatter. It might be that corneal changes caused by DM are more important in central zone than in the periphery. The combination between age-related and DM-related changes results in ageing of the overall cornea without differences between both zones. We observed that central 3 mm backscatter was higher than 5 mm in control subjects, implying a corneal backscatter

decrease from the apex towards periphery in these subjects. Rozema et al. (2011) determined this decrease may be due to an artifact resulting from the angle under which the cornea was illuminated in the peripheral areas.

In the present study, both central backscatter zones, 3 mm and 5 mm, were correlated with age and CCT (Figures 3.2.4 and 3.2.5). The increase of central corneal backscatter with CCT could be due to an increase of corneal hydration although, Smith et al. (1990) evidenced that variations on corneal thickness is caused by changes in mass content rather than water content of the cornea. With respect to increasing in corneal backscatter with age, it may be due to structural, physiological and morphological changes, which undergo corneas of diabetic patients, since T2DM patients showed higher corneal backscatter values than control age-matched group and ageing was not statistically different between both groups. However, diabetes duration or severity of DM was not correlated with any central corneal backscatter in T2DM. This lack of correlation between diabetes duration and central corneal backscatter might be due to wide range of the length of the disease in the sample, varying from 1 month to 40 years.

The increase of corneal central backscatter in T1DM patients was not correlated with age, CCT, diabetes duration or severity of DM.

Although previous studies have shown an increase of corneal backscatter with severity of DM (Morishige et al., 2001; Takahashi et al., 2007), this study could not find this relationship, due to the pilot character of the study, and therefore reduced sample size, and the fact that representation of the different DR stages was not considered in this study.

The measurements of corneal backscatter using optical density analysis showed homogeneity in both groups of participants (CV diabetic patients was 2.1% and for control subjects 2.3%).

The main limitation of this study is reduced sample size, but other limitation was that DR stages were not considered. Therefore, all conclusions must be interpreted with care. Although sample size is small and the methods used to quantify corneal backscatter have not yet been validated, the results obtained from this pilot study suggest the possibility to make further studies to confirm and to consolidate these

results in larger cohorts of diabetic patients, with different ranges of diabetes duration, and different stages of DR, as well as in prediabetic and healthy subjects.

In summary, the use of Scheimpflug imaging and external software for optical density calibration enabled detecting significant differences in central corneal backscatter between diabetic patients and healthy subjects. These results show a potential for optical quality measurements in monitoring changes caused by DM.

CHAPTER 4

Ocular Optical Quality and Diabetes Mellitus

4.1 TOTAL, CORNEAL, AND INTERNAL ABERRATIONS IN TYPE 1 AND TYPE 2 DIABETES MELLITUS PATIENTS

4.1.1 INTRODUCTION

The transparency, structure, and morphology of ocular components determine the sharpness of the retinal image. Changes in these characteristics imply a decrease of the quality of the retinal image (Liang and Williams, 1997).

The improvement of wavefront technology and its availability to clinical practice permitted a greater knowledge about the distribution of corneal and crystalline lens aberrations, and their contribution to total ocular aberrations. These new devices enable an improved visual performance of patients with different pathologies (Gobbe and Guillon, 2005; Schlegel et al., 2009) and surgical procedures (Oliveira et al., 2012).

It seems reasonable to think that any condition compromising the metabolism of ocular structures contributing to the formation of retinal image might alter the quality of that image. Previous studies have shown changes in optical quality in diabetic eyes (Shahidi et al., 2004; Wiemer et al., 2009), although the contribution of the cornea and crystalline lens to total ocular aberrations is unknown.

In the present study, total, corneal, and internal ocular HOAs (coma and spherical aberration) were determined in T1DM and T2DM patients with the aim of knowing the distribution of the HOAs in both groups, establishing the relationship between HOAs and ocular parameters, and investigating the potential of optical quality measurement as an aid for monitoring the condition.

4.1.2 PATIENTS AND METHODS

Subjects

This observational case series included eyes with DM. All patients provided informed written consent in accordance with the World Medical Association´s Declaration of Helsinki before the research. The local ethics committee approved the study.

Patients were recruited from the Department of Ophthalmology of the Vithas Medimar Hospital International, in Alicante. 14 from 7 patients with T1DM (6 men and 1woman) and 22 eyes of 11 patients with T2DM (9 men and 2 women) were studied.

Exclusion criteria were previous corneal or intraocular surgery, previous corneal or ocular disease, previous retinal photocoagulation, crystalline lens opacity or contact lens wear. Diabetic patients had a stable and well-controlled blood glucose levels. Measurements were obtained under natural pupil conditions of at least 5 mm in diameter and data analyzed for a 5 mm pupil size.

Methods

A comprehensive examination was performed in all cases, including the wavefront aberration analysis for distance (5 m) by means of the ray tracing aberrometry (iTrace, Tracey Technologies Corp., Houston, TX-USA) and the measurement of anterior segment using Scheimpflug imaging (Pentacam, Oculus Inc. Germany).

Aberrations measurement

Ocular and corneal aberrations were measured with the iTrace wavefront aberrometer. The iTrace aberrometer analyzes retinal spot patterns by means of ray tracing to determine ocular wavefront aberrations. An infrared beam is projected into the eye through different locations, and the system analyzes the retinal spot patterns to determine the wavefront (Cerviño et al., 2007). The system also includes a Placido disk-based corneal topography system that allows deriving corneal aberration data. Thus, this system also makes it possible to obtain the internal aberrations of the eye by subtracting corneal aberrations from total. Wavefront errors were recorded in Zernike terms, under monocular conditions, across 5 mm pupil size and up to the fourth order, since HOAs are dominated by 3rd order coma-like and spherical aberration (4th order) (Lombardo and Lombardo, 2010; Oliveira et al., 2012).

All measurements were carried out following a standardized procedure to minimize as much as possible the external sources of variability. The iTrace aberrometer is a monocular system; the contralateral eye was covered with an eye patch in all cases during the measurement procedure. Three repeated consecutive measurements were taken by the same examiner. All measurements were performed 3-4 seconds after blink to ensure appropriate spread of the tear film (Montés-Micó et al., 2004a) and the room was dark to provide pupil dilation.

Ocular parameters measurements

Scheimpflug photography was carried out using the Pentacam rotating Scheimpflug camera (Oculus Inc., Germany). This instrument uses the Scheimpflug principle to acquire cross-sectional images of the cornea and crystalline lens.

The analysis of the anterior segment included: (1) anterior and posterior surface topography of cornea with axial (sagittal), tangential, and elevation maps, (2) CCT measured by noncontact pachymetry based on true elevation data, (3) ACD, anterior chamber volume (ACV), and thickness of crystalline lens.

Three repeated consecutive measurements were taken by the same examiner. Again, an interval of 3-4 seconds was allowed from blink and the room was dark to provide pupil dilation.

Refraction notation

The spherocylindrical refractions were converted to vectorial notation using the power vector method as described in Ref. (Thibos et al., 1997). The length of this vector is a measure of the overall blurring strength (B) of the spherocylindrical refractive error.

Statistical Analysis

Data analysis was performed using SPSS for Windows (version 19, IBM Corp., Armonk, NY-USA). Non-parametric analysis was carried out in this study; a Wilcoxon test was used for comparisons between right eye and left eye in diabetic patients and each diabetic group. The U-Mann Whitney test was used to assess the significance of difference between T1DM and T2DM. Spearman correlation was used to assess the correlation between variables. Differences were considered statistically significant when the *p* value was less than 0.05.

4.1.3 RESULTS

Demographic data of both diabetic groups are summarized in Table 4.1.1. The thickness of crystalline lens was only measurable in two eyes with T1DM (14%) (Mean 2.55 ± 0.23 mm) and six eyes T2DM (27%) (Mean 2.65 ± 0.84 mm).

Differences between the diabetic groups were statistically significant for orthogonal component of astigmatism J0 (Z_2^2) (95% CI ± 0.285 D in T1DM, and 95% CI ± 0.155 D in T2DM patients). Mean ocular parameters were not significantly different between diabetic groups (Table 4.1.1).

There were no significant differences in total, internal or corneal wavefront aberrations between T1DM and T2DM patients (Tables 4.1.2, 4.1.3, and 4.1.4). Total HOAs were slightly higher in T1DM (95% CI ± 0.131 μm) than in T2DM patients (95% CI ± 0.108 μm), although the difference was not statistically significant. Except for coma, the magnitudes of the various ocular HOAs were lower than their respective corneal and internal components, indicating a partial balancing effect of corneal aberrations by internal aberrations.

	T1DM (n=14)		T2DM (n=22)		
Characteristics	**Mean (SD)**	**Range**	**Mean (SD)**	**Range**	***p*-value***
Age (year)	42.29 (9.19)	33 to 62	57.09 (6.44)	44 to 68	<0.001
M (D)	-1.13 (3.16)	-8.12 to 2.75	0.23 (0.77)	-0.75 to 2.12	0.072
J0 (D)	-0.286 (0.464)	-0.8 to 0.96	-0.039 (0.35)	-0.61 to 1.23	0.023
J45 (D)	-0.022 (0.433)	-1.15 to 0.96	0.028 (0.058)	0 to 0.22	0.876
B (D)	2.058 (2.703)	0 to 8.15	0.447 (0.758)	0 to 2.36	0.066
CCT (µm)	596.43 (19.39)	562 to 621	587.05 (42.97)	504 to 662	0.377
ACD (mm)	2.69 (0.41)	1.98 to 3.39	2.61 (0.29)	2.24 to 3.19	0.240
ACV (mm^3)	146.64 (34.94)	87 to 214	146 (29.96)	102 to 192	0.689
Ant K1 (D)	42.68 (1.42)	40.3 to 44.4	43.34 (1.96)	40.7 to 47	0.689
Ant K2 (D)	43.46 (0.99)	41.7 to 44.7	44.17 (2.25)	41.5 to 49.6	0.810
Ant Q (D)	-0.26 (0.12)	-0.49 to -0.1	-0.31 (0.12)	-0.56 to -0.11	0.240
Post K1 (D)	-6.10 (0.30)	-6.5 to -5.7	-6.10 (0.31)	-6.7 to -5.7	0.713
Post K2 (D)	-6.43 (0.32)	-6.9 to -6	-6.41 (0.48)	-7.7 to -5.9	0.511
Post Q (D)	-0.28 (0.31)	-0.75 to -0.07	-0.3 (0.14)	-0.48 to -0.02	0.713

M: Mean spherical equivalent, J0: orthogonal component 90 to 180 degrees of astigmatism, J45: orthogonal component 45 to 135 degrees of astigmatism, B: overall blurring strength of spherocylindrical refraction error, CCT: central corneal thickness, ACD: anterior chamber depth; ACV: anterior chamber volume, Q: asphericity, Ant: anterior, Post: posterior
*U Mann-Whitney test

Table 4.1.1: Demographic data of the diabetic groups.

From the Zernike coefficients studied, vertical coma component Z_3^{-1} had the highest value in T1DM (95% CI ± 0.176 μm) and T2DM patients (95% CI ± 0.129 μm).

Aberrations	T1DM	T2DM	*p*-value*
Total HOAs (μm)	0.634 (0.228)	0.527 (0.245)	0.267
Total Z_3^{-1} (μm)	-0.354 (0.306)	-0.300 (0.292)	0.553
Total Z_3^{1} (μm)	-0.046 (0.163)	0.024 (0.130)	0.203
Total Z_4^{0} (μm)	0.070 (0.106)	0.080 (0.917)	0.665

HOAs: higher order aberrations, Z_3^{-1}: coma 1 or vertical coma, Z_3^{1}: coma 2 or horizontal coma, Z_4^{0}: spherical aberration.
*U Mann-Whitney test

Table 4.1.2: Total aberrations in T1DM and T2DM patients. Mean (SD) values.

Aberrations	T1DM	T2DM	*p*-value*
Internal Z_3^{-1} (μm)	-0.380 (0.265)	-0.313 (0.264)	0.432
Internal Z_3^{1} (μm)	-0.024 (0.148)	0.029 (0.090)	0.180
Internal Z_4^{0} (μm)	-0.052 (0.099)	-0.030 (0.098)	0.665

HOAs: higher order aberrations, Z_3^{-1}: coma 1 or vertical coma, Z_3^{1}: coma 2 or horizontal coma, Z_4^{0}: spherical aberration
*U Mann-Whitney test

Table 4.1.3: Internal aberrations in T1DM and T2DM patients. Mean (SD) values.

Aberrations	T1DM	T2DM	*p*-value*
Corneal Z_3^{-1} (μm)	0.026 (0.094)	0.013 (0.087)	0.665
Corneal Z_3^{1} (μm)	-0.022 (0.813)	-0.015 (0.097)	0.785
Corneal Z_4^{0}(μm)	0.119 (0.433)	0.099 (0.048)	0.343

HOAs: higher order aberrations, Z_3^{-1}: coma 1 or vertical coma, Z_3^{1}: coma 2 or horizontal coma, Z_4^{0}: spherical aberration
*U Mann-Whitney test

Table 4.1.4: Corneal aberrations in T1DM and T2DM patients. Mean (SD) values.

Wilcoxon test revealed significant inter-eye differences in diabetic patients only for total, internal, and corneal horizontal coma. In T1DM patients, all Zernike terms were statistically different between eyes, except for internal horizontal coma, corneal vertical coma and corneal spherical aberration. However, in T2DM patients, only total horizontal coma and corneal horizontal coma were statistically different. In T1DM, correlation analysis showed that age was correlated with corneal vertical coma Z_3^{-1} ($r = 0.563$, $p=0.036$) and inversely with total HOAs ($r = -0.644$, $p=0.013$) (Figure 4.1.1). Posterior asphericity (Q) was significantly correlated with total HOAs ($r = 0.754$, $p=0.002$) (Figure 4.1.2), anterior Q was significantly correlated with total spherical aberration Z_4^0 ($r = 0.563$, $p=0.036$) and inversely correlated with internal vertical coma Z_3^{-1} ($r = -0.625$, $p=0.017$). In T2DM patients, age was correlated with total HOAs ($r = 0.821$, $p<0.001$) and inversely correlated with total and internal vertical coma Z_3^{-1} ($r = -0.782$ and -0.732, respectively; both $p<0.001$) (Figures 4.1.1, 4.1.3, and 4.1.4 respectively). CCT was correlated with total HOAs ($r = 0.499$, $p=0.018$) and inversely correlated with total (Figure 4.1.5) and internal vertical coma Z_3^{-1} ($r = -0.524$, $p=0.012$ and $r = -0.477$, $p=0.025$, respectively). ACV was inversely correlated with total HOAs ($r = -0.495$, $p=0.019$). Anterior Q was inversely correlated with total vertical coma Z_3^{-1} ($r = -0.453$, $p=0.034$).

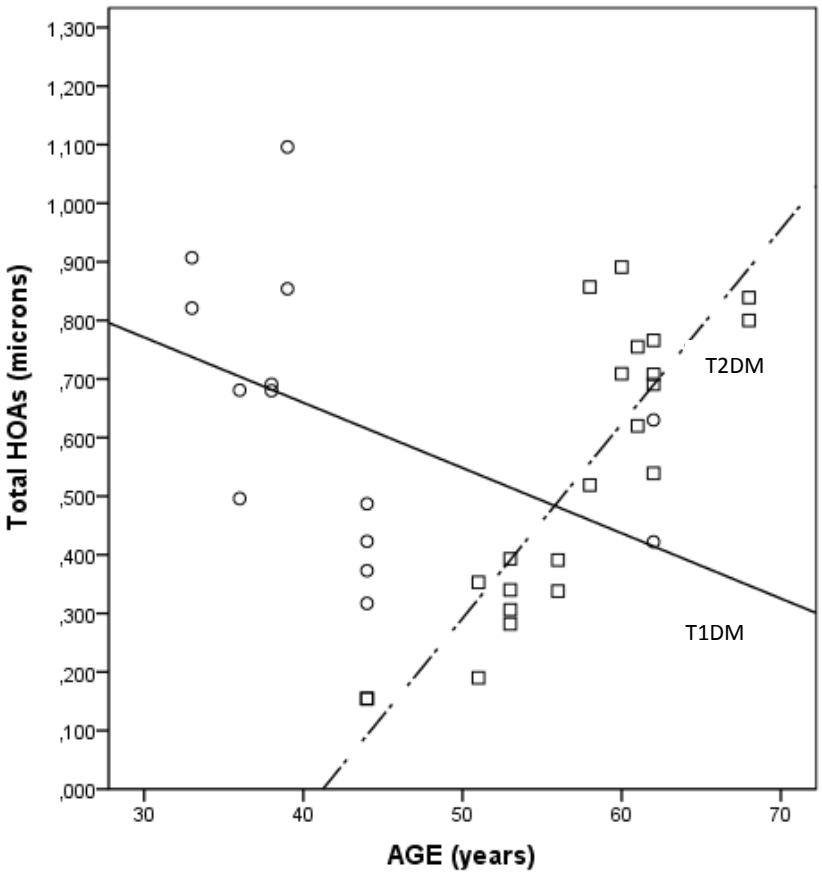

Figure 4.1.1: Correlations between total HOAs and age in T1DM patients (circles and solid line, r = -0.644; p=0.013) and T2DM patients (squares and dashed/dotted line, r = 0.821, p<0.001).

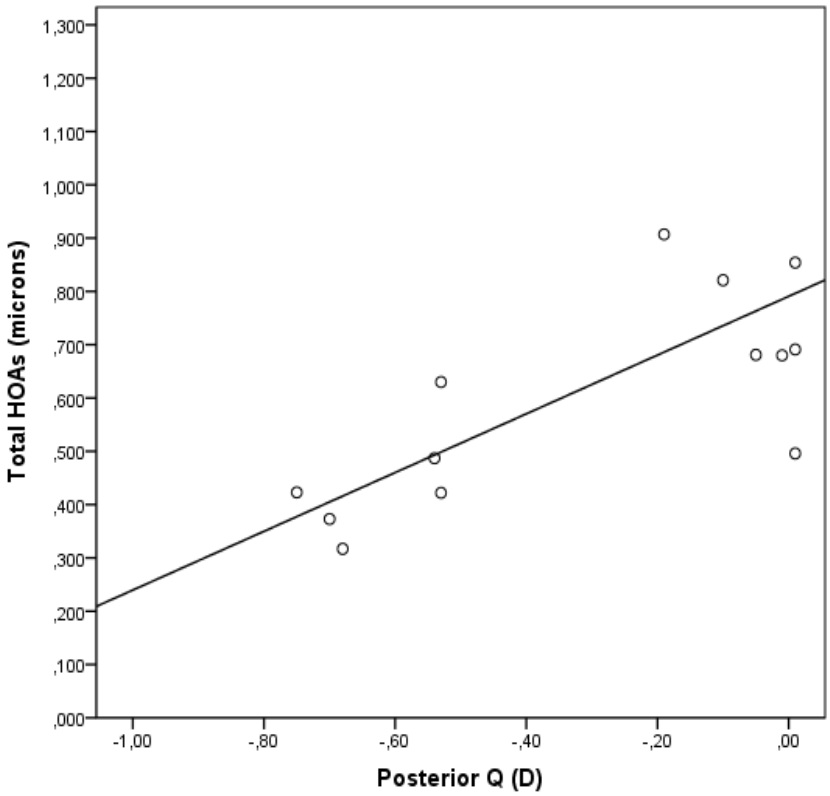

Figure 4.1.2: Correlation between total HOAs and posterior Q in T1DM patients (r = 0.754; p=0.002).

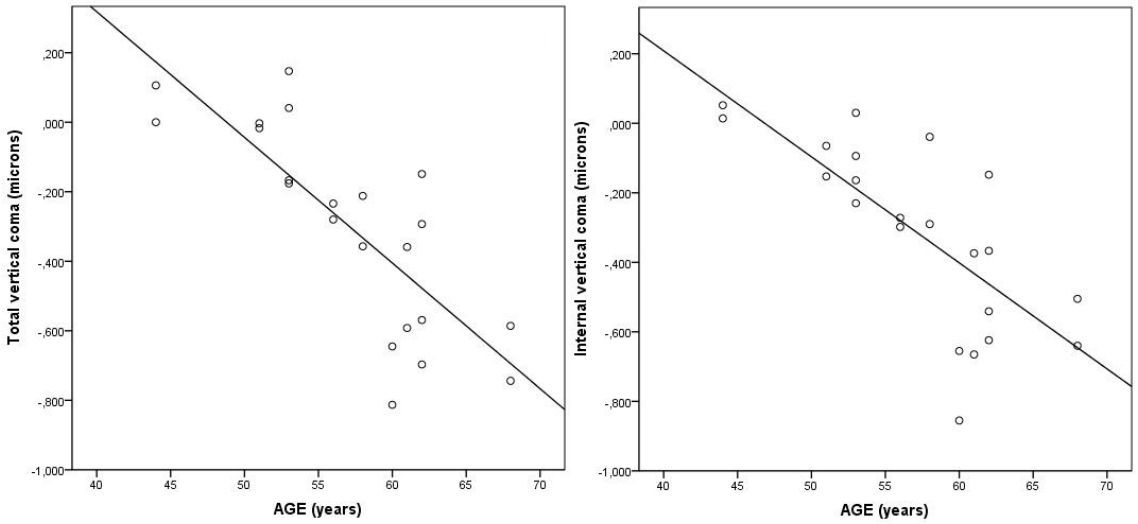

Figure 4.1.3 and Figure 4.1.4: Correlations between age and total vertical coma (Z_3^{-1}) and internal vertical coma (Z_3^{-1}) in T2DM patients (r = -0.782; p<0.00; r = -0.732; p<0.001; respectively).

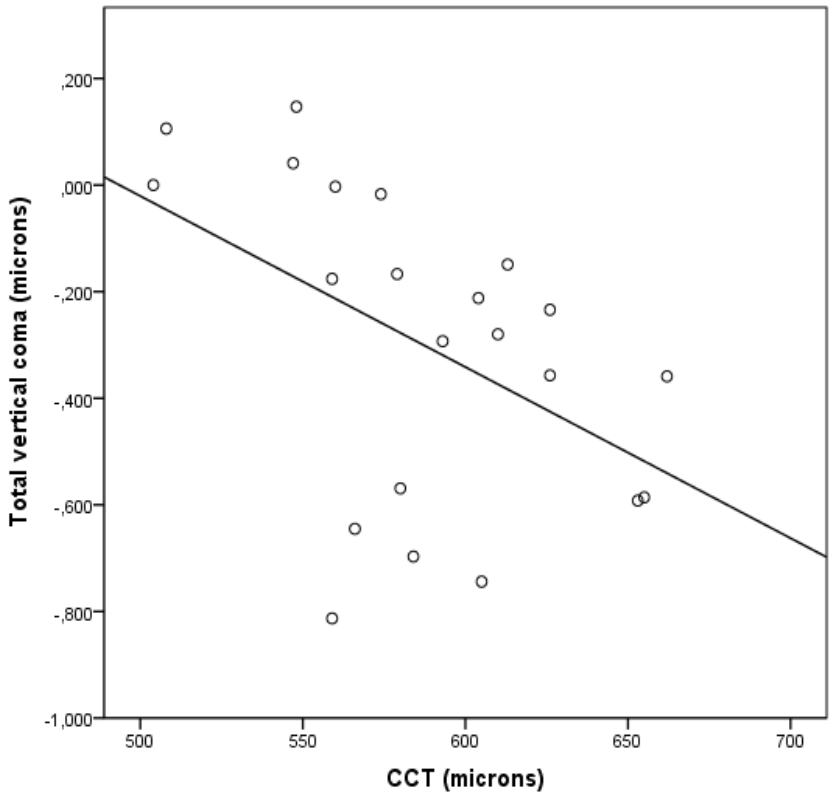

Figure 4.1.5: Correlation between total vertical coma (Z_3^{-1}) and CCT in T2DM patients (r = -0.524; p=0.012).

4.1.4 DISCUSSION

The retinal image quality is determined by the combination of corneal (anterior surface) and internal aberrations (posterior corneal surface and crystalline lens). In the presence of corneal and/or lens disorders, the optical structure of the eye is altered, causing changes in the ocular aberrations.

Alterations in tear film have been observed in diabetic patients, the most frequent being reduced tear secretion (Dogru et al., 2001; Goebbels, 2000; Ozdemir et al., 2003; Yoon et al., 2004), tear film instability (Dogru et al., 2001; Ozdemir et al., 2003; Yoon et al., 2004), higher grade of conjunctival squamous metaplasia (Dogru et al., 2001; Goebbels, 2000; Yoon et al., 2004), and lower cell density (Dogru et al., 2001; Yoon et al., 2004).

Corneal epithelial and endothelial cells show polymorphism, polimegatism and changes in the cellular coefficient of variation (Inoue et al., 2002; Rehany et al., 2000;

Roszkowska et al., 1999; Sánchez-Thorin, 1998). Some researchers indicate that patients with DM show changes in biomechanical behavior of the cornea, such as a tendency to present a greater CCT (Roszkowska et al., 1999) related to duration of DM (Calvo-Maroto et al., 2015) and higher corneal hysteresis (CH) values (Hager et al., 2009). The lens of diabetic patients has been found to be thicker and more convex than in healthy subjects (Bron et al., 1993; Brown and Hungerford, 1982). These alterations in corneal and lens thickness may induce changes in its anterior and posterior surfaces. Moreover, diabetic patients experience vitreous degeneration earlier than those without DM (Stitt et al., 1998).

Wavefront analysis is a useful tool for evaluating the optical quality of the eye. HOAs measurements show the consequences of ocular changes into visual quality. So in diabetic eyes, HOAs values may increase because of disease-related changes in the optics of the eye. Previously, CH has been suggested as an indicator of biomechanical changes caused by DM (Hager et al., 2009). It might be that HOA measurements in diabetic patients become a useful tool to evaluate and monitor in vivo and non-invasively diabetes-mediated changes. The present pilot study investigated total, internal, and corneal coma and spherical aberration in two groups of diabetic patients (T1DM and T2DM) to know the distribution of HOAs and establish a relationship between HOAs and ocular parameters.

Several studies have measured the aberrations of a large population, showing large inter-subject variability in ocular aberrations (Castejón-Mochón et al., 2002; Liang and Williams, 1997; Porter et al., 2001). In the present study, intra-subject inter-eye variability in total, internal, and corneal horizontal coma in diabetic patients has been found. T1DM patients showed inter-eye variability in more Zernike terms than T2DM patients.

Porter et al. (2001) in their study with 109 normal subjects (mean age 41 years) investigated the distribution of ocular aberrations across 5.7 mm pupil and showed that HOAs in any population are approximately zero except for spherical aberration which averages to a slightly positive values (+0.138 ± 0.103 μm). Castejón-Mochón et al. (2002) observed the mean value for every Zernike term (except second order) was lower than 0.03 μm across 5 mm pupil in 59 young subjects (mean age 24 ± 3 years); the mean total RMS for pupil of 5 mm was 1,49 μm, but HOAs had an impact of only 9.2%

on the total RMS. Wang et al. (2003) reported a value of total HOA RMS across 6 mm pupil of 0.305 µm ± 0.095 in 532 eyes (mean age 41 ± 10 years), and the mean coefficients for comatic components (Z_3^{-1}, Z_3^{1}) and spherical aberration (Z_4^{0}) were -0.055 ± 0.142 µm, 0.009 ± 0.106 µm, and 0.101 ± 0.103 µm, respectively.

The present study reports the values of coma and spherical aberration across 5mm pupil in two groups of diabetic patients, without significant differences in ocular parameters (Table 4.1.1). The T1DM group showed total HOAs values slightly higher than T2DM (Table 4.1.2). We found higher mean total HOAs in T1DM and T2DM patients than those reported by Wang et al. (2003) in their study. Total HOA RMS values were not reported in studies of Porter et al. (2001) and Castejón-Mochón et al. (2002). The mean of vertical coma component Z_3^{-1} in T1DM and T2DM patients was more negative than those showed by the studies mentioned above. Shahidi et al. (2004) found that HOAs, in their 22 chronic diabetics, were significantly higher than in normal subjects (mean age 52 ± 12 years and 6 mm pupil size), total HOA RMS value for diabetic patients reported was 0.45 ± 0.18 µm.

This study shows that the greatest contributor to total ocular aberrations was internal vertical coma Z_3^{-1} for both groups (Tables 4.1.2 and 4.1.3). Wang et al. (2003) in 114 subjects (mean age 42 ± 13 years) showed that the means for internal comatic coefficients Z_3^{-1} and Z_3^{1} were 0.060 ± 0.112 µm and 0.033 ± 0.137 µm across 5 mm pupil, respectively. These differences suggest that certain changes in posterior cornea or crystalline produced by DM are responsible for increased HOAs in diabetic patients.

With respect to anterior corneal HOAs, studies with healthy subjects reported that the HOAs are dominated by the 3rd-order and 4th-order Zernike terms (Lombardo and Lombardo, 2010; Montés-Micó et al., 2004a). We found slightly lower mean values of spherical aberration Z_4^{0} coefficients, and higher vertical coma Z_3^{-1} coefficients than those reported by Wang et al. (2003) (Table 4.1.4).

Some investigators have observed that internal surfaces compensate the aberrations from the anterior corneal aberrations in younger subjects, for this reason the total ocular HOAs were lower than anterior corneal aberrations (Artal et al., 2001; He et al., 2003). This process was significant in the horizontal/vertical astigmatism, horizontal coma, and spherical aberrations components, causing a decrease in their contribution to total ocular aberrations (Kelly et al., 2004). In this study, a partial balancing effect was

observed in spherical aberration Z_4^0 and vertical coma Z_3^{-1} but not in horizontal coma aberrations Z_3^1.

Some studies have demonstrated an increase of corneal or ocular coma with ageing (Dubbelman et al., 2007; Guirao et al., 2000; Wang et al., 2003).

Although it would be desirable, differences in HOAs for different age groups of DM could not be analyzed due to the sample size limitations. In T1DM patients, ageing was correlated with corneal vertical coma Z_3^{-1} ($p<0.05$) and inversely correlated with total HOAs ($p<0.05$) (Figure 4.1.1). In T2DM patients, age was correlated with total HOAs (Figure 4.1.1), and inversely with total and internal vertical coma Z_3^{-1} (both $p<0.01$) (Figures 4.1.3 and 4.1.4, respectively).

Moreover, CCT was correlated with total HOAs. However total (Figure 4.1.5) and internal vertical coma Z_3^{-1} becomes more negative with an increase of CCT ($p = 0.012$ and $p = 0.025$, respectively). We have not found that any parameters of the posterior corneal surface were correlated with internal vertical coma Z_3^{-1}.

Dubbelman et al. (2007) demonstrated that the posterior corneal surface compensates 3.5% of coma derived to anterior surface. Due to this compensation being negligible, they suggested that the principal contributors of total coma are anterior corneal surface and crystalline lens.

Considering our results, we observed that internal HOAs were higher than corneal HOAs. It can be therefore suggested that posterior cornea and crystalline lens changes caused by DM are responsible for this increase of HOAs. It is proposed that glycation and elevated concentration of AGEs are responsible for a premature aging in crystalline lens and basement membranes changes. As a consequence, these alterations would cause those T1DM patients to show slightly higher internal aberrations than those with T2DM despite being significantly younger than T2DM patients.

Although glucose levels and duration of DM might partly explain this increase, this data was not available for analysis.

Therefore, the idea that HOAs measurements could be a parameter for monitoring DM changes in the manner of CH was proposed by Hager et al. (2009). Although both parameters are indicative of DM progression, corneal changes

responsible of higher CH are in anterior and central stroma. Meanwhile, in our study we observed that changes in posterior cornea and crystalline lens cause higher values of HOAs.

Due to the limited sample size, the results of all these analyses must be interpreted as trends in diabetic patients that require further research. This pilot study has limited sample size as main limitation, but other limitations include the following: (1) including both eyes in the analysis, (2) lack of control sample of healthy subjects, although there is extensive literature on optical quality of healthy eyes, (3) not including information regarding duration of diabetes and HbA1c levels, although all diabetic patients had stable and well-controlled blood glucose levels.

In summary, this chapter describes the trends of wave aberration patterns observed on a small sample of T1DM and T2DM patients for 5 mm pupil size. We observed that these patients showed higher values of total and internal vertical coma. In T2DM, these increases seem to be primarily due to age-related changes of the crystalline lens. In T1DM we have not found correlations between both total and internal vertical coma and ocular parameters to explain these increases. These results show the clinical usefulness of optical quality measurements as an aid for monitoring changes due to DM, although further studies are needed to confirm the trends found here on larger cohorts of diabetic patients.

CHAPTER 5

State-of-the-Art in Fundus

Autofluorescence imaging methods

5.1 BASIC MECHANISM OF AUTOFLUORESCENCE

Fluorescence is the result of a three-stage process that occurs in exogenous and endogenous fluorophores. The process responsible for the fluorescence phenomenon is frequently illustrated using the Jablonski diagram (Johnson and Spence, 2010) (Figure 5.1).

The three stages involved in the AF phenomenon are described in the following:

Stage 1. Excitation. A photon with a defined energy ($h\upsilon_{EX}$) is provided by an external source and absorbed by the fluorophores in femtoseconds, causing an excited electronic single state (S_2). This process is very fast, on the order of 10^{-15} seconds.

Stage 2. Excited-State Lifetime. In this stage, the fluorophore undergoes conformational changes and may interact with its molecular environment, leading to energy dissipation. This process is also very fast, between 10^{-14} and 10^{-11} seconds. The first cause of energy loss is through vibrational relaxation, where the energy of electron is transferred as kinetic energy. This energy may remain in the same molecule or may be transferred to other vibrational states (S_1), being this process known as *internal conversion*, or to other molecules around the excited molecule, known as *vibrational relaxation*, where molecules may return to ground state (S_0).

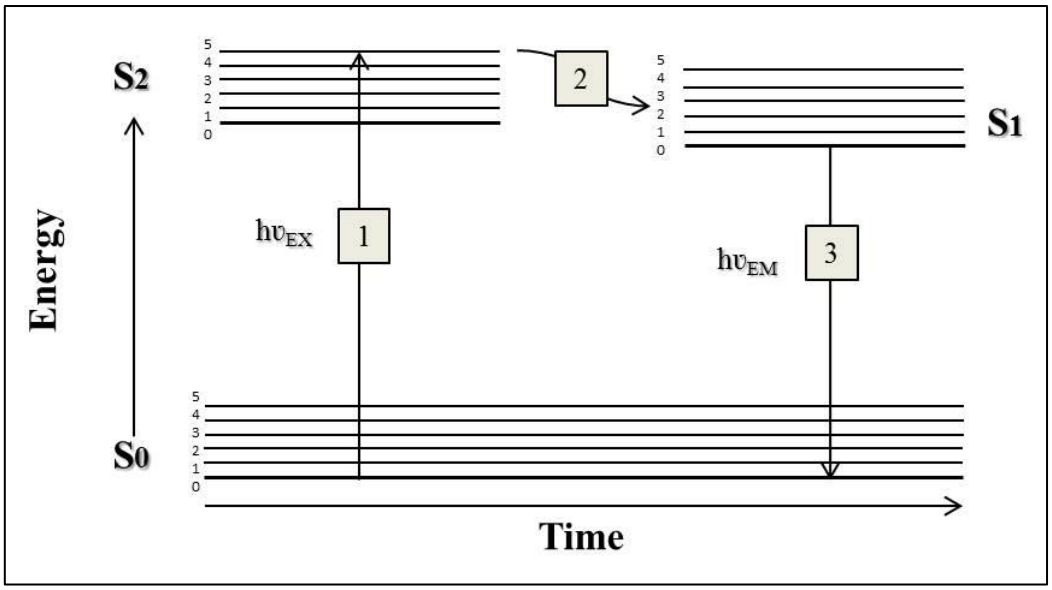

Figure 5.1: Jablonski diagram illustrating the basic mechanism of fluorescence. Bold lines represent the limits of electronic energy states. Within each electronic energy states are represented several vibrational energy states (Calvo-Maroto et al., 2016a).

When vibrational energy levels overlap electronic energy levels, the excited electron can have a transition from a vibrational level in one electronic state (S_1) to another vibrational level (S_2) in a lower electronic state. Other process can cause a decrease of fluorescence intensity such as collisional quenching, fluorescence resonance energy transfer and intersystem crossing (Johnson and Spence, 2010). Since fluorescence spectroscopy is sensitive to molecular dynamics during the lifetime in the excited state, the measurements of time-resolved fluorescence allow the detection of fluorophores according to the fluorescence decay time (Schweitzer et al., 2007).

Stage 3. Fluorescence emission. A photon of a particular energy ($h\upsilon_{EM}$) is emitted when the fluorophore returns to its ground state S_0. Due to energy dissipation through internal conversion and vibrational relaxation in the second stage, the energy of fluorescent photon is always less than that of the excited photon. Fluorescence emission is the slower stage of the whole process being in the order of 10^{-9} to 10^{-7} seconds.

Thus, the emitted electron has less energy than the absorbed photon that is at a longer wavelength. This difference between excitation and emission energies (or wavelengths) is called the Stokes shift. The Stokes shift allows that fluorescent emission can be detected from excitation photons.

The fluorescence process is cyclical, so the same fluorophore can be repeatedly excited and detected, and can generate detectable radiation. Both processes are fundamental to the sensitivity of fluorescence devices (Johnson and Spence, 2010). For polyatomic molecules, the electronics transitions represented in Figure 5.1 are replaced by broad energy spectra called *fluorescence excitation spectrum* and *fluorescence emission spectrum*. Both spectra show relative intensity of fluorescence through group consecutive wavelengths. So, the emission intensity depends of the excitation wavelength used. To define the emission spectrum of a particular fluorophore, the wavelength of maximum excitation is detected by means of fluorescence excitation spectrum, and the fluorophore is excited at that wavelength. The relative intensity of the fluorescence is measured at various wavelengths to obtain the emission spectrum.

The bandwidth of these spectra has an important interest for applications in which several different fluorophores are simultaneously detected. There are usually an overlay between the higher excitation wavelengths and the lower emission wavelengths (Johnson and Spence, 2010). This overlay must be eliminated by the suitable selection of an excitation filter and barrier or emission filter. If this is not the case, the brighter excitation light overlaps the weaker emitted fluorescence light leading to a decrease in contrast.

The manufacturers usually indicate the wavelength for the peak of the illumination excitation intensity and the wavelength for the peak of the fluorescence emission intensity.

5.2 OCULAR ENDOGENOUS FLUOROPHORES

Most ocular tissues exhibit natural fluorescence as a result of exposure to light. The molecules responsible for this AF are called ocular endogenous fluorophores. However, ocular AF can be also induced by certain fluorescing drugs, denominated exogenous fluorophores, which are used for specific diagnosis or therapeutic purposes, such fluorophotometry and fluoroangiography (Roberts, 2001). An overview of the ocular endogenous fluorophores located in the cornea, the crystalline lens and the retinal pigment epithelium (RPE) has been summarized in Table 5.1.

CORNEA

Corneal fluorescence is originated from endogenous fluorophores that are physiologically present in corneal structure. It is still uncertain which fluorophores are responsible for corneal AF, but some reports suggest that corneal AF may be caused by pyridine nucleotides (e.g. nicotinamide dinucleotide (NAD) and nicotinamide dinucleotide phosphate (NADP)) and flavoproteins (e.g. flavin adenine dinucleotide (FAD) and flavin mononucleotide (FMN)) resulting from impaired metabolism of corneal mitochondrial respiration (Chance et al., 1979; Rovati and Docchio, 2004). For this reason, corneal AF is considered an indicator of metabolic health of the cornea (Van Schaik and Van Best, 1997).

The flavoproteins fluoresce in their oxidized redox form (excitation maximum at 450 nm and emission maximum at 550 nm), whereas pyridine nucleotides fluoresce in their reduced redox state (excitation maximum around 366 nm and emission maximum at 450 nm) (Chance et al., 1979; Rovati and Docchio, 2004).

These fluorophores are located in the corneal epithelium and endothelium, whereas corneal AF is distributed over the cornea and decreasing from endothelium to epithelium layers (Rovati and Docchio, 2004). This distribution implies, as suggested by van Schaik et al. (1999a), that corneal AF cannot be only explained by these endogenous fluorophores.

In addition to these fluorophores, corneal AF can also be originated from glycosilated collagen via Maillard reaction, which eventually causes the formation of AGEs (Grandhee and Monnier, 1991). The excitation spectrum of AGEs fluorescence is 360-370 nm, with an emission spectrum around 430-450 nm (Sato et al., 2001).

Ocular Tissue	Study conditions	Endogenous fluorophores	Excitation wavelengths (nm)	Emission wavelengths (nm)
Cornea		Flavoproteins	λex= 450	λem= 550
	In vivo	Pyridine nucleotides	λex= 366	λem= 450
		AGE	λex= 360-370	λem= 430-450
	In vitro	-	-	
Lens		Tryptophan	λex= 290	λem= 340
	In vivo	Nontryptophan	λex= 364-472	λem= 437-523
		3-HGK	λex= 520	λem= 550
		AGE	λex= 360-370	λem= 430-450
	In vitro	Red	λex= 647	λem= 672
		Near-red	λex= 568	λem= 633
		Orange	λex= 568	λem= 591
RPE	*In vivo*	Lipofuscin	λex= 300-600	λem= 480-800
		Melanolipofuscin	λex= 364	λem= 540
	In vitro	Melanin	λex= 350-450	λem= 440-560

RPE: retinal pigment epithelium; AGE: advanced glycation end products; 3-HGK: hydroxykynurenina glucoside; λex: excitation wavelength; λem: excitation emission.

Table 5.1: Characteristics of ocular endogenous fluorophores.

LENS

Lens AF is produced as a result of the accumulation of fluorophores located in different parts of the lens. There are two AF bands in the human lens (Sparrow et al., 1992b): the age-independent ultraviolet (UV) band (maximum at around 290 nm for excitation and around 333 nm for emission) (Beneyto and Pérez, 2006), and the blue band (maximum at around 348 nm for excitation and around 420 nm for emission) that increases as a function of age (Beneyto and Pérez, 2006; Sandby-Møller et al., 2004).

Ultraviolet band is associated with the yellow pigment of ageing and cataract formation, and may be derived from tryptophan (Beneyto and Pérez, 2006; Sparrow et al., 1992b). Lens fibers are free from organelles, and lens proteins within these fibers,

such as crystallins (α, β and, γ) are long-lived, which facilitates the accumulation of AGEs throughout life (Abiko et al., 1999; Monnier and Cerami, 1981). This accumulation is assumed to contribute to the gradual decrease in tissue and organ function observed with ageing (Burd et al., 2012). All crystalline species show tryptophan fluorescence (excitation maximum at 290 nm and emission maximum around 340 nm) and their distribution is uniform throughout the lens cross sections (Jacobs and Krohn, 1981), as is the distribution of proteins (Sue Menko, 2002).

Blue band fluorescence has been related to the insolubilization of lens proteins associated with ageing (Yappert et al., 1992). Although the origin of this fluorophore is still unknown, kynurenine-type derivatives from photo-oxidation of tryptophan residues have been suggested as possible candidates. These derivatives have also been proposed by their photosensitive capacity for the production of reactive oxygen species, enhancing polypeptide cross-linking (Andley et al., 1997; Roberts, 2001). However, this source of lens AF is disputable because of the negligible fluorescence emission detected upon excitation of 3-hydroxy-kynurenine (3-HGK) in water at different pH (Kessel et al., 2002). This endogenous photosensitizer combined to long-wavelength UV light causes the fluorescence of non-tryptophan (Rovati and Docchio, 2004).

Non-tryptophan fluorophore is not present in the newborn and fetal lens (Rovati and Docchio, 2004), although there is an increase of water-insoluble proteins fractions within the lens with ageing and cataract formation (Lampi et al., 2014). Another phenomenon related to ageing is the photo-oxidation process that allows the cross-linking of water-soluble protein in the lens (Bessems et al., 1987). Both processes could facilitate the non-tryptophan fluorophore formation (Rovati and Docchio, 2004).

In addition to the photochemical process, the increase of this fluorophore intensity with age might be metabolically induced (Lampi et al., 2014). Excitation and emission spectra of nontryptophan fluorescence show peaks at longer wavelengths than tryptophan, typically excitation spectra from 364 to 472 nm and emission from 437 to 523 nm (Rovati and Docchio, 2004).

An additional suggestion for the blue band fluorophore would be oxidation products of ascorbic acid and AGEs such as argpyrimidine and pentosidine (Kessel et al., 2002; Sandby-Møller et al., 2004). However, the measurement of AGE-related fluorescence cannot be carried out by noninvasive techniques (Abiko et al., 1999).

Under *in vitro* conditions, red (excitation/emission maximum 647/672 nm), near-red (excitation/emission maximum 568/633 nm), and orange (excitation/emission maximum 568/591 nm) have been also found (Yu et al., 1979).

Another nontryptophan fluorophore has been observed in young eyes. It is produced from 3-HGK (Van Schaik and Van Best, 1997), is not protein bound, and has excitation and emission maxima of 520 and 550 nm, respectively.

RETINAL PIGMENT EPITHELIUM

Fundus AF (FAF) is mainly originated from lipofuscin. Liposfucin is the dominant fluorophore within the retina and is a product of the oxidative breakdown of photoreceptor outer segment located in the RPE (Sepah et al., 2014; Shen et al., 2014). Lipofuscin inhibits lysosomal degradation, is photoreactive and produces oxygen radicals that can reduce the phagocytic capacity of the RPE, RPE cell death and photoreceptor loss (Boulton et al., 2001; Boulton et al., 2004; Sparrow et al., 2003).

Lipofuscin is a heterogeneous group of bisretinoids containing a wide range of fluorophores with an excitation spectrum range from 300 to 600 nm and an emission spectrum from 480 to 800 nm (Durrani and Foster, 2012). The only known fluorophores of RPE liposfucin to date are N-retinylidine-N-retinylethanolamin (A2E), iso-A2E and other minor cis-isomers of A2E (Boulton et al., 2001; Boulton et al., 2004; Durrani and Foster, 2012; Sparrow et al., 2003; Sparrow and Boulton, 2005). Biosynthesis of A2E begins when all-trans retinal leaves the visual cycle to react with phosphatidylethanolamine (PE), thereby generating its precursor N-retinylidine-N-retinyl phosphatidylethanolamine (A2-PE). These fluorophores are formed by phosphate hydrolysis of A2-PE to phosphatidyl-pirydinium bisretinoid (Sparrow et al., 2003) (Figure 5.2). All-trans retinal originated from the visual cycle is a toxic aldehyde produced in the outer segments of the photoreceptor when exposed to light. The excess of all-trans retinal in photoreceptors causes bisretinoid formation, which upon oxidization produces lipofuscin (Sepah et al., 2014; Sparrow et al., 2003). Moreover, a contribution of malondialdehyde (MDA), 4-hydroxynoneual (HNE) and AGEs to the composition of lipofuscin has also been reported (Schutt et al., 2003).

Another fluorophore observed in the RPE is melanin. Although granules of natural melanin show weak fluorescence properties, it has been observed that these fluorescence capabilities increase after oxidative modification of dihydroxyphenylalanine (DOPA)-melanin and melanoprotein (Boulton et al., 2001).

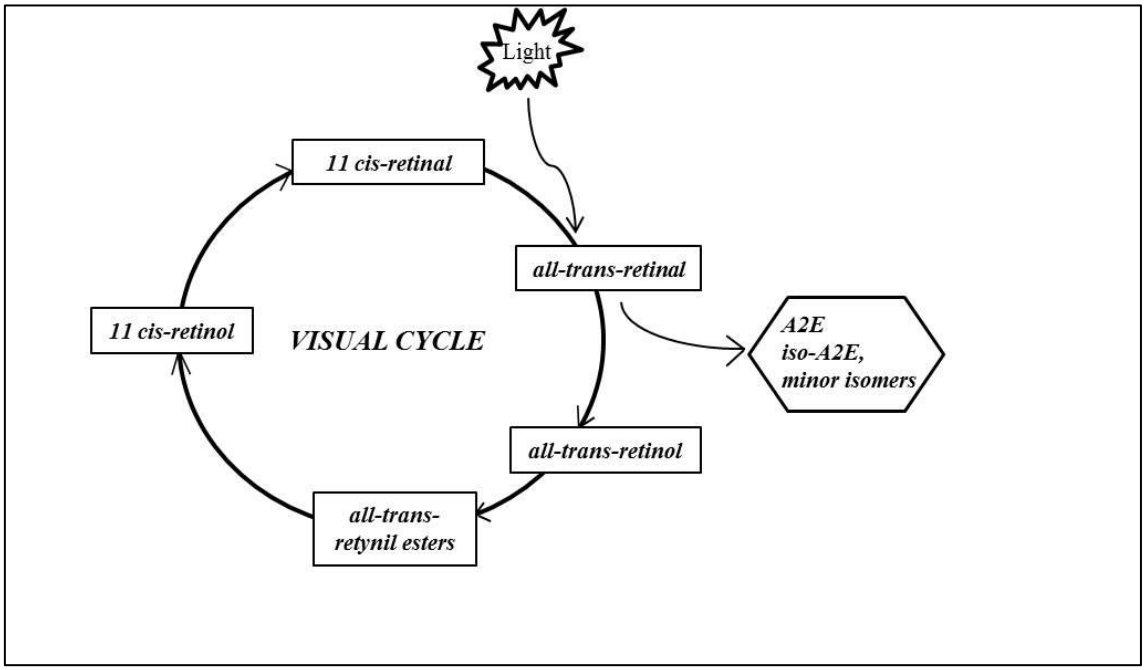

Figure 5.2: The visual cycle that represents several steps of lipofuscin metabolism and N-retinylidine-N-retinylethanolamin (A2E) formation (Calvo-Maroto et al., 2016b).

With ageing, the density of melanosomes in the RPE decreases, whereas an increase of complex granules containing melanin (melanolipofuscin and melanolysosomes) has been observed (Feeney-Burns et al., 1984). The excitation maximum shifts of isolated melanin are from 350 to 450 nm, and emission maximum extends from 440 to 560 nm, in which fluorescence intensity increases with ageing (Boulton et al., 2001). However, the excitation maximum for melanolipofuscin fluorescence is 364 nm, with an emission maximum at 540 nm (Rovati and Docchio, 2004).

These age-related fluorescence properties detected in melanosomes might be due to an association with other components, such as lipofuscin and/or oxidative degradation of melanin polymer from light or hydrogen peroxide (Kayatz et al., 2001).

Furthermore, the retina contains fluorophores such as proteins (haemoglobin and mitochondrial enzymes) with an excitation maximum around 400 nm, flavin and flavoproteins that absorb blue light with maximum at 450 nm and macular pigments whose excitation maximum is around 400-530 nm (Boulton et al., 2001).

5.3 CORNEAL AUTOFLUORESCENCE IN DIABETES MELLITUS

Corneal AF is considered a useful parameter to assess the metabolic state of the cornea (Laing et al., 1992; Van Schaik and Van Best, 1997). When the metabolism of corneal mitochondrial respiration is damaged by conditions such as hypoxia, a decrease of mitochondrial function implies an increase in the reduced pyridine nucleotide fluorescence signal and a decrease in oxidized flavoprotein fluorescence intensity (Masters, 1984).

Several studies have found that corneal AF is higher in diabetic patients than in control subjects (Kitaya et al., 1996; McNamara et al., 1998b; Stolwijk et al., 1992; Van Schaik et al., 1999a; Van Schaik et al., 1999b). The fluorophores responsible for corneal AF are the same in diabetic patients and healthy controls (Kitaya et al., 1996; Stolwijk et al., 1992; Van Schaik et al., 1999b), as previously described, located in the corneal epithelium and endothelium (Rovati and Docchio, 2004). Under hyperglycaemic conditions, there is an increase in corneal AF caused by an increment of flavoproteins within the respiratory chain (Kitaya et al., 1996; Stolwijk et al., 1992; Van Schaik et al., 1999b) .

However, corneal AF is not only caused by oxidized flavoproteins and pyridine nucleotides in a reduced state. The same distribution of corneal AF has been demonstrated in diabetic patients and control subjects characterized by a decrease in intensity from the endothelium to epithelium (Van Schaik et al., 1999a). In DM, diffusion of glucose from the aqueous humour through the cornea occurs when there is a breakdown of the blood-aqueous barrier, resulting in a glucose gradient in the cornea (Van Schaik and Van Best, 1997). An increase in non-enzymatic glycation in corneal

proteins and collagen (via the Maillard reaction) also occurs in DM, that results in an increase corneal AF (Van Schaik et al., 1999a).

Over the past decade, corneal AF in diabetic patients was explored and related to the level of DR (Kitaya et al., 1996; Mori et al., 1997; Roberts, 2001; Sandby-Møller et al., 2004; Van Schaik and Van Best, 1997). Because of the strong correlation reported with PDR (Stolwijk et al., 1992; Van Schaik et al., 1999a; Van Schaik et al., 1999b), AF could be considered a useful method for screening retinopathy diabetic population (Stolwijk et al., 1992). Prolonged high serum glucose levels usually increase retinopathy (Grandhee and Monnier, 1991) and the level of AGEs increases the severity of DR (Stolwijk et al., 1992). Stolwijk et al. (1992) observed a correlation between corneal AF and the severity of DR in T1DM patients and suggested two possible explanations for this correlation. The first explanation is related to the vascular component of DM, in which the severity of DR may be related to changes in lipid and protein metabolism, which could also affect the cornea. Thus, corneal metabolism undergoes a progressive impairment that is associated with an increase in corneal AF. The second explanation is related to the production of neovascularization-mediating substances in retinas with DR. These substances could reach the cornea, causing changes in corneal metabolism and resulting in increased corneal AF intensity (Rovati and Docchio, 2004; Stolwijk et al., 1992).

In addition, a significant correlation has been observed between corneal AF and diabetes duration, metabolic control (HbA1c) in young T1DM patients without retinopathy (Ishiko et al., 1998), and blood glucose changes in T1DM patients with PDR (Mori et al., 1997). However, corneal AF has been found to be independent of age in healthy controls, T1DM or T2DM patients (Stolwijk et al., 1990). Furthermore, a considerable variation in corneal AF throughout the day in diabetic patients with PDR has also been observed (Kitaya et al., 1996).

5.4 CRYSTALLINE LENS AUTOFLUORESCENCE IN DIABETES MELLITUS

Lens AF increases linearly with age in healthy individuals and depends strongly on the amount of sunlight received, namely UV radiation (Bleeker et al., 1986; Bordat et al., 1992; Van Best et al., 1998). Van Best el al. (1998) reported that the yearly increase in lens AF was around 35% larger than calculated from age dependency, and that lens transmittance was at least 130% larger than that calculated form age dependency (Van Best et al., 1998) . Van Best et al. (1998) observed an increase in lens AF and a decrease in lenticular transmittance, and suggested that this change could be attributed to an increase in exposure to solar UV.

With ageing, blue light transmission in the retina decreases because of increased absorption in the lens of blue spectral region (Broendsted et al., 2011), whereas the transmission of green to red light is modified (Rovati and Docchio, 2004). This increase in blue AF intensity with age and cataract formation may be induced metabolically, but has been also proposed to be the result of chronic UV exposure (Bleeker et al., 1986). Nuclear brunescent cataract acts as a filter for blue light, leading to impaired colour vision (Broendsted et al., 2011), as well as protecting the retina from cumulative photochemical damage (Boulton et al., 2001).

Cataract or opacity of the lens is formed by years of gradual decrease in lens transmission caused by an increase of scattering and absorption of light by the lens (Van Best et al., 1985a). A strong correlation between age and loss of blue light transmission was found in healthy lenses, thus, Broendsted et al. (2011) reported that the transmission at 480 nm was reduced by two-thirds at 80 years of age. These processes of decreased transmission could be derived from tryptophan or AGEs accumulation within the lens (Sparrow et al., 1992b). Tryptophan in lens protein undergoes photochemical changes that could be responsible for UV or blue fluorescence (Sparrow et al., 1992b). However, Pongor et al. (1984) demonstrated that lens UV or blue fluorescence is due to products of non-enzymatic glycation of “browned” protein.

In addition to age-related changes in light transmission, several studies have revealed an increase in fluorescence and a decrease in transmission with certain

conditions such as diabetes (Rovati and Docchio, 2004; Sparrow, et al., 1992b; Van Best et al., 1998). Several studies have reported that lens AF is higher in diabetic patients than in healthy subjects (Abiko et al., 1999; Bleeker et al., 1986; Bordat et al., 1992; Bron et al., 1993b; Burd et al., 2012; Sparrow et al., 1992b) and that lens transmission in subjects of about same age was higher in diabetic patients than in healthy subjects (Bleeker et al., 1986; Bordat et al., 1992; Broendsted et al., 2011; Van Best et al., 1985b; Van Best et al., 1998).

This increase in AF could be due to an association between the existence of the nuclear brunescent pigment and the blue/green fluorophores, which has been found to be higher in diabetic patients (Sparrow et al., 1992b). Moreover, non-enzymatic glycation of lens protein increases with age (Monnier and Cerami, 1981) and increased further in diabetes (Garlick et al., 1984). Green lens AF has been related to diabetes (Bleeker et al., 1986) and is considered to be the result of photoxidation of blue fluorophores (Yu et al., 1989).

Lens AF in T1DM patients is related to metabolic regulation and this increase was twice as fast as compared to healthy subjects (Bleeker et al., 1986). A correlation between fluorescence ratio and HbA1c levels has been reported in T1DM patients (Bron et al., 1993; Mori et al., 1997). Blue/green AF is increased in DM and this increase is dependent on duration of DM (Ishiko et al., 1998) and is related to diabetes control (Sparrow et al., 1992b).

The development of cataract is one of the most common complications of DM (Klein et al., 1985). In diabetic patients with cataract, non-enzymatic glycation of "browned" proteins exhibits fluorescence with maximum at around 370 nm for excitation and around 440 nm for emission (Pongor et al., 1984). Other wavelengths, with a fluorescence peak emission range centered in 520 nm, have also been observed in eyes with brunescent cataract (Sparrow et al., 1992b). An association between nuclear brunescence (pigmentation) and AF has been reported in diabetic patients (Sparrow et al., 1992b). The nuclear and cortical regions of the lens exhibit a high intensity of blue/green AF that could be due to a UV light-induced tryptophan photodegradation reaction or nonenzymatic glycation of lens proteins (Rovati and Docchio, 2004).

Lens AF measurement is a practical clinical technique to assess the yellow colouration and opalescence of the human lens nucleus. So, this measurement

technique, together with opacity grading, could be a useful tool for monitoring optical changes in the nuclear zone of the crystalline lens (Siik et al., 1993) and as a measure of cumulative tissue damage due to increased glucose in the plasma and interstitial fluids (Burd et al., 2012).

5.5 FUNDUS AUTOFLUORESCENCE

5.5.1 FUNDUS AUTOFLUORESCENCE IMAGING ACQUISITION

At present, FAF images can be obtained in clinical settings using commercially available devices based on steady-state technology, such as confocal scanning laser ophthalmoscopy (cSLO) and conventional fundus camera with modified filter settings according to excitation properties and emission spectra of endogenous ocular fluorophores, and by lifetime of fluorescence after short time excitation using time-resolved AF technology.

Detection of the steady state autofluorescence

Confocal Scanning Laser Ophthalmoscopy

The cSLO technique is based on confocal principle where a pinhole is conjugated with lens focal point, so it is called as confocal pinhole. This technique uses a point source that projects a low-power beam on the retina and a point detector, which have a common focal point so that scattered light does not fall on the detector, improving the signal/background ratio. Since a point source is used, the retina must be scanned both horizontally and vertically for building a two-dimensional image (Webb et al., 1987). Figure 5.3 represents a schematic diagram of the illumination and imaging paths in cSLO.

To reduce the background noise and improve image contrast, cSLO records several single images by standard video scanning rates, and the final FAF image is resulting from the average of several frames and pixel values normalization (Schmitz-Valckenberg and Fitzke, 2009; Ciardella and Eandi, 2009). The image size is a retinal

field of 30x30 degrees, although this size can be increased using additional lenses (Schmitz-Valckenberg and Fitzke, 2009).

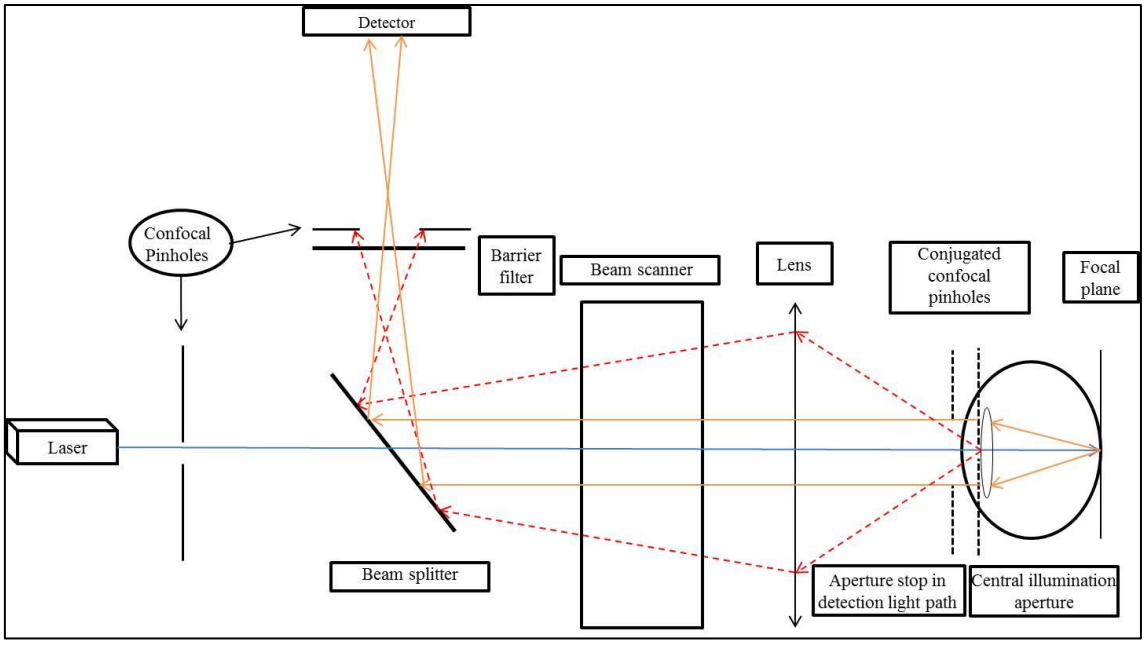

Figure 5.3: Schematic diagram of cSLO showing illumination and imaging paths (Calvo-Maroto et al., 2016a).

Several types of cSLO have been used to capture FAF images: the Zeiss prototype SM 30 4024 (ZcSLO, Zeiss, Oberkochen, Germany), the Rodenstock cSLO (RcSLO; Rodenstock, Weco, Düsseldorf, Germany), the Heidelberg Retinal Angiography system (HRA classic, HRA 2, Spectralis®, Heidelberg Engineering, Dossenheim, Germany), the F-10 (Nidek, Aichi, Japan) and the Optomap® Panoramic 200 Tx (Optomap; Optos, Scotland). Their excitation and detection wavelengths are summarized in Table 5.2.

The HRA 2 is a confocal scanning laser ophthalmoscope that uses a blue laser light with an excitation wavelength of 488 nm to illuminate the retina, and a barrier filter of 500 nm to provide FAF imaging (Bellmann et al., 2003). This device provides an automatic real-time imaging so that the final mean and normalized image is obtained during acquisition.

	Excitation wavelength (nm)	Detection wavelength (nm)	Resolution* (μm)	Field of view (degrees)
SPECTRALIS®	488	>500	5,10	20,30,55
F-10	490	510	16-20	40,60
Optomap® Panoramic 200 Tx	532	540-800	11,14	200

cSLO: Confocal scanning laser ophthalmoscope.
*Transversal resolution at the image plane.

Table 5.2: Technical characteristics of the commercially available cSLO devices.

The last improvement has been the combination of spectral-domain optical coherence tomography (SD-OCT) with cSLO fundus imaging known as Spectralis® (Spectralis SD-OCT, Heidelberg Engineering GMbH, Heidelberg, Germany). This combination allows simultaneous cSLO and OCT recordings, the registration of fundus imaging by cSLO and synchronous topographic alignment by OCT scans. This device presents several advantages with respect to HRA 2, such as an automated image alignment for correcting eye movements during image acquisition. Its dual-beam mode decreases eye motion artefact and ensures a structural correlation between OCT and FAF images without posterior images processing. Another advantage is the elimination of subjective operator placement in posterior scans for monitoring retinal diseases. This mode uses the map obtained from eye tracking to automatically place follow-up scans in the same location as the baseline scan. In addition, Spectralis® also offers FAF image acquisition by blue laser light AF and by multiple laser colours that provide diagnostic information from different retinal structures within a single examination. This last imaging mode can be observed using individual colour imaging (blue, green and infrared reflectance), offering structural details of different depths of the retina. Light penetration depth is dependent on the wavelength used, so the different wavelengths penetrate tissue to different depths and therefore provide structural information from different depths within the retina. Thus, the blue, green and infrared reflectance images give information about the nerve fiber layer, the retinal cells, and the choroid and RPE, respectively. The blue reflectance images allow observing spot changes in superficial retinal structures. The green reflectance images are very useful for assessment blood, blood vessels, and exudates. The infrared reflectance images show deeper structures in

the choroid and the RPE. Figure 5.4 shows high magnification of macular central zone from FAF image in a healthy subject, image obtained from Spectralis®.

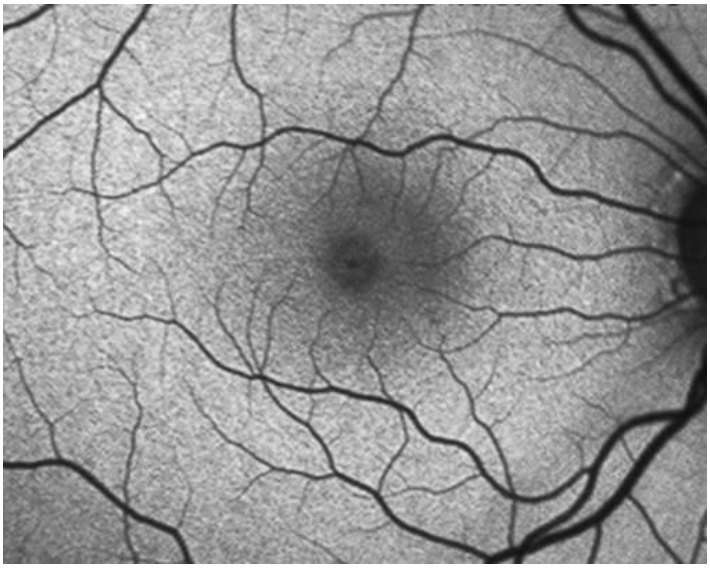

Figure 5.4: Central macular area in a healthy subject acquired with SPECTRALIS®. (Available at www.heidelbergengineering.com; Last accessed July 2016).

Another commercially available cSLO based system is the F-10 that also provides FAF imaging. This device has four different laser sources for different kinds of observation of retinal and choroidal images: infrared (excitation wavelength at 790 nm), red (excitation wavelength at 660 nm), green (excitation wavelength at 532 nm), and blue (excitation wavelength at 490 nm). The last excitation wavelength is used for acquiring FAF imaging. The image size has a field of view of 40º or 60º, an optical resolution of 16-20 μm and image resolution of up to 1024x720 pixels. The use of Retro Mode imaging technique employs an infrared wavelength (λ=790 nm) and an aperture with a modified central stop. This aperture is deviated laterally from the confocal light path, and may be positioned to the left or right side of the fundus. The scattered light passing through the deviated aperture gives a shadow to features such as subretinal deposits, thus enhancing the contrast and delineation of the features.

The Optomap® Panoramic 200 Tx is a non-mydriatic SLO with two laser wavelengths scanning at 532 nm (green laser) and 635 nm (red laser). Both images can be observed separately or superimposed by the software to yield semi-realistic colour

imaging. Green laser allows observation of the sensory retina from the RPE, while red laser visualizes the choroidal features. This device allows non-mydriatic high resolution images through 2 mm pupil diameter and by a special mirror design is able to acquire wide-field images of approximately 180-200^{o}. The optical resolution in FAF and fluorescein angiography imaging is 14 μm. For green-light FAF imaging, an excitation wavelength of 532 nm and detection wavelength range from 540 nm to 800 nm is used (Reznicek et al., 2013).

In a comparative study, Bellman et al. (2003) used ZcSLO, RcSLO and HRA classic for obtaining FAF imaging. As mentioned previously, all three use excitation wavelength of 488 nm and emission wavelengths above 500 nm for the HRA classic, above 515 nm for the Rodenstock cSLO and above 521 nm for the ZcSLO. The laser output was constant and comparable on all cSLOs with 230 μW for the ZcSLO, 255 μW for the RcSLO, and 265 μW for the HRA classic. They observed that image contrast and image brightness were significantly higher with the ZcSLO and HRA classic compared to RcSLO. They attributed these differences to the amount of light blocked by the different filters used, the size of pinhole aperture, the degree of amplification of argon laser and the sensitivity of the photodetector. Using a model eye, the highest background noise was measured with the ZcSLO and the lowest with the HRA classic. Thus, they concluded that the differences observed should be taken into account when FAF findings are obtained with different imaging devices (Bellmann et al., 2003). However, the Heidelberg Retinal Angiography (HRA classic, HRA 2 and HRA Spectralis®) is the only one currently available.

Conventional fundus cameras

In the past, the use of conventional fundus cameras for acquiring FAF imaging in the same range as the cSLO had several limitations such as low FAF signal, AF of the crystalline lens, and the nonconfocality of fundus camera, leading to light scattering. Delori et al. (1995) introduced an aperture in the illumination optics of the camera reducing the loss of contrast caused by light scattering and fluorescence from the crystalline lens, although the angle of view was reduced to 13°. This disadvantage and the complex design were the reasons why this device was not used by other clinicians (Delori et al., 1995). In 2003, Spaide introduced a modification in a commercially

available fundus camera moving the excitation and detection wavelengths towards the red end of the spectrum to avoid the fluorescence of the lens (excitation wavelength 500-610 nm, emission barrier filter 675-715 nm), and in 2008 introduced an additional modification of the filters (excitation wavelength 535-585 nm, emission barrier filter 615-715 nm) (Spaide, 2008).

Retinal camera system uses a continuous illumination ring of lower power with a high-energy white flash (300 watt-seconds) and a hole mirror as excitation beam, but also a wideband excitation filter. This combination allows that only the annulus of this mirror penetrates ocular media, reaching deep within the RPE, and excites any existing lipofuscin. The lipofuscin fluorescence signal is able to pass through the hole reaching the sensor on the retinal camera. The result is a single monochromatic and real time image that reveals either the presence or absence of lipofuscin. Figure 5.5 represents a schematic diagram of conventional fundus camera.

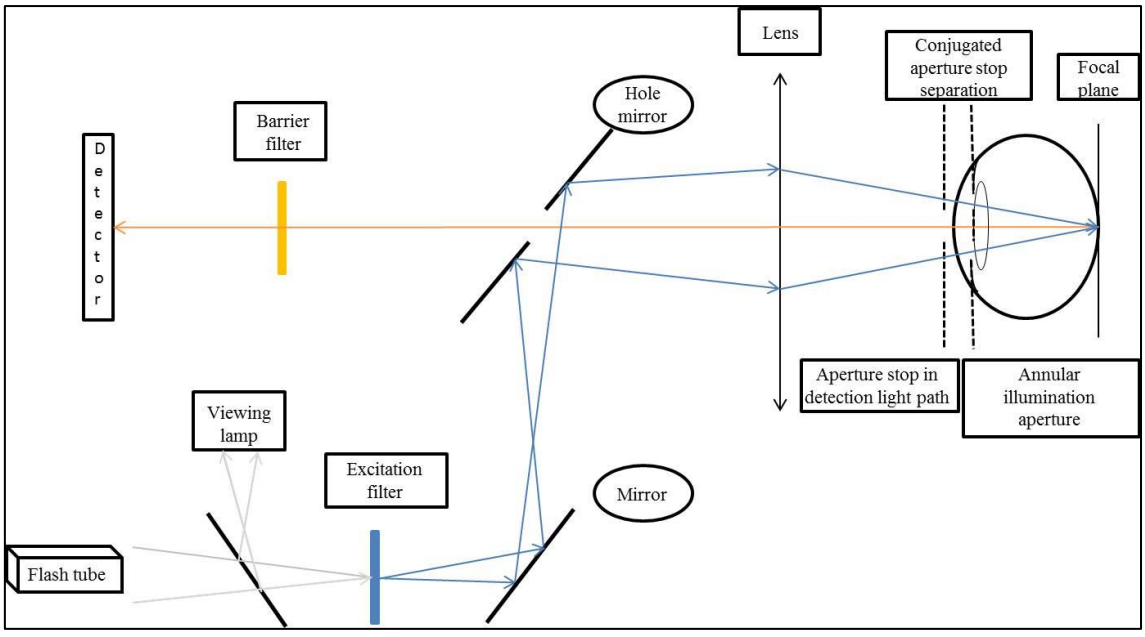

Figure 5.5: Schematic diagram of conventional fundus camera showing illumination and imaging paths (Calvo-Maroto et al., 2016a).

Currently, there are several commercially available digital retinal cameras which allow the acquisition of FAF images: CX-1 and CR-2 Plus fundus cameras (Canon, Tokyo), Visucam 200, Visucam 500, Visucam NM/FA and FF 450 Plus IR cameras (Carl Zeiss Meditec, Jena, Germany), TRC-50DX and TRC-50IX cameras (Topcon Medical Systems, Oakland, NJ). Their excitation and detection wavelengths are summarized in Table 5.3.

The CX-1 and CR-2 Plus cameras use an excitation wavelength range from 530 nm to 580 nm and a detection filter at 640 nm. Figure 5.6 shows high magnification of macular central zone from FAF image in a healthy subject acquired with the CR-2 Plus camera. Also, they have a full set of cobalt, blue, green and red filters to extract more in-depth information from the captured image. The cobalt and blue filters provide a view of retinal nerve fiber layer (RNFL), the blue filter also allows the visualization of the internal limiting membrane, retina folds, cysts and epiretinal membranes. The green filter enhances the vision of the retinal vasculature and highlights common findings such as hemorrhages, drusen and exudates. The red filter is useful for pigmentary disturbances, choroidal ruptures, choroidal nevi, and choroidal melanomes. And the red-free filter is used for evaluating the RNFL and the vascular structure of the retina as it relates to glaucoma, DR, and hypertension. According to the manufacturer, the CX-1 and CR-2 Plus cameras incorporate its own premium front lens, internal camera lenses, active pixel sensor in complementary metal–oxide–semiconductor with 18.0 megapixels that result in less chromatic distortion and spherical aberration. This allows that these cameras provide excellent colour reproduction and image detail. Because the optical pathway is free of aberration, AF filter is able to provide very precise views of the layers of the retina.

	Excitation wavelength (nm)	Detection wavelength (nm)	Resolution* (MP)	Field of view (degrees)
CX-1 /CR-2 Plus	530-580	>640	18	35,45
Visucam 200 /500	510-580	650-735	5.0	30,45
FF450 Plus	510-580	650-735	1.5-16.7	20,30,50
TRC-50DX /50IX	535-585	615-715		20,35,50

*Sensor resolution on megapixels (MP).

Table 5.3: Technical characteristics of the commercially available conventional fundus cameras.

Zeiss retinal cameras (Visucam 200, Visucam 500, Visucam NM/FA and FF 450 Plus IR) use excitation filter of 510-580 nm and a barrier filter in the range of 650-735 nm for acquiring FAF images (Creuzot-Garcher et al., 2014). Visucam 200 and Visucam 500 also determine the macular pigment optical density through reflectance of a single 460 nm wavelength (Creuzot-Garcher et al., 2014). FF 450 Plus IR obtains FAF images with a resolution of 4.1 megapixels through a black-and-white sensor known as Pike421b.

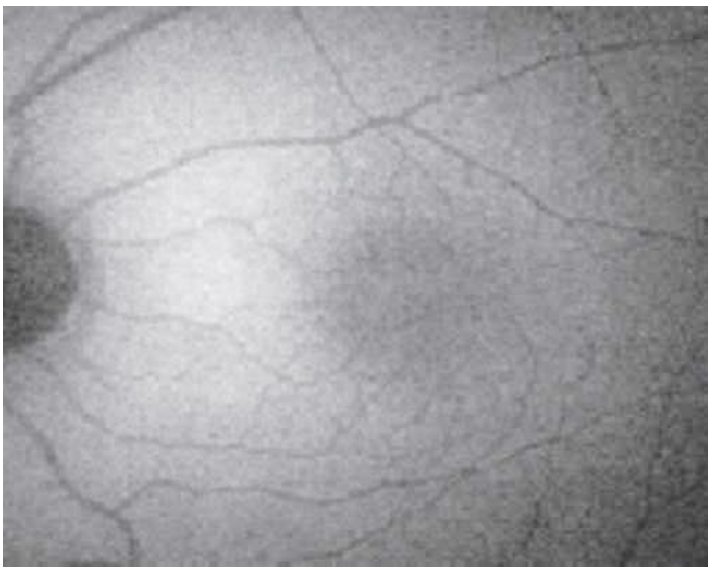

Figure 5.6: Central macular area in a healthy subject acquired with CR 2-Plus retinal camera. (Available at www.canon-europe.com; Last accessed July 2016).

The TRC-50DX and TRC-50IX use an excitation filter in the range of 500-610 nm and a barrier filter of 675-715 nm (Spaide, 2003; Muñoz et al., 2013). These devices present a mechanism of exchangeable filters for excitation and detection wavelengths. In addition, these devices can also be equipped by the last modification of Spaide filter characteristics, excitation band pass filter of 535-585 nm and barrier filter of 615-715 nm (Spaide, 2008).

In a comparative study between FF 450 Plus IR and TRC-50IX fundus cameras in which the Topcon fundus camera was equipped with older Spaide filters characteristics (Spaide, 2003), Muñoz et al. (2013) studied the quality of contrast in FAF imaging by comparing the contrast levels of the images provided by each device. They observed that the Carl Zeiss camera showed higher contrast values over the Topcon for FAF imaging. They suggested that this difference could be due to the illumination, reflectivity, and sensor capabilities. All these factors can be influenced by quality of optical system and the filters or by capability of the software used.

Comparison of technical characteristics between cSLO and conventional fundus camera

In this section, both steady state methods allowing FAF image acquisition in clinical acquisition and commercially available are compared. There are several technical and optical principles differences between both technologies, such as excitation and detection wavelengths, image acquisition and image processing capabilities. Thus, the obtained AF images differ between both devices (Bessho et al., 2009; Yamamoto et al., 2009). Lipofuscin fluorophore shows the most intense fluorescence in the RPE. This fluorophore is most efficiently excited at 380 nm, however this excitation wavelength cannot be used due to blockage by the absorption in the crystalline lens [towards], thus measurements of fluorescence can only be performed on the spectral range between 400nm and 900nm. In spite of this, lipofuscin has a wide excitation and emission spectra, between 300 and 600nm and between 480 and 800 nm, respectively (Calvo-Maroto et al., 2016b). However, there are other fluorophores present in anterior and posterior with respect to RPE cell monolayer which absorb visible light, such as melanin, macular pigments, flavins, piridyne nucleotides, and other proteins (Boulton et al., 2001). Although the difference of excitation and detection wavelengths would result in the detection of different complements of fluorophores

(Schmitz-Valckenberg et al., 2008a), it makes the discrimination of these fluorophores difficult.

The acquisition of FAF images by steady state techniques, cSLO and conventional fundus camera, cannot allow the discrimination of fundus fluorophores. The main difference between both methods is due to the optical principle used. The cSLO detects the fluorescence light of a small excited spot at the fundus via a large aperture. A fundus camera excites the whole field at the fundus simultaneously and the fluorescence light is detected through the reduced aperture. For FAF image acquisition, cSLO uses the confocal optics and scanning mode, the fundus camera employs band-pass filters, a ring illumination and a central field stop for excitation and the fluorescence exhibitions due to a beam of light at one single instance. The acquisition mode of fundus camera is particularly predisposed to pseudoautofluorescence phenomenon. This phenomenon is caused by fluorescence from anterior and posterior structures of the retina, mainly the crystalline lens (Schmitz-Valckenberg and Fitzke, 2009). This ocular dioptre has highly fluorescent properties in the short-wavelengths range (excitation between 400 and 600 nm with a peak emission at 520nm) that shows a common source or interference, and an emission peak similar to that of lipofuscin. In cSLO, a small volume of the lens is excited resulting in a small contribution of the fluorescence of the lens and the excitation light is reflected only from a single point, resulting in a weak secondary excitation of the lens. In fundus cameras, a large volume of the lens is excited, the excitation light is reflected from an extended field of the fundus and excites secondarily the lens. In addition, the lens AF would be also scattered inside the vitreous body and the optic nerve head, sending this light back toward the detector due to the reflective properties of these structures. Thus, the fluorescence of the optic disc, detected by fundus camera, is predominantly the fluorescence from the lens (Schmitz-Valckenberg and Fitzke, 2009). To avoid fluorescence signals from anterior ocular structures, fundus cameras use the principle of aperture separation, whereby the influence of the anterior ocular structures is eliminated by separation between entrance and exit aperture in the pupil plane. Thus, the area of aperture of the pupil plane has the same size for excitation as for the detection, so less fluorescence light is detectable from the fundus in comparison with cSLO.

Despite the differences in the optical principles used by both methods to avoid the influence of crystalline lens, both of them can also avoid it by using long excitation

wavelengths, since the use of shorter wavelengths could be an inconvenient due to the increase of the shorter wavelength absorption by the lens with ageing (Van Best et al., 1985b), leaving less light for excitation of the fluorophores in the RPE (Spaide, 2003).

The normalized fluorescence emission spectrum of the crystalline lens shows a decrease of 20% at 650 nm when excited at 468 nm (Schweitzer et al., 2007). Meanwhile, the influence of the crystalline lens fluorescence is also reduced using conventional fundus camera when the emission of lipofuscin (emission maximum at 600nm) is detected above 650 nm (Spaide, 2003).

The acquisition mode of conventional fundus camera allows adjustment of orientation and position of the camera, detector gain, and the intensity of the flash, although this task may be difficult to perform, apart from being time-consuming.

Park et al. (2013) used a cSLO (488 nm excitation wavelength) and digital fundus camera (530-580 nm excitation wavelength) and they found several differences in the pattern of normal FAF. The optic disc was uniformly dark with the cSLO device while it exhibited some AF signal with the digital fundus camera. This signal could be due to reflected light from the fluorescence measurement and a possible contribution from intrinsic collagen and elastin AF. This contribution has only been demonstrated by time-resolved measurements, thus the optic disc exhibits the long decay time of connective tissue (Schweitzer et al., 2004). Retinal vessels were less hypoautofluorescent with the fundus camera due to decreased haemoglobin absorbance at higher wavelengths, decreased signal collagen and elastine located in the vessel wall (Park et al., 2013).

In addition, images generated with 488 nm excitation wavelength are more affected by macular pigments than those generated with longer excitation wavelengths. Thus, the macular area is less fluorescent in images acquired using 488 nm excitation wavelength than those obtained with 530-580 nm excitation wavelengths (Figures 5.4 and 5.6).

Macular pigment is composed of yellow carotenoid pigments, namely lutein, zeaxanthin, and meso-zeaxanthin. These pigments are located in a layer anterior to the RPE, in the outer plexiform layer and partly in the inner plexiform layer (Delori et al., 2001), and they absorb light of 400-540 nm with absorption peak at 460 nm

(Wüstemeyer et al., 2002). This decreased absorption by macular pigments in FAF imaging obtained by the fundus camera provides a better visualization of foveal AF, such as choroidal vasculature, due to reflectance or intrinsic AF by long-wavelength excitation of the choroidal vasculature´s collagenous/elastin wall, allowing the detection of progression in foveal retinal disease (Chong et al., 2000).

FAF images obtained from cSLO (HRA) may allow a better visualization of cystoid macular oedema since the cysts may displace the blockage of macular pigments creating a window defect (Bessho et al., 2009). However, the cysts spaces could contain other fluorophores that are excited at 488 nm and not at 580 nm (Deli et al., 2013).

Spaide (2008) described that FAF from subretinal space might be originated from incompletely digested outer accumulation of A2E. The precursors of lipofuscin show AF with an emission spectrum from around 480 to 750 nm and an excitation spectrum from 320 to around 520 nm (Bui et al., 2006). Therefore, the different appearance observed in areas with subretinal fluid could be due to a difference in the excitation wavelengths used (Framme et al., 2004).

Another difference between both devices is related with the image processing capabilities: cSLO acquires a series of nine FAF images, being the final image calculated by averaging the previous nine. Thus, overall image quality and contrast are maximized with multiple image acquisition and mean image calculation. However, digital non-mydriatic fundus camera records images employing a single flash of nonconfocal light, which might imply that reflected or scattered light from fluorophores such as collagen, elastin or AGEs (Hammer et al., 2007) are captured at the image plane affecting the quality and contrast of the image (Delori et al., 1995; Park et al., 2013).

In conventional fundus camera, the brightness and contrast can be manually modified after the image is captured in order to optimize the visualization. However, there is not a standardization of these modifications, so the comparisons between images even captured with the same acquisition setting is not possible. The modification of contrast and brightness is made by image optimization (Schmitz-Valckenberg et al., 2008a), however cSLO uses an automatic normalization algorithm with normalization of the histogram, so the sensitivity of the signal is enhanced. In addition, by averaging of images the photon noise is reduced by the square root of the number of images, thus obtaining a better contrast in cSLO than in fundus cameras. Therefore, neither system

allows the quantitative assessment of absolute AF intensities (Schmitz-Valckenberg and Fitzke, 2009).

The development of measurement software integrated into the devices to establish a quantitative distribution of AF intensity might allow an improvement in assessment and monitoring of alterations related with retinal disease. Moreover, the development of an equivalency between FAF intensity obtained by cSLO and those by fundus camera might allow the comparison of the results acquired by both methods.

The cSLO post acquisition process allows more modifications and is more time-consuming compared to the fundus camera. The cSLO normalizes and averages all the captured images to reduce the noise and low sensitivity of the signal. This averaging procedure improves the signal-to-noise ratio and allows a better visualization of details. The number of processed images is limited for practical reasons, such as exposure time to the laser beam and the difficulty of correction for eye movements when increasing the number of captured images. Conventional fundus camera uses the maximum or near to maximum flash light intensity for a single image. However, the average of several images captured from fundus camera have not been demonstrated to reduce the noise and improve the visualization of details (Schmitz-Valckenberg et al., 2008a; Schmitz-Valckenberg and Fitzke, 2009).

The observation of certain retinal alterations by both technologies has reflected differences between both of them. Schmitz-Valckenberg et al. (2008a) compared FAF images from modified Topcon TRC-50IX and HRA 2 in patients with GA secondary to age-related macular degeneration (AMD). The modified Topcon TRC-50IX was equipped with older Spaide filters characteristics, excitation bandwidth of 500-610 nm and a barrier filter of 615-715 nm. They observed that agreements for atrophy quantification were similar between both image systems. In relation to FAF pattern classification of GA secondary to AMD, the Fundus Autofluorescence in age-related Macular degeneration (FAM) Study pattern classification established six different phenotypic patterns, focal, banded, diffuse and patchy. However, they classified FAF images in the two categories with prognostic value in relation to atrophy progression, none-focal and the banded-diffuse group (Bindewald et al., 2005) and they observed that this classification was possible in a higher number of images from cSLO (88%) compared to those from fundus cameras (69%). Thus, fundus camera showed less

capability for detecting disease markers than cSLO. This could be due to the nonconfocality property and the use of a mean image obtained from a series of single images from cSLO compared to one single image obtained with fundus cameras.

Deli et al. (2013) also compared a modified TRC-50IX and HRA 2 for studying the agreement in FAF patterns in healthy and pathological retinal structures. The modified fundus camera was equipped with the last modification of Spaide filter characteristics. They observed that cystoid macular oedema, lipid exudates and AF from the subretinal space were more visible from HRA 2 images. However, FAF image from fundus camera is better than HRA 2 when screening for foveal atrophy, because images from fundus camera were less influenced by macular pigments, and they also observed that image quality of FAF images from fundus camera was higher than HRA 2 in cases of advanced cataract and poor fixation. The AF changes in GA, RPE changes, drusen, and retinal haemorrhages were similar in both devices.

Detection of the time-resolved autofluorescence

Similarly to the steady-state methods for acquiring AF images, in this technique several fluorophores are excited. However, an important advantage of time-resolved measurements is the separation of fluorophores also in the case of overlapping spectra. In process of detection of only one photon during 10 to 100 excitation cycles, the probability for simultaneous detection of more than one photon is very low. The measured function is proportional to the probability density function of the investigated process, representing the dynamic fluorescence signal. If more than one photon is detected per excitation pulse, the lifetime will be determined systematically too short (Lakowicz, 1999). The contribution of each fluorophore can be determined by fitting the sum decay by a model function. First measurements of the time-resolved AF of the living human eye and of fundus specimen were published by Schweitzer et al. (2004).

Thus, the fluorescence emission intensity is detected as a function of time. The detection and posterior discrimination of ocular endogenous fluorophores at the fundus by methods mentioned above is not possible with high spatial resolution. There are two inconveniences, the transmission of the ocular media, particularly the absorption from the crystalline lens, and the high spectrally resolved fluorescence signal required. In

addition, the maximal exposure of the eye limits the radiation power and the exposure time (Schwitzer et al., 2003).

The measurements of fluorescence lifetime for discrimination of ocular endogenous fluorophores can be carried out by time-resolved AF methods (Marcu, 2012). For detection of the living fundus a cSLO combined with a time-correlated single photon (TCSPC) is used to compensate for the weak fluorescence signal from the eye (Schwitzer et al., 2003).

The maximal permissible exposure must be low enough no to cause damage in the eye. Because of its maximal permissible exposure, and the excitation power required for the calculation of decay, the time-resolved AF is only detectable by cSLO. The combination of cSLO with the principle of the aperture diaphragm division reduces the crystalline lens fluorescence (Schweitzer et al., 2005a).

The light source emits series of pulses at determined wavelengths with a specific frequency of repetition rate (Lakowicz, 1999). The fluorescence is detected in spectral channels and the fluorescence decay is detected using TCSPC (Schwitzer et al., 2003).

The fluorescence decay described in the Jablonski diagram is used for measuring time-resolved fluorescence allows differentiating several fluorophores according to the fluorescence decay time (Marcu, 2012). Thus, changes of endogenous fluorophores can be detected as early sign of disease, such as AMD or DM, despite of the strong fluorescence intensity of lipofuscin (Schweitzer et al., 2005b; Schweitzer et al., 2015).

5.5.2 NORMAL FUNDUS AUTOFLUORESCENCE IMAGING

FAF imaging allows a spatial distribution of lipofuscin in the RPE in vivo and that correlates to the intensity of the signal emitted. In healthy eyes the FAF distribution shows a characteristic pattern where the optic disc appears dark due to absence of RPE and no lipofuscin and retinal vessels exhibit a reduced FAF signal because of the absorption by blood. In macula area, especially around the fovea the FAF is also reduce due to the absorption of macular pigments, such as lutein, zeaxanthin and other pigments (Sepah et al., 2014). The parafoveal area tends to be higher than that of the fovea signal; however, it shows a reduced intensity when compared with the

background signal in peripheral areas of the retina. This diminution of FAF signal could be related to an increase of melanin, and a decrease concentration of lipofuscin in RPE cells (Schmitz-Valckenberg et al., 2008b). Figure 5.7 shows the FAF image of a healthy subject.

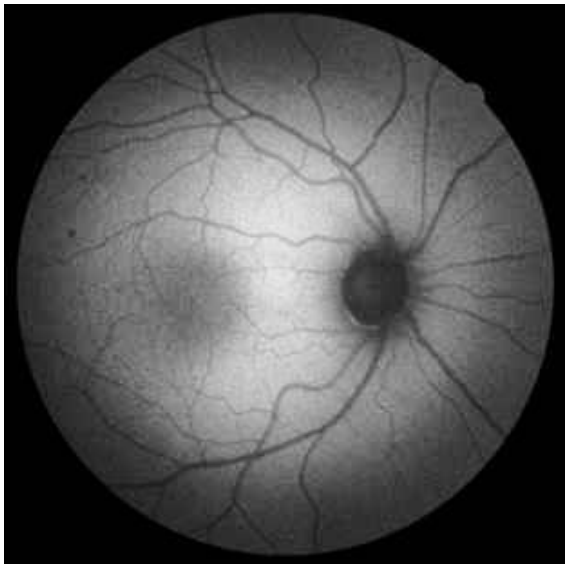

Figure 5.7: FAF image in a healthy subject. Note the hypofluorescence in the macular area and the increased signal in parafoveal zone (Calvo-Maroto et al., 2016b).

5.5.3 FUNDUS AUTOFLUORESCENCE IN DIABETES MELLITUS

FAF imaging allows the topographic mapping of lipofuscin distribution in the RPE (Kolomeyer et al., 2012; Samy et al., 2014). Lipofuscin morphology remains similar with ageing, however certain age-related changes are observed in the excitation spectral characteristics (Boulton et al., 1990) showing a decrease from shorter (250 nm) to longer (700 nm) wavelengths. Determination of the lipofuscin excitation spectrum presents several challenges because of the size, complexity and density of the granules (Boulton et al., 2004), but it has been proposed that lipofuscin has a broad-band absorption across the UV and visible spectrum (Boulton et al., 1990). Lipofuscin shows a yellow-orange fluorescence when it is excited with UV or blue light (Yin, 1996). The intensity represented in FAF images corresponds with lipofuscin accumulation, which increases with age (Boulton et al., 1990; Boulton et al., 2004; Feeney-Burns et al., 1984; Hunter et al., 2012; Rovati and Docchio, 2004).

FAF imaging is considered a useful tool for understanding the pathophysiologic mechanisms, diagnosis, and prognosis of retinal disease. In clinical practice is currently used for monitoring different maculopathies, such as AMD, and dystrophies. New applications of this technique include its use in diabetic patients with DME (Schmitz-Valckenberg et al., 2008b; Vujosevic et al., 2011).

In retinal disease, an increase in AF has been correlated with accumulation of lipofuscin in the RPE (Boulton et al., 2001; Boulton et al., 2004; Sparrow et al., 2003; Sparrow and Boulton, 2005), as a result of photoreceptor outer segment phagocytosis (Sepah et al., 2014). Moreover, lipofuscin is composed of a large number of molecules, mainly peroxidation products of proteins and lipids. For this reason, lipofuscin seems to be an indicator of oxidative damage (Vujosevic et al., 2011).

DR and DME are common ocular complications considered to be leading causes of blindness in diabetic patients (Ciulla et al., 2003). In urbanized countries DR is recognized as the leading cause of visual loss in working-age population while DME the major cause of legal blindness in patients with T2DM (Ciulla et al., 2003) .

In DR, the mechanism of lipofuscin accumulation in the retina is different compared with other retinal diseases. Xu et al. (2008) found that, in mice, lipofuscin granules accumulate in microglia cells much more than in RPE cells. These observations were used by Vujosevic et al. (2011) to explain their results, in part, namely that retinal sensitivity decreased in areas with increased FAF, indicating that the function of the neurosensory retina deteriorated when AF increased in T1DM and T2DM patients (Vujosevic et al., 2011).

Certain changes in the normal distribution of FAF have been observed in diabetic patients with DME. These FAF patterns are characterized by the presence of round or oval areas bordered by darker rims. The intensity of the FAF signal in these patients depends on cysts that are located in the outer plexiform and inner nuclear layers, where the accumulation of luteal pigment is maximum (McBain et al., 2008). These cysts could displace luteal pigment and avoid the normal blockage of foveal FAF (McBain et al., 2008; Smith et al., 2005).

The mechanical effect of cystoid macular oedema (CME) (Vujosevic et al., 2011) has been studied. The classification of DME has been widely studied, but there

are no unified criteria. Several researchers have proposed a DME classification based on FAF patterns in diabetic patients with clinical significant macular oedema (CSME), and described four types: (i) normal FAF; (ii) cystoid increased FAF (iFAF), where cystoid or petaloid was observed in the macular area, and iFAF area on the FAF image corresponded to cystoid oedema on optical coherence tomography (OCT) scans; (iii) spot iFAF, where sporadic iFAF is in the low FAF background damaged retinal structure that is, the reflection of every layer was blured; and (iv) irregular decreased FAF (dFAF), where the macula shows a mottled shape as well as irregular dFAF and subfoveal accumulation of a large amount of hard exudates was observed on OCT (Shen et al., 2014).

It has also been proposed that T2DM with spot iFAF is caused by displacement of macular pigments because of their correlation with cystic-like changes found on OCT (Shen et al., 2014). Bessho et al. (2009) explained that the iFAF intensity observed at 488 nm excitation is due to a reduction in the density macular pigments, which decreases the blockage of FAF intensity. However, when 580 nm FAF is used to obtain an FAF image, this blockage by the macular pigments is not produced. So, any diminution of macular pigment density has less of an effect and may result in lower sensitivity for detection of cystoid lesions.

However, Pece et al. (2010) determined that iFAF could be considered as "normal FAF", because it was caused by lack of zeaxanthin. Even though they accepted that cystoid iFAF was caused by changes in the distribution of macular pigments, Pece et al. (2010) observed that spot iFAF was not correlated with cystic-like changes although retinal structure was altered. Thus, spot iFAF was not caused by abnormal macular pigment distribution, but an increase in the death of photoreceptor cells in DME (Shen et al., 2014). The RPE cells accumulate photoreceptor outer segments to compensate for this process, which results in the abnormal accumulation of lipofuscin. This accumulation of lipofuscin could also damage the function of photoreceptor cells.

Those patients with irregular dFAF have a large amount of subfoveal hard exudates that may absorb the FAF signal, causing a decrease in FAF. In addition, these T2DM patients with dFAF show damaged photoreceptor layers, resulting in decreased lipofuscin production and FAF (Shen et al., 2014).

Although the hypothesis regarding the displacement of macular pigment in DME patients has been proposed by several investigators, Waldstein et al. (2012) demonstrated this displacement using macular pigment optical density (MPOD) measures. Waldstein et al. (2012) observed that the FAF intensity of these ovoid lesions was similar that peripheral zones where macular pigments density was very low, whereas the intensity of the surrounding rims was the same as that of zones with high macular pigments density. These lesions were correlated with intraretinal cysts on OCT imaging. The results of Waldstein et al. (2012) agree with the displacement of these macular pigments resulting from the cysts, leading to a loss of the normal blockage of the foveal FAF signal. Thus, 488 nm, 514 nm FAF and MPOD imaging have been demonstrated as sensitive and specific methods for clinical screening in DME patients (Waldstein et al., 2012).

Another hypothesis to explain changes in FAF pattern of diabetic patients with DME has been proposed by Vujosevic et al. (2011), who hypothesized that the increase of FAF intensity in DME areas was due to accumulation of oxidative products induced by activated microglia. This explanation was based in the activation of microglia by diabetes. So, this activation process could lead to the oxidation of proteins and lipids that have accumulated in the microglia because of diabetes progression (Xu et al., 2008). However, Holz et al. (2001) suggested that FAF observed in macular oedema may be related to retinal fluorophores (retinoids) in extracellular or intra- or subretinal fluid rather than lipofuscin patterns in the RPE (Holz, 2001).

Chung et al. (2012) observed that not all diabetic patients with DME had comparable levels of increased FAF. Although this observation could be due to the fact that excitation light at 488 nm is blocked by macular pigments and causes macular hypoautofluorescence, Chung et al. (2012) observed that those patients with improved DME did not show a significant decrease in FAF levels. Therefore, they suggested that residual FAF after an almost complete resolution of DME was related to the persistence of activated microglia or damaged cells, as well as residual displaced macular pigments. Moreover, they predicted that the increase in FAF intensity in DME would be due to the ineffectiveness of a compensatory function of retinal or glial cells to block AF of the RPE, and to an increase of active microglia at the fovea. Thus, if one of these conditions occurs, FAF intensity would be lower and if none of the conditions exists the FAF intensity would be at the lowest value.

FAF is almost absent at the foveola in normal eyes because of absorption by macular pigments, but the cone photoreceptors at the foveola have high concentrations of lutein and zeaxanthin pigments in their axons (Neelam et al., 2005). However, Chung et al. (2012) observed an increased FAF intensity at the foveola and proposed that this observation may indicate a serious damage to cone photoreceptor cells and leading to visual loss.

When macular oedema is improved, photoreceptors and retinal cells have the ability to obtain and stabilize macular pigments, indicating a good degree of physiological recovery. Consequently, the persistent high FAF after the resolution of DME could indicate a decrease in macular cell function and/or the persistent accumulation of oxidative products induced by microglial activation (Chung et al., 2012).

Although two hypotheses have been proposed to explain the changes in FAF in diabetic patients with DME, both are based on comparing FAF patterns. The disagreement between the two hypotheses lies in the mechanism responsible for the changes observed. The displacement of macular pigment is the most accepted hypothesis.

The use of conventional FAF technology in screening and monitoring DM has several limitations, such as: (i) the requirement for a clear ocular media, because significant cataract or vitreous opacity can affect the intensity of fluorescence coming from the retina; (ii) the relatively small image angle (usually 35 and 50º), such that its implementation as a monitoring tool for peripheral retinal changes into clinical practice is often technically difficult; (iii) the increased screening time to allow for reversal of pupil constriction secondary to flash intensity required for acquiring FAF images.

At present, there is no standardized protocol or metric to assess AF distribution in diabetic patients.

CHAPTER 6

Fundus Autofluorescence in Diabetes Mellitus

6.1 VISUAL FUNCTION AND FUNDUS AUTOFLUORESCENCE ASSESSMENT IN DIABETIC PATIENTS

6.1.1 INTRODUCTION

DR is a common complication of DM caused by a long-term damage to retinal microvasculature that implies visual impairment (American Diabetes Association, 2011; Ciulla et al., 2003; Fong et al., 2004). A combination of 35 studies determined that the overall prevalence of any DR was 34.6% among diabetic patients (Yau et al., 2012). The diabetes-induced mechanism that contributes to develop of DR remains understood (Ciulla et al., 2003; Fong et al., 2004).

RPE and choroid are essential layers to maintain the normal metabolism and function of the retina. Any alteration of these layer functions implies a degeneration of photoreceptors, visual impairment and even blindness (Han et al., 2007).

The main substrate for lipofuscin formation in the RPE is the undegradable end products that results from the phagocytosis of photoreceptor outer segment located in RPE (Sepah et al., 2014; Shen et al., 2014). In DR, lipofuscin contains numerous molecules mainly composed of peroxidation products from lipids and proteins (Schmitz-Valckenberg et al., 2008b) and it could be used as an indicator of oxidative

damage on the retina (Vujosevic et al., 2011). Thus, lipofuscin accumulation reflects the metabolic damage in RPE caused by disease (Rovati and Docchio, 2004).

The FAF imaging is a noninvasive method that represents the distribution of lipofuscin in the RPE layer in vivo. This technique is based on the retinal capacity for light emission of a specific wavelength from natural fluorophores, mainly lipofuscin, in the RPE. This process occurs when these molecules are excited by suitable wavelength of light. The intensity of FAF depends on amount and distribution of lipofuscin (Samy et al., 2014; Kolomeyer et al., 2012).

Some studies have shown specific FAF patterns for numerous ocular diseases such as DME (Chung et al., 2012; Shen et al., 2014; Vujosevic et al., 2011), CME (Bessho et al., 2009; Ebrahimiadib and Riazi-Esfahani, 2012) and, AMD (Mauschitz et al., 2012; Spaide, 2003). The results of these studies demonstrated that FAF could be helpful for reflecting the extent of retinal damage and monitoring the progression of disease (Kolomeyer et al., 2012; Sepah et al., 2014; Shen et al., 2014; Spaide, 2003).

The present pilot study evaluates FAF in diabetic patients and control subjects using the CR-2 Plus AF non-mydriatic retinal camera (Canon Inc, Tokyo) with the aim of identifying the utility of optimized-FAF imaging in early detection of DR. Retinal alterations were also related with visual function, quality of life and diabetes self-care management.

6.1.2 PATIENTS AND METHODS

Subjects

We studied 7 right eyes from 7 subjects with T2DM (4 men and 3 women) and 13 right eyes from 13 control subjects (9 men and 4 women). All patients provided informed written consent in accordance with the World Medical Association´s Declaration of Helsinki before the procedures took place.

Inclusion criteria were clear ocular media allowing recording high quality colour and FAF imaging. Exclusion criteria for both diabetic patients and normal subjects were

previous retinal photocoagulation and any retinal alteration affecting macula, such as AMD.

All diabetic patients were diagnosed with DM by a general practitioner from the National Health System.

The quality of life of diabetic and control groups was assessment by National Eye Institute Visual-Functioning Questionnaire-25 (VFQ-25) (Mangione et al., 2001). The reliability and validity of this questionnaire have been confirmed on patients with DR (Mangione et al., 1998). Diabetes Self-Management Questionnaire (DSMQ) (Schmitt et al., 2013) was administered in diabetic patients and a custom-made questionnaire to identify people at increased risk for undiagnosed diabetes (Herman et al., 1995).

Ocular examination included measurement of BCVA by Snellen chart, autorrefractometer, slit-lamp biomicroscopy, contrast sensitivity function (CSF), colour fundus and FAF imaging. VA was converted to logMAR scale. Colour fundus and FAF imaging were recorded after fasting blood glucose levels measurement.

Fasting blood glucose levels were measured from 8.00 a.m. to 10.00 a.m. HbA1c levels were provided by diabetic patients.

Questionnaires

VFQ-25 consists of 25 vision-targeted questions divided in 11 vision-related sub-scales: general vision rating (1), difficulty with near vision activities (3), difficulty with distance vision activities (3), limitations in social functioning due to vision (2), mental health symptoms due to vision (4), role difficulties due to vision (2), dependency on others due to vision (3), driving difficulties (3), limitations with peripheral vision (1), colour vision (1) and ocular pain (2). In addition, a single-item general health rating question is included (Mangione et al., 2001). The scale of this questionnaire can vary between 0 (worst possible score) and 100 (best possible score).

DSMQ is a questionnaire designed to assess the self-care behaviour related to the glycemic control. This questionnaire consists of 16 items divided in four subscales, Glucose Management, Dietary Control, Physical Activity and Health-Care Use (Schmitt et al., 2013). The scale transformed can vary between 0 and 10.

The new questionnaire developed to identify people at increased risk for undiagnosed diabetes is divided in three age ranges (20-44, 45-64, 65 or plus years of age). The questions are related to body mass index (BMI) and sedentary lifestyle, for ranges of 20-44 and 45-64 years of age. For range of 65 or plus years, questions are related to BMI, familiar antecedents (father, mother or brothers) and a question for women about their baby's weight at birth (Herman et al., 1995).

Methods

CSF measurements

CSF measurements were carried out with the Vistech 6500 chart (Vistech consultants, Inc., Dayton, OH-USA) which is a panel with 5 rows of 9 printed circular patches. The rows increase in spatial frequency from top to bottom of the chart, and on each row the contrast decreases from left to right. There are 5 spatial frequencies across the rows (1.5, 3, 6, 12 and 18 cycles per degree (cpd), respectively). The contrast decreases in increments of 0.12 log unit. The direction of the last patch correctly identified by the patient was recorded for each frequency. The patient was at 3 meters of chart and test was performed in a monocular way. The measurements were carried in photopic conditions (85cd/m^2).

Colour fundus and FAF imaging. Evaluation and image acquisition

Colour and FAF images were recorded with CR-2 Plus digital non-mydriatic retinal camera (Canon, Tokyo). Colour images were obtained and evaluated for potential changes in the optic nerve, blood vessels and macula. Following colour images, FAF images were taken using FAF mode (530-580 nm exciter filter and 640 nm barrier filter) in a dark room in order to prevent pupillary constriction. A single image was recorded per each eye.

The FAF images were saved as TIFF images and analysed by MATLAB 2013a software (Mathworks, Inc., Natick, MA-USA). All images were normalized and homogenized for a better visualization of retinal alterations and were called optimized-FAF images. Three images were obtained per eye, colour, FAF and optimized-FAF images. All images were divided into four spatial quadrants that correspond to

anatomical retinal quadrants: 1. Upper temporal area, 2. Lower temporal area, 3. Upper nasal area and 4. Lower nasal area. The optic nerve was considered the centre of the image (Figure 6.1.1), as it is commonly used for diagnostic staging of DR in clinical practice (Wilkinson et al., 2003).

These images were observed to find ophthalmic compatible signs with DR such as microaneurysms, capillary dilation, hard exudates, and haemorrhages in diabetic patients.

In control subjects the observation was focused on retinal epithelial defects and capillary dilation findings.

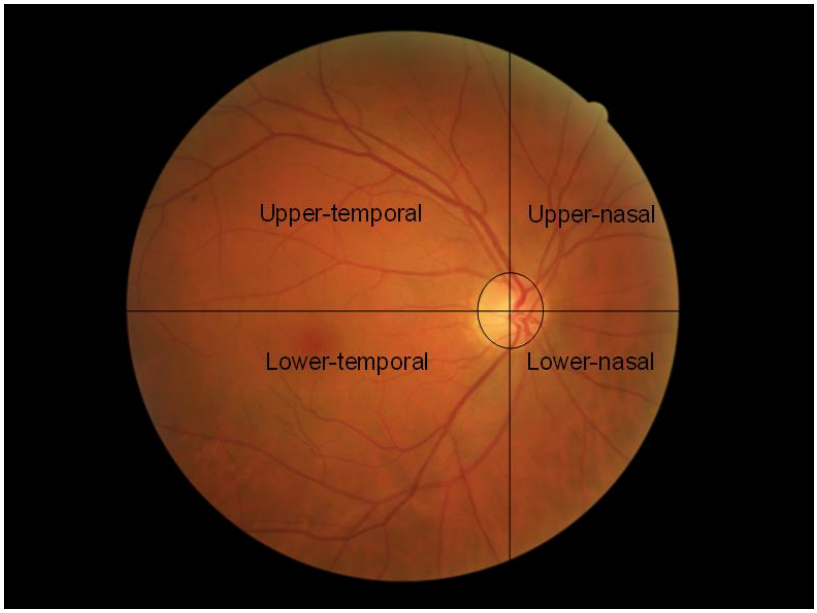

Figure 6.1.1: Division of fundus images into four quadrants centred at the optic nerve.

Statistical Analyses

In this pilot study only the right eye was considered for statistical analysis. Normality of data distribution for the different groups was determined using the Kolmogorov-Smirnov test. When parametric analysis was possible, the independent Student *t* test was used for comparisons between diabetic patients and control subjects. When parametric analysis was not possible, the U Mann Whitney test was used to

assess the significance of such difference. Differences in ophthalmic signs of different areas between three images were assessed by Kruskall-Wallis test. To determine which of pairwise comparisons were responsible for the overall difference between groups, separate Mann-Whitney U tests were performed on each pairwise (3 tests), alpha used 0.05/3=0.0167.

Correlation coefficients (Pearson or Spearman) were used to assess the correlation between variables. We considered values of $p<0.05$ to be statistically significant. All statistical analyses were performed using SPSS software (version 19, IBM Corp., Armonk, NY-USA).

6.1.3 RESULTS

The mean age of diabetic patients was 54.86 ± 10.25 years (range 45-71 years) and that of control subjects 40.77 ± 11.77 years (range 25-68 years) (p=0.014). Characteristics of diabetic and control groups are summarized in Table 6.1.1.

In the diabetic group, four patients were treated for high cholesterol values, two patients for high blood pressure values and two patients had problems with their thyroid gland. Within control group, one patient was being treated for high blood pressure and three showed cholesterol values higher than 200 mg/dL. The diabetic group did not show any complication.

The VFQ-25 questionnaire revealed that diabetic patients and control subjects presented similar visual function scores since differences were not statistically significant in each subscales (Table 6.1.1). In “General Health” subscale, control subjects showed higher scores (69.231 ± 18.125) than diabetic patients (64.286 ± 19.670) (p=0.438). However, “General Vision” subscale and Specific Vision subscales (“Social Functioning”, “Mental Health”, “Role Difficulties”, and “Dependency”) of diabetic subjects were higher compared to control subjects ($p>0.05$). Also, “Sum Scale” was slightly higher in diabetic patients (92.26 ± 4.14) than control subjects (87.62 ± 13.35) but not statistically different (p=0.817) (Table 6.1.1).

According to the scoring guide of DSMQ, where a cut-off score ≤ 6.0 in total score shows a suboptimal self-care, all diabetic patients had an adequate self-care with a

"Total Score" mean of 7.09 ± 0.85. "Glucose Management" subscale showed the highest score (8.89 ± 1.57) and "Physical Activity" was the lowest score (4.60 ± 2.43) (Table 6.1.2).

	Diabetic Patients (n=7)	**Control Subjects (n=13)**	***p*-value[§]**
Sex	4M, 3F	9M, 4F	
Age (yr)	54,86 (10,25)	40,77 (11,77)	0,014
LogMAR VA	0,04 (0,09)	0,01 (0,027)	0,438
Fasting Glucose Levels (mg/dL)	147 (16,65)	95,46 (8,40)	<0,001
HbA1c levels (%)	7,21 (1,12)	-	
Diabetes duration (months)	182,14 (140,74)	-	
General Health	64,29 (19,67)	69,23 (18,12)	0,438
General Vision	74,29 (9,76)	70,77 (15,52)	0,817
Ocular Pain	94,64 (9,83)	81,73 (16,63)	0,097
Distance Vision Activities	92,83 (8,91)	89,10 (14,18)	0,588
Near Vision Activities	83,10 (11,64)	91,66 (16,32)	0,311
Visual-Specific Social Functioning	98,21 (4,72)	95,19 (9,60)	0,699
Visual-Specific Mental Health	83,93 (9,45)	81,73 (24,53)	0,536
Visual-Specific Role Difficulties	92,86 (12,20)	86,538 (20,70)	0,588
Visual-Specific Dependency	100	92,95 (19,20)	0,588
Driving	79,76 (36,28)	73,07 (35,38)	0,536
Colour Vision	100	98,08 (6,93)	0,817
Peripheral Vision	96,43 (9,45)	88,46 (19,41)	0,536
Sum Scale	92,26 (4,14)	87,62 (13,35)	0,817

§ Mann-Whitney U test

LogMAR VA: Visual Acuity Logarithm of the Minimum Angle of Resolution; HbA1c: Glycated haemoglobin.

Table 6.1.1: Descriptive statistics and scoring of Visual Functioning Questionnaire-25 (VFQ-25) of the diabetic patients and control subjects. Mean (SD) values.

The questionnaire used in control subjects to assess the risk in undiagnosed people to have diabetes showed that 53% of control subjects had an increased risk of suffering diabetes. Age, fasting glucose levels and VA differences between control subjects with and without risk to develop DM were not statistically different.

Patients	Glucose Management	Dietary Control	Physical Activity	Health-Care Use	Total Score
1	6,66	7,5	8,88	5,55	7,083
2	10	6,66	3,33	7,77	7,5
3	6,66	6,66	2,22	6,66	5,625
4	10	9,16	2,22	10	8,125
5	10	7,5	4,44	8,88	7,916
6	8,88	7,5	4,44	8,88	6,739
7	10	0	6,67	2,22	6,667
Mean (SD)	8,89 (1,57)	6,43 (2,95)	4,60 (2,43)	7,14 (2,63)	7,09 (0,85)

Table 6.1.2: Scoring of Diabetes Self-Management Questionnaire (DSMQ) in diabetic patients.

The CSF measurements revealed that differences at 1.5, 3, 6, 12, 18 cpd were not statistically different between diabetic patients (45.0 ± 17.08, 67.43 ± 21.19, 66.71 ± 45.67, 35.29 ± 29.41, 10.43 ± 9.25, respectively) and control subjects (51.15 ± 18.16, 98.08 ± 31.92, 85.38 ± 34.06, 48.85 ± 26.92, 16.38 ± 8.56, respectively) ($p>0.05$) (Figure 6.1.2). There were not statistically differences in CSF measurements between control subjects with risk of developing DM compared to those without risk ($p>0.05$) (Figure 6.1.3).

In VFQ-25 questionnaire, “General Health”, “General Vision”, and “Role Difficulties” subscales were inversely correlated with fasting glucose levels ($r = -0.763$, $p=0.002$; $r = -0.640$, $p=0.018$; and $r = -0.709$, $p=0.007$, respectively) in control subjects. In diabetic patients, “General Health” was inversely correlated with HbA1c levels ($r = -0.784$ $p=0.037$).

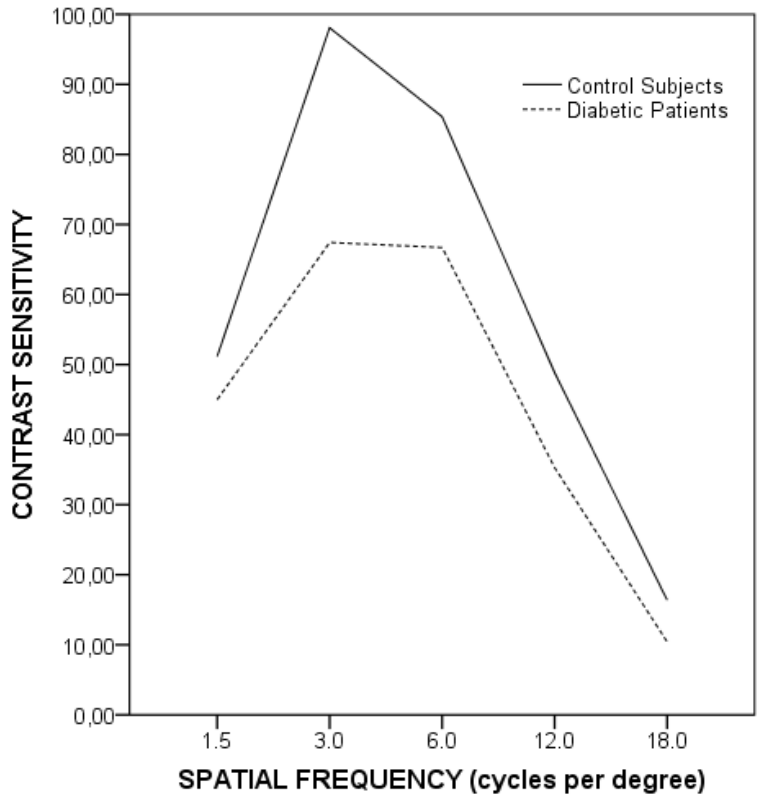

Figure 6.1.2: CSF between diabetic patients (solid line) and control subjects (dashed/dotted line) ($p>0.05$).

No significant correlations were found between contrast sensitivity scores and age, fasting glucose levels, LogMAR VA in control and diabetic subjects. Diabetes duration and HbA1c levels were not significant correlated with contrast sensitivity scores in diabetic patients.

In diabetic patients, statistically significant differences of compatible signs with microaneurysms and capillary dilation between colour, FAF and optimized-FAF images were found (Table 6.1.3, See Appendix 2). In all retinal areas, compatible signs with microaneurysms were less numerous in colour images compared with optimized-FAF and FAF images (Table 6.1.3, See Appendix 2). In colour versus FAF images, this decrease of ophthalmic signs observed was only statistically different for upper and lower temporal areas ($p=0.001$ and $p=0.007$, respectively). In colour versus optimized-FAF images, differences of compatible signs with microaneurysms were statistically different in all retinal areas ($p<0.0167$). However, these ophthalmic signs were only statistically different at upper temporal area in FAF images compared to optimized-FAF images ($p=0.016$) (Table 6.1.3, See Appendix 2).

Compatible signs with capillary dilation were more abundant in FAF and optimized-FAF images compared to colour images. However, differences were not statistically different between FAF and optimized-FAF images ($p>0.0167$) (Table 6.1.3, See Appendix 2). Number of capillary dilations of FAF images was statistically higher at upper and lower temporal areas compared to colour images ($p=0.001$). In colour versus FAF images, all retinal areas showed statistically significant differences in compatible signs with capillary dilations ($p<0.0167$) except upper nasal area ($p=0.017$). There were not statistically significant differences in compatible signs with haemorrhages and hard exudates between colour, FAF and optimized-FAF images ($p>0.05$) (Table 6.1.3, See Appendix 2).

In control subjects, number of epithelial defects and capillary dilations were statistically different between the three types of image ($p<0.001$) (Table 6.1.4, See Appendix 2). Both retinal defects were statistically different between colour versus FAF images, and colour versus optimized-FAF images ($p<0.0167$) (Table 6.1.4, See Appendix 2). In FAF versus optimized-FAF images, epithelial defects were only statistically different at upper and lower temporal areas ($p<0.0167$). However, statistically significant differences in capillary dilation number between FAF and optimized-FAF images were not found ($p>0.0167$) (Table 6.1.4, See Appendix 2).

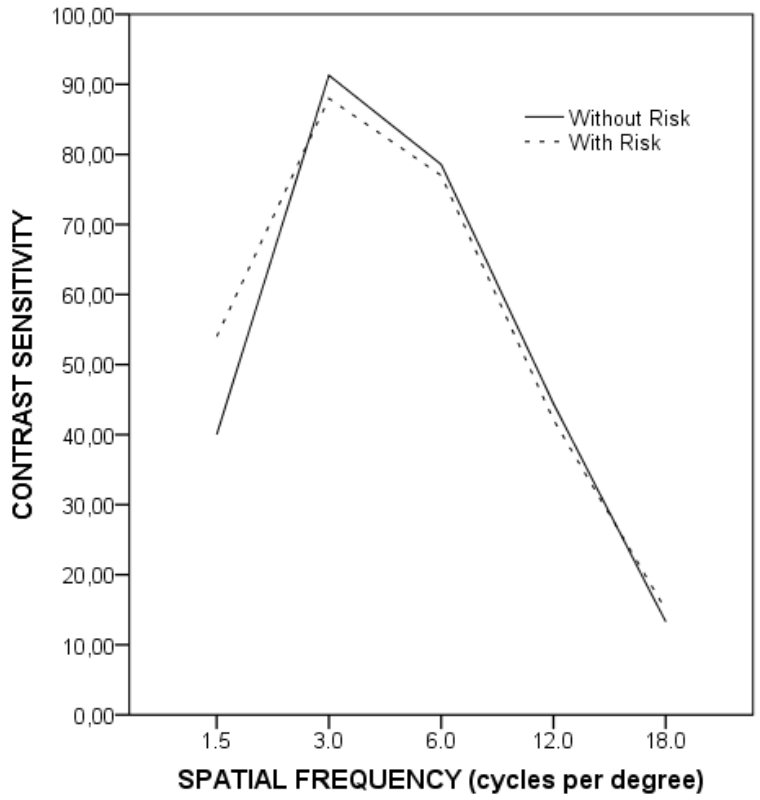

Figure 6.1.3: CSF between control subject with (dashed/dotted line) and without (solid line) risk of undergo DM.

Based in DSMQ questionnaire, control subjects were divided in two groups, control subjects with risk to develop DM and those without risk. Although a number of ophthalmic epithelial signs observed in optimized-FAF images were higher than colour and FAF images, these signs were only statistically different at lower temporal area of colour images ($p=0.035$). In FAF images, statistically significant differences between both groups were not found in any retinal area ($p>0.05$). In optimized-FAF images we only observed statistically differences at upper temporal area ($p=0.008$). Related to capillary dilations, we only observed statistically significant differences at lower temporal area in colour images ($p=0.014$). Statistical differences have not found in FAF images and optimized-FAF images between both groups of control subjects.

In diabetic patients, Spearman correlation revealed that compatible signs with microaneurysms observed at upper temporal and nasal areas in colour images were correlated with age in ($r = 0.845$, $p=0.017$; $r = 0.905$, $p=0.005$, respectively) and glucose levels were correlated with lower temporal area ($r = 0.919$, $p=0.003$). In FAF images, HbA1c levels were correlated with upper nasal area ($r = 0.955$, $p=0.001$) and diabetes

duration with lower nasal area ($r = 0.827$, $p=0.022$). In optimized-FAF images, diabetes duration was correlated with upper and lower nasal areas ($r = 0.757$, $p=0.049$; $r = 0.811$, $p=0.027$).

Compatible signs with capillary dilation were only correlated with HbA1c levels in upper nasal area ($r = 0.757$, $p=0.049$), and with glucose levels in lower nasal area ($r = 0.757$, $p=0.049$), in optimized-FAF images. In control subjects, Pearson correlation showed that epithelial defects observed at upper nasal area were correlated with age ($r = 0.613$, $p=0.026$) in FAF images. In optimized-FAF images, age was correlated with epithelial defects found at upper temporal area ($r = 0.587$, $p=0.035$).

Figure 6.1.4 shows colour, FAF and optimized-FAF images of diabetic patients and control subjects. FAF and optimized-FAF images of diabetic patients revealed retinal alterations while colour imaging did not present such alterations.

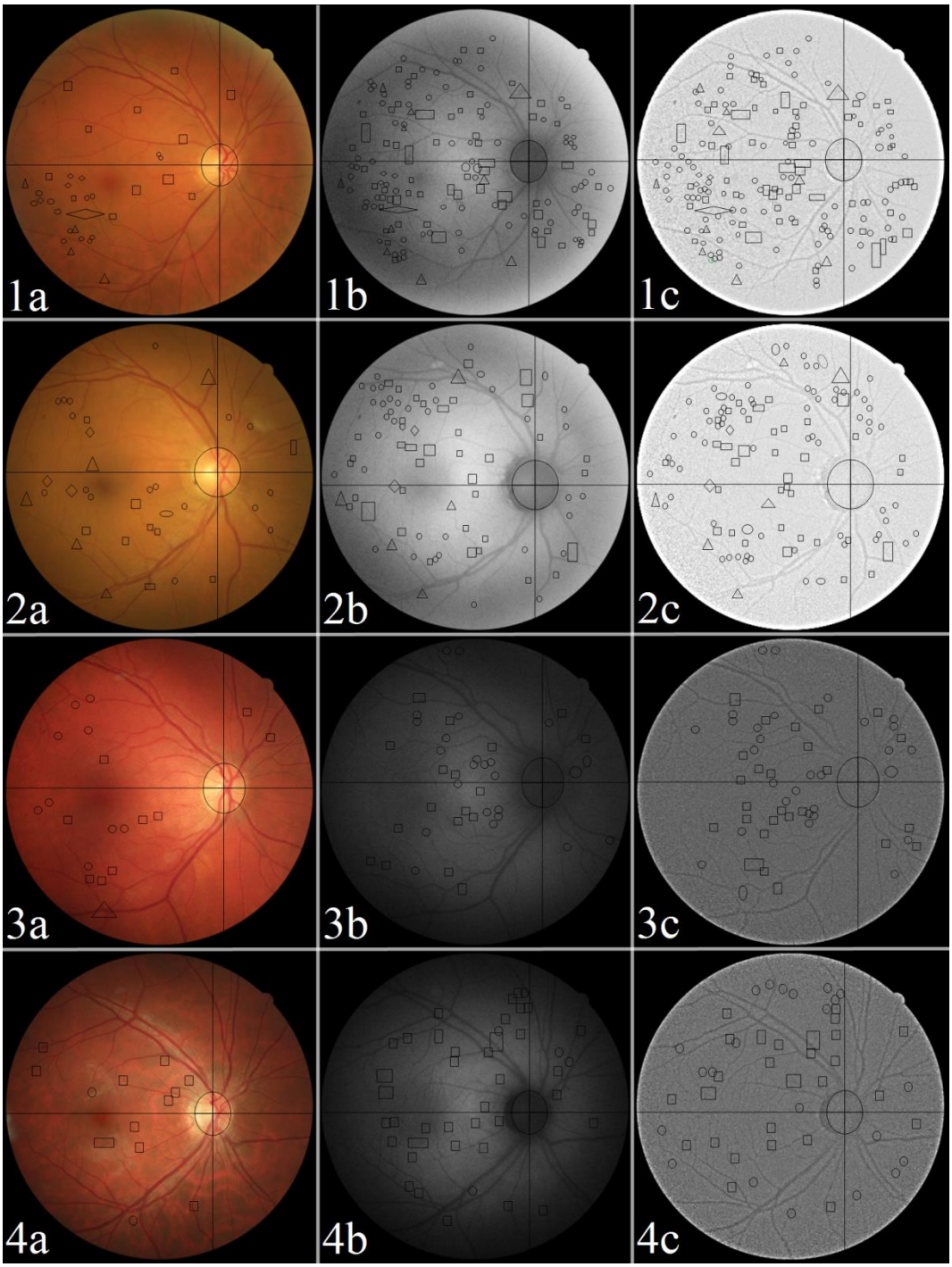

Figure 6.1.4: Colour fundus imaging (a), FAF imaging (b) and optimized-FAF (c) of 1: T1DM patient, diabetes duration 18 years; 2: T2DM patient, diabetes duration 30 years; 3: Control subject with risk of developing DM; 4: Control subject without risk of developing DM. Signs compatible with microaneurysms were represented by circles, capillary dilation by squares, haemorrhages by triangles, and hard exudates by rhombus.

6.1.4 DISCUSSION

The FAF is a non-invasive technique utilized mainly for detecting changes in metabolic activity at the RPE and it has been used in retinal diseases, such as AMD, DME and other retinal diseases to develop typical imaging features and to determine the extent of retinal damage (Kolomeyer et al., 2012; Sepah et al., 2014; Shen et al., 2014; Spaide, 2003).

DR is a common microvasculature complication in diabetic patients characterized by the presence of microaneurysms at the earliest stage, known as mild NPDR until the development of neovascularization and/or vitreous/prerretinal haemorrhage at the PDR, the latest stage of this complication. Several pathways such as polyol accumulation, AGEs, oxidative stress and activation of protein kinasa C (PKC) have been proposed as responsible of microvasculature damage (Fong et al., 2004).

In this pilot study we assessed FAF images using CR-2 Plus digital non-mydriatic retinal camera (Canon, Tokyo) in diabetic patients and control subjects with the aim of detecting early retinal signs of DM before impacting at the visual quality. We also studied visual function of both groups, self-care of diabetes and risk of developing diabetes by the use of questionnaires.

Diabetic patients showed significantly higher fasting glucose levels than control subjects ($p<0.001$) (Table 6.1.1). Diabetic subjects presented stable blood glucose levels (<200mg/dL) and HbA1c levels revealed a good glycaemic control (7.21 %) (Table 6.1.1). Thus, according to DSMQ questionnaire all diabetic patients had an adequate self-care of DM (Table 6.1.2) ("Total Score" > 6) (Schmitt et al., 2013).

A 53% of control subjects had a risk to develop diabetes according to the new questionnaire developed to identify undiagnosed people of diabetes (Herman et al., 1995), due to lack of practical exercise and/or high values of BMI.

Relative to visual function, several studies have analysed VFQ-25 questionnaire in diabetic patients (Gabrielian et al., 2010; Matza et al., 2008). In these studies determining that VFQ-25 is a better measure of visual function state in diabetic patients with DR than VA measure, due to degree of anxiety, fear and mental anguish related to

DR presence did not assessment by VA measure. The progression of DR was related with a decrease of "Specific-Vision Mental Health" (Gabrielian et al., 2010; Matza et al., 2008), "Role Difficulties", "Dependency" and "Driving" subscales (Gabrielian et al., 2010). However, in this study there are not differences in LogMAR VA, subscales scores and "Sum Scale" of VFQ-25 between diabetic patients and control subjects (Table 6.1.1). This lack of significant differences between both of group could be because our patients had well-controlled and to these patients did not show retinal alterations related to advanced stage of DR.

In this study, statistical correlations between LogMAR VA and VFQ-25 subscales were not found in diabetic patients nor control subjects. Although we found that fasting glucose levels were inversely correlated with "General Health" ($r = -0.763$ $p=0.002$), "General Vision" ($r = -0.640$ $p=0.018$) and "Role Difficulties" ($r = -0.709$ $p=0.007$) subscales in control subjects. In diabetic controls, HbA1c levels were inversely correlated with "General Health" subscale ($r = -0.784$ $p=0.037$).

In previous studies, contrast sensitivity scores were reduced in diabetic patients without retinopathy and it has been determined that contrast sensitivity measure could represent early retinal dysfunctions in diabetic patients without signs of DR (Georgakopoulos et al., 2011; Misra et al., 2010). In this study, spatial frequency scores of diabetic patients were lower than of control subjects, but not statistically different ($p<0.05$) (Figure 6.1.2). In addition to diabetes-related changes, this decrease could be explained partly by ageing because of a statistical difference in age between diabetic patients and control subjects.

Misra et al. (2010) in their study found an inversed statistically significant correlation between contrast sensitivity and LogMAR VA in diabetic patients without signs of DR, and they also demonstrate that HbA1c levels have a significant effect association with contrast sensitivity. However, we did not found statistically correlations between LogMAR VA, HbA1c levels, and contrast sensitivity frequencies in diabetic patients. These differences could be due to a difference in diabetes duration; although in study of Misra et al. (2010) this variable is unknown, it is possible their patients had duration of diabetes higher than our patients.

In control subjects with and without risk of developing diabetes spatial frequencies scores were similar, so there were not statistically differences at spatial

frequencies (Figure 6.1.3). This lack of statistic difference between control subjects could be due to absence of early ocular alterations related with diabetes.

In the FAF pattern of healthy eyes, the optic nerve head appears dark due to absence of lipofuscin, retinal vessels present a reduction of FAF signal due to absorption by blood and in the macular area, and FAF signal is also reduced especially around the fovea due to absorption of macular pigment, such as lutein, zeaxanthin and other pigments (Sepah et al., 2014). In DR, the mechanism of accumulation of lipofuscin in the retina is different from the other retinal diseases such as AMD (Sepah et al., 2014). In DR, age-related accumulation of lipofuscin in RPE, due to phagocytosis of outer segment photoreceptor, is not important in this retinal disease (Spaide, 2008). But, lipofuscin contains a large number of different products of peroxidation of lipids and proteins. So, lipofuscin is thought an indicator of oxidative damage in the retina (Vujosevic et al., 2011). Xu et al. (2008) showed that accumulation of lipofuscin was greater in microglia than in the RPE in this retinal disease. The pathophysiologic process of DR activates microglia; this activation allows the oxidation of proteins and lipids and therefore the accumulation of lipofuscin granules in the microglia in the development of diabetes.

In this study FAF images were normalized and homogenized for a better visualization of retinal alterations, and were compared to colour fundus images. We observed that all compatible signs with DR were statistically different between colour, FAF and optimized-FAF images (Table 6.1.3, See Appendix 2) (Figure 6.1.4). In FAF and optimized-FAF images we observed hypofluorescent granules that could be compatible signs with microaneurysms. Thus, we observed that these signs were statistically more numerous in optimized-FAF than colour images ($p<0.0167$). Related to compatible signs with capillary dilation, both temporal zones (upper and lower areas) showed statistically significant differences between colour and optimized-FAF images ($p<0.0167$). However, compatible signs with haemorrhages and hard exudates were not found statistically different between colour, FAF, and optimized-FAF images ($p>0.05$), although a number of hard exudates were slightly higher in colour images compared with FAF and optimized-FAF images. Hard exudates were identified as hyperfluorescent granules in FAF and optimized-FAF images. So compatible signs with microaneurysms and capillary dilation were more evident in FAF and optimized-FAF images compared with colour images but hard exudates were more difficult in their

identification in FAF and optimized-FAF images. Also optimized-FAF images showed compatible alterations with DR not visible in colour fundus, such as microaneurysms and capillary dilations. Xu et al. (2008) showed the pathophysiologic process of DR active microglia and therefore formation of lipofuscin granules. So we hypothesized that these alterations observed in optimized-FAF images could be show an early oxidative damage before formation of DR signs.

Although control subjects with risk to develop DM showed a large amount of epithelial defects compared to those without risk, these alterations were statistically different at lower temporal area of colour images, and at upper temporal area of optimized-FAF images. Capillary dilations numbers were only statistically different at upper temporal area in colour images ($p=0.008$) (Table 6.1.4, See Appendix 2). In control subjects with risk of developing DM, these epithelial alterations were more predominant in temporal areas and could correspond to local defects of RPE.

This study has limited sample size as main limitation, but the other limitation was that questionnaires were not validated in Spanish language. Therefore, all conclusions must be interpreted with care, as they need further confirmation in larger sample studies. In this study we have compared FAF and colour fundus imaging, although future comparative studies with other imaging models, such as OCT could also be significant for DR diagnosis.

In summary, this chapter shows visual function, contrast sensitivity, FAF and colour imaging in diabetic patients and control subjects. Diabetic patients had a good glycaemic control; however, we found that FAF imaging revealed alterations not visible in colour imaging that could be a sign of diabetes progression. Visual function and contrast sensitivity score were not statistically different between diabetic patients and control subjects. Although there is difficulty with image interpretation due to absence of protocols and measure system, in this study we considered that FAF and optimized-FAF images could be a complementary tool for detecting early signs of DR and for monitoring DM. Further studies are still needed to confirm these results and the exact mechanism of FAF changes in DM.

6.2 DIABETIC MACULAR OEDEMA ASSESSMENT BY FUNDUS AUTOFLUORESCENCE ANALYSIS USING A NON-MIDRIATIC RETINAL CAMERA

6.2.1 INTRODUCTION

DME is one of the major complications of DR and also one of the leading causes of severe visual loss in working-age population (Klein et al., 1998; Klein et al., 2008; World Health Organization, 2005). Although DME may appear at any stage of DR (Lopes de Faria et al., 1999), around 12% of patients with DR develop DME (Paulus and Gariano, 2009). T1DM patients can develop DME within the first five years following diagnosis (White et al., 2010), however around 5% of T2DM patients already have DME at time of diagnosis (Gundogan et al., 2016). The prevalence rate of DME is associated with duration, type of diabetes, proteinuria, gender, cardiovascular disease, high levels of HbA1c and the use of diuretics (White et al., 2010). In addition to glycaemic control and regulation of hypertension and hyperlipidaemia, there are several ophthalmic treatments intended to resolve DME, such as focal/grid laser photocoagulation (ETDRS Research Group, 1987; Olk, 1986), intravitreal injection of bevacizumab (IVB) (Haritoglou et al., 2006) or triamcinolone acetonide (Avitabile et al., 2005), and pars plana vitrectomy (Harbour and Smiddy, 1996).

In clinical practice, assessment of DME can be performed by means of fundus slit lamp biomicroscopy (Early Treatment Diabetic Retinopathy Study Research, 1985) or non-invasive imaging techniques such as OCT, which is currently considered a gold standard for diagnosing DME (Browning et al., 2004; Virgili et al., 2007).

FAF imaging is a non-invasive retinal imaging technique widely used for the assessment of age-related maculopathy and retinal dystrophy, among other ocular diseases (Spaide, 2008; Vaclavik et al., 2008). In healthy subjects, the macular area, particularly around the fovea, displays reduced AF intensity due to the absorption by macular pigments, such as lutein or zeaxanthin. The parafoveal area signal tends to be higher than that of the fovea signal; however, it shows a reduced intensity when compared with the background signal in peripheral areas of the retina (Schmitz-

Valckenberg et al., 2008b). Previous studies have shown FAF imaging as an useful tool for the detection and monitoring of DR (Calvo-Maroto et al., 2016c) and diabetic maculopathy (Dandekar et al., 2005; Roesel et al., 2009).

The present pilot study aimed to study FAF images obtained in diabetic patients with and without DME using the CR-2 Plus AF non-mydriatic retinal camera (Canon Inc, Tokyo) with the aim to determine the potential usefulness of FAF imaging in the detection of DME and establish correlations with OCT imaging and functional parameters.

6.2.2 PATIENTS AND METHODS

Subjects

We studied 32 right eyes from 32 subjects with DM (22 men and 10 women) and 10 right eyes from 10 healthy subjects (2 men and 8 women). Healthy subjects were recruited from University of Valencia and diabetic patients were recruited consecutively from the Doctor Peset University Hospital. All patients provided informed written consent in accordance with the World Medical Association´s Declaration of Helsinki before the procedures took place.

Inclusion criterion was clear ocular media allowing to record high quality colour and FAF imaging. Exclusion criteria for healthy subjects and diabetic patients were previous retinal photocoagulation and any retinal alteration affecting macular caused by systemic/ocular disease different from DM, such as AMD. Healthy subjects were considered as control subjects.

All diabetic patients were diagnosed of DM by a general practitioner (GP) from the primary care system. Diabetic patients group included T1DM and T2DM patients. Diabetic patients were classified into diabetic patients with and without DR. Those patients with DR were then subclassified according to the presence of DME. Ocular examination included autorrefractometry, slit-lamp biomicroscopy, OCT, colour fundus and FAF imaging. Four diabetic patients were dilated with tropicamide eye drops for acquiring fundus imaging. Colour fundus and FAF imaging were recorded after blood

analysis. The study was conducted as a single blind and an experienced optometrist explored FAF images.

Blood samples were collected from 8.00 a.m. to 10.00 a.m. These analyses included fasting glucose level, HbA1c levels, total cholesterol, high-density lipoprotein (HDL), low-density lipoprotein (LDL), and very low-density lipoprotein (VLDL) measurements.

Methods

Colour fundus and FAF imaging. Evaluation and image acquisition

Colour and FAF images were recorded with CR-2 Plus digital non-mydriatic retinal camera (Canon, Tokyo). Colour images were obtained and evaluated for potential changes in the optic nerve, blood vessels and macula. Following colour images, FAF images were taken using FAF mode (530-580 nm exciter filter and 640 nm barrier filter) in a dark room in order to prevent pupillary constriction. A single image was recorded per eye.

The FAF images were saved as TIFF images and analysed by MATLAB 2013a software (Mathworks, Inc., Natick, MA). All images were normalized and homogenized to a better visualization of retinal alterations, as per previous studies (Calvo-Maroto et al., 2016c).

After normalization and homogenezitation, imaging analysis was performed using NIH ImageJ medical imaging software (NIH ImageJ 1.47v, National Institutes of Health, Bethesda, MD-USA), developed by the National Institutes of Health and available as free download.

FAF images were calibrated according to Drasdo and Fowler (1974). Center of the macula was determined using anatomical references (Armadá Maresca et al., 2010) and was taken as a reference to define the different study zones. Therefore, three concentric circles with diameters of 1.7, 2.7 and 5.5 mm were analyzed, corresponding to foveal (including foveola and fovea), parafoveal, and perifoveal zones, respectively (Figure 6.2.1).

The macular zone contrast was enhanced by streatching histogram and signal-noise were reduced by median filter. Afterwards, FAF signal of different macular zones were quantified as grey level units (GU).

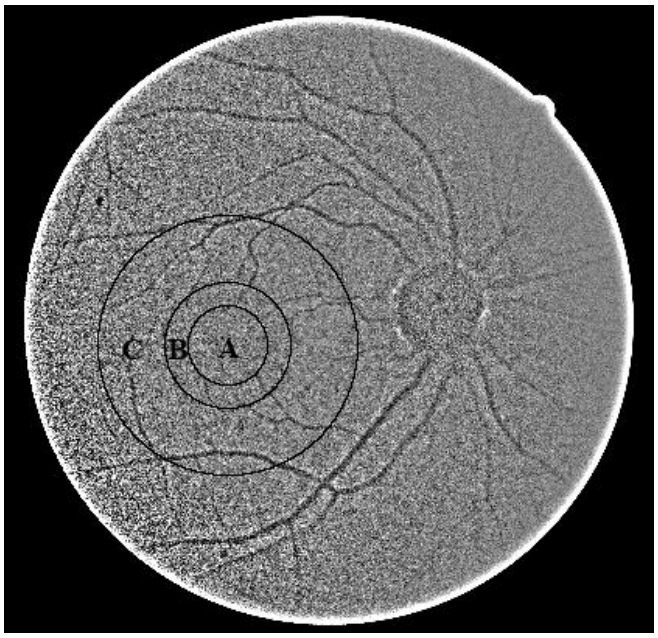

Figure 6.2.1: Division of FAF images intro three concentric rings centred at the fovea. A: Foveal Zone; B: Parafoveal Zone; C: Perifoveal Zone.

OCT measurements

OCT scanning was carried out with the Cirrus HD-OCT (Carl Zeiss Meditec, Inc., Dublin, CA-USA). The macular 512x128 cube scanning protocol was used for assessing volume and macular thickness. This scan protocol generates a cube of data through a 6 mm square grid by acquiring a series of 128 horizontal scan lines comprising 512 A-scans. Signal strength of 6 or higher was considered acceptable. Internal fixation was utilized to ensure proper alignment of the eye. All imaging was performed by an experienced ophthalmic photographer under the same conditions. Multiple measurements were taken and the one with best centration out of those with good signal strength was chosen for analysis.

Total macular thickness and macular volume over the central 6 mm centred at the fovea were obtained from the computation software output and used for statistical analysis.

Statistical Analysis

In the present study, only the right eye was considered for analysis. Normality of data distribution for the different groups was determined using the Kolmogorov-Smirnov test. When parametric analysis was possible, independent samples Student *t* test was used for comparisons between diabetic patients and control subjects, and one-way repeated measurements ANOVA test was used to assess differences between foveal, parafoveal, and perifoveal zones. When parametric analysis was not possible, Mann-Whitney U test and Friedman test were used to assess the significance of those differences, respectively. Bonferroni test was used as post-hoc analysis to determine which pairwise comparisons were responsible for the overall difference between groups. Kruskall-Wallis analysis was performed to evaluate differences between groups on FAF measurements.

Correlation coefficients (Pearson or Spearman) were used to assess the correlation between variables. P-values <0.05 were considered as statistically significant. All statistical analysis was carried out using SPSS software (version 19, IBM Corp., Armonk, NY-USA).

6.2.3 RESULTS

Qualitative analysis of FAF images performed by the optometrist revealed that FAF images from fifteen subjects were compatible with healthy subjects FAF patterns, ten subjects showed FAF patterns compatible with diabetic patients without DR, thirteen subjects provide FAF distribution compatible with diabetic patients without DME and four images were compatible with DME presence. However, there were really 10 control subjects, 13 diabetic patients without DR, 15 diabetic patients without DME and four with DME. Thus, 5 diabetic patients without DR were erroneously considered as control subjects, and 2 patients without DME as diabetic patients without RD in qualitative analysis of FAF images. Figure 6.2.2 shows colour, FAF, and normalized

and homogenized FAF images. FAF images revealed a hyperautofluorescence alteration compatible with cystoid DME.

Afterwards, quantitative analysis was performed with control subjects and diabetic patients diagnosed by the ophthalmologist. The mean age of control subjects was 57.50 ± 6.69 years (range 45 to 69 years) and that of diabetic patients 59.72 ± 7.87 years (range 40 to 75 years) ($p>0.05$). FAF measurements of control subjects (foveal zone: 105.65 ± 5.67 GU; parafoveal zone: 106.84 ± 5.42 GU; perifoveal zone: 106.93 ± 6.23 GU) were lower than those of diabetic patients (foveal zone: 110.05 ± 17.57 GU; parafoveal zone: 111.25 ± 17.77 GU; perifoveal zone: 111.46 ± 17.95 GU) but were not statistically significant ($p>0.05$). In control subjects, a repeated measurements ANOVA revealed differences in FAF measurements between foveal, parafoveal and perifoveal zones ($F(2,18) = 8.474$; $p=0.003$). Post-hoc analysis showed that FAF measurements in foveal zone were statistically different compared with those FAF levels in parafoveal and perifoveal zones ($p<0.05$). Besides, FAF measurements between parafoveal and perifoveal zones were not statistically different ($p>0.05$).

When diabetic patients group was divided according to the presence of DR, the mean age of diabetic patients without DR was 58.38 ± 9.36 years (range 40 to 75 years) and that of diabetic patients with DR was 60.63 ± 6.79 years (range 41 to 70 years) ($p>0.05$). The characteristics of both groups of diabetic patients are summarized in Table 6.2.1.

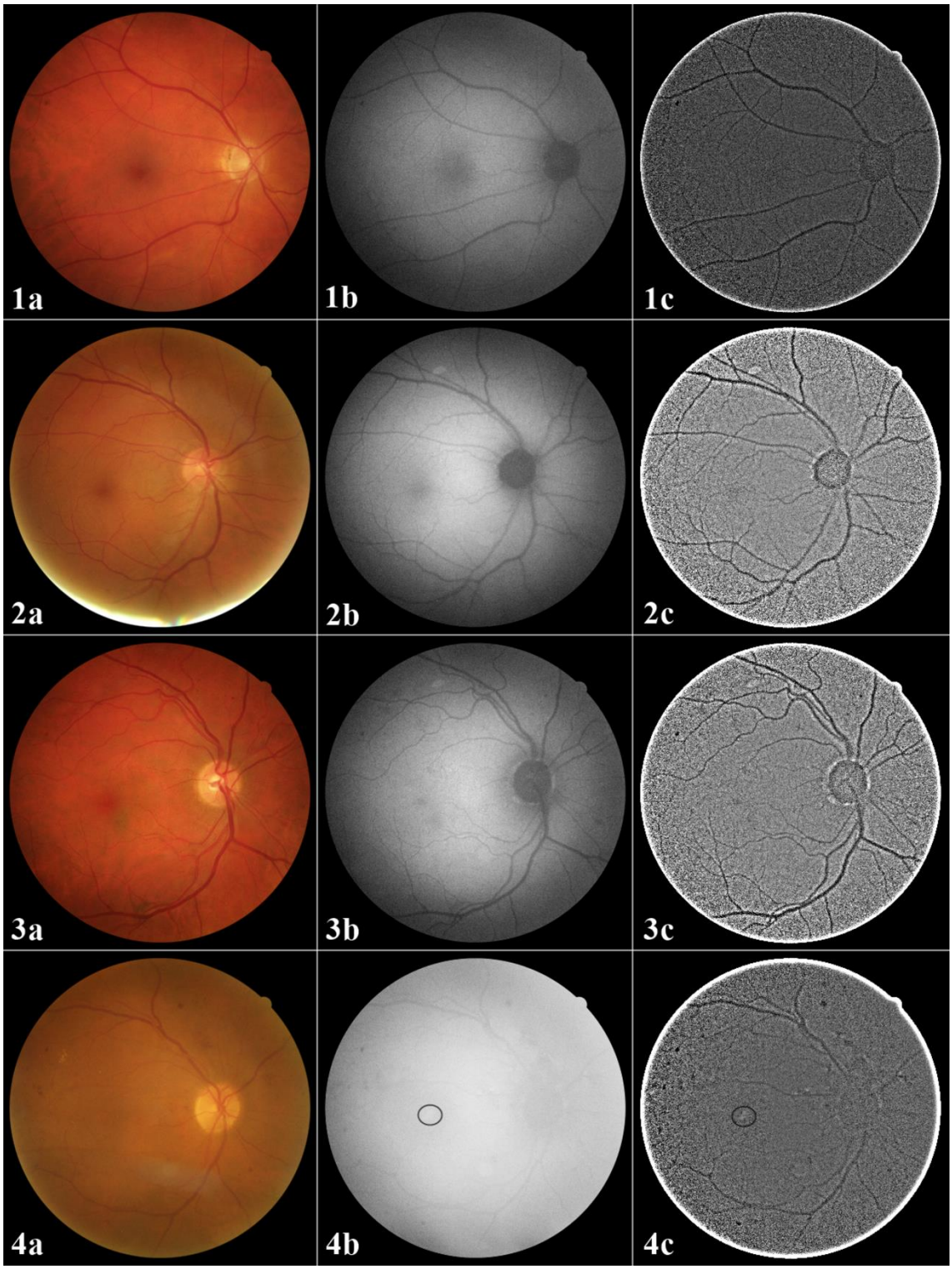

Figure 6.2.2: Colour fundus imaging (a), FAF imaging (b), and homogenized and normalized FAF imaging (c) of (1) control subject; (2) diabetic patient without diabetic retinopathy; (3) diabetic patient with diabetic retinopathy but not diabetic macular oedema; (4) diabetic patient with diabetic macular oedema. Signs compatible with cystoid alteration were represented by circle form.

In both groups of diabetic patients we found an acceptable metabolic control according to the ADA criteria (American Diabetes Association, 2016), based on the values of fasting blood glucose (without DR: 169.66 ± 61.96 mg/dL; with DR: 154.00 ± 70.48 mg/dL) and HbA1c levels (without DR: 7.34 ± 1.69 %; with DR: 7.97 ± 1.53%). Induced dilation was required in four patients with RD for acquiring FAF images.

	Diabetic patients without DR (n=13)	Diabetic patients with DR (n=19)	p-value*
Age (years)	58,38 (9,36)	60,63 (6,79)	0,437
BMI	27,89 (4,05)	29,83 (4,87)	0,259
Fasting Glucose Levels (mg/dL)	169,67 (61,96)	154 (70,48)	0,541
HbA1c Levels (%)	7,34 (1,69)	7,97 (1,53)	0,333
Cholesterol (mg/dL)	171,25 (24,39)	161,12 (40,98)	0,455
HDL (mg/dL)	40 (6,34)	47,31 (13,20)	0,065
LDL (mg/dL)	99, 66 (9,25)	88,28 (35,23)	0,31
VLDL (mg/dL)	31,58 (13,09)	23 (15,67)	0,141
Apolipoprotein A (g/L)	150,09 (17,80)	162,06 (33,25)	0,285
Apolipoprotein B (g/L)	100,45 (20,21)	83,76 (28,97)	0,109
FAF fovea (GU)	117,31 (23,51)	105,09 (9,97)	0,098
FAF parafovea (GU)	118,95 (23,60)	105,99 (10,02)	0,081
FAF perifovea (GU)	119,18 (23,70)	106,17 (10,38)	0,082

DR: Diabetic retinopathy; BMI: body mass index; HbA1c: glycosylated haemoglobin A1c; HDL: high density lipoprotein; LDL: low density lipoprotein; VLDL: very low density lipoprotein; FAF: Fundus autofluorescence; GU: grey levels units.
* Student *t* test

Table 6.2.1: Demographic data of diabetic patients with and without DR. Mean (SD) values.

In diabetic patients without DR, the mean macular volume was 9.67 ± 0.53 mm^3 and that of diabetic patients with DR was 10.34 ± 0.68 mm^3 ($p<0.01$). Difference of central macular thickness between diabetic patients without DR (266.28 ± 18.80 μm) and those with DR (274.55 ± 50.88 μm) was not statistically different ($p>0.05$).

FAF measurements of diabetic patients without DR (foveal zone: 117.30 ± 23.51 GU; parafoveal zone: 118.95 ± 23.60 GU; perifoveal zone: 119.18 ± 23.70 GU) were slightly higher than those with DR (foveal zone: 105.09 ± 9.97 GU; parafoveal zone: 105.99 ± 10.01 GU; perifoveal zone: 106.17 ± 10.38 GU), but were not statistically significant ($p>0.05$).

A one way repeated measurements ANOVA showed a significant effect of DM on FAF measurements in diabetic patients without DR ($F(2,24) = 25.841$ ($p<0.001$)) and in diabetic patient with DR ($F(2,36) = 13.217$ ($p<0.001$)). A post-hoc analysis determined that FAF measurements in foveal zone was statistically different compared with FAF in parafoveal and perifoveal zones ($p<0.05$) in diabetic patients with and without DR. However, FAF measurements between parafoveal and perifoveal zones were not statistically different in both groups ($p>0.05$).

Diabetic group with DR was divided according to the presence of DME. 15 diabetic patients did not show DME and four patients showed DME. The characteristics of both subgroups of diabetic patients are summarized in Table 6.2.2.

Mean macular volume in diabetic patients without DME was 10.15 ± 0.46 mm^3 and that of diabetic patients with DME was 11.05 ± 0.97mm^3 ($p<0.01$). Difference in central macular thickness between diabetic patients without DME (257.21 ± 26.58 μm) and those with DME (335.25 ± 72.76 μm) was also statistically different ($p<0.05$).

FAF measurements between diabetic patients without DME (foveal zone: 102.99 ± 9.78 GU; parafoveal zone: 103.91 ± 9.91 GU; perifoveal zone: 104.05 ± 10.34 GU) were significantly lower than those compared with DME (foveal zone: 112.97 ± 6.71 GU; parafoveal zone: 113.78 ± 6.41 GU; perifoveal zone: 114.15 ± 6.34 GU) ($p<0.05$) (Table 6.2.2) (Figure 6.2.3).

	Diabetic patients without DME (n=15)	Diabetic patients with DME (n=4)	p-value**
Age (years)	59,73 (7,27)	64 (3,26)	0,307
BMI	28,98 (4,36)	33,03 (6,00)	0,53
Fasting Glucose Levels (mg/dL)	163,46 (78,35)	123,25 (16,92)	0,35
HbA1c Levels (%)	8,11 (1,61)	7,55 (1,39)	0,521
Cholesterol (mg/dL)	158,67 (43,37)	168,5 (37,50)	0,262
HDL (mg/dL)	49,33 (12,76)	41,25 (14,45)	0,24
LDL (mg/dL)	82,30 (35,35)	103,25 (34,81)	0,226
VLDL (mg/dL)	22,64 (18,06)	24 (7,53)	0,245
Apolipoprotein A (g/L)	168 (33,67)	142,75 (26,67)	0,549
Apolipoprotein B (g/L)	80,61 (31,50)	94 (18)	0,163
FAF fovea (GU)	102,99 (9,78)	112,97 (6,71)	0,049
FAF parafovea (GU)	103,91 (9,91)	113,78 (6,41)	0,049
FAF perifovea (GU)	104,05 (10,34)	114,15 (6,34)	0,049

DME: diabetic macular edema; BMI: body mass index; HbA1c: glycosilated hemoglobin A1c; HDL: high density lipoprotein; LDL: low density lipoprotein; VLDL: very low density lipoprotein; FAF: Fundus autofluorescence; GU: grey levels units.
**U Mann-Whitney test

Table 6.2.2: Demographic data of diabetic patients with and without DME. Mean (SD) values.

In diabetic patients without DME, a one way repeated measurements ANOVA showed a significant effect to DM on FAF measurements ($F(2,28) = 8.575$, $p=0.001$). Post-hoc analysis revealed that FAF measurements in foveal zone was statistically different compared with those FAF in parafoveal and perifoveal zones ($p<0.05$). However, FAF measurements between parafoveal and perifoveal zones were not statistically different ($p>0.05$).

In diabetic patients with DME, a Friedman test revealed that FAF measurements were not statistically different between measured zones, $\chi^2 = 6.5$, $df = 2$, $p>0.05$.

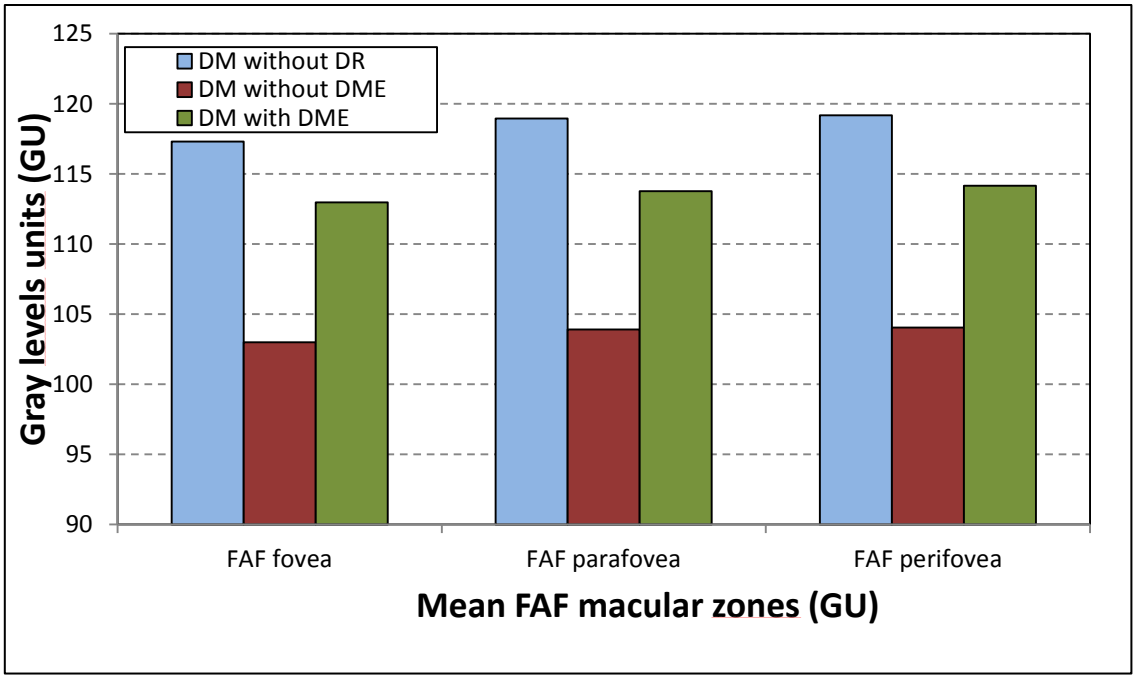

Figure 6.2.3: FAF signal measurements (GU) of macular zones (foveal, parafoveal, and perifoveal) in different groups of diabetic patients.

Kruskall-Wallis test showed that there was a significant effect of different stages of DM in macular volume (χ^2 = 11.752, df = 2, p=0.003). There was not a significant effect of any of the remaining variables studied (p>0.05).

Pearson´s correlation analysis showed in diabetic patients without DR that FAF measurements in foveal, parafoveal, and perifoveal zones were only correlated with fasting glucose levels (r = -0.685, p=0.014; r = -0.674, p=0.016; r = -0.676, p=0.016; respectively) (Figure 6.2.4).

In diabetic patients without DME, significant correlations were not found between different zones of FAF measurements with glucose levels (foveal zone: r = -0.017, p=0.957; parafoveal zone: r = 0.014, p=0.963; perifoveal zone: r = 0, p=0.999; respectively), or HbA1c levels (foveal zone: r = 0.035, p=0.915; parafoveal zone: r = 0.025, p=0.938; perifoveal zone: r = 0.040, p=0.902; respectively).

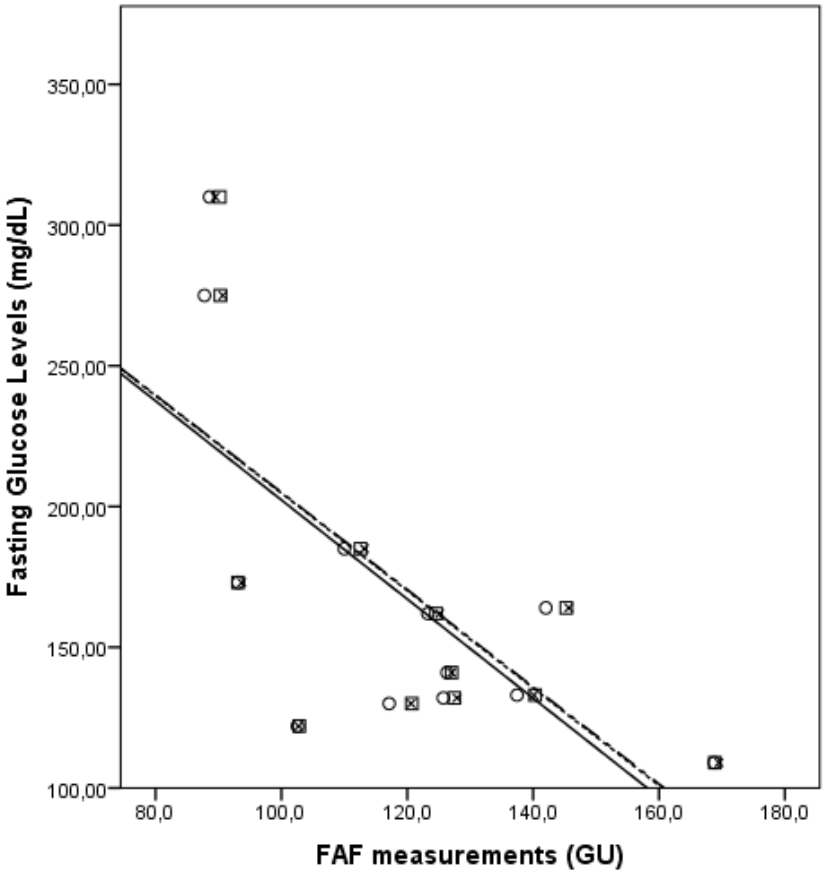

Figure 6.2.4: Correlations between FAF signal measurements in three macular zones and fasting glucose levels, in diabetic patients without DR. (Foveal: circles and solid line r = -0.685, p=0.014; Parafoveal: squares and dotted line r = -0.674, p=0.016; Perifoveal: crosses and dash-dot line r = -0.676, p=0.016).

In diabetic patients with DME, we showed a scatter diagram between FAF measurements in the different zones and HbA1c levels (Figure 6.2.5). By way of guidance, Spearman coefficients was calculated to provide the possible values of correlation between FAF measurements and HbA1c levels (foveal zone: r = 1.00, p<0.001; parafoveal zone: r = 1.00, p<0.001; perifoveal zone: r = 1.00, p<0.001).

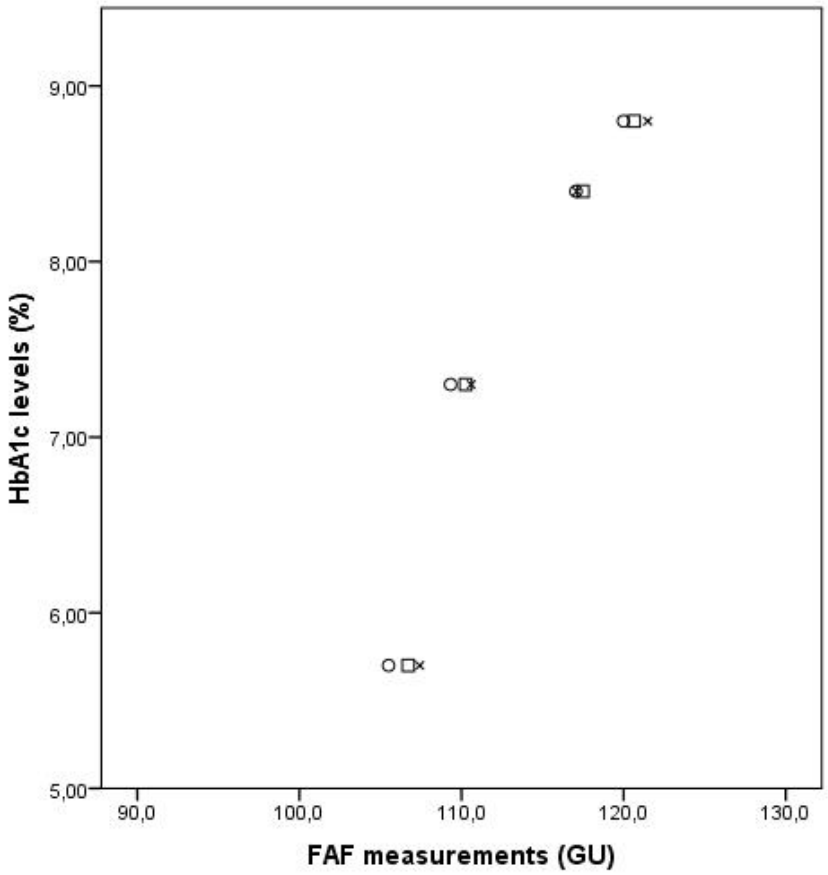

Figure 6.2.5: Scatter diagram between FAF signal measurements in three macular zones and HbA1c levels, in diabetic patients with DME. (Foveal: circles; Parafoveal: squares; Perifoveal: crosses).

6.2.4 DISCUSSION

FAF imaging is a non-invasive technique based in the retinal capacity for emitting light of a determined wavelength from natural fluorophores, mainly lipofuscin in the RPE (Delori et al., 1995). This technique is used for assessing changes in the metabolic activity of the RPE (Samy et al., 2014) and has been used as a complementary tool for understanding the pathophysiological mechanisms, diagnosing certain retinal diseases and macular dystrophies progression, and identifying predictive markers (Kolomeyer et al., 2012; Rovati and Docchio 2004; Schmitz-Valckenberg, et al., 2008b).

DME is a common complication of DR characterized by swelling or accumulation of blood and fluids within one disk diameter from the foveal centre leading to a severe visual loss (Klein et al., 1998; Klein et al., 2008; World Health

Organization, 2005). Although there is no unified criteria for DME classification, some authors have divided DME into focal and subtypes (Bresnick, 1986) while others, according to fluorescein angiographic findings, have classified DME into focal or diffuse (Browning and Fraser, 2005). In relation to FAF imaging, several authors have provided a qualitative assessment of FAF image and demonstrated four characteristic patterns in patients with DME: *normal*, *cystoid increased FAF (iFAF)*, where cystoid is observed within the macular area; *spot iFAF*, sporadic iFAF is in the low FAF background damaged retina; and *irregular decrease FAF (dFAF)*, where macula shows a mottled shape as well as irregular dFAF and subfoveal accumulation of a large amount of hard exudates observed on OCT (Vujosevic et al., 2011).

Previous studies have qualitatively observed hyperautofluorescence in diabetic patients with DME using cSLO (Bessho et al., 2009; Chung et al., 2012; Vujosevic et al., 2011) or fundus camera (Bessho et al., 2009), and other authors have quantified FAF signal in diabetic patients with DME (Yoshitake et al., 2015). In the present pilot study FAF images were acquired using the CR2-Plus digital non-mydriatic retinal camera (Canon, Tokyo). FAF images were qualitatively assessed by an experienced optometrist and afterwards, FAF signal was quantified in control subjects, diabetic patients without DR, with DR, and with DME. The FAF signal was analysed in three clinical zones: foveal, parafoveal, and perifoveal (Figure 6.2.1). We observed that FAF signal in control subjects were lower than those values in diabetic patients in all studied zones, although not statistically different ($p>0.05$). However the diabetic group showed a wide variation of FAF values due to different stages of ocular DM that might cause this difference was not statistically different.

When the diabetic patient group was divided according to the different stages of ocular DM, FAF values in diabetic patients without DR were slightly higher than those values obtained for patients with DR in all zones analysed, although these differences were not statistically significant ($p>0.05$) (Table 6.2.1). These differences possibly respond to the characteristic lesions of DR, causing a hypoautofluorescent signal that is not easily visible in colour images compared with FAF images, such as microaneurysms (Calvo-Maroto et al., 2016c).

When FAF signal was compared between diabetic patients with and without DME, it was observed that diabetic with DME showed higher FAF signal values and

signs compatible with cystoid alteration, compared to those without DME in all zones ($p<0.05$) (Table 6.2.2) (Figures 6.2.2 and 6.2.3). This macular hyperautofluorescence could be due to a lateral displacement of macular pigments causing a reduction of macular pigments density and avoiding the blocking of the AF signal (Bessho et al., 2009). Fundus retinal cameras use longer excitation wavelengths and hence, macular pigments may be less affected by blockage of these, located especially in highest density in the foveal area. Another hypothesis that could explain this hyperautofluorescence is the existence of unknown fluorophores within the macular oedema responsible of this fluorescence. Vujosevic et al. (2011) hypothesized that this could be caused by accumulation of oxidative products induced by activated microglia in which lipofuscin accumulates.

A recent study by Yoshitake et al. (2015) quantified the FAF intensity in diabetic patients with DME compared to those patients with DR without CSME. They found that parafoveal subfield showed lower FAF signal values in diabetic patients with DME compared to those without DME ($p<0.05$). However, patients with DME showed higher signal levels in the central subfield, although not significantly ($p>0.05$). In the present study, the foveal zone of patients without RD and without DME showed lower values than parafoveal and perifoveal zones ($p<0.01$), but differences were not statistically different between parafoveal and perifoveal zones ($p>0.05$). Likewise, in diabetic patients with DME, differences between the three zones were not statistically different ($p>0.05$).

These differences in the results reported might be due to differences on the size of the zones studied and the devices used. The present study used the CR-2 Plus, a digital non-mydriatic retinal camera, for acquiring FAF imaging, while Yoshitake et al. (2015) used a cSLO based Heidelberg Retina Angiograph 2 (Heidelberg Engineering Inc. Franklin, MA-USA). Both techniques show differences in the optical principles, excitation and emission barrier filter wavelengths, image acquisition and image processing.

Although there were not statistically differences on FAF measurements between the three groups of diabetic patients, diabetic subjects without DR showed higher FAF values than those with and without DME in all zones studied. It could be that the RPE function gets damaged by diabetes, and it is possible that phagocytosis of photoreceptor

outer segments decrease causing lower amounts of fluorophore debris, including lipofuscin (Yoshitake et al., 2015). Thus, this decrease in phagocytosis might explain the decrease in FAF signal of diabetic patients with DR compared to FAF signal of those without DR. It may be speculated that hyperautofluorescence signal in diabetic eyes with DME compared to those without DME might due to existence of unknown fluorophores inside the DME. It might be also due to cyst size, thus our diabetic patients might show a relatively small oedema size and consequently a lower FAF signal than diabetic patients without DR or even, the maximum excitation/emission wavelengths of responsible fluorophores of FAF might not be identify by excitation/detection wavelengths used in this non-mydriatic retinal fundus camera.

There are conflicting reports according to the effect of the lipid profile on RD or DME. Some authors showed that patients with high total cholesterol and LDL levels are more likely to have retinal hard exudates compared to patients with normal lipid profile (Chew et al., 1996). Other authors observed that retinal exudates of DME are associated with either LDL or cholesterol, or both (Idiculla et al., 2012). However, Ozer et al. (2009) could not show a significant correlation between serum lipid and DME. The same observation applies to DR, triglycerides, HDL and cholesterol. Miljanovic et al. (2004) did not find association between lipid profiles and DR progression or PDR. Benarous et al. (2011) reported that there is no association between DR and lipid profile, although CSME was associated with serum lipids.

In the present study it may be observed that LDL and cholesterol levels were higher in patients with DME compared to those without DME, but this difference was not statistically different ($p>0.05$) (Table 6.2.2). However, diabetic patients with RD showed lower values of these lipid parameters than those without RD ($p>0.05$) (Table 6.2.1).

Regarding to serum metabolic markers, Sasongko et al. (2011) showed that serum apolipoproteins (apo-A, apo-B and apo-B/apoA ratio) are stronger biomarkers of DR compared to traditional lipids. Apo-A is the structural protein of HDL and better reflects lipid accumulation in peripheral tissues and it has anti-inflammatory, antioxidant, and atheroprotective effects. However, apoB is associated with the LDL fraction and is a predictor of cardiovascular risk and a proinflammatory mediator. Previous studies have shown that serum apo-B was associated with increased risk of

PDR that was observed in diabetes with macrovascular and microvascular complications (Hill and McQueen, 1997). The results reported in the present pilot study show that this marker was higher in diabetic patients with DME compared to those without DME, although not statistically different ($p>0.05$) (Table 6.2.2). Correlations between serum lipids and metabolic markers with different stage of DM were not found.

A low metabolic control has been considered as risk factor of DM progression (American Diabetes Association, 2016; Klein et al., 1998). Glucose levels of diabetic patients without DR were correlated with all FAF zones in the present study (foveal zone: $r = -0.685$, $p=0.014$; parafoveal zone: $r = -0.674$, $p=0.016$; perifoveal zone: $r = -0.676$, $p=0.016$) (Figure 6.2.4). These correlations might confirm that excitation wavelengths used by fundus camera avoid blockage of macular pigments in diabetic without DR. However, those patients without DME showed the lowest values of FAF measurements and did not show correlations with metabolic control parameters. In diabetic patients with DME, scatter diagram showed a possible lineal correlation between FAF measurements and HbA1c levels (Figure 6.2.5). And, correlation values (foveal zone: $r = 1.00$, $p<0.001$; parafoveal zone: $r = 1.00$, $p<0.001$; perifoveal zone: $r = 1.00$, $p<0.001$) showed that FAF measurements tends to increase with poor glycaemic control however, these results must be interpreted with care because of sample size is not enough large to establish definitive findings. It can be speculated that an accumulation of unknown fluorophores or oxidative products, suggested by Vujosevic et al. (2011), was a result of poor metabolic control in patients with DME.

To the best of the author's knowledge, this is the first pilot study of FAF quantification in diabetic patients with DME using a non-mydriatic retinal camera. The main limitation of this study is the reduced sample size, and therefore all the results must be interpreted with care, and further studies in larger cohorts of diabetic patients and healthy subjects are needed to confirm the trends and conclusions reported here.

In conclusion, this chapter shows FAF measurements in three macular zones in healthy subjects, diabetic patients without DR, without DME, and with DME. Statistically significant differences in FAF measurements between healthy subjects and diabetic patients were not found, neither between with and without DR diabetic patients. However FAF signal was statistically different between patients with and without DME. According to the metabolic parameters studied, fasting glucose and HbA1c levels were

correlated with FAF measurements in all macular zones. Therefore, FAF signal measurements using digital non-mydriatic retinal camera might be a complementary tool for assessment and management of DME in patients with DR.

CHAPTER 7

Discussion

DM is a clinical syndrome characterized by chronic hyperglycaemia associated with long-term damage of different organs, especially eyes, kidneys, heart, blood vessels, and nerves. In clinical practice, DM is usually diagnosed and controlled by glucose (World Health Organization, 1999) or HbA1c levels (American Diabetes Association, 2010) measurements. Although a good control of these levels is essential to avoid developing complications, the duration and poor glycaemic control of this disease is considered an important risk factor on complications development.

As previously mentioned in Chapter 1, DM is associated with several ocular complications, such as keratopathy (Inoue et al., 2001), cataract (Ederer et al., 1981; Klein et al., 1985; Nielsen and Vinding 1984), glaucoma (Şahin et al., 2009), refractive changes, chronic inflammation of the eyelids, lachrymal gland dysfunction, oculomotor nerve paralysis, DR or DME (American Academy of Ophthalmology, 2016; Williams et al., 2004). Therefore, this PhD thesis aims to determine the clinical usefulness of non-invasive optical quality metrics and FAF imaging analysis on early detection of ocular changes caused by DM and the management of disease progression to improve quality of life in diabetic patients.

The first part of this PhD thesis is focused on corneal complications caused by DM and how these complications affect to corneal optical quality. For that purpose, a new metric of corneal backscatter has been developed using Scheimpflug imaging from Pentacam rotation Scheimpflug camera and the NIH ImageJ medical imaging software.

The first study has shown that CCT values in long-term diabetic patients (those diagnosed and treated for 10 years or more) were significantly higher than those with short-term diabetes (<1 year since diagnosis) ($p<0.001$). And ECD values were significantly lower in long-term diabetic patients compared with short-term diabetes ($p<0.001$). When both diabetic groups were compared with their respective control age-matched groups, CCT and ECD values were not statistically different between short-term diabetic patients and its age-matched control group ($p>0.05$), however these parameters were statistically different between long-term diabetic patients and its respective control group ($p<0.001$). Also, this study confirmed the effect of diabetes duration and poor control of glycaemic levels on CCT and ECD changes in T2DM patients. Thus, CCT values were significantly different for a 7.5% HbA1c cut-off value, ECD for both 7.0% and 7.5% HbA1c cut-off values, and MANOVA test indicated a significantly effect of diabetes duration on CCT and ECD values.

To determine how these structural and morphological changes affect to corneal transparency and therefore, its optical quality, a second study assessed this corneal property by measuring the central corneal backscatter with the aim to provide a complementary tool for monitoring corneal changes caused by DM. In clinical practice, several devices have been used to measure light backscatter by digital analysis of the images obtained with slit-lamp, OCT or Scheimpflug camera, and to assess the quality of ocular tissues.

Scheimpflug imaging analysis was used to develop a new metric of corneal backscatter by optical density calibration from NIH ImageJ medical imaging software. Two central zones, 3 and 5 mm, were analysed in diabetic patients and control subjects. Corneal backscatter, in both zones, was statistically higher in diabetic patients compared with their respective control age-matched group ($p<0.05$ in both cases). T2DM showed higher values of corneal backscatter, in both analysed zones, than T1DM, but not statistically different ($p>0.05$ in both cases). Although the image resolution was not enough to distinguish the different corneal layers, this study provides distribution of ocular backscatter along central corneal thickness. These profiles showed a similar pattern in all groups studied, although diabetic patients showed a higher peak of corneal backscatter in the anterior corneal layers compared with control subjects, and the highest peak observed corresponded to T2DM. Since these peaks of corneal backscatter profile are located in the anterior corneal layer so, it suggested that these peaks might

correspond to the interface between the tear film and the epithelium-Bowman´s membrane.

Previous studies have demonstrated that this increase of corneal light scattering in diabetic patients might be suitable for early detection of diabetic complications using specific (Morishige et al., 2001; Takahashi et al., 2007) or modified devices (Patel et al., 2007). Holden et al. (1994) did not detect any difference between diabetic patients and normal control group using the Case 2000 CCD (charged couple device) Scheimpflug slit image camera (part of the Oxford Modular Cataract Image Analysis System [OMCIAS]). However, this PhD thesis provides a new quantification of corneal backscatter by optical devices widely used in clinical practice and available to clinical practitioners.

Thus, this first part of the PhD thesis shows that diabetic patients undergo morphological and structural corneal changes that might compromise corneal transparency and therefore its optical quality. Corneal properties, such as transparency, was assessed and quantified by light backscatter. Results of this pilot study showed diabetic patients had higher central corneal backscatter values than healthy controls. Although an increase of corneal backscatter does not imply a reduction in visual quality, these results show a decreased on corneal optical quality due to ocular complications that might be caused by duration of disease or poor glycaemic control in diabetic patients. Therefore, corneal backscatter measurements may be useful tool to assess corneal complications, and therefore, to detect early ocular changes and progression of DM.

The purpose of the second part of this PhD thesis was to assess ocular optical quality in diabetic patients by HOAs measurements and to know the relative contribution of optical components to the total aberrations of the eye.

The transparency, structure and morphology of ocular components determine the sharpness of the retinal image, and therefore any alteration in these characteristics implies a decrease in the quality of retinal image (Liang and Williams, 1997). As previously mentioned in Chapter 1, ocular components (mainly cornea and crystalline lens) undergo several changes caused by DM, so it seems reasonable to think that these changes might cause an increase of HOAs and hence a decrease in retinal image quality.

This study has reported HOAs up to fourth order across 5 mm pupils in T1DM and T2DM patients without differences in ocular parameters. This study shows that there were not differences in total, internal or corneal aberrations between studied groups. Total HOAs were higher in T1DM patients than in T2DM patients, but not statistically significant ($p>0.05$). Also, a partial balancing between corneal and internal components was observed in horizontal/vertical astigmatism, horizontal coma, and spherical aberrations components. Considering all studied Zernike coefficients, vertical coma had the highest value in T1DM and T2DM patients, and the internal vertical coma was the highest contributor of total optical aberrations for both groups. Although healthy subjects were not included in this study, there are several studies with larger sample size of healthy subjects. Wang et al. (2003) in their study with healthy subjects and similar age to T1DM patients of this study, reported values of internal comatic coefficients lower than to those found in this study. Thus, it suggested that changes in posterior cornea or crystalline lens caused by DM might be responsible of this increase in HOAs measurements in diabetic patients. In T2DM patients this increase might be due to age-related changes of the crystalline lens, however in T1DM was not found any correlation with ocular parameters to explain this increase.

Therefore, HOAs measurements show the consequences of ocular changes related to DM into visual quality, and might be considered a tool for monitoring changes in ocular structures in diabetic patients. CH has been also proposed to be a useful tool for assessment DM changes, although corneal changes responsible of CH changes are located in anterior and central stroma (Hager et al., 2009). However, this study has reported that changes in posterior cornea and crystalline lens cause higher HOAs measurements. Therefore, this study provides the clinical usefulness of optical quality as an aid for monitoring changes caused by DM.

In view of the above, the ocular quality study of optical components and retinal image (light backscatter and HOAs measurements, respectively), provide useful information about the effects of ocular complications on visual quality in diabetic patients, also these measurements show the progression of DM. Therefore, these non-invasive parameters of ocular quality might be a complementary tool for monitoring and assessing ocular complications caused by DM.

The third part of this PhD thesis is focused on the two main retinal complications of DM, i.e. DR and DME, and their assessment by FAF imaging using a non-invasive retinal camera. This PhD thesis provides an overview about the state of the art of the basis of this mechanism, taking into account the different ocular endogenous fluorophores and the optical principles in which the widely used devices for acquiring FAF imaging are based. Also, this PhD thesis has studied the potential for detecting these retinal complications by a non-mydriatic camera and it has been proposed a new quantification for the FAF signal.

The most common retinal complications caused by DM are DR and DME. DR is caused by long-term damage to retinal microvasculature that involves visual impairment (American Diabetes Association, 2011; Fong et al., 2004). According to several authors, the prevalence of any DR is around 34% among diabetic patients (Yau et al., 2012).

The FAF imaging is a non-invasive technique that provides a lipofuscin distribution in the RPE in vivo (Kolomeyer et al., 2012; Samy et al., 2014). Lipofuscin fluorophore is the undegradable end product resulting from the phagocytosis of receptor outer segment located in RPE (Sepah et al., 2014; Shen et al., 2014). The lipofuscin accumulation shows the metabolic damage in RPE caused by retinal diseases (Rovati and Docchio, 2004). In DR, lipofuscin granules contain peroxidation products from lipids and proteins (Schmitz-Valckenberg et al., 2008b), and therefore it has been proposed as an indicator of oxidative damage on the retina (Vujosevic et al., 2011).

In this PhD thesis, DR was assessed by FAF imaging using a non-mydriatic retinal camera in diabetic patients and healthy controls. Retinal alterations were also related to quality of life and diabetes self-care management.

The FAF imaging was analysed by MATLAB 2013b software and all images were normalized and homogenized for a better visualization of retinal alterations. These images were called optimized-FAF images. Colour, FAF, and optimized-FAF images were divided onto four quadrants corresponding to anatomical retinal quadrants.

All diabetic patients showed stable blood glucose levels (<200mg/dL) and glycaemic control (<7.5%). According to DSMQ questionnaire all diabetic patients had an adequate self-care of DM. In diabetic patients, compatible signs with mycroaneurisms and capillary dilation were more abundant in FAF and optimized-FAF

imaging than those observed in colour imaging, for all retinal quadrants. Compatible signs with mycroaneurisms were only statistically different at one quadrant in FAF images compared to optimized-FAF images ($p=0.016$). For compatible signs with capillary dilation, differences were not statistically different between FAF and optimized-FAF images (>0.0167).

A 53% of control subjects had risk to develop diabetes according to questionnaire to identify undiagnosed people of diabetes. In these subjects, the number of epithelial defects and capillary dilations were statistically different between the three types of images ($p<0.001$). However, post hoc analysis showed that differences in capillary dilation number were not statistically significant between FAF and optimized-FAF images ($p>0.0167$).

Compatible signs with microaneurysms, observed as hypofluorescent granules, and capillary dilation were more evident in FAF and optimized-FAF images compared with colour images. However hard exudates, identified as hyperfluorescent granules in FAF and optimized-FAF images, were more difficult to be identified in both type of FAF images. Thus, optimized-FAF and FAF imaging showed retinal alterations not visible in colour imaging, such as mycroaneurisms and capillary dilation, suggesting that optimized-FAF and FAF imaging could show an early oxidative damage before formation of DR signs and could be an interesting tool for detecting early signs of diabetes progression, since Xu et al. (2008) showed that pathophysiologic process of DR actives microglia and therefore the formation of lipofuscin granules.

Another study of this PhD thesis provides an assessment of DME in diabetic patients with optimized-FAF and FAF imaging using the same retinal camera for determining their usefulness for detecting this retinal complication. In this study were enrolled diabetic patients without DR, without DME, and with DME and age-matched healthy controls. Firstly, a qualitative analysis of FAF images was done, concluding that those diabetic patients with DME showed hyperfluorescent zones compatible with cystoid DME in macular area. Afterwards, a quantitative analysis of FAF images was carried out. For this purpose, FAF images were normalized and homogenized by MATLAB 2013b and image analysis was done with NIH ImageJ medical imaging software. After calibrating FAF imaging, macular area was divided onto three zones: foveal, parafoveal, and perifoveal zones, and FAF signal was measured as GU.

In control subjects, FAF signals were lower than those measured in diabetic patients in all studied zones, but not statistically significant ($p>0.05$). In the diabetic group it was observed a wide variation in FAF signal that might be due to different stages of DR that diabetic patients presented. When diabetic group was divided according to the presence of DR, FAF signals were slightly lower in diabetic patients with DR compared to those patients without DR in all zones that were analysed, but not statistically significant ($p>0.05$). However, when FAF signal was measured in diabetic patients with and without DME, it was observed that patients with DME showed higher FAF signal values and compatibles signs with cystoid alteration compared to those patients without DME in all zones ($p<0.05$). There are several hypotheses about these hyperfluorescent zones. They could be the result of the displacement of macular pigments, consequently avoiding de blockage of macular pigments, they might be due to the existence of unknown fluorophores within oedema responsible of this AF signal, or as Vujosevic et al. (2011) reported, they could be caused by accumulation of oxidative products induced by microglia in which lipofuscin accumulates. According to the metabolic control, it was observed that HbA1c and fasting glucose levels were correlated with FAF signals in the three zones that were studied.

Previous studies have assessed qualitatively DME using cSLO and there have been proposed different retinal patterns to describe it. Several authors compared FAF images from cSLO and fundus camera in diabetic patients with DME, and they concluded that CME is always observed with an excitation wavelength of 488 nm (cSLO) and rarely with 580 nm (fundus camera). FAF intensity has been quantified in diabetic patients with DME compared with diabetic patients without DR by Yoshitake et al. (2015) using cSLO. They reported that parafoveal zone showed lower FAF signal values in diabetic patients with DME compared to those without DME ($p<0.05$). However, patients with DME showed higher signal levels in the foveal zone, although not statistically significant ($p>0.05$). In this study, foveal zone showed lower FAF signals compared to parafoveal and perifoveal zones in diabetic patients without DME and those without DR ($p<0.05$), however differences between parafoveal and perifoveal zones were not statistically significant ($p>0.05$). These differences could be due to differences in the optical principles, excitation and emission barrier filters of the devices employed, or even to the size of the studied zones.

According to the pilot studies of this thesis, FAF and optimized-FAF images acquired with non-mydriatic retinal fundus cameras might be useful complementary tools for assessment and monitoring retinal complications by DM. Although there are necessary further studies with larger sample sizes, results obtained show that fundus retinal camera is able to detect early signs that are compatible with DR progression, and also hyperfluorescent zones compatible with cystoid in patients with DME. Nevertheless, measurements of FAF signals obtained with this device cannot be directly compared with those of other studies because of there is not standardized protocol or measurement system.

CHAPTER 8

Conclusions and Future Work

In the present PhD thesis the consequences of ocular changes caused by DM in ocular optical quality through the corneal backscatter and ocular HOAs measurements have been studied. Also, it has been assessed the usefulness of FAF imaging acquired with non-mydriatic retinal cameras on detecting and monitoring retinal complications of DM, mainly RD and DME. According to these results, this PhD thesis provides several non-invasive complementary tools that might be part of the diagnostic and monitoring tests that are performed daily in clinical practice. Results obtained from these studies should be considered as preliminary indications, because they are pilot studies requiring further analysis with larger sample sizes to confirm them. Since DM is a systemic disease with a great healthcare impact due to its increased prevalence, development of diabetic complications and high mortality associated rate, these non-invasive measurements of corneal light backscatter, HOAs and FAF signals could help the DM screening and the early diagnosis of complications that could improve the quality of life of diabetic patients.

Then, the main conclusions of these studies are listed below:

- T2DM causes a significant alteration in corneal structure and function in the long term, confirming the effect of diabetes duration and poor glycaemic control in CCT and ECD values.

- People with DM show higher values of central corneal backscatter compared to control age-matched subjects. Corneal optical density analysis might be a useful tool for monitoring and assessing the ocular changes caused by DM.
- Diabetic patients show higher values of total and internal vertical coma. Therefore, optical quality measurements might be playing a role in monitoring changes due to DM.
- FAF and optimized-FAF imaging show significant alterations related to DR that are not observed in standard colour imaging. Therefore, FAF and optimized-FAF imaging could be useful complementary tools for detecting early alterations associated with the development and progression of DR.
- People with DME show higher values of FAF signals and compatible signs with cystoid alterations compared to those patients without DME. Thus, FAF and optimized-FAF imaging obtained by non-mydriatic retinal cameras might be useful complementary tools for assessing and monitoring DME in diabetic patients with DR.

These conclusions for the different studies of this PhD thesis establish the basis for future research lines and potential studies, such as:

1. Development of standardized metrics of light backscatter values from Scheimpflug imaging.
2. Increase the sample of T1DM, T2DM patients with different degrees of DR and include people with risk to develop DM in optical quality measurements.
3. Development of standardized metric of FAF signal and achieve equivalence between measurements from the devices widely used for acquiring FAF imaging, i.e., cSLO and non-mydriatic retinal camera.
4. Establish ranges of normality in FAF signal in healthy controls in different decades of age.
5. Increase the sample of diabetic patients with DME and DR and include people with risk of developing DM in studies of FAF imaging to compare with healthy control measurements.

REFERENCES

ABIKO, T., ABIKO, A., ISHIKO, S., TAKEDA, M., HORIUCHI, S., & YOSHIDA, A. 1999. Relationship between Autofluorescence and Advanced Glycation End Products in Diabetic Lenses. *Exp Eye Res*, 68, 361–66.

AKRAM, A., NIAZI, M.K., ISHAQ, M., & AZAD, N. 2003. Frequency of Diabetics in Asteroid Hyalosis Patients. *J Ayub Med Coll Abbottabad*, 15, 10–1.

AMERICAN ACADEMY OF OPHTHALMOLOGY RETINA/VITREOUS PANEL. 2016. Preferred Practice Pattern Guidelines. Diabetic Retinopathy. San Francisco, CA, USA: American Academy of Ophthalmology. Available at www.aao.org.

AMERICAN DIABETES ASSOCIATION. 2005. Diagnosis and Classification of Diabetes Mellitus. *Diabetes Care*, 28 (Suppl 1), S37–42.

AMERICAN DIABETES ASSOCIATION. 2010. Diagnosis and Classification of Diabetes Mellitus. *Diabetes Care*, 33 (Suppl 1), S62–69.

AMERICAN DIABETES ASSOCIATION. 2011. Diagnosis and Classification of Diabetes Mellitus. *Diabetes Care*, 34 (Suppl 1), S62–69.

AMERICAN DIABETES ASSOCIATION. 2016. Glycemic Targets. Sec. 5. In: Standards of Medical Care in Diabetes 2016. *Diabetes Care*, 39 (Suppl 1), S39–46.

ANDLEY, U.P., SAWARDEKAR, M.A., & BURRIS, J.L. 1997. Action Spectrum for Photocross-Linking of Human Lens Proteins. *Photochem Photobiol*, 65, 556–59.

APPLEGATE, R.A., BALLENTINE, C., GROSS, H., SARVER, E.J. & SARVER, C.A. 2003. Visual Acuity as a Function of Zernike Mode and Level of Root Mean Square Error. *Optom Vis Sci*, 80, 97–105.

APPLEGATE, R.A., SARVER, E.J. & KHEMSARA, V. 2002. Are All Aberrations Equal? *J Refract Surg*, 18, S556–62.

ARMADÁ MARESCA, F., FOSNECA SANDOMINGO, A., ENCINAS MARTIN, J.L., GARCÍA-ARUMÍ, J., GÓMEZ-ULLA, F., RUIZ MORENO, J. & VILAPLANA, D. 2010. Patología Y Cirugía de La Macula. Madrid, Spain: Sociedad Española de Oftalmología.

ARTAL, P. 2014. Optics of the Eye and Its Impact in Vision: A Tutorial. *Adv Opt Photon*, 6, 340–67.

ARTAL, P., BERRIO, E., GUIRAO, A. & PIERS, P. 2002. Contribution of the Cornea and Internal Surfaces to the Change of Ocular Aberrations with Age. *J Opt Soc Am A Opt Image Sci Vis*, 19, 137–43.

ARTAL, P., FERRO, M., MIRANDA, I. & NAVARRO, R. 1993. Effects of Aging in Retinal Image Quality. *J Opt Soc Am A*, 10, 1656–62.

ARTAL, P., & GUIRAO, A. 1998. Contributions of the Cornea and the Lens to the Aberrations of the Human Eye. *Opt Lett*, 23, 1713–15.

ARTAL, P., GUIRAO, A., BERRIO, E. & WILLIAMS, D.R. 2001. Compensation of Corneal Aberrations by the Internal Optics in the Human Eye. *J Vis*, 1, 1–8.

ARTAL, P., GUIRAO, A., BERRIO, E., PIERS, P. & NORRBY, S. 2003. Optical Aberrations and the Aging Eye. *Int Ophthalmol Clin*, 43, 63–77.

AVITABILE, T., LONGO, A. & REIBALDI, A. 2005. Intravitreal Triamcinolone Compared with Macular Laser Grid Photocoagulation for the Treatment of Cystoid Macular Edema. *Am J Ophthalmol*, 140, 695–702.

BELLMANN, C., RUBIN, G.S., KABANAROU, S.A., BIRD, A.C. & FITZKE, F.W. 2003. Fundus Autofluorescence Imaging Compared with Different Confocal Scanning Laser Ophthalmoscopes. *Br J Ophthalmol*, 87, 1381–86.

BENAROUS, R., SASONGKO, M.B., QURESHI, S., FENWICK, F., DIRANI, M., WONG, T.Y. & LAMOUREUX, E.L. 2011. Differential Association of Serum Lipids with Diabetic Retinopathy and Diabetic Macular Edema. *Invest Ophthalmol Vis Sci*, 52, 7464–9.

BENEYTO, P., & PÉREZ, T.M. 2006. Study of Lens Autofluorescence by Fluorophotometry in Pregnancy. *Exp Eye Res*, 82, 583–87.

BESSEMS, G.J., KEIZER, E., WOLLENSAK, J. & HOENDERS, H.J. 1987. Non-Tryptophan Fluorescence of Crystallins from Normal and Cataractous Human Lenses. *Invest Ophthalmol Vis Sci*, 28, 1157–63.

BESSHO, K., GOMI, F., HARINO, S., SAWA, M., SAYANAGI, K., TSUJIKAWA, M. & TANO, Y. 2009. Macular Autofluorescence in Eyes with Cystoid Macula Edema, Detected with 488 Nm-Excitation but Not with 580 Nm-Excitation. *Graefes Arch Clinl Exp Ophthalmol*, 247, 729–34.

BINDEWALD, A., SCHMITZ-VALCKENBERG, S., JORZIK, J.J., DOLAR-SZCZASNY, J., SIEBER, H., KEILHAUER, C., WEINBERGER, A.W., DITHMAR, S., PAULEIKHOFF, D., MANSMANN, U. & WOLF, S. 2005. Classification of Abnormal Fundus Autofluorescence Patterns in the Junctional Zone of Geographic Atrophy in Patients with Age Related Macular Degeneration. *Br J Ophthalmol*, 89, 874–78.

BLEEKER, J.C., VAN BEST, J.A., VRIJ, L., VAN DER VELDE, E.A. & OOSTERHUIS, J.A. 1986. Autofluorescence of the Lens in Diabetic and Healthy Subjects by Fluorophotometry. *Invest Ophthalmol Vis Sci*, 27, 791–4.

BORDAT, B., LAUDEHO, A., GUIRGUIS, I.R. & ARNAUD, C. 1992. [Study of the Crystalline Lens by Fluorophotometry in 60 Control Subjects and 56 Diabetics]. *J Fr Ophtalmol*, 15, 113–8.

BOULTON, M., DOCCHIO, F., DAYHAW-BARKER, P., RAMPONI, R. & CUBEDDU, R. 1990. Age-Related Changes in the Morphology, Absorption and Fluorescence of Melanosomes and Lipofuscin Granules of the Retinal Pigment Epithelium. *Vision Res*, 30, 1291–303.

BOULTON, M., RÓZANOWSKA, M. & RÓZANOWSKI, B. 2001. Retinal Photodamage. *J Photochem Photobiol B*, 64, 144–61.

BOULTON, M., ROZANOWSKA, M., ROZANOWSKI, B. & WESS, T. 2004. The Photoreactivity of Ocular Lipofuscin. *Photochem Photobiol Sci*, 3, 759–64.

BRAUNSTEIN, R.E., JAIN, S., MCCALLY, R.L., STARK, W.J., CONNOLLY, P.J. & AZAR, D.T. 1996. Objective Measurement of Corneal Light Scattering after Excimer Laser Keratectomy. *Ophthalmology*, 103, 439–43.

BRESNICK, G.H. 1986. Diabetic Macular Edema. A Review. *Ophthalmology* 93, 989–97.

BROENDSTED, A.E., HANSEN, M.S., LUND-ANDERSEN, H., SANDER, B. & KESSEL, L. 2011. Human Lens Transmission of Blue Light: A Comparison of Autofluorescence- Based and Direct Spectral Transmission Determination. *Ophthalmic Res*, 46, 118–24.

BRON, A.J., SPARROW, J., BROWN, N.A., HARDING, J.J. & BLAKYTNY, R. 1993. The Lens in Diabetes." *Eye (Lond)*, 7, 260–75.

BROWN, N., & HUNGERFORD, J. 1982. The Influence of the Size of the Lens in Ocular Disease. *Trans Ophthalmol Soc U K*, 102, 359–63.

BROWNING, D.J., MCOWEN, M.D., BOWEN, R.M. JR. & O'MARAH, T.L. 2004. Comparison of the Clinical Diagnosis of Diabetic Macular Edema with Diagnosis by Optical Coherence Tomography. *Ophthalmology*, 111, 712–5.

BROWNING, D.J., & FRASER, C.M. 2005. Regional Patterns of Sight-Threatening Diabetic Macular Edema. *Am J Ophthalmol*, 140, 117-24.

BUI, T.V., HAN, Y., RADU, R.A., TRAVIS, G.H. AND MATA, N.L. 2006. Characterization of Native Retinal Fluorophores Involved in Biosynthesis of A2E and Lipofuscin-Associated Retinopathies. *J Biol Chem*, 281, 18112–9.

BURD, J., LUM, S., CAHN, F. & IGNOTZ, K. 2012. Simultaneous Noninvasive Clinical Measurement of Lens Autofluorescence and Rayleigh Scattering Using a Fluorescence Biomicroscope. *J Diabetes Sci Technol*, 6, 1251–9.

BUSTED, N., OLSEN, T. & SCHMITZ, O. 1981. Clinical Observations on the Corneal Thickness and the Corneal Endothelium in Diabetes Mellitus. *Br J Ophthalmol*, 65, 687–90.

CALVO-MAROTO, A.M., CERVIÑO A., PEREZ-CAMBRODÍ, R.J., GARCÍA-LÁZARO, S. & SANCHIS-GIMENO, J.A. 2015. Quantitative Corneal Anatomy: Evaluation of the Effect of Diabetes Duration on the Endothelial Cell Density and Corneal Thickness. *Ophthalmic Physiol Opt*, 35, 293–8.

CALVO-MAROTO, A.M., ESTEVE-TABOADA, J.J., DOMINGUEZ-VICENT, A., PÉREZ-CAMBRODÍ R.J. & CERVIÑO, A. 2016a. Confocal Scanning Laser Ophthalmoscopy versus Modified Conventional Fundus Camera For Fundus Autofluorescence. *Expert Rev Med Devices*, 13, 965-78.

CALVO-MAROTO, A.M., ESTEVE-TABOADA, J.J., PEREZ-CAMBRODI, R.J., MADRID-COSTA, D. & CERVIÑO, A. 2016c. Pilot Study on Visual Function and Fundus Autofluorescence Assessment in Diabetic Patients. *J Ophthalmol*, 2016, 2016, 1287847.

CALVO-MAROTO, A.M., PEREZ-CAMBRODI, R.J., ALBARAN-DIEGO, C., PONS, A. & CERVIÑO, A. 2014. Optical Quality of the Diabetic Eye: A Review. *Eye (Lond)*, 28, 1271–80.

CALVO-MAROTO, A.M., PEREZ-CAMBRODI, R.J., GARCIA-LAZARO, S., FERRER-BLASCO, T. & CERVIÑO, A. 2016b. Ocular Autofluorescence in Diabetes Mellitus. A Review. *J Diabetes*, 8, 619–28.

CASTEJÓN-MOCHÓN, J.F., LÓPEZ-GIL, N., BENITO, A. & ARTAL, P. 2002. Ocular Wave-Front Aberration Statistics in a Normal Young Population. *Vision Res*, 42, 1611–7.

CERVIÑO, A., HOSKING, S.L., MONTES-MICO, R. & BATES, K. 2007. Clinical Ocular Wavefront Analyzers. *J Refract Surg*, 23, 603–16.

CHANCE, B., SCHOENER, B., OSHINO, R., ITSHAK, F. & NAKASE, Y. 1979. Oxidation-Reduction Ratio Studies of Mitochondria in Freeze-Trapped Samples. NADH and Flavoprotein Fluorescence Signals. *J Biol Chem*, 254, 4764–71.

CHENG, H., BARNETT, J.K., VILUPURU, A.S., MARSACK, J.D., KASTHURIRANGAN, S., APPLEGATE, R.A. & ROORDA, A. 2004. A Population Study on Changes in Wave Aberrations with Accommodation. *J Vis*, 4, 272–80.

CHEW, E.Y., KLEIN, M.L., FERRIS, F.L. 3RD, REMALEY, N.A., MURPHY, R.P., CHANTRY, K., HOOGWERF, B.J. & MILLER, D. 1996. Association of Elevated Serum Lipid Levels with Retinal Hard Exudate in Diabetic Retinopathy. Early Treatment Diabetic Retinopathy Study (ETDRS) Report 22. *Arch Ophthalmol*, 114, 1079–84.

CHONG, N.H., ALEXANDER, R.A., GIN, T., BIRD, A.C. & LUTHERT, P.J. 2000. TIMP-3, Collagen, and Elastin Immunohistochemistry and Histopathology of Sorsby's Fundus Dystrophy. *Invest Ophthalmol Vis Sci*, 41, 898–902.

CHOO, M, PRAKASH, K., SAMSUDIN, A., SOONG, T., RAMLI, N. AND KADIR, A. 2010. Corneal Changes in Type II Diabetes Mellitus in Malaysia. *Int J Ophthalmol*, 3, 234–6.

CHUNG, H., PARK, B., SHIN, H.J. & KIM, H.C. 2012. Correlation of Fundus Autofluorescence with Spectral-Domain Optical Coherence Tomography and Vision in Diabetic Macular Edema. *Ophthalmology*, 119, 1056–65.

CIARDELLA, A.P, & EANDI, C.M. 2009. Fundus Autofluorescence. In J.F. Arevalo (Ed.), *Retinal Angiography and Optical Coherence* (pp. 419–30). New York: Springer.

CIULLA, T.A., AMADOR, A.G. & ZINMAN, B. 2003. Diabetic Retinopathy and Diabetic Macular Edema: Pathophysiology, Screening, and Novel Therapies. *Diabetes Care*, 26, 2653-64.

COHEN, M.P., HUD, E., WU, V.Y., & SHEARMAN, C.W. 2008. Amelioration of Diabetes-Associated Abnormalities in the Vitreous Fluid by an Inhibitor of Albumin Glycation. *Invest Ophthalmol Vis Sci*, 49, 5089–93.

CONGET, I. 2002. [Diagnosis, Classification and Pathogenesis of Diabetes Mellitus]. *Rev Esp Cardiol*, 55, 528-35.

COPT, R.P., THOMAS, R. & MERMOUD, A. 1999. Corneal Thickness in Ocular Hypertension, Primary Open-Angle Glaucoma, and Normal Tension Glaucoma. *Arch Ophthalmol*, 117, 14–6.

COUSEN, P., CACKETT, P., BENNETT, H., SWA, K. & DHILLON, B. 2007. Tear Production and Corneal Sensitivity in Diabetes. *J Diabetes Complications*, 21, 371–3.

CREUZOT-GARCHER, C., KOEHRER, P., PICOT, C., AHO, S., & BRON, A.M. 2014. Comparison of Two Methods to Measure Macular Pigment Optical Density in Healthy Subjects. *Invest Opthalmoly Vis Sci*, 55, 2941-6.

DANDEKAR, S.S., JENKINS, S.A., PETO, T., SCHOLL, H.P., SEHMI, K.S., FITZKE, F.W., BIRD, A.C. & WEBSTER, A.R. 2005. Autofluorescence Imaging of Choroidal Neovascularization due to Age-Related Macular Degeneration. *Arch Ophthalmol*, 123, 1507–13.

DE BROUWERE, D., GINIS, H., KYMIONIS, G., NAOUMIDI, I., & PALLIKARIS, I. 2008. Forward Scattering Properties of Corneal Haze. *Optom Vis Sci*, 85, 843–8.

DE WAARD, P.W., IJSPEERT, J.K., VAN DEN BERG, T.J., & DE JONG, P.T. 1992. Intraocular Light Scattering in Age-Related Cataracts. *Invest Ophthalmol Vis Sci*, 33, 618–25.

DELI, A., MOETTELI, L., AMBRESIN, A. & MANTEL, I. 2013. Comparison of Fundus Autofluorescence Images Acquired by the Confocal Scanning Laser Ophthalmoscope (488 Nm Excitation) and the Modified Topcon Fundus Camera (580 Nm Excitation). *Int Ophthalmol*, 33, 635–43.

DELORI, F.C., DOREY, C.K., STAURENGHI, G., AREND, O., GOGER, D.G., & WEITER, J.J. 1995. In Vivo Fluorescence of the Ocular Fundus Exhibits Retinal Pigment Epithelium Lipofuscin Characteristics. *Invest Ophthalmol Vis Sci*, 36, 718–29.

DELORI, F.C., GOGER, D.G., HAMMOND, B.R., SNODDERLY, D.M. & BURNS, S.A. 2001. Macular Pigment Density Measured by Autofluorescence Spectrometry : Comparison with Reflectometry and Heterochromatic Flicker Photometry. *J Opt Soc Am A Opt Image Sci Vis*, 18, 1212–30.

DIABETIC RETINOPATHY STUDY RESEARCH GROUP, ETDRS. 1985. Photocoagulation for Diabetic Macular Edema. Early Treatment Diabetic Retinopathy Study Report Number 1. Early Treatment Diabetic Retinopathy Study Research Group. *Arch Ophthalmol*, 103, 1796–806.

DIABETIC RETINOPATHY STUDY RESEARCH GROUP, ETDRS. 1987. Treatment Techniques and Clinical Guidelines for Photocoagulation of Diabetic Macular Edema. Early Treatment Diabetic Retinopathy Study Report Number 2. Early Treatment Diabetic Retinopathy Study Research Group. *Ophthalmology*, 94, 761–74.

DOGRU, M., KATAKAMI, C., & INOUE, M. 2001. Tear Function and Ocular Surface Changes in Noninsulin-Dependent Diabetes Mellitus. *Ophthalmology*, 108, 586–92.

DRASDO, N., & FOWLER, C.W. 1974. Non-Linear Projection of the Retinal Image in a Wide-Angle Schematic Eye. *Br J Ophthalmol*, 58, 709–14.

DUBBELMAN, M., SICAM, V.A. & VAN DER HEIJDE, R.G. 2007. The Contribution of the Posterior Surface to the Coma Aberration of the Human Cornea. *J Vis*, 7, 1–8.

DUKE-ELDER, W.S. 1925. Changes In Refraction In Diabetes Mellitus. *Br J Ophthalmol*, 9, 167–87.

DURRANI, K., & FOSTER, C.S. 2012. Fundus Autofluorescence Imaging in Posterior Uveitis. *Semin Ophthalmol*, 27, 228–35.

EBRAHIMIADIB, N., & RIAZI-ESFAHANI, M. 2012. Autofluorescence Imaging for Diagnosis and Follow-up of Cystoid Macular Edema. *J Ophthalmic Vis Res*, 7, 261–7.

EDERER, F., HILLER, R. & TAYLOR, H.R. 1981. Senile Lens Changes and Diabetes in Two Population Studies. *Am J Ophthalmol*, 91, 381–95.

EFRON, N., MUTALIB, H.A., PEREZ-GOMEZ, I. & KOH, H.H. 2002. Confocal Microscopic Observations of the Human Cornea Following Overnight Contact Lens Wear. *Clin Exp Optom*, 85, 149–55.

EVA, P.R., PASCOE, P.T. & VAUGHAN, D.G. 1982. Refractive Change in Hyperglycaemia: Hyperopia, Not Myopia. *Br J Ophthalmol*, 66, 500–5.

FEENEY-BURNS, L., HILDERBRAND, E.S. & ELDRIDGE, S. 1984. Aging Human RPE: Morphometric Analysis of Macular, Equatorial, and Peripheral Cells. *Invest Ophthalmol Vis Sci*, 25, 195–200.

FEIST, R.M., MORRIS, R.E., WITHERSPOON, C.D., BLAIR, N.P., TICHO, B.H. & WHITE, M.F. 1990. Vitrectomy in Asteroid Hyalosis. *Retina*, 10, 173–7.

FIGUEROA-ORTIZ, L.C., JIMÉNEZ RODRÍGUEZ, E., GARCÍA-BEN, A. & GARCÍA-CAMPOS, J. 2011. Study of Tear Function and the Conjunctival Surface in Diabetic Patients. *Arch Soc Esp Oftalmol*, 86, 107–12.

FONG, D.S., AIELLO, L.P., FERRIS, F.L. & KLEIN, R. 2004. Diabetic Retinopathy. *Diabetes Care*, 27, 2540–53.

FRAMME, C., SCHÜLE, G., BIRNGRUBER, R., ROIDER, J., SCHÜTT, F., KOPITZ, J., HOLZ, F.G.& BRINKMANN, R. 2004. Temperature Dependent Fluorescence of A2-E, the Main Fluorescent Lipofuscin Component in the RPE. *Curr Eye Res*, 29, 287–91.

FRAUNFELDER, F.W. & RICH, L.F. 2002. Laser-Assisted in Situ Keratomileusis Complications in Diabetes Mellitus. *Cornea*, 21, 246–8.

FRIEND, J. & THOFT, R.A. 1984. The Diabetic Cornea. *Int Ophthalmol Clin*, 24, 111–23.

GABBAY, K.H. 1973. The Sorbitol Pathway and the Complications of Diabetes. *N Engl J Med*, 288, 831–6.

GABRIELIAN, A., HARIPRASAD, S.M., JAGER, R.D., GREEN, J.L. AND MIELER, W.F. 2010. The Utility of Visual Function Questionnaire in the Assessment of the Impact of Diabetic Retinopathy on Vision-Related Quality of Life. *Eye (Lond)*, 24, 29–35.

GARLICK, R.L., MAZER, J.S., CHYLACK, L.T. JR., TUNG, W.H. & BUNN, H.F. 1984. Nonenzymatic Glycation of Human Lens Crystallin. Effect of Aging and Diabetes Mellitus. *J Clin Invest*, 74, 1742–9.

GEKKA, M., MIYATA, K., NAGAI, Y., NEMOTO, S., SAMESHIMA, T., TANABE, T., MARUOKA, S., NAKAHARA, M., KATO, S. & AMANO, S. 2004. Corneal Epithelial Barrier Function in Diabetic Patients. *Cornea*, 23, 35–7.

GENUTH, S., ALBERTI, K.G., BENNETT, P., BUSE, J., DEFRONZO, R., KAHN, R., KITZMILLER, J., KNOWLER, W.C., LEBOVITZ, H., LERNMARK, A., NATHAN, D., PALMER, J., RIZZA, R., SAUDEK, C., SHAW, J., STEFFES, M., STERN, M., TOUMILEHTO, J. & ZIMMET, P. 2003. Follow-up Report on the Diagnosis of Diabetes Mellitus. *Diabetes Care*, 26, 3160-7.

GEORGAKOPOULOS, C.D., ELIOPOULOU, M.I., EXARCHOU, A.M., TZIMIS, V., PHARMAKAKIS, N.M. & SPILIOTIS, B.E. 2011. Decreased Contrast Sensitivity in Children and Adolescents with Type 1 Diabetes Mellitus. *J Pediatr Ophthalmol Strabismus*, 48, 92–7.

GLASSER, A., & CAMPBELL, M.C. 1999. Biometric, Optical and Physical Changes in the Isolated Human Crystalline Lens with Age in Relation to Presbyopia. *Vision Res*, 39, 1991–2015.

GOBBE, M., & GUILLON, M. 2005. Corneal Wavefront Aberration Measurements to Detect Keratoconus Patients. *Cont Lens Anterior Eye*, 28, 57–66.

GÖBBELS, M., SPITZNAS, M. & OLDENDOERP, J. 1989. Impairment of Corneal Epithelial Barrier Function in Diabetics. *Graefes Arch Clin Exp Ophthalmol*, 227, 142–4.

GOEBBELS, M. 2000. Tear Secretion and Tear Film Function in Insulin Dependent Diabetics. *Br J Ophthalmol*, 84, 19–21.

GOLDMAN, J.N., BENEDEK, G.B., DOHLMAN, C.H. & KRAVITT, B. 1968. Structural Alterations Affecting Transparency in Swollen Human Corneas. *Invest Ophthalmol*, 7, 501–19.

GRANDHEE, S.K., & MONNIER V.M. 1991. Mechanism of Formation of the Maillard Protein Cross-Link Pentosidine: Glucose, Fructose, and Ascorbate as Pentosidine Precursors. *J Biol Chem*, 266, 11649–53.

GRUS, F.H., SABUNCUO, P., DICK, H.B., AUGUSTIN, A.J. & PFEIFFER, N. 2002. Changes in the Tear Proteins of Diabetic Patients. *BMC Ophthalmol*, 2: 4.

GUIRAO, A., & ARTAL, P. 2000. Corneal Wave Aberration from Videokeratography: Accuracy and Limitations of the Procedure. *J Opt Soc Am A Opt Image Sci Vis*, 17, 955–65.

GUIRAO, A., GONZÁLEZ, C., REDONDO, M., GERAGHTY, E., NORRBY, S. & ARTAL, P. 1999. Average Optical Performance of the Human Eye as a Function of Age in a Normal Population. *Invest Ophthalmol Vis Sci*, 40, 203–13.

GUIRAO, A., REDONDO, M. & ARTAL, P. 2000. Optical Aberrations of the Human Cornea as a Function of Age. *J Opt Soc Am A Opt Image Sci Vis*, 17, 1697–702.

GUNDOGAN, F.C., YOLCU, U., AKAY, F., ILHAN, A., OZGE, G. & UZUN, S. 2016. Diabetic Macular Edema. *Pak J Med Sci* 32, 505–10.

GWINUP, G., & VILLARREAL, A. 1976. Relationship of Serum Glucose Concentration to Changes in Refraction. *Diabetes*, 25, 29–31.

HAGER, A., WEGSCHEIDER, K. & WIEGAND, W. 2009. Changes of Extracellular Matrix of the Cornea in Diabetes Mellitus. *Graefes Arch Clin Exp Ophthalmol*, 247, 1369–74.

HAMMER, M., KÖNIGSDÖRFFER, E., LIEBERMANN, C., FRAMME, C., SCHUCH, G., SCHWEITZER, D. & STROBEL, J. 2008. Ocular Fundus Auto-Fluorescence Observations at Different Wavelengths in Patients with Age-Related Macular Degeneration and Diabetic Retinopathy. *Graefes Arch Clin Exp Ophthalmol*, 246, 105–14.

HAN, M., GIESE, G., SCHMITZ-VALCKENBERG, S., BINDEWALD-WITTICH, A., HOLZ, F.G., YU, J., BILLE, J.F. & NIEMZ, M.H. 2007. Age-Related Structural Abnormalities in the Human Retina-Choroid Complex Revealed by Two-Photon Excited Autofluorescence Imaging. *J Biomed Opt*, 12, 024012.

HARBOUR, J.W., & SMIDDY, W.E., FLYNN H.W. JR. & RUBSAMEN, P.E. 1996. Vitrectomy for Diabetic Macular Edema Associated with a Thickened and Taut Posterior Hyaloid Membrane. *Am J Ophthalmol*, 12, 405–13.

HARITOGLOU, C., KOOK, D., NEUBAUER, A., WOLF, A., PRIGLINGER, S., STRAUSS, R., GANDORFER, A., ULBIG, M. & KAMPIK, A. 2006. Intravitreal Bevacizumab (Avastin) Therapy for Persistent Diffuse Diabetic Macular Edema. *Retina*, 26, 999–1005.

HASSAN, I.A., WICKRAMASINGHE, Y.A. & SPENCER, S.A. 2003. Effect of a Change in Global Metabolic Rate on Peripheral Oxygen Consumption in Neonates. *Arch Dis Child Fetal Neonatal Ed*, 88, F143–6.

HE, J.C., GWIAZDA, J., THORN, F. & HELD, R. 2003. Wave-Front Aberrations in the Anterior Corneal Surface and the Whole Eye. *J Opt Soc Am A Opt Image Sci Vis*, 20, 1155–63.

HERBER, S., GRUS, F.H., SABUNCUO, P. & AUGUSTIN, A.J. 2001. Two-Dimensional Analysis of Tear Protein Patterns of Diabetic Patients. *Electrophoresis*, 22, 1838–44.

HERMAN, W.H., SMITH, P.J., THOMPSON, T.J., ENGELGAU, M.M. & AUBERT, R.E. 1995. A New and Simple Questionnaire to Identify People at Increased Risk for Undiagnosed Diabetes. *Diabetes Care*, 18, 382–7.

HERSE, P.R. 1988. A Review of Manifestations of Diabetes Mellitus in the Anterior Eye and Cornea. *Am J Optom Physiol Opt*, 65, 224–30.

HILL, S.A., & MCQUEEN, M.J. 1997. Reverse Cholesterol Transport--a Review of the Process and Its Clinical Implications. *Clin Biochem*, 30, 517–25.

HOLDEN, R., SHUN-SHIN, G.A. & BROWN, N.A. 1994. Central Corneal Light Scatter in Long-Term Diabetics. *Eye (Lond)*, 8, 44–5.

HOLZ, F.G. 2001. [Autofluorescence Imaging of the Macula.] *Ophthalmologe*, 98, 10-8.

HOWLAND, H.C., & HOWLAND, B. 1977. A Subjective Method for the Measurement of Monochromatic Aberrations of the Eye. *J Opt Soc Am*, 67, 1508–18.

HUGOD, M., STORR-PAULSEN, A., NORREGAARD, J.C., NICOLINI, J., LARSEN, A.B. & THULESEN, J. 2011. Corneal Endothelial Cell Changes Associated with Cataract Surgery in Patients with Type 2 Diabetes Mellitus. *Cornea*, 30, 749–53.

HULST, H.C. 1981. *Light Scattering by Small Particles*. *Light Scattering by Small Particles*. Mineola, NY: Dover Publications.

HUNTER, J.J., MORGAN, J.I., MERIGAN, W.H., SLINEY, D.H., SPARROW, J.R. & WILLIAMS, D.R. 2012. The Susceptibility of the Retina to Photochemical Damage from Visible Light. *Prog Retin Eye Res*, 31, 28-42.

INTERNATIONAL DIABETES FEDERATION (IDF). 2015. IDF Diabetes Atlas, Seventh Edition. International Diabetes Federation. Brussels, Belgium.

IDICULLA, J., NITHYANANDAM, S., JOSEPH, M., MOHAN, V.A., VASU, U. & SADIQ, M. 2012. Serum Lipids and Diabetic Retinopathy: A Cross-Sectional Study. *Indian J Endocrinol Metab*, 16 (Suppl 2), S492–4.

INOUE, K., KATO, S., OHARA, C., NUMAGA, J., AMANO, S. & OSHIKA, T. 2001. Ocular and Systemic Factors Relevant to Diabetic Keratoepitheliopathy. *Cornea*, 20, 798–801.

INOUE, K, KATO, S., INOUE, Y., AMANO, S. & OSHIKA. T. 2002. The Corneal Endothelium and Thickness in Type II Diabetes Mellitus. *Jpn J Ophthalmol*, 46, 65–9.

INTERNATIONAL EXPERT COMMITTEE. 2009. International Expert Committee Report on the Role of the A1C Assay in the Diagnosis of Diabetes. *Diabetes Care*, 32, 1327-34.

INTERNATIONAL ORGANIZATION FOR STANDARDIZATION. 2008. Ophthalmic Optics and Instruments -- Reporting Aberrations of the Human Eye. Geneva, Swiizerland, ISO.

ISHIKO, S., YOSHIDA, A., MORI, F., ABIKO, T., KITAYA, N., KONNO, S. & KATO, Y. 1998. Corneal and Lens Autofluorescence in Young Insulin-Dependent Diabetic Patients. *Ophthalmologica*, 212, 301–5.

JACOBS, R., & KROHN, D.L. 1981. Fluorescence Intensity Profile of Human Lens Sections. *Invest Ophthalmol Vis Sci*, 20, 117–20.

JOHNSON, I., & SPENCE, M.T.Z. 2010. *The Molecular Probes Handbook. A Guide to Fluorescent Probes and Labeling Technologies*. Carsbad, CA, USA: Invitrogen Life Technologies.

JOYCE, N.C. 2003. Proliferative Capacity of the Corneal Endothelium. *Prog Retin Eye Res*, 22, 359-89.

KAYATZ, P., THUMANN, G., LUTHER, T.T., JORDAN, J.F., BARTZ-SCHMIDT, K.U., ESSER, P.J. & SCHRAERMEYER, U. 2001. Oxidation Causes Melanin Fluorescence. *Invest Ophthalmol Vis Sci*, 42, 241–6.

KELLY, J.E., MIHASHI, T. & HOWLAND, H.C. 2004. Compensation of Corneal Horizontal/vertical Astigmatism, Lateral Coma, and Spherical Aberration by Internal Optics of the Eye. *J Vis*, 4, 262–71.

KESSEL, L., KALININ, S., NAGARAJ, R.H., LARSEN, M. & JOHANSSON, L.B. 2002. Time-Resolved and Steady-State Fluorescence Spectroscopic Studies of the Human Lens with Comparison to Argpyrimidine, Pentosidine and 3-OH-Kynurenine. *Photochem Photobiol*, 76, 549–54.

KING, H., AUBERT, R.E. & HERMAN, W.H. 1998. Global Burden of Diabetes, 1995-2025: Prevalence, Numerical Estimates, and Projections. *Diabetes Care*, 21, 1414–31.

KINNUNEN, K., PUUSTJÄRVI, T., TERÄSVIRTA, M., NURMENNIEMI, P., HEIKURA, T., LAIDINEN, S., PAAVONEN, T., UUSITALO, H. & YLÄ-HERTTUALA, S. 2009. Differences in Retinal Neovascular Tissue and Vitreous Humour in Patients with Type 1 and Type 2 Diabetes. *Br J Ophthalmol*, 93, 1109–15.

KLEIN, B.E., KLEIN, R. & MOSS, S.E. 1985. Prevalence of Cataracts in a Population-Based Study of Persons with Diabetes Mellitus. *Ophthalmology*, 92, 1191–6.

KLEIN, R., KLEIN, B.E., MOSS, S.E. & CRUICKSHANKS, K.J. 1998. The Wisconsin Epidemiologic Study of Diabetic Retinopathy: XVII. The 14-Year Incidence and Progression of Diabetic Retinopathy and Associated Risk Factors in Type 1 Diabetes. *Ophthalmology*, 105, 1801–15.

KLEIN, R., KLEIN, B.E., MOSS, S.E., DAVIS, M.D. AND DEMETS, D.L. 1989. The Wisconsin Epidemiologic Study of Diabetic Retinopathy. X. Four-Year Incidence and Progression of Diabetic Retinopathy When Age at Diagnosis Is 30 Years or More. *Arch Ophthalmol*, 107, 244–9.

KLEIN, R., KNUDTSON, M.D., LEE, K.E., GANGNON, R. & KLEIN, B.E. 2008. The Wisconsin Epidemiologic Study of Diabetic Retinopathy XXII. The Twenty-Five-Year Progression of Retinopathy in Persons with Type 1 Diabetes. *Ophthalmology*, 115, 1859–68.

KOLOMEYER, A.M., NAYAK, N.V., SZIRTH, B.C. & KHOURI, A.S. 2012. Fundus Autofluorescence Imaging in an Ocular Screening Program. *Int J Telemed Appl*, 2012, 806464.

LAING, R.A., CHIBA, K., TSUBOTA, K. & OAK, S.S. 1992. Metabolic and Morphologic Changes in the Corneal Endothelium: The Effects of Potassium Cyanide, Iodoacetamide, and Ouabain. *Invest Ophthalmol Vis Sci*, 33, 3315–24.

LAKOWICZ, J.R. 1999. *Principles of Fluorescence Spectroscopy*. New York: Kluwer Academic/Plenum Publishers.

LAMPI, K.J., WILMARTH, P.A., MURRAY, M.R. & DAVID, L.L. 2014. Lens B-Crystallins: THE Role of Deamidation and Related Modifications in Aging and Cataract. *Prog Biophys Mol Biol*, 115, 21–31.

LEE, J.S., OUM, B.S., CHOI, H.Y., LEE, J.E. & CHO, B.M. 2006. Differences in Corneal Thickness and Corneal Endothelium Related to Duration in Diabetes. *Eye (Lond)*, 20, 315–8.

LEE, J.S., PARK, W.S., LEE, S.H., OUM, B.S. & CHO B.M. 2001. A Comparative Study of Corneal Endothelial Changes Induced by Different Durations of Soft Contact Lens Wear. *Graefes Arch Clin Exp Ophthalmol*, 239, 1–4.

LEGRO, R.S., KUNSELMAN, A.R., DODSON, W.C. & DUNAIF, A. 1999. Prevalence and Predictors of Risk for Type 2 Diabetes Mellitus and Impaired Glucose Tolerance in Polycystic Ovary Syndrome: A Prospective, Controlled Study in 254 Affected Women. *J Clin Endocrinol Metab*, 84, 165–9.

LIANG, J., & WILLIAMS, D.R. 1997. Aberrations and Retinal Image Quality of the Normal Human Eye. *J Opt Soc Am. A Opt Image Sci Vis*, 14, 2873–83.

LIANG, J., WILLIAMS, D.R. & MILLER, D.T. 1997. Supernormal Vision and High-Resolution Retinal Imaging through Adaptive Optics. *J Opt Soc Am A Opt Image Sci Vis*, 14, 2884–92.

LJUBIMOV, A.V., HUANG, Z.S., HUANG, G.H., BURGESON, R.E., GULLBERG, D., MINER, J.H., NINOMIYA, Y., SADO, Y. & KENNEY, M.C. 1998. Human Corneal Epithelial Basement Membrane and Integrin Alterations in Diabetes and Diabetic Retinopathy. *J Histochem Cytochem*, 46, 1033–41.

LLEÓ, A., MARCOS, A., CALATAYUD, M., ALONSO, L., RAHHAL, S.M. & SANCHIS-GIMENO, J.A. 2003. The Relationship between Central Corneal Thickness and Goldmann Applanation Tonometry. *Clin Exp Optom*, 86, 104–8.

LØGSTRUP, N., SJØLIE, A.K., KYVIK, K.O. & GREEN, A. 1996. Lens Thickness and Insulin Dependent Diabetes Mellitus: A Population Based Twin Study. *Br J Ophthalmol*, 80, 405–8.

LOMBARDO, M., & LOMBARDO, G. 2010. Wave Aberration of Human Eyes and New Descriptors of Image Optical Quality and Visual Performance. *J Cataract Refract Surg*, 36, 313–31.

LOPES DE FARIA, J.M., JALKH, A.E., TREMPE, C.L. & MCMEEL, J.W. 1999. Diabetic Macular Edema: Risk Factors and Concomitants. *Acta Ophthalmol Scand*, 77, 170–5.

LUNDQUIST, O., & ÖSTERLIN, S. 1994. Glucose Concentration in the Vitreous of Nondiabetic and Diabetic Human Eyes. *Graefes Arch Clin Exp Ophthalmol*, 232, 71–4.

MAHDY, M.A., EID, M.Z., MOHAMMED, M.A., HAFEZ, A. & BHATIA, J. 2012. Relationship between Endothelial Cell Loss and Microcoaxial Phacoemulsification Parameters in Noncomplicated Cataract Surgery. *Clin Ophthalmol*, 6, 503–10.

MANGIONE, C.M., LEE, P.P., GUTIERREZ, P.R., SPRITZER, K., BERRY, S., & HAYS R.D. 2001. Development of the 25-Item National Eye Institute Visual Function Questionnaire. *Arch Ophthalmol*, 119, 1050–8.

MANGIONE, C.M., LEE, P.P., PITTS, J., GUTIERREZ, P., BERRY, S. & HAYS, R.D. 1998. Psychometric Properties of the National Eye Institute Visual Function Questionnaire (NEI-VFQ). NEI-VFQ Field Test Investigators. *Arch Ophthalmol*, 116, 1496–504.

MARCOS, S., BARBERO, S., LLORENTE, L. & MERAYO-LLOVES, J. 2001. Optical Response to LASIK Surgery for Myopia from Total and Corneal Aberration Measurements. *Invest Ophthalmol Vis Sci*, 42, 3349–56.

MARCU, L. 2012. Fluorescence Lifetime Techniques in Medical Applications. *Ann Biomed Eng*, 40, 304–31.

MASTERS, B.R. 1984. Noninvasive Redox Fluorometry: How Light Can Be Used to Monitor Alterations of Corneal Mitochondrial Function. *Curr Eye Res*, 3, 23–6.

MATZA, L.S., ROUSCULP, M.D., MALLEY, K., BOYE, K.S. & OGLESBY, A. 2008. The Longitudinal Link between Visual Acuity and Health-Related Quality of Life in Patients with Diabetic Retinopathy. *Health Qual Life Outcomes*, 6, 95.

MAUSCHITZ, M.M., FONSECA, S., CHANG, P., GÖBEL, A.P., FLECKENSTEIN, M., JAFFE, G.J., HOLZ, F.G. & SCHMITZ-VALCKENBERG, S. 2012. Topography of Geographic Atrophy in Age-Related Macular Degeneration. *Invest Ophthalmol Vis Sci*, 53, 4932–9.

MCBAIN, V.A., FORRESTER, J.V. & LOIS, N. 2008. Fundus Autofluorescence in the Diagnosis of Cystoid Macular Oedema. *Br J Ophthalmol*, 92, 946–9.

MCCALLY, R.L., FREUND, D.E., ZORN, A., BONNEY-RAY, J., GREBE, R., DE LA CRUZ, Z. & GREEN, W.R. 2007. Light-Scattering and Ultrastructure of Healed Penetrating Corneal Wounds. *Invest Ophthalmol Vis Sci*, 48, 157–65.

MCNAMARA, N.A., BRAND, R.J., POLSE, K.A., & BOURNE, W.M. 1998. Corneal Function during Normal and High Serum Glucose Levels in Diabetes. *Invest Ophthalmol Vis Sci*, 39, 3–17.

MILJANOVIC, B., GLYNN, R.J., NATHAN, D.M., MANSON, J.E. & SCHAUMBERG D.A. 2004. A Prospective Study of Serum Lipids and Risk of Diabetic Macular Edema in Type 1 Diabetes. *Diabetes*, 53, 2883–92.

MISRA, S., SAXENA, S., KISHORE, P., BHASKER, S.K., MISRA, A. & MEYER, C.H. 2010. Association of Contrast Sensitivity with LogMAR Visual Acuity and Glycosylated Hemoglobin in Non-Insulin Dependent Diabetes Mellitus. *J Ocul Biol Dis Infor*, 3, 60–3.

MÓDIS, L. JR., SZALAI, E., KERTÉSZ, K., KEMÉNY-BEKE, A., KETTESY, B. AND BERTA, A. 2010. Evaluation of the Corneal Endothelium in Patients with Diabetes Mellitus Type I and II. *Histol Histopathol*, 25, 1531–7.

MONNIER, V.M., & CERAMI, A. 1981. Nonenzymatic Browning in Vivo: Possible Process for Aging of Long-Lived Proteins. *Science*, 211, 491–3.

MONTÉS-MICÓ, R., ALIÓ, J.L., MUÑOZ, G., PÉREZ-SANTONJA, J.J. & CHARMAN, W.N. 2004a. Postblink Changes in Total and Corneal Ocular Aberrations. *Ophthalmology*, 111, 758–67.

MONTÉS-MICÓ, R., CÁLIZ, A. & ALIÓ, J.L. 2004b. Wavefront Analysis of Higher Order Aberrations in Dry Eye Patients. *J Refract Surg*, 20, 243–7.

MORENO-BARRIUSO, E., LLOVES, J.M., MARCOS, S., NAVARRO, R., LLORENTE, L. & BARBERO, S. 2001. Ocular Aberrations before and after Myopic Corneal Refractive Surgery: LASIK-Induced Changes Measured with Laser Ray Tracing. *Invest Ophthalmol Vis Sci*, 42, 1396–403.

MORI, F., ISHIKO, S., ABIKO, T., KITAYA, N., KATO, Y., KANNO, H. & YOSHIDA, A. 1997. Changes in Corneal and Lens Autofluorescence and Blood Glucose Levels in Diabetics: Parameters of Blood Glucose Control. *Curr Eye Res* 16, 534–8.

MORIKUBO, S., TAKAMURA, Y., KUBO, E., TSUZUKI, S. & AKAGI, Y. 2004. Corneal Changes after Small-Incision Cataract Surgery in Patients with Diabetes Mellitus. *Arch Ophthalmol*, 122, 966–9.

MORISHIGE, N., CHIKAMA, T.I., SASSA, Y. & NISHIDA, T. 2001. Abnormal Light Scattering Detected by Confocal Biomicroscopy at the Corneal Epithelial Basement Membrane of Subjects with Type II Diabetes. *Diabetologia*, 44, 340–5.

MOSS, S.E., KLEIN, R. & KLEIN, B.E. 2001. Asteroid Hyalosis in a Population: The Beaver Dam Eye Study. *Am J Ophthalmol*, 132, 70–5.

MUÑOZ, J.M., COCO, R.M., SANABRIA, M.R., CUADRADO, R. & BLANCO, E. 2013. Autofluorescence Images with Carl Zeiss versus Topcon Eye Fundus Camera: A Comparative Study. *J Ophthalmol*, 2013: 309192.

NEELAM, K., O'GORMAN, N., NOLAN, J., O'DONOVAN, O., AU EONG, K.G. & BEATTY, S. 2005. Macular Pigment Levels Following Successful Macular Hole Surgery. *Br J Ophthalmol*, 89, 1105–8.

NÍ DHUBHGHAILL, S., ROZEMA, J.J., JONGENELEN, S., RUIZ HIDALGO, I., ZAKARIA, N. & TASSIGNON, M.J. 2014. Normative Values for Corneal Densitometry Analysis by Scheimpflug Optical Assessment. *Invest Ophthalmol Vis Sci*, 55, 162–8.

NIELSEN, N.V. & VINDING, T. 1984. The Prevalence of Cataract in Insulin-Dependent and Non-Insulin-Dependent-Diabetes Mellitus. *Acta Ophthalmol (Copenh)*, 62, 595–602.

OKAMOTO, F., SONE, H., NONOYAMA, T. & HOMMURA, S. 2000. Refractive Changes in Diabetic Patients during Intensive Glycaemic Control. *Br J Ophthalmol*, 84, 1097–102.

OLIVEIRA, C.M., FERREIRA, A. & FRANCO, S. 2012. Wavefront Analysis and Zernike Polynomial Decomposition for Evaluation of Corneal Optical Quality. *J Cataract Refract Surg*, 38, 343-56.

OLK, R.J. 1986. Modified Grid Argon (blue-Green) Laser Photocoagulation for Diffuse Diabetic Macular Edema. *Ophthalmology*, 93, 938–50.

OLSEN, T. 1982. Light Scattering from the Human Cornea. *Invest Ophthalmol Vis Sci*, 23, 81–6.

OSHIKA, T., KLYCE, S.D., APPLEGATE, R.A., HOWLAND, H.C. & EL DANASOURY, M.A. 1999. Comparison of Corneal Wavefront Aberrations after Photorefractive Keratectomy and Laser in Situ Keratomileusis. *Am J Ophthalmol*, 127, 1–7.

OZDEMIR, M., BUYUKBESE, M.A., CETINKAYA, A., OZDEMIR, G. 2003. Risk Factors for Ocular Surface Disorders in Patients with Diabetes Mellitus. *Diabetes Res Clin Pract*, 59, 195–9.

OZER, P.A., UNLU, N., DEMIR, M.N., HAZIROLAN, D.O., ACAR, M.A. & DUMAN, S. 2009. Serum Lipid Profile in Diabetic Macular Edema. *J Diabetes Complications*, 23, 244–8.

PARK, S.P., SIRINGO, F.S., PENSEC, N., HONG, I.H., SPARROW, J., BARILE, G., TSANG, S.H. & CHANG, S. 2013. Comparison of Fundus Autofluorescence between Fundus Camera and Confocal Scanning Laser Ophthalmoscope-Based Systems. *Ophthalmic Surg Lasers Imaging Retina*, 44, 536–43.

PATEL, S.V., WINTER, E.J., MCLAREN, J.W. AND BOURNE, W.M. 2007. Objective Measurement of Backscattered Light from the Anterior and Posterior Cornea in Vivo. *Invest Ophthalmol Vis Sci*, 48, 166–72.

PAULUS, Y.M., & GARIANO, R.F. 2009. Diabetic Retinopathy: A Growing Concern in an Aging Population. *Geriatrics*, 64, 16–20.

PECE, A., ISOLA, V., HOLZ, F., MILANI, P. & BRANCATO, R. 2010. Autofluorescence Imaging of Cystoid Macular Edema in Diabetic Retinopathy. *Ophthalmologica*, 224, 230–5.

PEPONIS, V., BONOVAS, S., KAPRANOU, A., PEPONI, E., FILIOUSSI, K., MAGKOU, C. & SITARAS, N.M. 2004. Conjunctival and Tear Film Changes after Vitamin C and E Administration in Non-Insulin Dependent Diabetes Mellitus. *Med Sci Monit*, 10, CR213–7.

PEPONIS, V., PAPATHANASIOU, M., KAPRANOU, A., MAGKOU, C., TYLIGADA, A., MELIDONIS, A., DROSOS, T. & SITARAS, N.M. 2002. Protective Role of Oral Antioxidant Supplementation in Ocular Surface of Diabetic Patients. *Br J Ophthalmol*, 86, 1369–73.

PEREZ-VIVES, C., BELDA-SALMERON, L., GARCIA-LAZARO, S., MADRID-COSTA, D. & FERRER-BLASCO. T. 2011. Adaptative optics, wavefront aberrations and visual simulation. *J Emmetropia*, 2, 103-9.

PIÑERO, D.P., ORTIZ, D. & ALIO, J.L. 2010. Ocular Scattering. *Optom Vis Sci*, 87, E682–96.

PONGOR, S., ULRICH, P.C., BENCSATH, F.A. & CERAMI, A. 1984. Aging of Proteins: Isolation and Identification of a Fluorescent Chromophore from the Reaction of Polypeptides with Glucose. *Proc Natl Acad Sci U S A*, 81, 2684–8.

PORTER, J., GUIRAO, A., COX, I.G. & WILLIAMS, D.R. 2001. Monochromatic Aberrations of the Human Eye in a Large Population. *J Opt Soc Am A Opt Image Sci Vis*, 18, 1793–803.

QUADRADO, M.J., POPPER, M., MORGADO, A.M., MURTA, J.N. & VAN BEST, J.A. 2006. Diabetes and Corneal Cell Densities in Humans by In Vivo Confocal Microscopy. *Cornea*, 25, 761–8.

REHANY, U, Y ISHII, M LAHAV, AND S RUMELT. 2000. Ultrastructural Changes in Corneas of Diabetic Patients: An Electron-Microscopy Study. *Cornea*, 19, 534–38.

REZNICEK, L., DABOV, S., HARITOGLU, C., KAMPIK, A., KERNT, M. AND NEUBAUER, A.S. 2013. Green-Light Fundus Autofluorescence in Diabetic Macular Edema. *Int J Ophthalmol*, 6, 75–80.

ROBERTS, J.E. 2001. Ocular Phototoxicity. *J Photochem Photobiol B*, 64, 136–43.

ROESEL, M., HENSCHEL, A., HEINZ, C., DIETZEL, M., SPITAL, G. & HEILIGENHAUS, A. 2009. Fundus Autofluorescence and Spectral Domain Optical Coherence Tomography in Uveitic Macular Edema. *Graefes Arch Clin Exp Ophthalmol*, 247, 1685–9.

ROSZKOWSKA, A.M., TRINGALI, C.G., COLOSI, P., SQUERI, C.A. & FERRERI, G. 1999. Corneal Endothelium Evaluation in Type I and Type II Diabetes Mellitus. *Ophthalmologica*, 213, 258–61.

ROVATI, L., & DOCCHIO, F. 2004. Autofluorescence Methods in Ophthalmology. *J Biomed Opt*, 9, 9–21.

ROVATI, L., FANKHAUSER, F., DOCCHIO, F. & VAN BEST, J. 1998. Diabetic Retinopathy Assessed by Dynamic Light Scattering and Corneal Autofluorescence. *J Biomed Opt*, 3, 357–63.

ROZEMA, J.J., TRAU, R., VERBRUGGEN, K.H. & TASSIGNON, M.J. 2011. Backscattered Light from the Cornea before and after Laser-Assisted Subepithelial Keratectomy for Myopia. *J Cataract Refract Surg*, 37, 1648–54.

ŞAHIN, A., BAYER, A., ÖZGE, G. & MUMCUOĞLU, T. 2009. Corneal Biomechanical Changes in Diabetes Mellitus and Their Influence on Intraocular Pressure Measurements. *Invest Ophthalmol Vis Sci*, 50, 4597–604.

SAITO, J., ENOKI, M., HARA, M., MORISHIGE, N., CHIKAMA, T. & NISHIDA, T. 2003. Correlation of Corneal Sensation, but Not of Basal or Reflex Tear Secretion, with the Stage of Diabetic Retinopathy. *Cornea*, 22, 15–8.

SAITO, Y., OHMI, G., KINOSHITA, S., NAKAMURA, Y., OGAWA, K., HARINO, S. & OKADA, M. 1993. Transient Hyperopia with Lens Swelling at Initial Therapy in Diabetes. *Br J Ophthalmol*, 77, 145–8.

SAMY, A., LIGHTMAN, S., ISMETOVA, F., TALAT, L. & TOMKINS-NETZER, O. 2014. Role of Autofluorescence in Inflammatory/infective Diseases of the Retina and Choroid. *J Ophthalmol*, 2014, 418193.

SÁNCHEZ-THORIN, J.C. 1998. The Cornea in Diabetes Mellitus. *Int Ophthalmol Clin*, 38, 19–36.

SANCHIS-GIMENO, J.A., LLEÓ-PÉREZ, A., ALONSO, L., RAHHAL, M.S. & MARTÍNEZ-SORIANO, F. 2005. Corneal Endothelial Cell Density Decreases with Age in Emmetropic Eyes. *Histol Histopathol*, 20, 423–7.

SANDBY-MØLLER, J., THIEDEN, E., ALSHEDE PHILIPSEN, P., SCHMIDT, G., & WULF, H.C. 2004. Ocular Lens Blue Autofluorescence Cannot Be Used as a Measure of Individual Cumulative UVR Exposure." *Photodermatol Photoimmunol Photomed*, 20, 41–6.

SASONGKO, M. B., WONG, T.Y., NGUYEN, T.T., KAWASAKI, R., JENKINS, A., SHAW, J., & WANG, J.J. 2011. Serum Apolipoprotein AI and B Are Stronger Biomarkers of Diabetic Retinopathy than Traditional Lipids. *Diabetes Care*, 34, 474–79.

SATO, E., MORI, F., IGARASHI, S., ABIKO, T., TAKEDA, M., ISHIKO, S. & YOSHIDA, A. 2001. Corneal Advanced Glycation End Products Increase in Patients with Proliferative Diabetic Retinopathy. *Diabetes Care*, 24, 479–82.

SCHLEGEL, Z., LTEIF, Y., BAINS, H.S. & GATINEL, D. 2009. Total, Corneal, and Internal Ocular Optical Aberrations in Patients with Keratoconus. *J Refract Surg*, 25 (Suppl 10), S951–7.

SCHMITT, A., GAHR, A., HERMANNS, N., KULZER, B., HUBER, J. & HAAK, T. 2013. The Diabetes Self-Management Questionnaire (DSMQ): Development and Evaluation of an Instrument to Assess Diabetes Self-Care Activities Associated with Glycaemic Control. *Health Qual Life Outcomes*, 11, 138.

SCHMITZ-VALCKENBERG, S. & FITZKE, F.W. 2009. Imaging Techniques of Fundus Autofluorescence. In *Fundus Autofluorescence* (pp. 48–60). Philadelphia: Lippincott Williams & Wilkins.

SCHMITZ-VALCKENBERG, S., FLECKENSTEIN, M., GÖBEL, A.P., SEHMI, K., FITZKE, F.W., HOLZ, F.G. & TUFAIL, A. 2008a. Evaluation of Autofluorescence Imaging with the Scanning Laser Ophthalmoscope and the Fundus Camera in Age-Related Geographic Atrophy. *Am J Ophthalmol*, 146, 183–92.

SCHMITZ-VALCKENBERG, S., HOLZ, F.G., BIRD, A.C. & SPAIDE, R.F. 2008b. Fundus Autofluorescence Imaging: Review and Perspectives. *Retina*, 28, 385–409.

SCHULTZ, R.O., MATSUDA, M., YEE, R.W., EDELHAUSER, H.F. AND SCHULTZ, K.J. 1984. Corneal Endothelial Changes in Type I and Type II Diabetes Mellitus. *Am J Ophthalmol*, 98, 401–10.

SCHUTT, F., BERGMANN, M., HOLZ, F.G. & KOPITZ, J. 2003. Proteins Modified by Malondialdehyde, 4-Hydroxynonenal, or Advanced Glycation End Products in Lipofuscin of Human Retinal Pigment Epithelium. *Invest Ophthalmol Vis Sci*, 44, 3663–8.

SCHWARTZMAN, M.L., ISEROVICH, P., GOTLINGER, K., BELLNER, L., DUNN, M.W., SARTORE, M., GRAZIA PERTILE, M., LEONARDI, A., SATHE, S., BEATON, A., TRIEU, L. & SACK, R. 2010. Profile of Lipid and Protein Autacoids in Diabetic Vitreous Correlates with the Progression of Diabetic Retinopathy. *Diabetes* 59, 1780–8.

SCHWEITZER, D., BEUERMANN, B., HAMMER, M., SCHWEITZER, F., RICHTER, S., LEISTRITZ, L., SCIBOR, M., THAMM, E., KOLB, A. & ANDERS, R. 2005b. [Fundus Spectrometry in Age-Related Maculopathy]. *Klin Monbl Augenheilkd*, 222, 396–408.

SCHWEITZER, D., DEUTSCH, L., KLEMM, M., JENTSCH, S., HAMMER, M., PETERS, S., HAUEISEN, J., MÜLLER, U.A. & DAWCZYNSKI, J. 2015. Fluorescence Lifetime Imaging Ophthalmoscopy in Type 2 Diabetic Patients Who Have No Signs of Diabetic Retinopathy. *J Biomed Opt*, 20, 61106.

SCHWEITZER, D., HAMMER, M. & SCHWEITZER, F. 2005a. [Limits of the Confocal Laser-Scanning Technique in Measurements of Time-Resolved Autofluorescence of the Eye-Ground]. *Biomed Tech (Berl)*, 50, 263–7.

SCHWEITZER, D., HAMMER, M., SCHWEITZER, F., ANDERS, R., DOEBBECKE, T., SCHENKE, S., GAILLARD, E.R. & GAILLARD, E.R. 2004. In Vivo Measurement of Time-Resolved Autofluorescence at the Human Fundus. *J Biomed Opt*, 9, 1214–22.

SCHWEITZER, D., SCHENKE, S., HAMMER, M., SCHWEITZER, F., JENTSCH, S., BIRCKNER, E., BECKER, W. & BERGMANN, A. 2007. Towards Metabolic Mapping of the Human Retina. *Microsc Res Tech*, 70, 410–9.

SCHWIEGERLING, J. 2000. Theoretical Limits to Visual Performance. *Surv Ophthalmol*, 45, 139-46.

SCHWITZER, D., HAMMER, M., SCHWEITZER, F., SCHENKE, S.& GAILLARD, R. 2003. Evaluation of Time-Resolved Autofluorescence Images of the Ocular Fundus. In Wagniéres G. (Ed.), *Diagnostic Optical Spectroscopy in Biomedicine II*. Proc SPIE, Optical Society of America.

SEBAG, J. 1993. Abnormalities of Human Vitreous Structure in Diabetes. *Graefes Arch Clin Exp Ophthalmol*, 231, 257–60.

SEPAH, Y.J., AKHTAR, A., SADIQ, M.A., HAFEEZ, Y., NASIR, H., PEREZ, B., MAWJI, N., DEAN, D.J., FERRAZ, D., & NGUYEN, Q.D. 2014. Fundus Autofluorescence Imaging: Fundamentals and Clinical Relevance. *Saudi J Ophthalmol*, 28, 111–6.

SHAHIDI, M., BLAIR, N.P., MORI, M. & ZELKHA, R. 2004. Optical Section Retinal Imaging and Wavefront Sensing in Diabetes. *Optom Vis Sci*, 81, 778–84.

SHAHIDI, M., & YANG, Y. 2004. Measurements of Ocular Aberrations and Light Scatter in Healthy Subjects. *Optom Vis Sci*, 81, 853–7.

SHAW, J.E., SICREE, R.A. & ZIMMET, P.Z. 2010. Global Estimates of the Prevalence of Diabetes for 2010 and 2030. *Diabetes Res Clin Pract*, 87, 4-14.

SHEN, Y., XU, X & LIU, K. 2014. Fundus Autofluorescence Characteristics in Patients with Diabetic Macular Edema. *Chin Med J (Engl)*, 127, 1423–8.

SIHOTA, R., LAKSHMAIAH, N.C., TITIYAL, J.S., DADA, T. & AGARWAL, H.C. 2003. Corneal Endothelial Status in the Subtypes of Primary Angle Closure Glaucoma. *Clin Exp Ophthalmol*, 31, 492–5.

SIIK, S., AIRAKSINEN, P.J., TUULONEN, A. & NIEMINEN, H. 1993. Autofluorescence in Cataractous Human Lens and Its Relationship to Light Scatter. *Acta Ophthalmol (Copenh)*, 71, 388–92.

SMITH, G.T., BROWN, N.A. & SHUN-SHIN, G.A. 1990. Light Scatter from the Central Human Cornea. *Eye (Lond)*, 4, 584–8.

SMITH, G., COX, M.J., CALVER, R. & GARNER, L.F. 2001. The Spherical Aberration of the Crystalline Lens of the Human Eye. *Vision Res*, 41, 235–43.

SMITH, R.T., KONIAREK, J.P., CHAN, J., NAGASAKI, T., SPARROW, J.R. & LANGTON, K. 2005. Autofluorescence Characteristics of Normal Foveas and Reconstruction of Foveal Autofluorescence from Limited Data Subsets. *Invest Ophthalmol Vis Sci*, 46, 2940–6.

SPAIDE, R.F. 2003. Fundus Autofluorescence and Age-Related Macular Degeneration. *Ophthalmology*, 110, 392–9.

SPAIDE, R. 2008. Autofluorescence From The Outer Retina And Subretinal Space. *Retina*, 28, 5–35.

SPARROW, J.R., & BOULTON, M. 2005. RPE Lipofuscin and Its Role in Retinal Pathobiology. *Exp Eye Res*, 80, 595-606.

SPARROW, J.M., BRON, A.J., BROWN, N.A., & NEIL, H.A. 1990. Biometry of the Crystalline Lens in Early-Onset Diabetes. *Br J Ophthalmol*, 74, 654–60.

SPARROW, J.M., BRON, A.J., BROWN, N.A. & NEIL, H.A. 1992b. Autofluorescence of the Crystalline Lens in Early and Late Onset Diabetes. *Br J Ophthalmol*, 76, 25–31.

SPARROW, J.M., BRON, A.J., PHELPS BROWN, N.A. & NEIL, H.A. 1992a. Biometry of the Crystalline Lens in Late Onset Diabetes: The Importance of Diabetic Type. *Br J Ophthalmol*, 76, 428–33.

SPARROW, J.R., FISHKIN, N., ZHOU, J., CAI, B., JANG, Y.P., KRANE, S., ITAGAKI, Y. & NAKANISHI, K. 2003. A2E, a Byproduct of the Visual Cycle. *Vision Res*, 43, 2983–90.

STITT, A.W., MOORE, J.E., SHARKEY, J.A., MURPHY, G., SIMPSON, D.A., BUCALA, R., VLASSARA, H. & ARCHER, D.B. 1998. Advanced Glycation End Products in Vitreous: Structural and Functional Implications for Diabetic Vitreopathy. *Invest Ophthalmol Vis Sci*, 39, 2517–23.

STOLWIJK, T.R., VAN BEST, J.A., BOOT, J.P. & OOSTERHUIS, J.A. 1990. Corneal Autofluorescence in Diabetic and Penetrating Keratoplasty Patients as Measured by Fluorophotometry. *Exp Eye Res*, 51, 403–9.

STOLWIJK, T.R., VAN BEST, J.A., OOSTERHUIS, J.A. & SWART, W. 1992. Corneal Autofluorescence: An Indicator of Diabetic Retinopathy. *Invest Ophthalmol Vis Sci*, 33, 92–7.

STORR-PAULSEN, A., NORREGAARD, J.C., AHMED, S., STORR-PAULSEN, T. & PEDERSEN, T.H. 2008. Endothelial Cell Damage after Cataract Surgery: Divide-and-Conquer versus Phaco-Chop Technique. *J Cataract Refract Surg*, 34, 996–1000.

STORR-PAULSEN, A., SINGH, A., JEPPESEN, H., NORREGAARD, J.C. & THULESEN, J. 2014. Corneal Endothelial Morphology and Central Thickness in Patients with Type II Diabetes Mellitus. *Acta Ophthalmol*, 92, 158–60.

STRATTON, I.M., ADLER, A.I., NEIL, H.A., MATTHEWS, D.R., MANLEY, S.E., CULL, C.A., HADDEN, D., TURNER, R.C & HOLMAN, R.R. 2000. Association of Glycaemia with Macrovascular and Microvascular Complications of Type 2 Diabetes (UKPDS 35): Prospective Observational Study. *BMJ*, 321, 405–12.

SUDHIR, R.R., RAMAN, R. & SHARMA, T. 2012. Changes in the Corneal Endothelial Cell Density and Morphology in Patients with Type 2 Diabetes Mellitus: A Population-Based Study, Sankara Nethralaya Diabetic Retinopathy and Molecular Genetics Study (SN-DREAMS, Report 23). *Cornea*, 31, 1119–22.

SUE MENKO, A. 2002. Lens Epithelial Cell Differentiation. *Exp Eye Res*, 75, 485–90.

SUZUKI, S., OSHIKA, T., OKI, K., SAKABE, I., IWASE, A., AMANO, S. & ARAIE, M. 2003. Corneal Thickness Measurements: Scanning-Slit Corneal Topography and Noncontact Specular Microscopy versus Ultrasonic Pachymetry. *J Cataract Refract Surg*, 29, 1313–8.

TAKAHASHI, N., WAKUTA, M., MORISHIGE, N., CHIKAMA, T., NISHIDA, T. & SUMII, Y. 2007. Development of an Instrument for Measurement of Light Scattering at the Corneal Epithelial Basement Membrane in Diabetic Patients. *Jpn J Ophthalmol*, 51, 185–90.

THE DIABETES CONTROL AND COMPLICATIONS TRIAL RESEARCH GROUP, DCCT. 1993. The Effect of Intensive Treatment of Diabetes on the Development and Progression of Long-Term Complications in Insulin-Dependent Diabetes Mellitus. *N Engl J Med*, 329, 977–86.

THIBOS, L.N., WHEELER, W. & HORNER, D. 1997. Power Vectors: An Application of Fourier Analysis to the Description and Statistical Analysis of Refractive Error. *Optom Vis Sci*, 74, 367–75.

THIBOS, L.N., APPLEGATE, R.A., SCHWIEGERLING, J.T., WEBB, R. 2000. Standards for Reporting the Optical Aberrations of Eyes. *J Refract Surg*, 18, S652–60.

THIBOS, L.N., HONG, X., BRADLEY, A. & CHENG, X. 2002. Statistical Variation of Aberration Structure and Image Quality in a Normal Population of Healthy Eyes. *J Opt Soc Am A Opt Image Sci Vis*, 19, 2329–48.

UK PROSPECTIVE DIABETES STUDY (UKPDS) GROUP. 1998a. Intensive Blood-Glucose Control with Sulphonylureas or Insulin Compared with Conventional Treatment and Risk of Complications in Patients with Type 2 Diabetes (UKPDS 33). *Lancet*, 352, 837-53.

UK PROSPECTIVE DIABETES STUDY (UKPDS) GROUP. 1998b. Effect of Intensive Blood-Glucose Control with Metformin on Complications in Overweight Patients with Type 2 Diabetes (UKPDS 34). UK Prospective Diabetes Study (UKPDS) Group. *Lancet*, 352, 854–65.

ULLRICH, K., & PESUDOVS, K. 2012. Comprehensive Assessment of Nuclear and Cortical Backscatter Metrics Derived from Rotating Scheimpflug Images. *J Cataract Refract Surg*, 38, 2100–7.

UNWIN, N., SHAW, J., ZIMMET, P. & ALBERTI, K.G. 2002. Impaired Glucose Tolerance and Impaired Fasting Glycaemia: The Current Status on Definition and Intervention. *Diabet Med*, 19, 708–23.

VACLAVIK, V., VUJOSEVIC, S., DANDEKAR, S.S., BUNCE, C., PETO, T. & BIRD, C. 2008. Autofluorescence Imaging in Age-Related Macular Degeneration Complicated by Choroidal Neovascularization. A Prospective Study. *Ophthalmology*, 115, 342–6.

VAMBERGUE, A. & FAJARDY, I. 2011. Consequences of Gestational and Pregestational Diabetes on Placental Function and Birth Weight. *World J Diabetes*, 2, 196–203.

VAN BEST, J.A., TSOI, E.W., BOOT, J.P. & OOSTERHUIS, J.A. 1985b. In Vivo Assessment of Lens Transmission for Blue-Green Light by Autofluorescence Measurement. *Ophthalmic Res*, 17, 90–5.

VAN BEST, J.A., VAN DELFT, J.L. & KEUNEN, J.E. 1998. Long Term Follow-up of Lenticular Autofluorescence and Transmittance in Healthy Volunteers. *Exp Eye Res*, 66, 117–23.

VAN BEST, J.A., VRIJ, L. & OOSTERHUIS, J.A. 1985a. Lens Transmission of Blue-Green Light in Diabetic Patients as Measured by Autofluorophotometry. *Invest Ophthalmol Vis Sci*, 26, 532–6.

VAN DEN BERG, T.J. 1995. Analysis of Intraocular Straylight, Especially in Relation to Age. *Optom Vis Sci*, 72, 52-9.

VAN DEN BERG, T.J. 1997. Light Scattering by Donor Lenses as a Function of Depth and Wavelength. *Invest Ophthalmol Vis Sci*, 38, 1321–32.

VAN DEN BERG, T.J., FRANSSEN, L. & COPPENS, J.E. 2009. Straylight in the Human Eye: Testing Objectivity and Optical Character of the Psychophysical Measurement. *Ophthalmic Physiol Opt*, 29, 345–50.

VAN DEN BERG, T.J., FRANSSEN, L. & COPPENS, J.E. 2010. Ocular Media Clarity and Straylight. In Dart A.D., Beshare J.C., Dana R. (Eds.), *Encyclopedia of the Eye*. Oxford, UK: Elsevier/Academic Press.

VAN DEN BERG, T.J., & IJSPEERT, J.K. 1995. Light Scattering in Donor Lenses. *Vision Res*, 35, 169–77.

VAN DEN BERG, T.J., & SPEKREIJSE, H. 1999. Light Scattering Model for Donor Lenses as a Function of Depth. *Vision Res*, 39, 1437–45.

VAN SCHAIK H.J., ALKEMADE, C., SWART, W. & VAN BEST, J.A. 1999b. Autofluorescence of the Diabetic and Healthy Human Cornea in Vivo at Different Excitation Wavelengths. *Exp Eye Res*, 68, 1–8.

VAN SCHAIK, H.J, & VAN BEST, J.A. 1997. A Solid Fluorescence Reference for Corneal Autofluorescence Measurements. *Exp Eye Res*, 64, 121–3.

VAN SCHAIK, H.J., COPPENS, J., VAN DEN BERG, T.J. & VAN BEST, J.A. 1999a. Autofluorescence Distribution Along the Corneal Axis in Diabetic and Healthy Humans. *Exp Eye Res*, 69, 505–10.

VIRGILI, G., MENCHINI, F., DIMASTROGIOVANNI, A.F., RAPIZZI, E., MENCHINI, U., BANDELLO, F. & CHIODINI, R.G. 2007. Optical Coherence Tomography versus Stereoscopic Fundus Photography or Biomicroscopy for Diagnosing Diabetic Macular Edema: A Systematic Review. *Invest Ophthalmol Vis Sci*, 48, 4963-73.

VUJOSEVIC, S., CASCIANO, M., PILOTTO, E., BOCCASSINI, B., VARANO, M. & MIDENA, E. 2011. Diabetic Macular Edema: Fundus Autofluorescence and Functional Correlations. *Invest Ophthalmol Vis Sci*, 52, 442–8.

WALDSTEIN, S.M., HICKEY, D., MAHMUD, I., KIIRE, C.A., CHARBEL ISSA, P. & CHONG, N.V. 2012. Two-Wavelength Fundus Autofluorescence and Macular Pigment Optical Density Imaging in Diabetic Macular Oedema. *Eye (Lond)*, 26, 1078–85.

WANG, L., DAI, E., KOCH, D.D. & NATHOO, A. 2003. Optical Aberrations of the Human Anterior Cornea. *J Cataract Refract Surg*, 29, 1514–21.

WANG, J., SIMPSON, T.L. & FONN, D. 2004. Objective Measurements of Corneal Light-Backscatter during Corneal Swelling, by Optical Coherence Tomography. *Invest Ophthalmol Vis Sci*, 45, 3493–8.

WEBB, R.H., HUGHES, G.W. & DELORI, F.C. 1987. Confocal Scanning Laser Ophthalmoscope. *Appl Opt*, 26, 1492–9.

WEGENER, A., & LASER-JUNGA, H. 2009. Photography of the Anterior Eye Segment according to Scheimpflug's Principle: Options and Limitations - A Review. *Clin Exp Ophthalmol*, 37, 144-54.

WEISS, J.N., RAND, L.I., GLEASON, R.E. & SOELDNER, J.S. 1984. Laser Light Scattering Spectroscopy of in Vivo Human Lenses. *Invest Ophthalmol Vis Sci*, 25, 594–8.

WESTON, B.C., BOURNE, W.M., POLSE, K.A. & HODGE, D.O. 1995. Corneal Hydration Control in Diabetes Mellitus. *Invest Ophthalmol Vis Sci*, 36, 586–95.

WHITE, N.H., SUN, W., CLEARY, P.A., TAMBORLANE, W.V., DANIS, R.P., HAINSWORTH, D.P. & DAVIS, M.D. 2010. Effect of Prior Intensive Therapy in Type 1 Diabetes on 10-Year Progression of Retinopathy in the DCCT/EDIC: Comparison of Adults and Adolescents. *Diabetes*, 59, 1244–53.

WHITING, D.R., GUARIGUATA, L., WEIL, C. & SHAW, J. 2011. IDF Diabetes Atlas : Global Estimates of the Prevalence of Diabetes for 2011 and 2030. *Diabetes Res Clin Pract*, 94, 311-21.

WIEMER, N.G., DUBBELMAN, M., HERMANS, E.A., RINGENS, P.J., & POLAK, B.C. 2008b. Changes in the Internal Structure of the Human Crystalline Lens with Diabetes Mellitus Type 1 and Type 2. *Ophthalmology*, 115, 2017–23.

WIEMER, N.G., DUBBELMAN, M., KOSTENSE, P.J., RINGENS, P.J. & POLAK, B.C. 2008a. The Influence of Diabetes Mellitus Type 1 and 2 on the Thickness, Shape, and Equivalent Refractive Index of the Human Crystalline Lens. *Ophthalmology*, 115, 1679–86.

WIEMER, N.G., DUBBELMAN, M., RINGENS, P.J. & POLAK, B.C. 2009. Measuring the Refractive Properties of the Diabetic Eye during Blurred Vision and Hyperglycaemia Using Aberrometry and Scheimpflug Imaging. *Acta Ophthalmol*, 87, 176–82.

WILD, S., ROGLIC, G., GREEN, A., SICREE, R. & KING, H. 2004. Global Prevalence of Diabetes: Estimates for the Year 2000 and Projections for 2030. *Diabetes Care*, 27, 1047–53.

WILKINSON, C.P., FERRIS, F.L. 3RD., KLEIN, R.E., LEE, P.P., AGARDH, C.D., DAVIS, M., DILLS, D., KAMPIK, A., PARARAJASEGARAM, R. & VERDAGUER J.T. 2003. Proposed International Clinical Diabetic Retinopathy and Diabetic Macular Edema Disease Severity Scales. *Ophthalmology*, 110, 1677–82.

WILLIAMS, R., AIREY, M., BAXTER, H., FORRESTER, J., KENNEDY-MARTIN, T. & GIRACH, A. 2004. Epidemiology of Diabetic Retinopathy and Macular Oedema: A Systematic Review. *Eye (Lond)*, 18, 963–83.

WORLD HEALTH ORGANIZATION. 1999. Definition, Diagnosis And Classfication Of Diabetes Mellitus And Its Complications. In Part 1: Diagnosis And Classification Of Diabetes Mellitus. World Health Organization: Geneva, Switzerland.

WORLD HEALTH ORGANIZATION. 2005. Prevention of Blindness from Diabetes Mellitus. World Health Organization: Geneva, Switzerland.

WÜSTEMEYER, H., JAHN, C., NESTLER, A., BARTH, T. & WOLF, S. 2002. A New Instrument for the Quantification of Macular Pigment Density: First Results in Patients with AMD and Healthy Subjects. *Graefes Arch Clin Exp Ophthalmol*, 240, 666–71.

XU, H., CHEN, M., MANIVANNAN, A., LOIS, N. & FORRESTER, J.V. 2008. Age-Dependent Accumulation of Lipofuscin in Perivascular and Subretinal Microglia in Experimental Mice. *Aging Cell*, 7, 58–68.

YAMAMOTO, M., KOHNO, T. & SHIRAKI, K. 2009. Comparison of Fundus Autofluorescence of Age-Related Macular Degeneration between a Fundus Camera and a Confocal Scanning Laser Ophthalmoscope. *Osaka City Med J*, 55, 19–27.

YAPPERT, M.C., LAL, S. & BORCHMAN, D. 1992. Age Dependence and Distribution of Green and Blue Fluorophores in Human Lens Homogenates. *Invest Ophthalmol Vis Sci*, 33, 3555–60.

YAU, J.W., ROGERS, S.L., KAWASAKI, R., LAMOUREUX, E.L., KOWALSKI, J.W., BEK, T., CHEN, S.J., DEKKER, J.M., FLETCHER, A., GRAUSLUND, J., HAFFINER, S., HAMMAN, R.F., IKRAM, M.K., KAYAMA, T., KLEIN, B.E., KLEIN, R., KRISHNAIAH, S., MAYURASAKORN, K., O´HARE, J.P., ORCHARD, T.J., PORTA, M.M., REMA, M., ROY, M.S., SHARMA, T., SHAW, J., TAYLOR, H., TIELSCH, J.M., VARMA, R., WANG, J.J., WANG, N., WESTS, S., XU, L., YASUDA, M., ZHANG, X., MITCHELL, P. & WONG, T.Y. 2012. Global Prevalence and Major Risk Factors of Diabetic Retinopathy. *Diabetes Care*, 35, 556–64.

YIN, D. 1996. Biochemical Basis of Lipofuscin, Ceroid, and Age Pigment-like Fluorophores. *Free Radic Biol Med*, 21, 871-88.

YOKOI, M., YAMAGISHI, S., SAITO, A., YOSHIDA, Y., MATSUI, T., SAITO, W., HIROSE, S., OHGAMI, K., KASE, M. & OHNO, S. 2007. Positive Association of Pigment Epithelium-Derived Factor with Total Antioxidant Capacity in the Vitreous Fluid of Patients with Proliferative Diabetic Retinopathy. *Br J Ophthalmol*, 91, 885–7.

YOON, K.C., IM, S.K. & SEO, M.S. 2004. Changes of Tear Film and Ocular Surface in Diabetes Mellitus. *Korean Jf Ophthalmol*, 18, 168–74.

YOSHITAKE, S., MURAKAMI, T., UJI, A., UNOKI, N., DODO, Y., HORII, T. & YOSHIMURA, N. 2015. Clinical Relevance of Quantified Fundus Autofluorescence in Diabetic Macular Oedema. *Eye (Lond)*, 29, 662–69.

YU, N.T., KUCK, J.F.JR., & ASKREN, C.C. 1979. Red Fluorescence in Older and Brunescent Human Lenses. *Invest Ophthalmol Vis Sci*, 18, 1278–80.

YU, N.T., BARRON, B.C. & KUCK, J.F.JR. 1989. Distribution of Two Metabolically Related Fluorophors in Human Lens Measured by Laser Microprobe. *Exp Eye Res*, 49, 189–94.

Webs

SPECTRALIS® Information. Available at: *https://www.heidelbergengineering.com/* [Last accessed January 2017]

F-10. The NIDEK Digital Ophthalmoscope. Available at: *http://www.dfv.com.au/downloads/Nidek-f10-paper-01.pdf* [Last accessed January 2017]

Nidek F-10 Digital Ophthalmoscope. Available at: *https://www.mivision.com.au/nidek-f-10-digital-ophthalmoscope/* [Last accessed January 2017]

200 Tx Brochure. Available at:

https://www.optos.com/Global/documents/au_200Tx_Brochure.pdf [Last accessed January 2017]

Canon. Karolinska Institute, st. Erik´Eye Hospital, Sweden. Case Study. Available at: *http://www.canon.co.uk/Images/Karolinska%20FAF_tcm14-1087862.pdf* [Last accessed January 2017]

CX-1. Digital Retinal Camera mydriatic & non-mydriatic. Available at: *http://www.canon-europe.com/images/Canon_Brochure_CX-1_tcm13-737180.pdf* [Last accessed January 2017]

CR-2 Plus AF. Non-mydriatic retinal camera. Available at: *http://www.canon-europe.com/images/canon%20non-myd%20family%20brochure_tcm13-1261648.pdf* [Last accessed January 2017]

FF450plus Fundus Camera with VISUPAC from ZEISS. Available at: *http://applications.zeiss.com/C1257A290053AE30/0/7630DC2E072A128FC1257D4F00399380/$FILE/ff450plus-sensors-and-technical-data.pdf* [Last accessed January 2017]

Visucam 200. Available at: *http://applications.zeiss.com/C1257A290053AE30/0/D7C52747225E8972C1257A29005EFC3E/$FILE/VISUCAM-200_EN.pdf* [Last accessed January 2017]

Visucam 500. Available at: *http://applications.zeiss.com/C1257A290053AE30/0/C2028E1ECA36678AC1257A29005F002E/$FILE/VISUCAM-500_EN.pdf* [Last accessed January 2017]

FF450plus Fundus Camera with VISUPAC. Available at: *http://applications.zeiss.com/C1257A290053AE30/0/BB63B1821569CC0BC1257BE8004D69A5/$FILE/FI_FF450_Downloads_Brochure.pdf* [Last accessed January 2017]

APPENDIX 1

Publications resulting from the Thesis

This Thesis has resulted in the following peer-reviewed publications:

1. Optical quality of the diabetic eye: a review. Eye (London) 2014; 28(11): 1271-1280. Impact Factor: 2.082. Position: 21/57. Ophthalmology Section of the Journal Citation Report.
2. A pilot study on total, corneal, and internal aberrations in insulin-dependent and non-insulin-dependent diabetes mellitus patients. Graefe's Archive for Clinical and Experimental Ophthalmology 2015; 253(4): 645-653. Impact Factor: 1.991. Position: 23/56. Ophthalmology Section of the Journal Citation Report.
3. Quantitative corneal anatomy: evaluation of the effect of diabetes duration on the endothelial cell density and corneal thickness. Ophthalmic and Physiological Optics 2015; 35(3); 293-298. Impact Factor: 2.567. Position: 15/56. Ophthalmology Section of the Journal Citation Report.
4. Pilot study on visual function and fundus autofluorescence assessment in diabetic patients. Journal of Ophthalmology 2016; 2016:1287847. Impact Factor: 1.463. Position: 34/56. Ophthalmology Section of the Journal Citation Report.
5. Ocular autofluorescence in diabetes mellitus. A review. Journal of Diabetes 2016; 8(5): 619-628. Impact Factor: 2.5. Position: 79/133. Endocrinology & Metabolism Section of the Journal Citation Report.
6. Confocal scanning laser ophthalmoscopy versus modified conventional fundus camera for fundus autofluorescence. Expert Review of Medical Devices 2016;

13(10): 965-978. Impact Factor: 1.762. Position: 40/76. Engineering, Biomedical Section of the Journal Citation Report.

7. Corneal backscatter in insulin-dependent and non-insulin-dependent diabetes mellitus patients. A pilot study. Arquivos Brasileiros de Oftalmologia 2016 (accepted for publication). Impact Factor: 0.494. Position: 55/56. Ophthalmology Section of the Journal Citation Report.
8. Diabetic macular oedema assessment by fundus autofluorescence analysis using a non-mydriatic retinal camera. Pilot study. BMC Journal 2016 (submitted).

APPENDIX 2

Table 6.1.3

Table 6.1.4

Compatible signs	Image type				*p* value post-hoc test[b]		
Mycroaneurisms	**Colour**	**FAF**	**Optimized-FAF**	***p* value[a]**	**Colour vs FAF**	**Colour vs – Optimized FAF**	**FAF vs – Optimized-FAF**
Upper temporal area	4,43 ± 3,82	28,43 ± 6,29	42,57 ± 12,98	< 0,001	0,001	0,001	0,016
Lower temporal area	7,28 ± 3,95	23,43 ± 8,54	35,71 ± 11,98	0,001	0,007	0,001	0,073
Upper nasal area	1,14 ± 1,46	4,14 ± 2,27	12,14 ± 9,12	0,005	0,017	0,004	0,097
Lower nasal area	1,86 ± 2,27	9,00 ± 5,60	13,71 ± 8,48	0,007	0,026	0,002	0,318
Capillary dilation							
Upper temporal area	3,43 ± 2,15	22,71 ± 5,74	19,86 ± 2,34	0,001	0,001	0,001	0,209
Lower temporal area	3,86 ± 1,86	19,86 ± 7,42	16,57 ± 3,55	0,001	0,001	0,001	0,383
Upper nasal area	0,43 ± 0,53	2,71 ± 1,70	5,00 ± 4,28	0,02	0,017	0,017	0,535
Lower nasal area	0,43 ± 0,53	4,71 ± 3,95	4,14 ± 4,06	0,01	0,004	0,017	0,805
Hemorrhages							
Upper temporal area	1,14 ± 1,46	2,14 ± 2,11	2,29 ± 2,50	0,516	-	-	-
Lower temporal area	3,00 ± 1,63	2,71 ± 1,60	2,86 ± 1,95	0,914	-	-	-
Upper nasal area	-	-	-	-	-	-	-
Lower nasal area	0,43 ± 0,79	0,43 ± 0,79	0,43 ± 0,79	1	-	-	-
Hard exudates							
Upper temporal area	1,43 ± 2,23	0,71 ± 1,50	1,14 ± 2,61	0,819	-	-	-
Lower temporal area	1,57 ± 2,93	1,28 ± 2,98	1,28 ± 2,98	0,823	-	-	-
Upper nasal area	-	-	-	-	-	-	-
Lower nasal area	-	-	-	-	-	-	-

[a] Kruskall-Wallis test; [b] Mann-Whitney U test; FAF= Fundus autofluorescence

Table 6.1.3: Distribution of retinal alterations observed in colour, FAF, and optimized-FAF images in diabetic patients.

	Image type				*p* value post-hoc test		
Epithelial defects	**Color**	**FAF**	**Optimized-FAF**	***p* value**	**Color vs FAF**	**Color vs – Optimized-FAF**	**FAF vs – Optimized FAF**
Upper temporal area	1,92 ± 2,06	10,08 ± 4,60	19,61 ± 7,69	< 0,001[a]	< 0,001[c]	< 0,001[c]	< 0,001[c]
Lower temporal area	1,15 ± 1,28	9,61 ± 6,65	18,77 ± 9,04	< 0,001[a]	< 0,001[c]	< 0,001[c]	0,008[c]
Upper nasal area	0,85 ± 1,40	3,08 ± 2,29	5,61 ± 3,69	< 0,001[b]	0,007[d]	<0,001[d]	0,048[c]
Lower nasal area	0,92 ± 1,60	3,08 ± 2,06	5,61 ± 3,20	< 0,001[b]	0,01[d]	<0,001[d]	0,026[c]
Capillary dilation							
Upper temporal area	3,85 ± 2,91	13,77 ± 4,21	12,23 ± 3,63	< 0,001[a]	< 0,001[c]	< 0,001[c]	0,328[c]
Lower temporal area	4,15 ± 2,73	13,15 ± 7,20	13,00 ± 4,08	< 0,001[a]	< 0,001[c]	< 0,001[c]	0,947[c]
Upper nasal area	0,69 ± 1,18	3,08 ± 1,98	3,15 ± 1,62	< 0,001[a]	0,001[c]	< 0,001[c]	0,915[c]
Lower nasal area	0,54 ± 0,97	2,69 ± 2,21	3,31 ± 1,97	< 0,001[b]	0,001[d]	<0,001[d]	0,462[c]

[a] One-way ANOVA test; [b] Kruskall-Wallis test; [c] Unpaired *t* test; [d] Mann-Whitney U test; FAF: Fundus autofluorescence

Table 6.1.4: Distribution of retinal alterations observed in colour, FAF, and optimized-FAF images in control subjects